

**SPATIO-TEMPORAL ANALYSIS OF  
RAINFALL AND REGIONAL  
GROUNDWATER MODELLING OF THE  
WEST COAST BASINS OF INDIA**

**Thesis**

**Submitted in partial fulfillment of the requirements for the degree of  
Doctor of Philosophy**

by

**CHYTHANYA KRISHNAN**



**DEPARTMENT OF WATER RESOURCES AND OCEAN  
ENGINEERING  
NATIONAL INSTITUTE OF TECHNOLOGY KARNATAKA  
SURATHKAL, MANGALORE – 575025  
APRIL 2023**

**SPATIO-TEMPORAL ANALYSIS OF  
RAINFALL AND REGIONAL  
GROUNDWATER MODELLING OF THE  
WEST COAST BASINS OF INDIA**

**Thesis**

**Submitted in partial fulfillment of the requirements for the degree of  
Doctor of Philosophy**

by

**CHYTHANYA KRISHNAN**

Under the guidance of

**Prof. AMAI MAHESHA**

Professor,

Dept. of Water Resources and Ocean Engineering  
NITK, Surathkal



**DEPARTMENT OF WATER RESOURCES AND OCEAN  
ENGINEERING  
NATIONAL INSTITUTE OF TECHNOLOGY KARNATAKA  
SURATHKAL, MANGALORE – 575025**

**APRIL 2023**

## DECLARATION

*By the Ph.D. Research Scholar*

I hereby *declare* that the Research Thesis entitled **Spatio-temporal Analysis of Rainfall and Regional Groundwater Modelling of the West Coast Basins of India** which is being submitted to the **National Institute of Technology Karnataka, Surathkal** in partial fulfilment of the requirements for the award of the Degree of **Doctor of Philosophy in Water Resources and Ocean Engineering Department** is a *bonafide report of the research work* carried out by me. The material contained in this Research Thesis has not been submitted to any University or Institution for the award of any degree.



158013 AM15F13, CHYTHANYA KRISHNAN

(Register Number, Name & Signature of the Research Scholar)

Department of Water Resources and Ocean Engineering

Place: NITK-Surathkal

Date: 05/04/2023

## CERTIFICATE

This is to certify that the Research Thesis entitled **Spatio-temporal Analysis of Rainfall and Regional Groundwater Modelling of the West Coast Basins of India** submitted by CHYTHANYA KRISHNAN (Register Number: 158013 AM15F13) as the record of the research work carried out by her, is *accepted as the Research Thesis submission* in partial fulfilment of the requirements for the award of degree of **Doctor of Philosophy**.

  
Prof. Amaj Mahesha 2023

Research Guide

(Name and Signature with Date and Seal)



  
5/4/23  
Chairman - DRPC

(Signature with Date and Seal)

Chairman (DRPC)  
Dept. of Water Resources & Ocean Engineering

## ACKNOWLEDGMENTS

*Thanks to Almighty!*

I am forever grateful to my research guide, **Prof. Amai Mahesha**, for his supervision, valuable inputs and patience during my PhD study. Sir, You have always been calm and supportive during the difficult times of my PhD journey.

Let me express my gratitude to my RPAC members **Prof. K Swaminathan** and **Dr. Ramesh H.** for their valuable inputs and suggestions.

Let me express my thanks to, **Prof. G. S. Dwarakish**, **Prof. Amai Mahesha**, **Prof. Amba Shetty**, **Prof. B. M. Dodamani**, the former Heads of Department and **Dr. Varija K**, the present Head of Department for granting me use the departmental facilities required for my PhD work.

I sincerely acknowledge the help and support from all the faculties, staff and the research scholars of Department of Water Resources and Ocean Engineering.

To my family, **Mrs. Usha K K** and **Mr. Kunhikrishnan K**, my parents for always believing in me and supporting me throughout my PhD journey. My sister, **Ms. Chandhana Krishnan** for building my confidence during the tough times. To my grandmother **Mrs. Padmini K. K.** and my grandfather **Late Mr. T. V. Balan Nambiar** for the blessings and love. I also express my heartfelt thanks to **Mr. C. Balan** and **Mrs. Yemuna P.** for their support and love.

To my pillar of strength, my husband – **Mr. Athul C. Balan** for his endless support that helped me conquer my fears and insecurities. Thank You!

To my little one, **Ms. Anvika Athul**, for understanding that her mother needs to work and wait for her turn to play!

To all my friends who have extended their support and love, **Dr. Soumya S.**, **Dr. Dineshkumar M.**, **Dr. Sinan**, **Dr. Nithya**, **Ms. Anjali**, **Dr. Beena**, **Dr. Rishikesh**, **Mr. Parthasarathy**, **Mrs. Ashwitha**, **Dr. Tom**, **Mr. Rony**, **Dr. Dinu**, **Mr. Athul**, **Dr. Anjana**, **Dr. Anaswara**, **Dr. Minu**, **Mrs. Sruthi**, **Miss Jubina**, **Dr. Sylus**, and all other research scholars.

*Chythanya Krishnan*

## ABSTRACT

---

The Indian summer monsoon (June to September) is the backbone of the country's agriculture and allied sectors, exhibiting spatial and temporal variability across the Indian subcontinent. A growing body of research on climate change indicated the varying and patterns of the Indian summer monsoon. The Indian west coast is among the densely populated region with undulating topography. The region has the Western Ghats to the west and the Arabian sea to the east. Demands from agriculture and allied sectors in conjunction with the growing population have adversely affected the groundwater reserves in the region. The scenario has worsened owing to changing rainfall regimes over the recent decades. In this context, the present study aims at understanding the spatio-temporal patterns of rainfall and groundwater levels in the west coast basins of India. The feasibility of applying machine learning models in simulating the region's groundwater levels was also investigated. The west coast basins are categorised by the Central Water Commission (Ministry of Water Resources and Ganga Rejuvenation, Govt. of India) as sub-basin of Bhatsol and others, sub-basin of Vasishti and others, sub-basin of Netravati and others, sub-basin of Varrar and others and the sub-basin of Periyar and others. The departure analysis assessed the decadal variability and epochal behaviour of annual and seasonal rainfall in the west coast basins. The annual and seasonal rainfall departures displayed decadal variability among the west coast basins. The decades from 1980 to 1989 and from 2000 to 2009 were observed as the driest decade common among the west coast basins. An increase in dry rainfall-year frequency was noted after 1980 for Periyar, Varrar, and Netravati basins. Wavelet power spectrum analysis was conducted to examine the role of teleconnections in the region. Inter-annual periodicities of 2-4-years and 4-8-years were predominantly exhibited by Bhatsol, Vasishti, and Periyar basins with varying wavelet power for southwest monsoon rainfall. At the same time, Netravati and Varrar basins presented few short periodicities of 2-4-year band confined to early decades. However, statistically significant inter-decadal oscillations of 12-16-year period were evident among all the basins with moderate wavelet power. The inter-annual and inter-decadal variability in the distribution of southwest monsoon rainfall (or Indian summer monsoon) is clear from the periodicities obtained from the wavelet spectra. The widely used Sen's slope estimator investigated rainfall and groundwater level trends at annual and seasonal scales. The statistical significance was examined by the modified Mann-Kendall test (mMK).

Southwest monsoon rainfall indicated a significant decline of -2.48mm/year, -6.57mm/year, and -5.34mm/year at 5% significance level in the Periyar, Varrar, and Netravati basins respectively. The Vasishti basin indicated a significant increase of +5.89% in average winter rainfall per decade. The influence of parent distribution on the test power of the mMK test was analysed by Monte Carlo simulation of the generalised extreme value (GEV) distribution. The rank-based Mann-Kendall test may not attain the threshold power of 0.8 owing to heavy-tailed distribution or scale parameters. The trajectory of trends was extracted using the singular spectrum analysis (SSA) for rainfall and groundwater level time series. Significant trends by mMK for the monsoon and post-monsoon GWLs indicated a greater number of falls than rises. An average significant fall of -0.032m/year, i.e., a 7m decline in 12.3% wells was observed for monsoon, while -0.042m/year i.e., 0.92m fall in 11% wells, was indicated during the post-monsoon season. The artificial neural network (ANN) and support vector machines (SVM) were incorporated to examine the feasibility of machine learning models in predicting groundwater levels in the west coast basins. Type I models included abstraction and meteorological variables as predictors, while type II used only meteorological variables as predictors. The machine learning models, namely ANN1, ANN2, SVM1, and SVM2, performed well in predicting groundwater levels during the test period from 2012 to 2017. All four models showcased promising results for RMSE metrics with more than 93% of models in each category associated with an RMSE<0.2m. About 60.53% ANN1, 58.13% ANN2 models, 56.93% SVM1 models, and 55.26% SVM2 models exhibited an  $R^2 > 0.7$ , indicating the accountability of both ANN and SVM approach in predicting the groundwater levels (GWLs). The present study emphasizes the rainfall patterns on the west coast of India and the feasibility of using simple machine-learning algorithms to simulate groundwater level without an extensive hydrogeological dataset.

**Keywords:** Artificial neural network (ANN), Departure analysis, Mann-Kendall, Monte-Carlo, Singular spectrum analysis (SSA), Support vector machine (SVM), Test power analysis, Trend analysis, Wavelet power spectrum, West coast basins

## CONTENTS

<b>Abstract</b> .....	<b>i</b>
<b>Contents</b> .....	<b>iii</b>
<b>List of figures</b> .....	<b>vii</b>
<b>List of Tables</b> .....	<b>xi</b>
<b>CHAPTER 1</b> .....	<b>1</b>
<b>INTRODUCTION</b> .....	<b>1</b>
1.1 INTRODUCTION.....	1
1.2 SCOPE OF STUDY.....	1
1.3 OBJECTIVES.....	3
1.4 ORGANIZATION OF THE THESIS.....	3
<b>CHAPTER 2</b> .....	<b>5</b>
<b>LITERATURE REVIEW</b> .....	<b>5</b>
2.1 GENERAL.....	5
2.2 RAINFALL STUDIES IN THE PAST.....	5
2.3 PAST LITERATURE ON GROUNDWATER STUDIES.....	6
2.4 MACHINE LEARNING BASED GROUNDWATER PREDICTIONS.....	9
2.5 PROBLEM FORMULATION.....	10
<b>CHAPTER 3</b> .....	<b>13</b>
<b>STUDY AREA</b> .....	<b>13</b>
3.1 STUDY AREA.....	13
3.2 DATA USED.....	15
<b>CHAPTER 4</b> .....	<b>17</b>
<b>SPATIO-TEMPORAL ANALYSIS OF RAINFALL</b> .....	<b>17</b>
4.1 INTRODUCTION.....	17
4.2 METHODOLOGY.....	17
4.2.1 Departure Analysis (D%).....	17
4.2.2 Wavelet Power Spectrum Analysis.....	18
4.3 RESULTS AND DISCUSSIONS.....	19



4.3.1 Spatio-temporal Analysis of Rainfall.....	19
4.3.2 Coefficient of Variation (CV).....	22
4.3.3 Departure Analysis (D % ).....	23
4.3.3.1 Annual rainfall departures.....	23
4.3.3.2 Winter rainfall departures.....	27
4.3.3.3 Pre-monsoon rainfall departures.....	30
4.3.3.4 Southwest-monsoon rainfall departures.....	33
4.3.3.5 Post-monsoon rainfall departures.....	37
4.3.4 Wavelet Spectrum.....	40
4.3.4.1 Annual rainfall wavelet spectrum.....	40
4.3.4.2 Winter rainfall power spectrum.....	42
4.3.4.3 Pre-monsoon rainfall power spectrum.....	43
4.3.4.4 South-west monsoon rainfall spectrum.....	46
4.3.4.5 Post-monsoon rainfall spectrum.....	48
4.4 CLOSURE.....	50
<b>CHAPTER 5.....</b>	<b>55</b>
<b>TREND ANALYSIS OF RAINFALL AND GROUNDWATER LEVELS.....</b>	<b>55</b>
5.1 INTRODUCTION.....	55
5.2 METHODODOLOGY.....	56
5.2.1 Mann-Kendall (MK) Test.....	56
5.2.2 Sen’s Slope Estimator (SE).....	58
5.2.3 Power Analysis of mMK Test.....	58
5.2.4 Singular Spectrum Analysis (SSA).....	60
5.3 RESULTS AND DISCUSSIONS.....	61
5.3.1 mMK and SE Rainfall Trends.....	62
5.3.2 Power of mMK Test.....	70
5.3.3 SSA- rainfall Trends.....	78

5.3.4 mMK and SE Groundwater Level Trends.....	84
5.3.5 SSA – PMGWL Trends.....	88
5.4 CLOSURE.....	89
<b>CHAPTER 6.....</b>	<b>93</b>
<b>GROUNDWATER LEVEL PREDICTIONS.....</b>	<b>93</b>
6.1 INTRODUCTION.....	93
6.2 METHODOLOGY.....	93
6.2.1 Artificial Neural Networks (ANN).....	93
6.2.2 Support Vector Machines (SVM).....	94
6.2.3 Model Training, Testing and Performance Evaluation.....	95
6.3 RESULTS AND DISCUSSIONS.....	96
6.3.1 ANN-GWL Predictions.....	96
6.3.2 SVM-GWL Model Predictions.....	98
6.3.3 Basin-wise ANN Model Performance.....	99
6.3.4 Basin-wise SVM Model Performance.....	101
6.4 CLOSURE.....	106
<b>CHAPTER 7.....</b>	<b>109</b>
<b>CONCLUSIONS.....</b>	<b>109</b>
7.1 SPATIOTEMPORAL ANALYSIS OF RAINFALL.....	109
7.2 TREND ANALYSIS OF RAINFALL AND GROUNDWATER LEVELS....	111
7.3 GROUNDWATER LEVEL PREDICTIONS.....	112
7.4 LIMITATIONS AND SCOPE FOR FUTURE RESEARCH.....	113
APPENDIX 1.....	115
APPENDIX 2.....	121

APPENDIX 3.....	141
APPENDIX 4.....	141
APPENDIX 5.....	153
REFERENCES.....	165
PUBLICATIONS.....	181
BIODATA.....	182

## LIST OF FIGURES

<b>Table</b>		<b>Page</b>
<b>No.</b>	<b>Figure Caption</b>	<b>No.</b>
3.1	Location map of the study area indicating major basins: 1- Bhatsol and others, 2- Vasishti and others, 3- Netravati and others, 4- Varrar and others, and 5- Periyar and others.	14
3.2	Location of observation wells, rainfall and temperature grids	16
4.1	Average rainfall totals of the west coast basins during 1950~2017.	22
4.2	Coefficient of variation (CV) for annual and seasonal rainfall (1950~2017).	23
4.3	Departures of annual rainfall from 1950 to 2017. The red-line indicates 10-year moving average	25
4.4	Departures of winter rainfall from 1950 to 2017. The red line indicates 10-year moving average	28
4.5	Departures of pre-monsoon rainfall from 1950 to 2017. The redline indicates 10-year moving average	31
4.6	Departures of south-west monsoon rainfall from 1950 to 2017. The red-line indicates 10-year moving-average	35
4.7	Departures of post- monsoon rainfall from 1950 to 2017. The red-line indicates 10-year moving-average	38
4.8	Wavelet power spectrum of annual rainfall.	41
4.9	Wavelet power spectrum of winter rainfall.	43
4.10	Wavelet power spectrum of pre-monsoon rainfall	45
4.11	Wavelet power spectrum of south-west monsoon rainfall.	47
4.12	Wavelet power spectrum of south-west monsoon rainfall	49

5.1	Rainfall trends for a) annual, b) southwest monsoon, c) pre-monsoon, d) winter and e) post-monsoon by mMK and SE	65
5.2	Test power analysis of mMK with varying position, scale, and shape parameters	73
5.3	SSA extracted annual rainfall trends at selected sample grids	79
5.4	SSA extracted winter rainfall trends at sample selected grids	81
5.5	SSA extracted pre-monsoon rainfall trends at sample selected grids	82
5.6	SSA extracted southwest monsoon rainfall trends at sample selected grids	83
5.7	SSA extracted post-monsoon rainfall trends at sample selected grids	84
5.8	mMK and SE trends of seasonal groundwater levels	86
5.9	SSA extracted post-monsoons GWL (PMGWL) trends for sample wells	89
6.1	Basin-wise violin plots for R2 of ANN and SVM models	103
6.2	Basin-wise violin plots for RMSE of ANN and SVM models	104
6.3	Basin-wise distribution map of R2 testing for ANN and SVM models	105

## LIST OF TABLES

<b>Table No.</b>	<b>Table Caption</b>	<b>Page No.</b>
3.1	The west coast river basins	14
4.1	India Meteorological Department (IMD) classification of rainfall regimes based on percentage departures (D%).	18
4.2	Basin-wise annual rainfall (mm) statistics for 68 years (1950~2017)	20
4.3	Basin-wise seasonal rainfall (mm) statistics during 1950~2017	21
4.4	Annual rainfall departures from 1950 to 2017. LE – large excess, E – excess, D – deficit, S – scanty rainfall years	26
4.5	Winter rainfall departures from 1950 to 2017. LE – large excess, E – excess, D – deficit, S – scanty rainfall years, NR – no rainfall years	29
4.6	Pre-monsoon rainfall departures from 1950 to 2017. LE – large excess, E – excess, D – deficit, S – scanty rainfall years	32
4.7	Southwest monsoon rainfall departures from 1950 to 2017. LE – large excess, E – excess, D – deficit, S – scanty rainfall years	36
4.8	Post- monsoon rainfall departures from 1950 to 2017. LE – large excess, E – excess, D – deficit, S – scanty rainfall years	39
5.1	Basin-wise mMK and SE trends of annual and seasonal rainfall	64
5.2	Grid-wise Mmk and SE trends of annual and seasonal rainfall	66
5.3	ML estimated GEV parameters for annual rainfall time series	74
5.4	Seasonal groundwater level (GWLs) trends by mMK and SE	87
6.1	RMSE metrics of ANN and SVM models for testing phase	97
6.2	R2 metrics of ANN and SVM models for testing phase	97
6.3	Basin-wise R2 (testing phase) metrics of ANN1 models	99

6.4	Basin-wise R2 (testing phase) metrics of ANN2 models	99
6.5	Basin-wise RMSE (testing phase) metrics of ANN1 models	100
6.6	Basin-wise RMSE (testing phase) metrics of ANN2 models	100
6.7	Basin-wise R2 (testing phase) metrics of SVM1 models	101
6.8	Basin-wise R2 (testing phase) metrics of SVM2 models	103
6.9	Basin-wise RMSE (testing phase) metrics of SVM1 models	103
6.10	Basin-wise RMSE (testing phase) metrics of SVM2 models	103

## INTRODUCTION

---

---

### 1.1 GENERAL

India occupies about 4% of land globally and accounts for 24% of world population, while accredited with greater than 30% of total irrigated area world-wide (FAO 2013). Between 2000 and 2010, global ground water depletion for irrigation rose, with India accounting for 23% of the increase (Dalin et al. 2017). Even in rain-fed areas, weak Indian summer monsoons leads to greater groundwater extraction for agriculture and thereby resulting in aquifer level depletion. The average yearly precipitation of India has decreased approximately from 4000 billion cubic meters (BCM) (CWC 2005) to 3566 BCM (CWC 2016) over ten years. Decreasing rainfall trends can adversely affect the groundwater systems by reducing the recharge, groundwater levels, and discharge, thereby propagating into groundwater droughts. Declining groundwater levels can be an indicator of depletion in the storage (Mishra and Singh 2010). Therefore, it is imperative to assess the impact of climate change on India's rainfall regimes, owing to the monsoon-driven seasonality in the annual rainfall, geographical complexity, growing population, and varied climatic zones.

### 1.2 SCOPE OF STUDY

India has been enlisted among the most vulnerable drought-prone countries globally due to an increased frequency of widespread drought occurrences since the mid-nineties. Over the last five decades, drought has been reported once in every three years (Mishra and Singh 2010). Being an agriculture-based country, the southwest monsoons (June to September) play a significant role in the social and economic stability, meeting agricultural, industrial and domestic water demands in India through surface and groundwater resources. Studies have shown that out of 36 meteorological sub-divisions, three regions including Kerala indicated significant decline in southwest monsoon rainfall (Guhathakurta and Rajeevan 2008). Rainfall variations have been reported along the west coast of India by Preethi et. al. (2017). Increasing rainfall trends in northern region and declining trends in the southern region from 1970 to 2014 was reported in the study. Under this context,



assessment of rainfall variabilities and spatial cum temporal pattern along the west coast is inevitable for strategic planning and management of existing water resources.

Though blessed with numerous rivers, easy access to private well construction, cost and maintenance problems related to surface water irrigation systems, absence of stringent water policies etc., paves way for groundwater withdrawals at an alarming rate. With a growing population, water demand from groundwater reserves increases, resulting in the declining water table and seawater intrusion. This scenario becomes more adverse under changing rainfall patterns associated with climate change. A fall of more than 2m in the decadal water table has been reported in the states of Kerala (CGWB, 2019a), Karnataka (CGWB, 2019b), and coastal districts of Maharashtra (CGWB 2019c). The groundwater development stage has crossed approximately 50% in the coastal region (CGWB, 2018), and a decline in groundwater availability is reported (Shaji et al., 2008). Recent years have witnessed an increase in the deepening of dug wells and a hike in private bore well construction (CGWB, 2013).

Though numerical models have proven to be efficient in examining the groundwater flow processes, uncertainty/lack of hydro-geological, meteorological and topographical data, along with the computational cost has resulted in extensive application of machine learning approaches in sub-surface hydrology. Recent decades have witnessed the machine learning approaches gaining momentum in hydrology and groundwater level (GWL) prediction studies. The present study therefore, attempts to close this gap by examining the rainfall variations among the west coast basins of India, as well as investigate the feasibility in applying machine learning techniques to efficiently the groundwater levels in the west coast region of India.

### **1.3 RESEARCH OBJECTIVES**

1. Comprehensive analysis of rainfall regimes and trends in understanding the rainfall patterns in the region.
2. Regional-scale assessment of spatio-temporal variations in the groundwater levels of the west coast basins of India.
3. Evaluation of the applicability of artificial neural network (ANN) models in achieving the intended purpose of regional-scale groundwater level predictions over spatially, hydro-geologically and meteorologically heterogenous hard-rock regions of the west coast basins of India.
4. Assessment of the predictive capacity of support vector machines (SVM) models for regional-scale groundwater level predictions and establishing a comparative assessment with the ANN models.

### **1.4 ORGANIZATION OF THESIS**

The thesis report comprises of seven chapters as enlisted below:

- Chapter 1 (Introduction) presents the general overview of the study and the research objectives.
- Chapter 2 (Literature Review) briefs about the past research and understanding on the rainfall and groundwater studies.
- Chapter 3 (Study Area) presents the details of the study area and the data used in this research.
- Chapter 4 (Rainfall Analysis) describes the rainfall distribution, departures and the periodicities of rainfall at annual and seasonal scales in the west coast basins of India.
- Chapter 5 (Trend Analysis) deals with the trend detection studies on rainfall and groundwater levels at annual and seasonal scales.
- Chapter 6 (Groundwater level predictions) consists of groundwater level prediction studies employing Artificial Neural Network (ANN) and Support Vector Machines (SVM).
- Chapter 7 (Conclusions) presents the summary and key findings from the present research.



### LITERATURE REVIEW

---

#### 2.1 GENERAL

Water scarcity is one of the challenges faced by developing countries like India, owing to the growing population, increasing suburban and urban communities, climate change effects, and lack of prompt regulatory guidelines (Vörösmarty et al. 2010). Easy accessibility to high-yielding aquifers, increased private well construction, initial cost and maintenance challenges in public water supply from surface water resources, and deteriorating water quality in the rivers due to pollution has led to over-exploitation of groundwater resources (Mohanavelu et al. 2020). Over the past decades, a surge in climate change studies indicated the changing rainfall patterns over the Indian subcontinent. Anthropogenic stresses combined with climate change can threaten India's socio-economic stability and food security. Efficient monitoring and prediction can aid in the sustainable management and allocation of existing groundwater reserves for future socio-economic growth and bio-diversity conservation.

Over the years, physically-based numerical models have been utilized for groundwater level simulation and predictions. Despite their popularity, a lack of accurate data on hydrogeology, abstraction, aquifer recharge, etc., could lead to incorrect estimates. In this context, recent decades have witnessed a growing quantum of research on the feasibility of applying data-driven models for hydrological predictions. Despite their flaws and being termed as “black box” models, past literature has revealed the ability of machine learning models in hydrology prediction studies.

#### 2.2 RAINFALL STUDIES IN THE PAST

Climate change has now been identified as a potential threat to Earth, affecting the hydrological cycle's environmental dynamics and various drivers. Numerous studies have assessed the impact of climate change on multiple components of the hydrological cycle (Bothale and Katpatal 2016; Ramos et al. 2020). Subsequently, precipitation and temperature distribution changes have been addressed globally with varying scenarios and

catchment types (Krishnakumar et al. 2009; Sheikh et al. 2015; Bisht et al. 2018;). In context to rising global concerns over the impacts of climate change (IPCC 2007), numerous studies investigating the trends in hydrological variables have been carried out by researchers employing different stochastic and statistical methods (Caloiero et al. 2011; Masih et al. 2011; Hu et al. 2012; Beck et al. 2015; Jain et al. 2017; Zhang et al. 2019). The trend analyses have been extensively applied as a practical approach in investigating the patterns and trends of rainfall at multiple temporal and spatial scales (De Luís et al. 2000; Partal and Kahya 2006; Alijani et al. 2008; Zhang et al. 2008, 2009; Caloiero et al. 2011; De Luis et al. 2011; Liang et al. 2011; Ngongondo et al. 2011; Tabari and Talaei 2011; Coscarelli and Caloiero 2012; Thomas and Prasannakumar 2016).

In the recent past, investigations were carried out on the trends of annual and seasonal rainfall regimes in India at different spatio-temporal scales, employing various techniques and methodologies (Guhathakurta and Rajeevan 2008; Rajeevan et al. 2008; Mondal et al. 2015; Thomas and Prasannakumar 2016; Kothawale and Rajeevan 2017). Guhathakurta and Rajeevan (2008) have reported significant trends (both decreasing and increasing) for annual and southwest monsoon rainfall over India. An overall declining trend was observed over the entire India for annual and southwest monsoon rainfall despite few variations along with peninsular and West Central India for 141 years (Mondal et al., 2015). Increasing and declining rainfall trends were observed for a period of 115 years, from 1901 to 2015, over the meteorological sub-divisions of India before and after 1950, respectively (Praveen et al. 2020). Land use / land cover changes could be attributed as a primary factor behind the increasing trends in frequency and intensity of rainfall extremes in India, apart from sea surface temperature and main monsoonal wind strength (Falga and Wang 2022).

### **2.3 PAST LITERATURE ON GROUNDWATER STUDIES**

Recent years have witnessed increasing research linking groundwater dynamics to climate change (Chen et al. 2004; Panda et al. 2007; Vaux 2011; Kuss and Gurdak 2014; Tirogo et al. 2016; Smerdon 2017). Relationships between historic climatic variables and long-term groundwater levels have been established across the globe (Jan et al. 2007; Panda et al. 2007; Shahid and Hazarika 2010; Weider and Boutt 2010; Tabari et al. 2012; Chen et al. 2016; Whittemore et al. 2016; Le Brocque et al. 2018;). Several studies have identified a significant relationship between long-term groundwater levels and teleconnection

patterns driven by El-Nino Southern Oscillation (ENSO) and North Atlantic Oscillation (NAO) in England (Holman et al. 2011), Canadian Prairies (Perez-Valdivia et al. 2012), west coast and central United States (Whittemore et al. 2016; Velasco et al. 2017) and European region (Rust et al. 2018). While long-term groundwater level responses could be attributed to the periodicity of teleconnection patterns, seasonal variability can be related to local precipitation and evapotranspiration, besides anthropogenic activities (Holman et al. 2011).

A substantial number of studies have employed the non-parametric Mann-Kendall test for trend detection of long-term groundwater levels (Shamsudduha et al. 2009; Panda et al. 2012; Daneshvar Vousoughi et al. 2013). A mixed trend in groundwater levels was obtained for agricultural areas worldwide. In the Mazandaran province of Iran, it was attributed to changes in temperature and relative humidity (Tabari et al. 2012). Significant declining trends in the long-term groundwater levels were observed in Ardabil plains, Iran (Daneshvar Vousoughi et al. 2013). Precipitation was the influencing factor responsible for declining groundwater levels compared to evapotranspiration and streamflow in eastern China (Yan et al. 2015). Increased precipitation intensity in New England, causing higher runoff, was related to negative groundwater level trends despite increased mean and annual precipitation (Shanley et al. 2016).

Inter-annual rainfall variations were responsible for the groundwater level trends observed in Burkina Faso, West Africa (Tirogo et al. 2016). Extreme rainfall during wet years was not sufficient to offset the magnitude of severe declining trends in the groundwater levels due to the preceding dry years in the agricultural catchment of southern Queensland, Australia (Le Brocque et al. 2018). Besides human-induced activities, climate change involving rainfall and evapotranspiration contributed to the driving forces causing the groundwater decline in Northwest China (Li et al. 2020). Though anthropogenic activities aggravate the groundwater decline, the precipitation anomalies can be a significant factor influencing the regional hydrological cycle on an interannual timescale (Eltahir and Yeh 1999).

Groundwater level trends have been investigated by many researchers in various parts of India; the declining trends in groundwater levels have been attributed to variability in rainfall, recurrent droughts, extremes in rainfall and temperature, increased extraction (Panda et al. 2007, 2012; Thakur and Thomas 2011; Krishan et al. 2014; Pophare et al. 2014; Kumar et al. 2018) and increased irrigation area attributed to power subsidy (Sishodia et al. 2016). Prominent declining groundwater level trends were indicated in the drought-

prone Ghataprabha basin of Karnataka (Pathak and Dodamani 2019). The study also emphasized the relationship linking meteorological and groundwater droughts using copula methods. The association between climate variability and land use/landcover changes on the groundwater trends in major urban cities of India was analyzed by Mohanavelu et. al. 2020. A Gravity Recovery and Climate Experiment (GRACE) study on groundwater anomaly by Asoka et al. (2017) from 2002 to 2013 indicated a significant declining trend of 2cm per year in the major areas of north India and northeast India. Tiwari et. al. (2011) reported a rise in groundwater tables after 2005 in many parts of southern India. Survivor bias-based groundwater stress information based on a percentage of dry wells or defunct wells would yield vital information on the groundwater recovery in south India (Hora et al. 2019).

Chatterjee et. al. (2020) reported significantly declining post-monsoon groundwater levels in contrast to pre-monsoon season in the Murshidabad district of West Bengal. The disparity in the recharge-discharge process owing to the over-exploitation of groundwater resources was accredited for the declining groundwater levels. A reduction of 20% in the cropping intensity nation-wise could be expected under the groundwater depletion scenario in India (Jain et. al. 2021). Substitution of groundwater irrigation by surface irrigation systems may not offset the cropping intensity reduction due to yearly rainfall regime variability. Shallow-depth groundwater displayed faster responses than deeper groundwater to global climatic responses in the Indus-Ganges-Brahmaputra-Meghna (IGBM) aquifer system. Unsustainable groundwater abstraction in the IGBM basin was the primary factor influencing groundwater level changes in the basin system (Malakar et. al. 2021). A substantial decline in the depth to groundwater levels during the pre-monsoon and post-monsoon season was identified in the districts of Jharkhand from 1996 to 2018 by Swain et. al. (2022). Groundwater level studies conducted across various parts of India at varying spatial scales have primarily indicated declining levels for pre-monsoon and/or post-monsoon seasons in recent decades. Most studies have linked the decline to either changing rainfall/abstraction/land use land cover, / increased private well construction for agriculture/ or a combination of above-stated factors.

## 2.4 MACHINE LEARNING BASED GROUNDWATER LEVEL PREDICTIONS

Monthly groundwater level (GWL) simulations using different artificial neural network (ANN) models using GWL, temperature and precipitation as input parameters were conducted by Coulibaly et al. (2001) in the Gondo aquifer, Burkina Faso. The results qualified recurrent neural network (RNN) as the best model compared to radial basis function (RBF)-ANN and static structure input delay ANN. Feed-forward neural network (FNN) with Levenberg- Marquardt (LM) algorithm proved to be the best model for forecasting monthly GWL in the island of Crete, Greece using precipitation, past GWL, temperature and river discharge as input variables (Daliakopoulos et al. 2005). FNN model with LM algorithm was found efficient in simulating monthly GWL in Tabriz aquifer, Iran (Nourani et al. 2008) and Messara Valley, Crete, Greece (Tsanis et al. 2008). FNN-GWL simulations indicated that groundwater abstraction for agriculture was the primary driver resulting in declining GWLs in the Shiyang river basin, China, from FNN GWL simulations. Antecedent GWLs at different time intervals were used as predictor variables for simulating monthly GWLs in western Jilin province, China by ANN and integrated time series (ITS) models. ANN model was found to be superior to ITS models (Yang et al. 2009). A monthly average GWL of ten wells were employed as input for simulating the output GWL of an individual well in southern Taiwan by Chen et al. (2011) by combining self-organizing maps (SOM) with backpropagation (BP)-ANN. The study highlighted the predictive accuracy of multi-site SOM-BP-ANN compared to single ANN and Auto-Regressive Integrated Moving Average (ARIMA) models.

The study conducted by Trichakis et al (2011) in the karstic Edward's aquifer (USA), using the multi-layer perceptron (MLP), indicated that pumping rate information from individual wells was vital for simulation daily GWLs in Karstic aquifers. Even though data-driven models are associated with drawbacks such as low-generalization issues, overtraining, using irrelevant predictor variables and tuning parameters, extensive data requirement by the conventional models have urged the researchers to employ machine learning models in groundwater quantity as well as quality predictions (Rajaei et al. 2019). The adaptive neuro-fuzzy inference system (ANFIS) proved superior to ANNs for GWL predictions in Mashhad plain, Iran (Shirmohammadi et al. 2013) and Langat Basin, Malaysia (Khakhi et al. 2015). Past GWL was the prime predictor in simulating the GWLs in a coastal aquifer of south Korea, apart from rainfall and tidal height by support vector machines (SVM) models (Yoon et al. 2011).



A significant amount of research was conducted in India for GWL predictions employing machine learning models as well. Nayak et al. (2006) studied the utility of applying ANN in efficiently predicting GWLs in the Godavari delta system. Krishna et al. (2008) examined the utility of various training algorithms in simulating monthly GWLs using ANN models in a coastal aquifer in Andhra Pradesh. The Levenberg- Marquardt (LM) algorithm was found efficient compared to Bayesian regularization and radial basis function (RBF) training algorithms. Banerjee et al. (2009) simulated the monthly GWL in four wells in the Kurmapally watershed, Hyderabad, using the FNN-LM model by varying recharge and pumping conditions. The adaptive learning rate back-propagation (GDX) algorithm was observed as superior to the Bayesian regularization (BR) algorithm and LM for simulating weekly GWL simultaneously for 18 wells in a humid tropical area in eastern India (Mohanty et al. 2015). The study considered antecedent weekly GWL of 18 wells, pan evaporation, the water level in the drain, rainfall, abstraction rate from 18 wells, and river stage as input variables, developing an FNN model with 40 input nodes and 18 output nodes. Wavelet-SVM models were efficient in forecasting GWLs in the urbanized city of Vishakhapatnam, compared to ANN and auto-regressive moving average (ARIMA) models (Suryanarayana et al. 2014). Mukherjee and Ramachandran (2018) used Gravity Recover Experiment (GRACE) satellite-terrestrial water storage (TWS) in addition to rainfall, temperature, wind and humidity for GWL predictions. The study indicated that the SVM model outperformed ANN and linear regression models; furthermore, TWS data served as a prime factor in model simulations. ANN models were superior to multiple linear regression (MLR) models for GWL predictions in a basin in Japan (Sahoo and Jha 2014). The emotional artificial neural network coupled with genetic algorithm (EANN-GA) was effective in comparison to the emotional artificial neural network (EANN), generalized regression neural network (GRNN), and the conventional feedforward neural network (FFNN) for groundwater level predictions in a coastal aquifer using tidal height, rainfall and groundwater levels as predictors (Roshni et al. 2020). The deep neural network (DNN) model was found to be relatively superior to ANFIS and support vector machines (SVM) models in predicting regional groundwater levels at 18 agro-climatic zones of India (Mohapatra et al. 2021).

## **2.5 PROBLEM FORMULATION**

Numerous studies have analyzed the trends and spatio-temporal variations of rainfall and groundwater at varying scales across India. However, a comprehensive analysis of the rainfall and groundwater level studies over the west coast of India was not attempted in the past. The present study investigates the spatio-temporal patterns of rainfall and groundwater levels on a regional scale over the west coast basins of India. Past literature established the utility of machine learning (ML) models in capturing the complex dynamics of groundwater flow and has been extensively applied in sub-surface hydrology studies. Most studies have relied on the performance statistics from a small-scale in-situ prediction model. However, limited studies have attempted to examine the applicability of Artificial neural networks (ANN) and other ML approaches to regional-scale GWL predictions (Mohapatra et al. 2021). The accountability of ML approaches in performing GWL predictions over a large scale helps to build confidence in ML as a suitable candidate for regional-scale GWL predictions under data-scarce conditions. The present study, therefore, attempts to close this gap by examining the feasibility of applying ML algorithms to regional-scale GWL predictions encompassing in-situ measurements from spatially and meteorologically heterogeneous hard-rock region of the west coast basins of India using seasonal groundwater datasets. The application of ML to an extensive collection of spatially heterogeneous wells in the study area is the first of its kind.



#### 3.1 STUDY AREA

The study area (Fig. 3.1) comprises the west coast river basins of India, encompassing the river basins of west-flowing rivers south of the Tapi river, as defined by the Central Water Commission, Ministry of Water Resources, Govt. of India. The basin has an area of 1,12,117sq. km. stretched between 8.7°N and 21°N latitude, 73° 0' E to 77° 30' E longitude having approximately 3.41% of the country's total geographical area. The region covers parts of Gujarat, Maharashtra, Dadra & Nagar Haveli, Goa, Daman & Diu, Karnataka, Kerala, Puducherry, and part of Tamil Nadu states. The rivers originating in India's Western Ghats drain into the Arabian Sea. Bhatsol, Vasishti, Netravati, Chaliyar, and Periyar are among the major rivers of the west coast basin. Accordingly, the entire area is sub-divided into five major basins by the Central Water Commission (Ministry of Water Resources, Govt. of India) as sub-basin of Bhatsol and others (coastal regions of Gujarat and Maharashtra), sub-basin of Vasishti and others (Konkan and Goa coast), sub-basin of Netravati and others (coastal Karnataka and north Kerala), sub-basin of Varrar and others (Central Kerala and part of Puducherry state) and sub-basin of Periyar and others (south Kerala and parts of Tamil Nadu). The basin-wise areal distribution and the major rivers flowing through them are given in Table 3.1. The region cover major cities such as Navsari, Valsad, Thane, Mumbai, Panaji, Udupi, Mangalore, Calicut, Cochin, Trivandrum, and Kanyakumari. The region falls under the Humid to Per-humid climatic zone according to the Thornthwaite classification (1948). The average annual maximum and minimum temperatures range from 35°C to 41.5°C and 6°C to 12°C, respectively (Mudbhatkal et al. 2017).

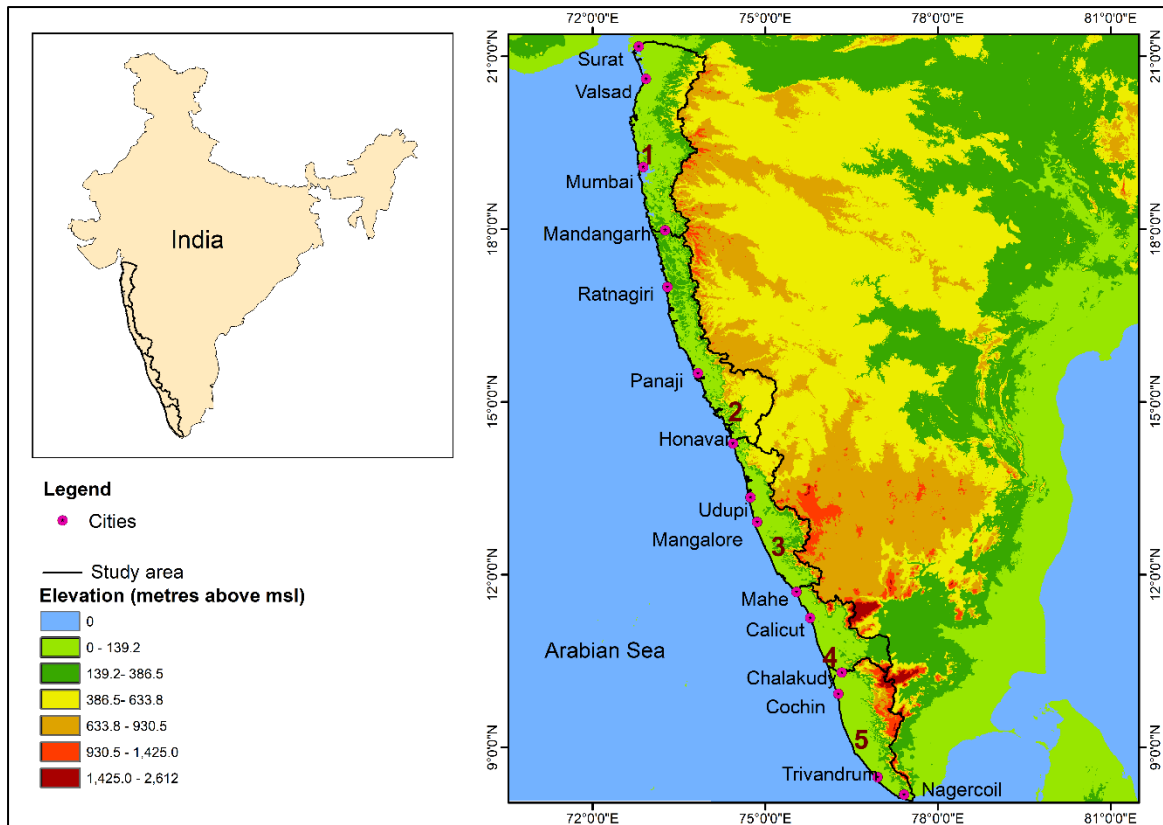


**Fig. 3.1** Location map of the study area indicating major basins: 1- Bhatsol and others, 2- Vasishti and others, 3- Netravati and others, 4- Varrar and others, and 5- Periyar and others.

**Table 3.1. The west coast river basins**

Basins	Area (sq.km)	Major rivers
Bhatsol	29,348.90	Purna, Ambika, Damanganga, Savitri, Bhatsai, Vaitarna, Ulhas, Amba and Kundalika.
Vasishti	27,473.95	Vasishti, Kajvi, Vaghotan, Gad, Mandavi, Gangavali (Bedti), Tadri and Varahi.
Netravati	18,762.09	Sharavati, Haladi, Sita, Gurpur, Netravati, Shiriya, Chandragiri, and Valapattanam
Varrar	14,164.70	Mahe, Kuttiyadi, Chaliyar, Kadalundi, and Bharathapuzha.
Periyar	21,895.21	Chalakuadi, Periyar, Muvattupuzha, Minachil, Manimala, Pamba, Achankovil, Attingal, Neyyar Vamanapuram and Tambraparani

Note: For convenience, the basins are referred to without “others” phrase.

The Indian monsoon consisting of the southwest monsoon (June –September) and northeast monsoon (October - December), is the most crucial factor influencing the regional water balance. The monsoon rainfall meets the population's agricultural and water supply demands across the coastal districts of Tamil Nadu (Kanyakumari), Kerala, Karnataka, Goa, Maharashtra, and Gujarat. The land-use/land cover change has affected the region's numerous river regimes, affecting the available surface water resources (Mudbhatkal et al. 2017).

Southern peninsular India, including the west coasts basins, consists of crystalline hard rock aquifer systems. Though hard rocks neither transmit nor hold water, fractured and weathered hard rocks form water-holding formations. The weathered zone includes the principal water-bearing aquifers, underlain by semi-fractured rock followed by bedrock. Major hydrogeological formations in the region are crystalline rocks consisting of Charnockites, Khondalites, Gneiss, and Schist. Alluvium and laterites are found along the river banks and valley regions (CGWB 2014). About 88% of the aquifer systems of Kerala are made of Charnockites, Khondalites, and Gneisses. Sedimentary formations are found along the western sides of the state. Weathered and fractured gneiss, granite, and schist are the major water-bearing formations along coastal Karnataka. Schist forms the major water-bearing formation in the state of Goa, along with beach sands and laterites. Coastal Maharashtra comprises of Basaltic rocks (Deccan traps) along with laterites and schist. Coastal Gujarat are underlain with igneous fissured formations. Groundwater in the weathered zone's form the shallow aquifers which is mainly under water table conditions and semi-confined to confined zones are observed in the fissures, cracks, and joints of the hard-rock deeper aquifers. Due to the hard-rock aquifer systems of peninsular India, the annual groundwater recharge is limited to 0.1m to 0.15m due to the crystalline rock formations' low infiltration and storage capacity in the region (CGWB 2019). Thus, groundwater replenishment may become challenging once the aquifers are over-exploited. The situation will worsen under varying rainfall patterns in context to the climate change scenario.

### **3.2 DATA USED**

Daily gridded precipitation ( $0.25^0 \times 0.25^0$ ) data and temperature data ( $1^0 \times 1^0$ ) from 1950-2017 were collected from the India Meteorological Department (IMD). The development of all India high-resolution gridded datasets and its comparison with the

existing datasets can be found elsewhere (Pai et al. 2014). Annual and seasonal rainfall analyses were carried out extensively on the study area, and the seasons are defined as per the India Meteorological Department as winter (January-February), pre-monsoon (March-May), southwestmonsoon (June-September), and post-monsoon (October–December). The seasonal groundwater levels for January (winter), May (pre-monsoon), August (southwestmonsoon), and November (post-monsoon) were obtained from the Central Ground Water Board (CGWB). The dataset consists of 418 monitoring wells with groundwater levels recorded for 22 years (1996-2017). The descriptive statistics, namely mean, standard deviation, and coefficient of variation, were determined for each rainfall grid and averaged over the basins on seasonal and annual time scales. The rainfall and temperature grids and the observation wells are presented in Fig. 3.2.

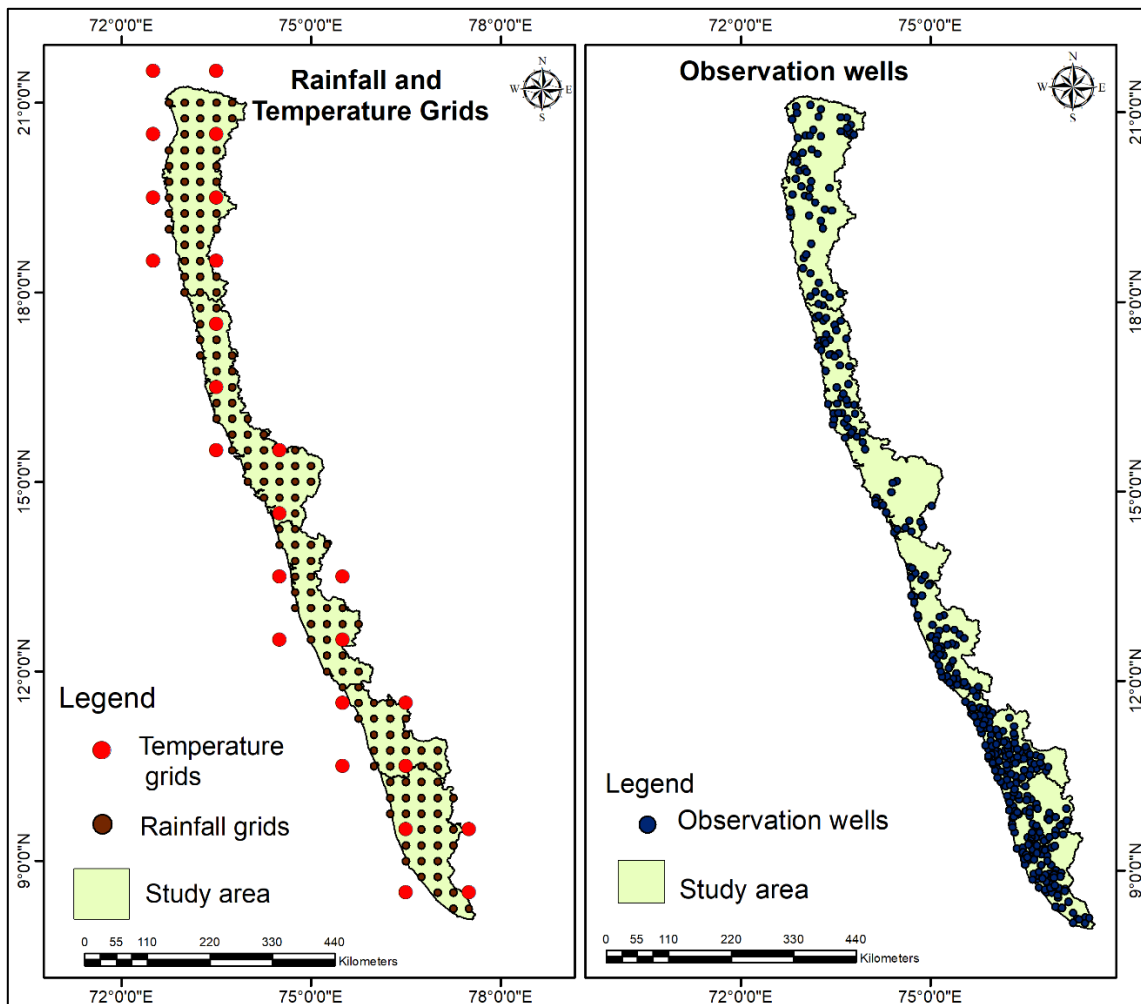


**Fig. 3.2. Location of observation wells, rainfall and temperature grids.**

**SPATIO-TEMPORAL ANALYSIS OF RAINFALL**

---

**4.1 INTRODUCTION**

The west coast basins receive large-scale precipitation primarily from southwest monsoon rainfall (Indian summer) from June to September and marginally from post-monsoon rainfall (Northeast monsoon) from October to December, along with meagre winter and pre-monsoon rainfall. Inter-annual and inter-decadal variability of the southwest monsoons were reported earlier on various spatial scales (Nair et al. 2018; Revadekar et al. 2018; Mishra et. al. 2022). In addition, the changing variability of northeast monsoon rainfall during recent decades has been a matter of concern (Nageswararao et al. 2019). Under the context of climate change, examining the rainfall patterns is vital, which may yield valuable information on the annual to decadal variabilities of rainfall regimes. Changing rainfall regimes could pose a detrimental impact on the region's water security and socio-economic stability. Information on rainfall departures and associated variabilities could assist in managing the existing water resources and adequately planning strategies for future consumption under the presumed risk of climate change. This chapter presents the departure and wavelet power spectrum analyses of the annual and seasonal rainfall for the west coast basins of India.

**4.2 METHODOLOGY****4.2.1 Departure Analysis (D%)**

The departure analysis (D%) was computed using Eq. (4.1).

$$D\% = \frac{X_i - X_m}{X_m} \times 100 \quad (4.1)$$



where  $X_i$  = precipitation for series  $i$  and  $X_m$  = mean annual precipitation (Thomas and Prasannakumar 2016). Since monsoon contributes predominantly (>80%) to the total annual rainfall, seasonal scale rainfall departures can provide better insights into the excess or deficit rainfall. The decade-wise percentage departure of yearly and seasonal rainfall and frequency of large excess, excess, deficit, scanty, and no rain years (Table 4.1) were obtained to understand the temporal patterns of rainfall in the study area.

**Table 4.1 India Meteorological Department (IMD) classification of rainfall regimes based on percentage departures (D%)**

Definition	Terminology
Large excess	Percentage departure of realized rainfall from normal rainfall is +60% or more
Excess	Percentage departure of realized rainfall from normal rainfall is +20% to +59%
Normal	Percentage departure of realized rainfall from normal rainfall is between -19% to +19%
Deficit	Percentage departure of realized rainfall from normal rainfall is between -20% to -59%
Scanty	Percentage departure of realized rainfall from normal rainfall is between -60% to -99%
No rain	Percentage departure of realized rainfall from normal rainfall is -100% or more

#### 4.2.2 Wavelet Power Spectrum Analysis

The wavelet analysis is a multi-resolution analysis decomposing a signal into time-frequency representations, enabling us to extract information on the frequency content's amplitude within the signal and its temporal variations (Guimaraes Santos et al. 2003). Unlike Fourier transforms, which account for the frequency content in the signal but fail to determine the time-frequency evolution, wavelet transform could be adopted for localized high-frequency events or contain scale-variable processes.

The timescale wavelet transformation is given as (Labat 2005):

$$W_{\psi}^x(a, \tau) = \frac{1}{\sqrt{a}} \int_{-\infty}^{+\infty} x(t) \psi^*\left(\frac{t - \tau}{a}\right) dt \quad (4.2)$$

where  $a$  = scale factor  $\tau$  = localization,  $t$  = time,  $x(t)$  = time-series signal and  $\psi^*$  = conjugate of the wavelet function  $\psi$ . The continuous wavelet transforms were performed to determine annual and seasonal rainfall periodicity using a Morlet wavelet, a continuous and complex-valued wavelet. Additionally, the Morlet wavelet function describes the shape of hydrological signals well and provides an optimum balance between time and frequency localization (Kumar and Foufoula-Georgiou 1997; Torrence and Compo 1998; Grinsted et al. 2004; Labat 2005; Kang and Lin 2007).

The Morlet wavelet function chosen for wavelet analysis is:

$$\psi(t) = e^{-i\omega_0 t} e^{(-t^2/2)} \quad (4.3)$$

where  $\psi(t)$  = wavelet function,  $i$  = imaginary symbol of a complex number;  $\omega_0$  = non-dimensional frequency ( $\omega_0 = 6$ ), and  $t$  = time.

## 4.3 RESULTS AND DISCUSSIONS

### 4.3.1 Spatio-Temporal Analysis of Rainfall

Comprehensive analysis of annual, seasonal and monthly scale rainfall totals was conducted to evaluate the spatial and temporal variations of rainfall along the west coast basins. The descriptive statistics for varying timescales of basin-wise historical (1950~2017) rainfall totals are given in Tables 4.2 & 4.3. The historical rainfall totals for annual ( $R_{AN}$ ), winter ( $R_{WN}$ ), pre-monsoon ( $R_{PRM}$ ), southwest monsoon ( $R_{SW}$ ) and post-monsoon ( $R_{POM}$ ), averaged over the basins are presented (Fig. 4.1 a-e) as violin plots which exhibit the central tendency as well as the kernel density of the basin-wise rainfall data distribution. For convenience, the basins are referred to without the “others” phrase throughout the chapter. Examination of historical data (1950~2017) indicates that the Netravati basin receives the highest average annual ( $\bar{R}_{AN}$ ) rainfall of 3702 mm and average southwest monsoon rainfall ( $\bar{R}_{SW}$ ) of 3169mm, while Varrar receives the minimum  $\bar{R}_{AN} = 2249$  mm and Periyar with minimum  $\bar{R}_{SW} = 1318$ mm. While average rainfall totals for post-monsoon ( $\bar{R}_{POM}$ ), winter ( $\bar{R}_{WN}$ ), and pre-monsoon ( $\bar{R}_{PRM}$ ) are found to be decreasing from south to north (Periyar to Bhatsol) (Fig. 4.1, Table 4.3).

The percentage contribution of southwest monsoon season to annual rainfall increases from south to north basins, with Periyar (58.14%), Varrar (70.28%), Netravati (85.63%), Vasishti (90.92%), and Bhatsol (95.48%) respectively (Table 4.3). This signifies that, in the study region, the contribution of non-monsoon rains decreases from south to north along the west coast. This is evident from the shape of peninsular India, which tapers off towards the south and receives a share of northeast monsoon rains. Periyar (23.65%) and Varrar (17.76%) receive a considerable amount of post-monsoon ( $R_{POM}$ ) from October to December compared to Netravati (8.35%), Vasishti (6.17%), and Bhatsol (3.77%) basins (Table 4.3). Winter rainfall contributes a meagre share to the west coast basin's annual rainfall budget (Table 4.3). Periyar and Varrar also receive higher pre-monsoon (summer) showers (16.35% and 11.27%, respectively) compared to other basins (Table 4.3). The seasonal rainfall distribution for the west coast basins are given in Appendix 1.

**Table 4.2 Basin-wise annual rainfall (mm) statistics for 68 years (1950~2017)**

Basins	Rainfall (mm)				
	Mean	SD	CV (%)	Minimum rainfall(mm)	Maximum rainfall(mm)
Periyar	2268	395	17	1392	3026
Varrar	2249	455	20	1265	3866
Netravati	3702	596	16	2528	6233
Vasishti	2995	460	15	1910	4043
Bhatsol	2500	456	18	1592	3446

Note: For convenience, the basins are referred to without the “others” phrase.

SD refers to Standard Deviation. CV corresponds to the Coefficient of Variation expressed in percentage (%).

**Table 4.3 Basin-wise seasonal rainfall (mm) statistics during 1950~2017**

Seasons	Rainfall (mm)	Basins				
		Periyar	Varrar	Netravati	Vasishti	Bhatsol
Winter (R <sub>WN</sub> )	Mean	42	15	5	1	0.9
	SD	35	17	8	5	1
	CV(%)	83	112	156	285	164
	Contribution to annual rainfall %	1.86	0.67	0.14	0.06	0.04
Pre-monsoon (R <sub>PRM</sub> )	Mean	370	254	217	85	17
	SD	126	104	118	68	23
	CV (%)	34	41	54	80	135
	Contribution to annual rainfall %	16.35	11.27	5.86	2.85	0.69
Southwest monsoon (R <sub>SW</sub> )	Mean	1318	1582	3169	2723	2387
	SD	315	414	573	443	450
	CV (%)	24	26	18	16	19
	Contribution to annual rainfall %	58.14	70.28	85.63	90.92	95.48
Post-monsoon (R <sub>POM</sub> )	Mean	536	400	310	185	94
	SD	150	124	102	87	64
	CV (%)	28	31	33	47	68
	Contribution to annual rainfall %	23.65	17.76	8.35	6.17	3.77

Note: For convenience, the basins are referred to without the “others” phrase.

SD refers to Standard Deviation. CV corresponds to the Coefficient of Variation expressed in percentage (%).

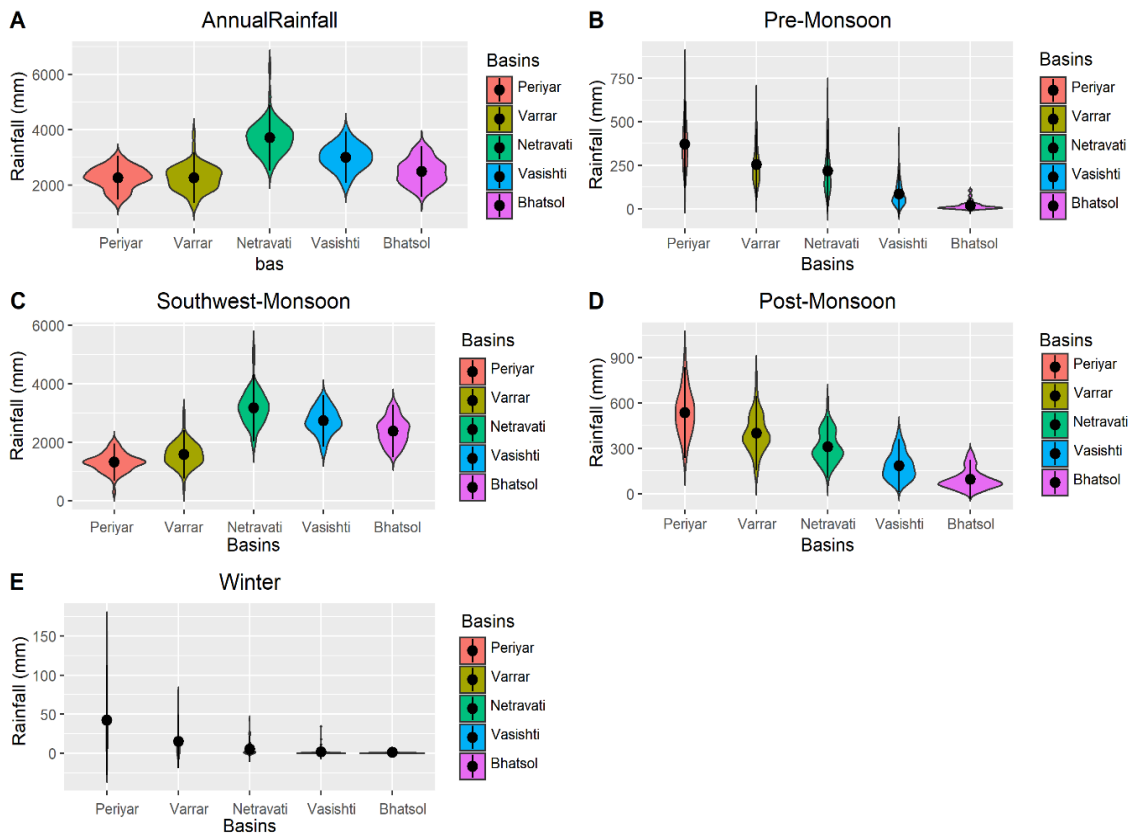


**Fig. 4.1 Average rainfall totals of the west coast basins during 1950~2017.**

### 4.3.2 Coefficient of variation (CV)

The spatial distribution of CV for annual and seasonal rainfall between 1950~2017 was explored and is presented in Fig. 4.2. The spatial variation in annual rainfall ( $R_{AN}$ ) from the seacoast to inland increases from 0.16 to 0.64.  $R_{AN}$  has the most minor variability in rainfall dispersion with the lowest CV of all seasons (Fig. 4.2). Distinct south-to-north pattern is visible for pre-monsoon and post-monsoon rainfall, with Periyar, Varrar, and Netravati basins showing relatively lesser variation than the north basins, ie. Vasishti and Bhatsol. The southwest monsoon rainfall showed a similar pattern to annual rainfall but with higher CV values. The results indicate the reliability of  $R_{SW}$  (with minor inter-annual variations) to other seasons in contributing to  $R_{AN}$ . Furthermore, any variations in the rainfall regimes, primarily comprising of southwest monsoons owing to climate change may alter the regional water balance over the study area.

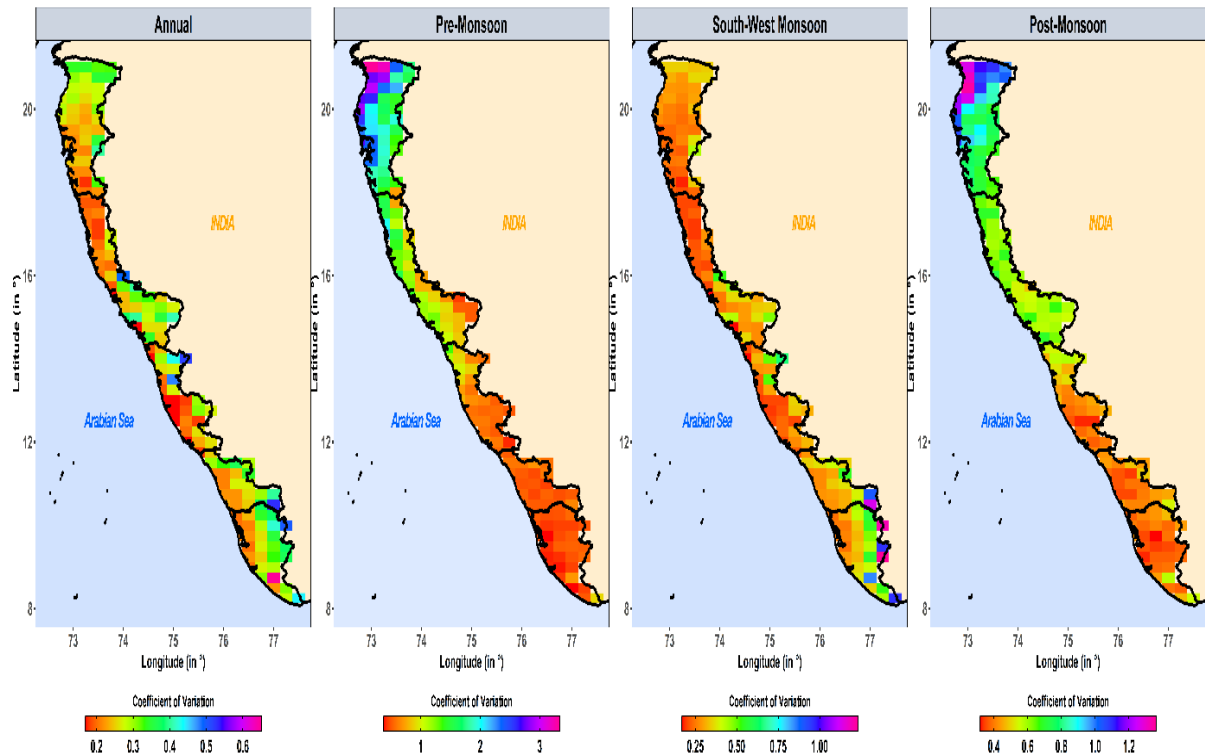


**Fig. 4.2 Coefficient of variation (CV) for annual and seasonal rainfall (1950~2017).**

### 4.3.3 Departure Analysis (D %)

The rainfall departures were examined to evaluate the year-wise distribution of rainfall amounts concerning the long-term normal for 68 years, from 1950 to 2017. Following the scheme from the India Meteorological Department (IMD) classification of precipitation distribution based on percentage deviation, D%, as given in Table 4.1., basin-averaged percentage departure of annual ( $R_{AN}$ ) and seasonal rainfall with the number of years having excess (E), large excess (LE), deficit (D), scanty (S) and no rain (NR) years along with the decadal mean are presented in Fig. 4.3 to Fig. 4.7 and Tables 4.4 to 4.8.

#### 4.3.3.1 Annual rainfall departures

Though deficit and excess years were observed throughout the period among the west coast basins, decadal variability in the rainfall regimes was observed from the departure analysis. The decade from 1980 to 1990 appeared to be the driest decade homogeneously for the entire region, owing to a greater number of below normal years as well as deficit years for the annual rainfall ( $R_{AN}$ ) as given in Fig. 4.3 and Table 4.4 except Vasishti basin wherein decades from 1960 to 1980 were the driest. The Bhatsol basin experienced both above and below- normal  $R_{AN}$  from 1950 to 2017 as given in Fig. 4.3. The basin experienced four excess years from 1950 to 1961, after which below- normal

years were greater in number from 1960 to 1990, in particular the decade from 1980 to 1990 with a decadal mean departure of -8% against a normal rainfall of 2500mm as given in Table 4.4. After the year 2002 frequency of above normal years for  $R_{AN}$  indicated a rise in the basin, though the year 2015 indicated a deficit year with -29.4% departure for  $R_{AN}$ .

Vasishti basin experienced wet years during the early decades from 1950 to 1960. However, the presence of any excess years was lacking (Fig. 4.3). Greater deficit years ( $D = 5$ ) compared to excess years ( $E=1$ ) were observed during the period from 1960 to 1990, with a decadal mean of -6.8% (1960~1969), -8.7% (1970~1979) and -0.9% (1980~1989). From 1990 to 1999, the basin experienced greater wet years and two excess years ( $E = 2$ ) with a decadal mean of +10.6%. Both above and below normal years were observed from 2000 to 2017 in the basin for  $R_{AN}$ , while the year 2015 marked a deficit year with a departure of -34.3% against a normal of 2995mm.

The Netravati basin indicated greater above normal years from 1950 to 1970  $\{(E = 2, LE = 1) > D=1\}$  with a decadal mean of +8.1% (1950~1959) and +2.7% (1960~1969). After the year 1980, the frequency of below normal years indicated a rise in the basin with greater deficit years ( $D =4 > E = 1$ ) during 1980 to 2017. A decadal mean of -4.5% (1980~1989), -6.1% (2000~2009) and -4.2% (2010~2017) were obtained for  $R_{AN}$  in the basin (Table 4.4). The later decades namely from 2000 to 2017, indicated a below normal  $R_{AN}$  phase for Netravati basin as given in Fig. 4.3 The years 1987, 2002 and 2016 indicated deficit departures of -31.7%, -24.7% and -28.1% respectively in the basin.

The  $R_{AN}$  distribution in the Varrar basin indicated above normal years in substantial numbers from 1950 to 1980  $\{(E = 7, LE = 1) > D = 0\}$ , with decadal mean of +13.4% (1950~1959), +9.5% (1960~1969) and +6.8% (1970~1979). From 1980 onwards, below normal years prevailed in the basin, with greater deficit years ( $D = 9$ ) than excess ( $E=1$ ) from 1980 to 2017, indicated with a decadal mean of -8.3% (1980~1989), -2% (1990~1999), -13.5% (2000~2009) and -7.4% (2010~2017) as given in Table 4.4. The shift in the rainfall departures could be clearly observed for the Varrar basin (Fig. 4.3) exhibiting positive decadal mean during early decades while negative mean decadal departures during the later decades. The basin experienced major deficit  $R_{AN}$  during 2003, 2005 and 2016 with departures of -37.3%, -40.8% and -43.7% respectively against a normal  $R_{AN}$  of 2249mm.

In the Periyar basin, above normal rainfall events occurred from 1950 to 1970 ( $D = 0 < E = 4$ ) with positive mean departures of +9.7% (1950-1959) and +9% (1960-1969) against a normal  $R_{AN}$  rainfall of 2268mm. From 1970 onwards, negative departures or in

other words, below normal rainfall years were observed in the basin ( $D = 12 > E = 2$ ) with decadal mean of -2.2% (1970-1979), -19% (1980-1989), -3.6% (2000-2009) and -1.5% (2010-2017) as given in Table 4.4. Among the deficit years, the years 1986, 2005 and 2016 experienced high departures of -38.7%, -37.6% and -31.3% against a normal  $R_{AN}$  of 2268mm. The decades 1980 ~ 1989 and 2000~2009 witnessed mostly negative departures for annual rainfall for the entire west coast basins (Table 4.4).

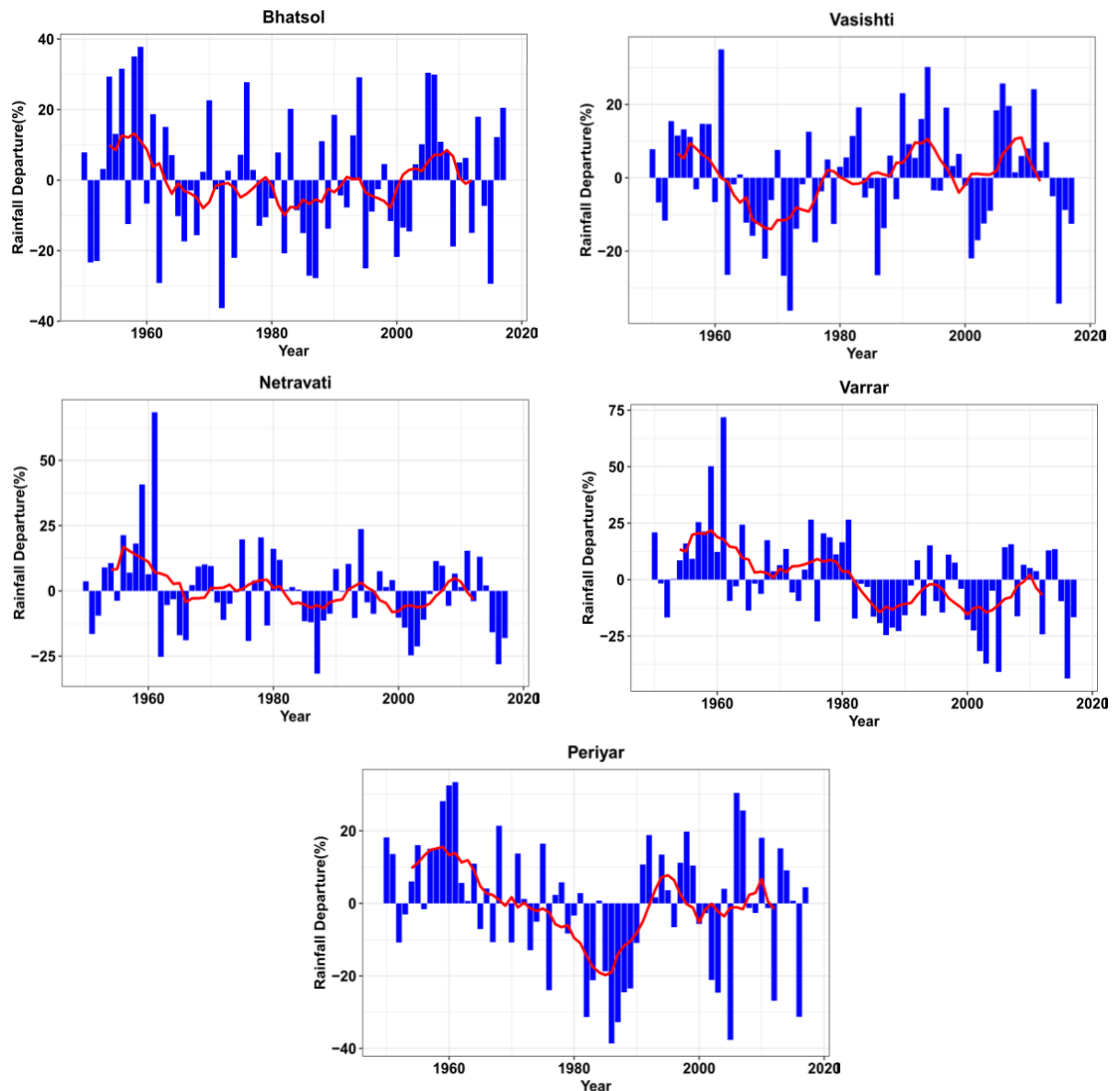


**Fig. 4.3** Departures of annual rainfall from 1950 to 2017. The red-line indicates 10-year moving average



**Table 4.4 Annual rainfall departures from 1950 - 2017. LE- large excess, E - excess, D- deficit and S -Scanty rainfall years.**

Decade	Periyar and Others			Varrar and Others				Netravati and Others				Vasishti and Others			Bhatsol and Others		
	Decadal mean D%	E	D	Decadal mean D%	E	LE	D	Decadal mean D%	E	LE	D	Decadal mean D%	E	D	Decadal mean D%	E	D
1950- 1959	9.7	1	0	13.4	4	0	0	8.1	2	0	0	6.7	0	0	9.9	4	2
1960-1969	9	3	0	9.5	1	1	0	2.7	0	1	1	-6.8	1	2	-3.8	0	1
1970-1979	-2.2	0	1	6.8	2	0	0	0.03	1	0	0	-8.7	0	2	-2.13	2	2
1980-1989	-19	0	6	-8.3	1	0	3	-4.5	0	0	1	-0.9	0	1	-8	1	3
1990-1999	7.2	0	0	-2	0	0	0	3.2	1	0	0	10.6	2	0	0.46	1	1
2000-2009	-3.6	2	3	-13.5	0	0	4	-6.1	0	0	2	0.85	1	1	2.53	2	1
2010-2017	-1.5	0	2	-7.4	0	0	2	-4.2	0	0	1	-2.11	1	1	1.28	1	1
Total		6	12		8	1	9		4	1	5		5	7		11	11

#### 4.3.3.2 Winter rainfall departures

Winter rainfall ( $R_{WN}$ ) exhibited inconsistent and unpredictable pattern throughout the study region as presented in Fig. 4.4. The Bhatsol basin experienced highly erratic  $R_{WN}$  with 46 deficit/scanty/no rainfall years ( $D = 3$ ,  $S = 25$  and  $NR = 18$ ) while 17 excess years ( $E = 2$  and  $LE = 15$ ) for a time period of 68 years against a normal of 1mm of rainfall as given in Table 4.5. The anomalous values of departures above 100% could be attributed to excess or large excess rainfall events, though a rainfall of 3mm was calculated to be excess  $R_{WN}$  against a normal of 1mm from 1950 to 2017.

Deficit and scanty winter rainfall years ( $D = 8$ ,  $S = 23$  and  $NR = 20$ ) were observed for Vasishti basin similar to Bhatsol as given in Table 4.5 and Fig.4.4. Only 13 excess years ( $E = 5$  and  $LE = 8$ ) were observed for  $R_{WN}$ , distributed mainly after the year 2000. Winter rainfall was observed to be irregular for the Netravati basin, with no rainfall ( $NR$ ) = 8, scanty ( $S$ ) = 25 and deficit ( $D$ ) = 16 (total = 49) compared to 16 excess years ( $E = 3$  and  $LE = 13$ ) out of 68-year time period analysed. The pattern is unreliable with sparse events of wet years (either excess or large excess) dispersed between long dry years. Relatively greater wet years were observed in the basin after the year 2000. The Varrar basin exhibited deficit ( $D$ ) = 12, scanty ( $S$ ) = 27 and no rainfall ( $NR$ ) = two years, while 18 excess years ( $E = 1$  and  $LE = 17$ ) were observed against a normal of 15.1mm of  $R_{WN}$ . The temporal variation in the  $R_{WN}$  for the basin is unreliable with events of excess years occurring in between the deficit/scanty years as presented in Table 4.5 and Fig.4.4.

The Periyar basin received meagre  $R_{WN}$  throughout the period from 1950 to 2017 with  $NR = 0$ . The basin received both wet ( $E = 11$  and  $LE = 14$ ) and dry ( $D = 19$  and  $S = 19$ )  $R_{WN}$  intermittently as given in Table 4.5 and Fig.4.4.

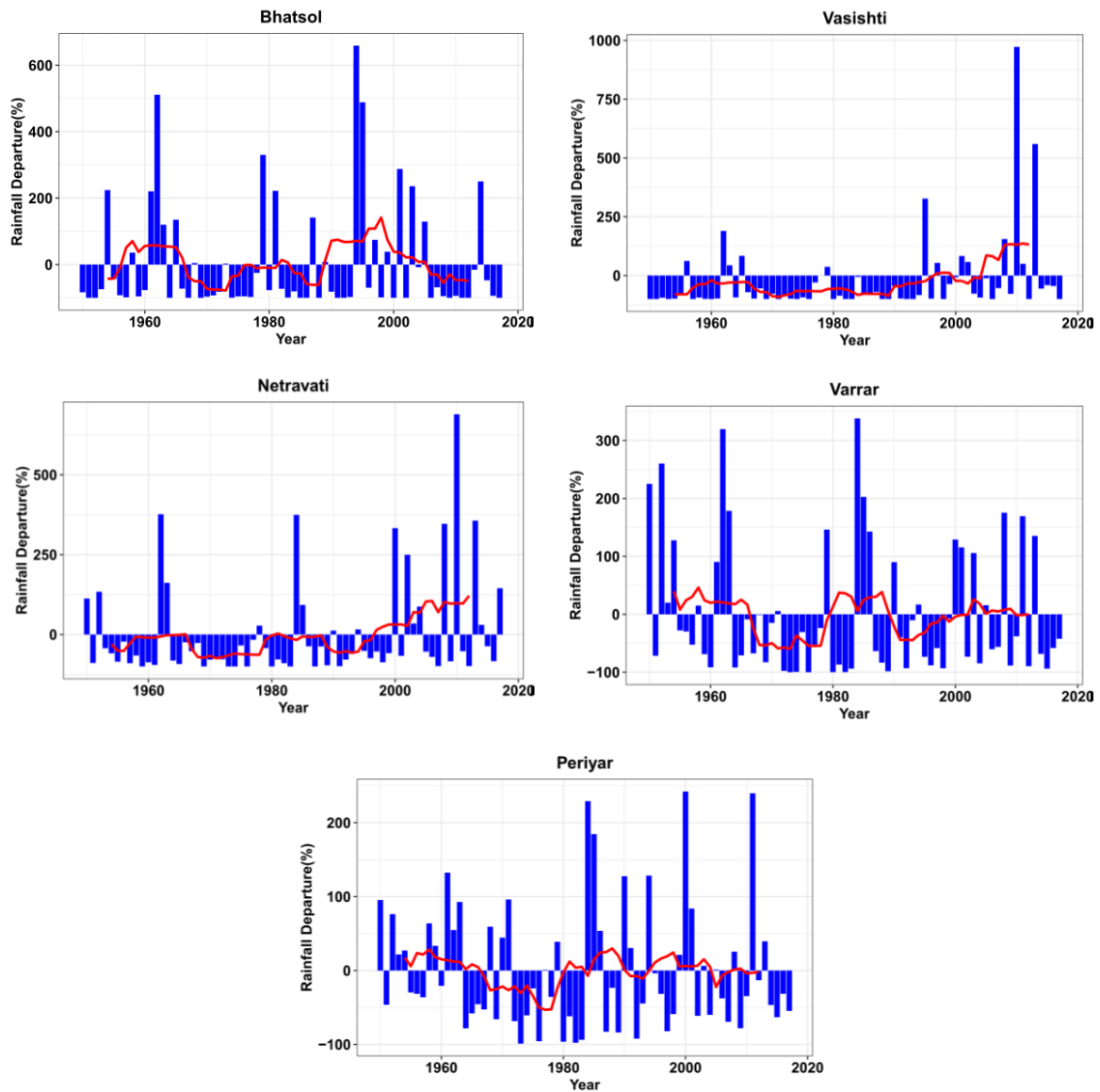


**Fig. 4.4** Departures of winter rainfall from 1950 to 2017. The red line indicates 10-year moving average

Table 4.5 Winter rainfall departures from 1950 to 2017. LE- large excess, E - excess, D- deficit, S -Scanty and NR -no rainfall years.

	Periyar and Others					Varrar and Others					Netravati and Others					Vasishti and Others					Bhatsol and Others								
	Decadal mean D %	E	LE	D	S	Decadal mean D %	E	LE	D	S	NR	Decadal mean D %	E	LE	D	S	NR	Decadal mean D %	E	LE	D	S	NR	Decadal mean D %	E	LE	D	S	NR
1950-1959	17.4	3	3	4	0	39.8	1	3	3	2	0	-30.7	0	2	3	4	1	-80.0	0	1	0	5	4	-42.7	1	1	1	5	2
1960-1969	1.8	1	3	4	2	17.5	0	3	0	5	0	-2.1	0	2	3	4	1	-29.8	1	2	1	4	2	54.2	0	4	0	2	3
1970-1979	-20.3	2	1	2	4	-36.7	0	1	3	2	2	-59.5	1	0	2	3	3	-64.9	1	0	1	4	3	-35.1	0	1	1	6	1
1980-1989	-7.2	1	2	1	6	5.8	0	3	0	7	0	-17.1	0	2	2	3	3	-82.6	0	0	0	4	5	-25.8	0	2	0	4	3
1990-1999	-0.6	2	2	3	2	-35.7	0	1	2	4	0	-53.3	0	0	3	5	0	-28.0	1	1	2	3	3	71.3	1	3	0	4	2
2000-2009	5.3	1	2	1	4	17.9	0	4	1	4	0	67.7	1	4	1	4	0	-12.5	1	2	1	3	1	8.1	0	3	0	2	4
2010-2017	4.5	1	1	4	1	-10.7	0	2	3	3	0	118.7	1	3	2	2	0	155.0	1	2	3	0	2	-37.6	0	1	1	2	3
Total		11	14	19	19		1	17	12	27	2		3	13	16	25	8		5	8	8	23	20		2	15	3	25	18

#### 4.3.3.3 Pre-Monsoon rainfall departures

The pre-monsoon rainfall ( $R_{PRM}$ ) exhibited spatial homogeneity relatively in percentage departures over the west-coast basins. Early decades from 1950-1970 experienced greater above-normal years spatially among the basins. Later decades from 1980-2000 exhibited increased deficit cum scanty years as indicated in Table 4.6, over the entire region. Interestingly, the decade from 2000 to 2010 experienced considerable positive departures among the five basins. The Bhatsol basin experienced positive  $R_{PRM}$  departures during the early decades with consecutive excess years from 1955-1962 ( $LE = 3$ , and  $E = 5$ ); the decade also experienced a large excess seasonal rainfall of 105mm in the year 1956 against a normal  $R_{PRM}$  of 17.3mm (1950~2017). The decades from 1970 to 2000 witnessed deficit cum scanty  $R_{PRM}$  events in substantial numbers except for large excess  $R_{PRM}$  during the years 1974 and 1990 as given in Table 4.6 and Fig.4.5. From the year 2000 onwards, both excess and scanty years were spread across the basin with positive departures prominent during 2000 to 2009 (decadal mean of +48.3% ), while negative departures during 2011 to 2017 (decadal mean of -23%).

A similar pattern was identified for the Vasishti basin with excess to large excess  $R_{PRM}$  ( $LE = 7$  and  $E = 1$ ) during the early decades from 1950 to 1970, with a large excess  $R_{PRM}$  of 231mm (year:1956) and 399mm (year: 1961) against a normal  $R_{PRM}$  of 85.9mm. Deficit cum scanty  $R_{PRM}$  years followed from 1970 to 2000  $\{(D = 14$  and  $S = 8) > E = 5\}$  except for a large excess  $R_{PRM}$  during 1970 (159mm) and 1990 (212mm). After the year 2000, the basin experienced both excesses and deficit years, with a positive decadal mean of +21.9% during 2000~2009 and a negative mean of -19.2% during 2010~2017 (Table 4.6 and Fig. 4.5).

Excess and large excess pre-monsoon rainfall were observed in the Netravati basin from 1950 to 1962 ( $LE = 5$  and  $E = 1$ ) with large excess rainfall of 486.2mm (year: 1955), 491.5mm (year:1956) and 633.4mm (year: 1961) against normal rainfall of 217.6mm. The deficit and scanty years were pronounced from 1980 to 1999  $\{(D = 12$  and  $S = 1) > (E = 2$  and  $LE = 1)\}$ . Both excess, as well as deficit years, were noticed in the basin during later decades, with a positive decadal mean of +20.5% during 2000~2009 and negative mean of -14.8% during 2010~2017 (Table 4.6 and Fig.4.5). Varrar basin experienced above normal  $R_{PRM}$  years during the early decades from 1955 to 1965 with events of large excess ( $LE = 4$ ) as well as excess ( $E = 4$ )  $R_{PRM}$  rainfall. Large excess seasonal rainfall of 599.4mm (year

:1955), 498.4mm (year: 1960) and 460.5mm(year : 1961) were observed in the basin against a normal of 253.8mm. From 1980 to 1999, below normal years with prominent numbers of deficit and scanty years were detected in the basin  $\{(D = 9 \text{ and } S = 2) > E=2\}$  as presented in Table 4.6 and Fig. 4.5 From 2000 onwards, below and above normal  $R_{PRM}$  years were observed in the basin with positive decadal mean of +8.8% (2000~2009) and -11.3% (2010~2017). Similar to other west coast basins, Periyar basin also witnessed above normal pre-monsoon rainfall with 6 excess and 2 large excess rainfall years between 1950 to 1970. Large excess rainfall of 635mm (year: 1956) and 767mm (year :1960) were observed in the basin. From 1970 to 1999, deficit and scanty rainfall years were prevalent in the basin with deficit (D) = 15 and scanty (S) = 1 while, excess (E) years= 4. From 2000 onwards, both positive and negative departures were observed in the basin for pre-monsoon rainfall with a decadal mean of +9.5% (2000~2009) and +1% (2010~2017).

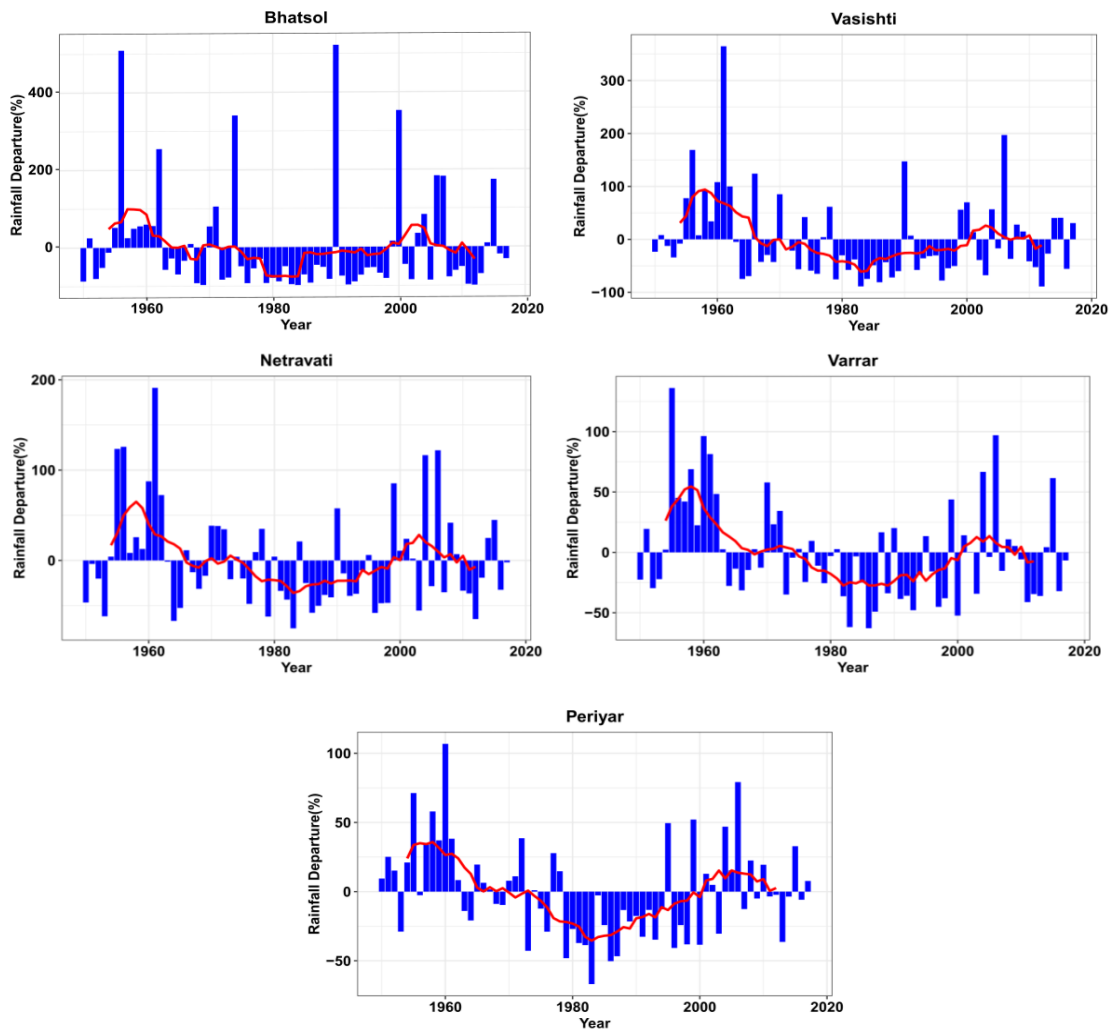


**Fig. 4.5 Departures of pre-monsoon rainfall from 1950 to 2017. The redline indicates 10-year moving average**

**Table 4.6 Pre-monsoon rainfall departures from 1950 to 2017. LE- large excess, E - excess, D- deficit and S -Scanty rainfall years.**

	Periyar and Others					Varrar and Others					Netravati and Others					Vasishti and Others					Bhatsol and Others				
	Decadal mean D%	E	LE	D	S	Decadal mean D%	E	LE	D	S	Decadal mean D%	E	LE	D	S	Decadal mean D%	E	LE	D	S	Decadal mean D%	E	LE	D	S
1950- 1959	24.0	5	1	1	0	26.2	3	2	3	0	16.8	1	2	2	1	31.1	1	3	2	0	48.4	5	1	1	2
1960-1969	12.8	1	1	1	0	13.1	1	2	2	0	18.0	0	3	2	1	43.3	0	4	3	2	0.1	1	2	3	3
1970-1979	-3.1	2	0	3	0	2.7	3	0	3	0	0.9	4	0	2	1	-8.5	1	2	3	2	2.0	1	2	3	4
1980-1989	-32.8	0	0	7	1	-25.6	0	0	4	2	-33.9	1	0	7	1	-59.5	0	0	5	5	-75.5	0	0	3	7
1990-1999	-11.2	2	0	5	0	-16.3	2	0	5	0	-10.4	1	1	5	0	-12.9	1	1	6	1	-5.0	0	1	1	7
2000-2009	9.5	2	1	2	0	8.8	0	2	2	0	20.5	2	2	3	0	21.9	2	2	2	1	48.4	1	4	1	4
2010-2017	1.1	1	0	1	0	-11.3	0	1	4	0	-14.8	2	0	3	1	-19.3	3	0	4	1	-23.0	0	1	2	3
Total		13	3	20	1		9	7	23	2		11	8	24	5		8	12	25	12		8	11	14	30

#### 4.3.3.4 Southwest monsoon rainfall departures

The Bhatsol basin experienced above normal rainfall years with 4 excess years from 1954 to 1960 indicated by a positive decadal mean of +8.7% (1950~1959) for the southwest monsoon rainfall ( $R_{SW}$ ). The rainfall during the years 1954, 1958 and 1959 experienced a positive departure above 30% against a normal  $R_{SW}$  rainfall of 2387mm (Table 4.7 and Fig 4.6). Dry years with below normal rainfall years predominantly occurred (25 years with negative departures and 15 years with positive departures), in the basin from 1960 to 1999. The decade from 1980 to 1989 was observed as the driest decade with 7 below normal rainfall years denoted with a mean departure of -7.1%. Above normal  $R_{SW}$  years were witnessed in the basin from the 2000 onwards, with an excess rainfall departure of +34.7% and +29.1% during the years 2005 and 2006 respectively. The year 2009 and 2015 indicated a deficit year during the same decade with -25.7% and -31.7% departures. The  $R_{SW}$  departures are similar to the  $R_{AN}$  departures obtained for the basin in Fig.4.3.

The Vasishti basin exhibited predominantly above normal  $R_{SW}$  years from 1950 to 1961 with an excess rainfall of 3441mm (+26.4% departure) in the year 1961 against a normal of 2722mm, after which dry years were prevalent in the basin up to 1980 ( $E = 1 < D = 5$ ) with mean departures of -9.4% (1960~1969) and -8.4% (1970~1979). Though 1980 to 1989 was considered to be the driest decade throughout the study region for  $R_{SW}$ , Vasishti basin experienced both positive and negative departures for  $R_{SW}$  ( $E = 1$  and  $D = 1$ ) with a decadal mean of +2.7% as given in Table 4.7. From 1990 to 2017, the region experienced a rise in the frequency of above normal  $R_{SW}$  years ( $E = 6 > D = 2$ ), with excess rainfall of 3352mm (year: 2005), 3439mm (year: 2007) and 3515mm (year: 2011). The basin experienced major deficit years during 1962 and 2015 with -37.3% and -37.5% departures respectively (Fig. 4.6).

The Netravati basin experienced wet phase of  $R_{SW}$  from 1950 to mid-1980s with 6 excess years and 1 large excess year, with an  $R_{SW}$  of 5207mm (64% departure, year: 1961) against a normal of 3169mm. Though later decades exhibited both above and below normal  $R_{SW}$  years, prominent dry phase of  $R_{SW}$  was indicated after the year 2000, sufficed with negative mean departures of -8.3% (2000~2009) and -3.6% (2010~2017). The latter decade also experienced two deficit years during 2015 and 2016 observed with departures of -22.6% and -24% respectively. Similar to the annual rainfall departures, Varrar basin



indicated a clear shift in the  $R_{sw}$  departures after the decade 1980 ~ 1989. Early decades from 1950 to 1982 witnessed a plethora of above normal rainfall events with 9 excess (E) and 2 large excess (LE) years compared to 3 deficit years(D) for  $R_{sw}$  departures. The years 1959 and 1961 witnessed large excess  $R_{sw}$  departures with 2644mm (D% of 67%) and 2988mm (D% of 88%) respectively as presented in Table 4.7 and Fig. 4.6. In contrast, the  $R_{sw}$  entered a dry epoch with 24 below normal years compared to 12 above normal years from 1982 to 2017. The departures indicated 1 scanty and 10 deficit years compared to 2 excess years from 1982 to 2017. The year 2005 was denoted as scanty year with departure of -70%, while 2016 was a deficit year with -41.3% departure from normal. The Periyar basin exhibited above normal  $R_{sw}$  years from 1950 to 1970 with an excess rainfall of 1909mm (D% of 44.8%) and 2044.3mm (D% of 55%) in the year 1959 and 1961 respectively against a normal of 1318mm (Table 4.7 and Fig. 4.6). From 1970 to 1989, the basin experienced an abundance of below normal  $R_{sw}$  years, especially from 1980 to 1990 indicated by decadal mean of -13.4%. Though both above and below normal  $R_{sw}$  departures followed in the later years, negative departures outnumbered from 2000 onwards indicated by mean departures of -9% (2000~2009) and -1.8% (2010~2017) respectively. The year 2005 was a scanty year with a departure of -76.7%.

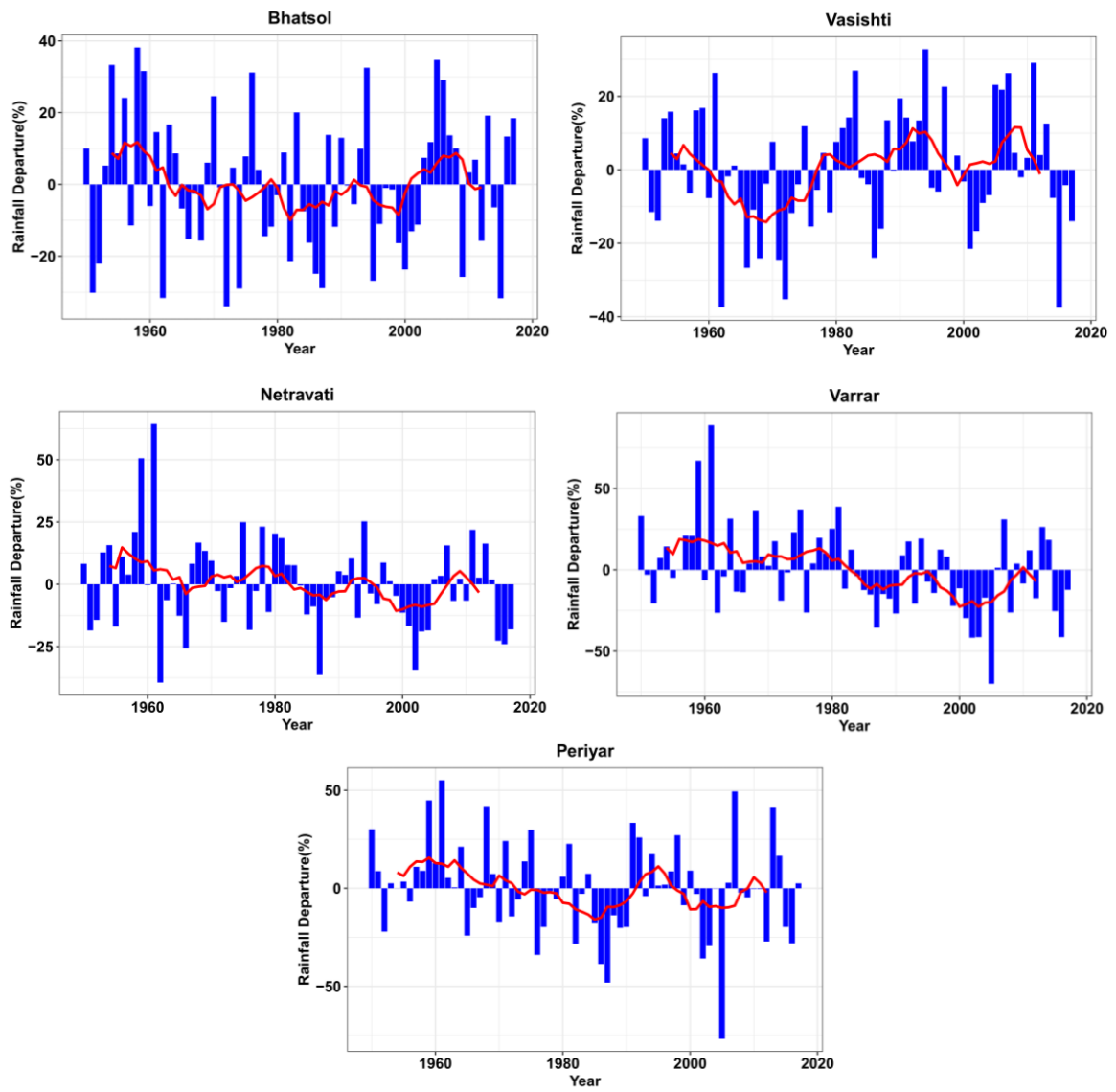


**Fig. 4.6** Departures of southwest monsoon rainfall from 1950 to 2017. The red-line indicates 10-year moving-average

**Table 4.7 Southwest monsoon rainfall departures from 1950 to 2017. LE- large excess, E - excess, D- deficit and S -Scanty rainfall years.**

Decade	Periyar and Others				Varrar and Others					Netravati and Others					Vasishti and Others			Bhatsol and Others		
	Decadal mean D%	E	D	S	Decadal mean D%	E	LE	D	S	Decadal mean D%	E	LE	D	S	Decadal mean D%	E	D	Decadal mean D%	E	D
1950- 1959	8.1	2	1	0	13.6	3	1	1	0	7.3	2	0	0	0	4.6	0	0	8.7	4	2
1960-1969	10.6	3	1	0	10.5	2	1	1	0	1.9	0	1	2	0	-9.4	1	3	-3.2	0	1
1970-1979	-3.1	2	1	0	6.8	2	0	1	0	0.9	2	0	0	0	-8.4	0	2	-1.8	2	2
1980-1989	-13.4	1	4	0	-3.4	2	0	1	0	-1.5	1	0	1	0	2.7	1	1	-7.1	1	3
1990-1999	8.3	3	0	0	-2.5	0	0	3	0	2.5	1	0	0	0	10.3	2	0	-0.7	1	1
2000-2009	-9.1	1	2	1	-20.1	1	0	4	1	-8.3	0	0	1	0	1.6	3	1	3.3	2	2
2010-2017	-1.8	1	2	0	-6.0	1	0	2	0	-3.6	1	0	2	0	-1.8	1	1	0.9	0	1
Total		13	11	1		11	2	13	1		7	1	6	0		8	8		10	12

#### 4.3.3.5 Post-Monsoon rainfall departures

The post-monsoon rainfall ( $R_{POM}$ ) depicted large excess as well as scanty rainfall dispersed irregularly across the study period similar to that of winter rainfall mainly in Bhatsol and Vasishti basins as presented in Table 4.8 and Fig. 4.7. Though both above and below normal  $R_{POM}$  departures were distributed in the Bhatsol basin, presence of large excess departures ( $LE = 4$ ) from 1950 to 1959 and ( $LE = 4$  and  $E = 2$ ) from 1990 to 1999, led to a substantial positive decadal mean of +33.1% (1950 to 1959) and +30% (1990 to 1999), for  $R_{POM}$  decadal distribution during these decades. The large excess rainfall above 190mm in the years 1951, 1955, 1956, 1959, 1993, 1998, 1999 and 2009, against a mean post-monsoon rainfall of 95.4mm, resulted in large positive departures above 100%. Dry epoch was observed from 1960 onwards in the Bhatsol basin, indicated by a decadal mean of -22.2%, -11.6% and -16.09% for the decades 1960 to 1969, 1970 to 1979 and 1980 to 1989 respectively. Alternate wet and dry decades followed from 1990 onwards, with decadal mean of +30% (1990~1999), -25% (2000~2009) and 14.9% (2010~2017).

The presence of large excess rainfall above 295mm against a normal of 185mm in the years 1953, 1955, 1956, 1966, 1993, 1996 and 1998 led to positive decadal mean of +27.6% (1950~1959), +6.95% (1960~1969) and +25.6% (1990~1999) in the Vasishti basin. Negative departures in substantial numbers  $\{(D = 14 \text{ and } S = 3) > (E = 4)\}$  led to negative decadal mean from 1970 to 1979 (-13.3%), from 1980 to 1989 (-26.2%) and from 2000 to 2009 (-20.5%). Later years from 2010 onwards indicated both above and below normal years for the post-monsoon rainfall in the Vasishti basin with two large excess rainfall of 406.8mm (year: 2009) and 355.3mm (year: 2010). Similar pattern was indicated by Netravati basin for  $R_{POM}$  with excess years during the early decades from 1950 to 1959 ( $E = 5 > D = 2$ ) and from 1990 to 1999 ( $E = 6 > D = 1$ ) with a decadal mean of +10.1% (1950~1959) and +20.8% (1990~1999) as given in Fig. 4.7 and Table 4.8. The decade from 1970 to 1989 indicated dry years with 7 deficit (D) years compared to 1 excess and 1 large excess year for the post-monsoon rainfall, indicated by a decadal mean of -8.9% (1970~1979) and -14.8% (1980~1989). From 2000 onwards above and below normal post-monsoon rainfall years were distributed in the basin, with the latter being in greater numbers. A large excess rainfall of 606mm against a normal 309mm, leading to a +96% departure was noticed in 2010.

Early decades from 1950 to 1979 experienced both above and below- normal post-monsoon rainfall in the Varrar basin, while excess years being predominant  $\{(E = 8 \text{ and } LE = 2) > (D = 3 \text{ and } S = 1)\}$  with two large excess rainfall of 657.9mm (65.2% departure) and 780mm (95.8% departure) in the years 1966 and 1977 respectively against a normal of 398.3mm. However, the decade from 1980 to 1999 was the driest decade, with nine years of below normal years ( $D = 3 \text{ and } S = 1$ ) against a single excess year in 1987 (Fig. 4.7 and Table 4.8). The decade from 1990 to 1999 experienced wet years with five excess to 2 deficit years with a decadal mean of +10.2%. Later decades from 2000 to 2010 witnessed both wet and dry years, with a substantial number of deficit years ( $D = 6 \text{ and } S = 1$ ), with a large excess rainfall of 668mm (67% departure) in 2010.

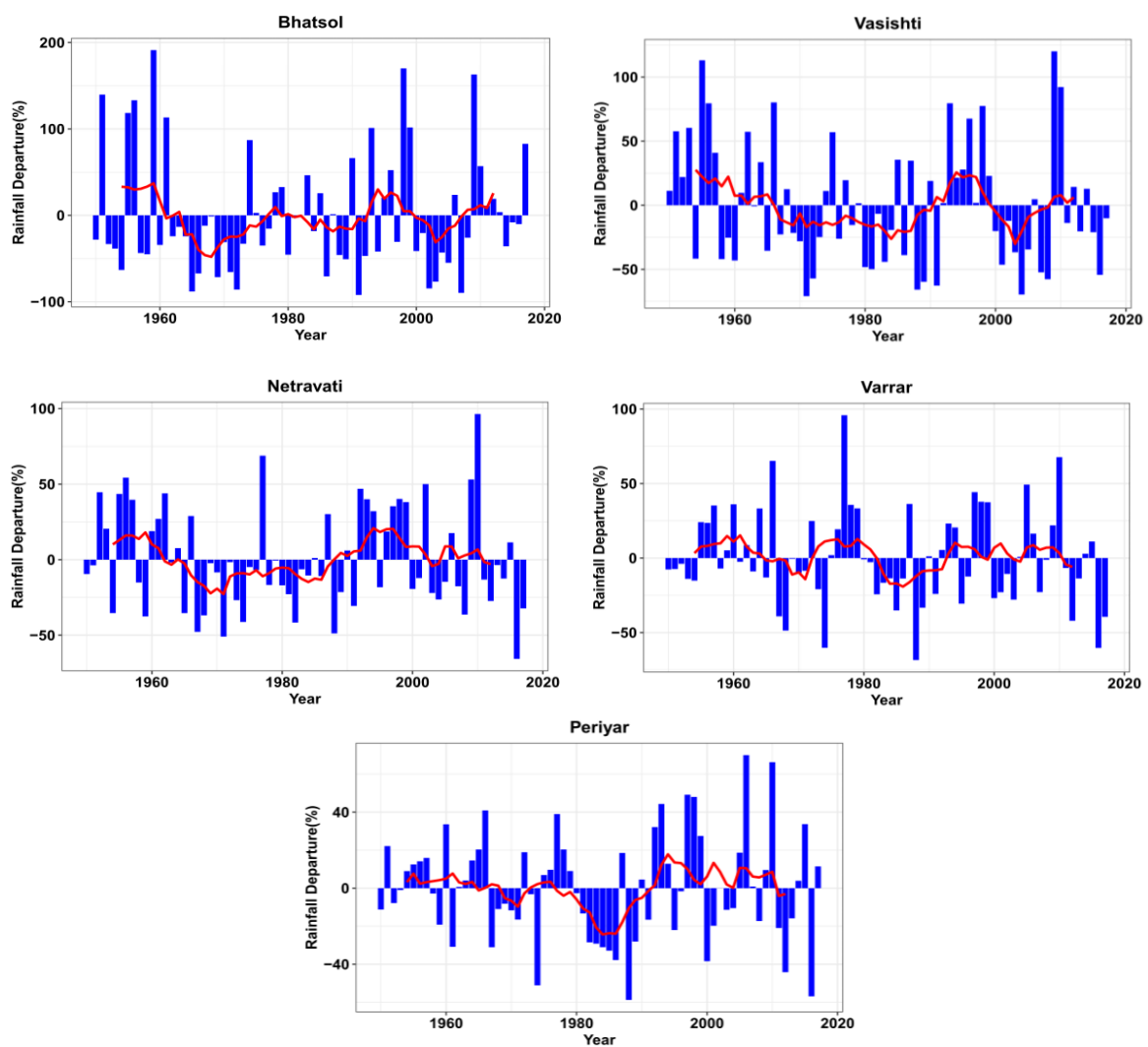


**Fig. 4.7 Departures of post- monsoon rainfall from 1950 to 2017. The redline indicates the 10-year moving average**

**Table 4.8 Post-monsoon rainfall departures from 1950 to 2017. LE- large excess, E - excess, D- deficit and S -Scanty rainfall years.**

Decade	Periyar and Others				Varrar and Others					Netravati and Others					Vasishti and Others				Bhatsol and Others					
	Decadal mean D%	E	LE	D	Decadal mean D%	E	LE	D	S	Decadal mean D%	E	LE	D	S	Decadal mean D%	E	LE	D	S	Decadal mean D%	E	LE	D	S
1950-1959	3.17	1	0	0	3.30	3	0	0	0	10.13	5	0	2	0	27.57	3	3	3	0	33.09	0	4	5	1
1960-1969	3.31	3	0	2	3.03	2	1	2	0	0.21	3	0	3	0	6.95	2	1	4	0	-22.29	0	1	3	3
1970-1979	2.14	2	0	1	11.13	3	1	1	1	-8.92	0	1	3	0	-13.34	1	0	4	1	-11.66	2	1	3	2
1980-1989	-24.36	0	0	7	-17.25	1	0	3	1	-14.81	1	0	4	0	-26.27	2	0	4	2	-16.09	2	0	3	1
1990-1999	17.82	5	0	1	10.26	5	0	2	0	20.85	6	0	1	0	25.64	3	3	0	1	30.02	2	4	3	1
2000-2009	0.18	0	1	1	-2.41	2	0	4	0	-2.78	2	0	3	0	-20.50	0	1	6	1	-25.01	1	1	5	3
2010-2017	-2.82	1	1	3	-10.07	0	1	2	1	-5.84	0	1	2	1	-0.06	0	1	3	0	14.93	1	1	1	0
Total		12	2	15		16	3	14	3		17	2	18	1		11	9	24	5		8	12	23	11

The Periyar basin highlighted similar  $R_{POM}$  distribution like Varrar, with relatively wet years from 1950 to 1979. Though the basin experienced both above and below normal  $R_{POM}$  years intermittently throughout the period. However, the decade from 1980 to 1990 was the driest decade with nine below-normal years out of which 7 were deficit years. From 1990 to 1999, excess years dominated the basin ( $E = 6$ ) with a decadal mean of +17.8%. Both positive and negative departures were noticed in the basin after 2000. The basin experienced two large excess years in 2006 (912.7mm) and 2010 (892.8mm).

#### **4.3.4 Wavelet Spectrum Analysis**

The wavelet power spectrum analysis of basin averaged rainfall was conducted to examine the annual and seasonal rainfall periodicities. The information on periodicities could explain the yearly as well as decadal variabilities in the rainfall regimes over the west coast basins.

##### **4.3.4.1 Annual rainfall wavelet spectrum**

The wavelet power spectra of annual rainfall ( $R_{AN}$ ) in the Bhatsol basin indicated a strong 2-3-year band from the mid-1950s to the early 1960s. Spectra enclosed in the white line indicate statistically significant at a 5% significance level, as given in Fig. 4.8. Moderate power bands were dispersed during the mid-1970s and throughout 1980~1990 and later years (after 2010). A moderate power in the 4-8-year band was noticed during the early decades up to the early 1980s, while the 4-6-year band during the 1990s. Interdecadal oscillations in the 8-16-year spectrum were obtained after 1990. Wavelet spectra for the annual rainfall ( $R_{AN}$ ) in the Bhatsol basin indicated strong intra-decadal oscillations mainly during the earlier decades, while inter-decadal oscillations were observed after the 1980s.

The Vasishti basin exhibited similar periodicity as that of the Bhatsol basin with strong 2-4-year oscillations during the late-1950s to early 1960s (Fig. 4.8). Moderate 4-6-year spectrum was visible during the early 1970s. Moderate to low power periodicities within 2-4-year periods were observed intermittently across the decades between early 1970s, 1990 to 2000 and after 2010. Mild 8-year and 16-year oscillations were displayed from the early decades with more power confined after the 1980s. The presence of intermittent 2-4-year and 4-6-year variations could be attributed to the intra-decadal variations in the annual rainfall of the Vashisti basin. Vasishti basin depicted prominent 16-year oscillations indicating the decadal modulations in the  $R_{AN}$  pattern in the basin.

Strong 2-4-year periodicity was found during the early years from 1955 to 1965 in the Netravati basin for the annual rainfall spectrum. Moderate to low power 2-4-year band was observed during the mid-1970s to 1980 and a very mild spectrum from 1990 to 2000. A strong periodicity in the 2-4-year band was lacking after 1990. Interdecadal oscillations of mild power (8 -16-year bands) were observed throughout the timeframe (Fig. 4.8). Similar periodicities were indicated by the wavelet power spectrum of  $R_{AN}$  in the Varrar basin.

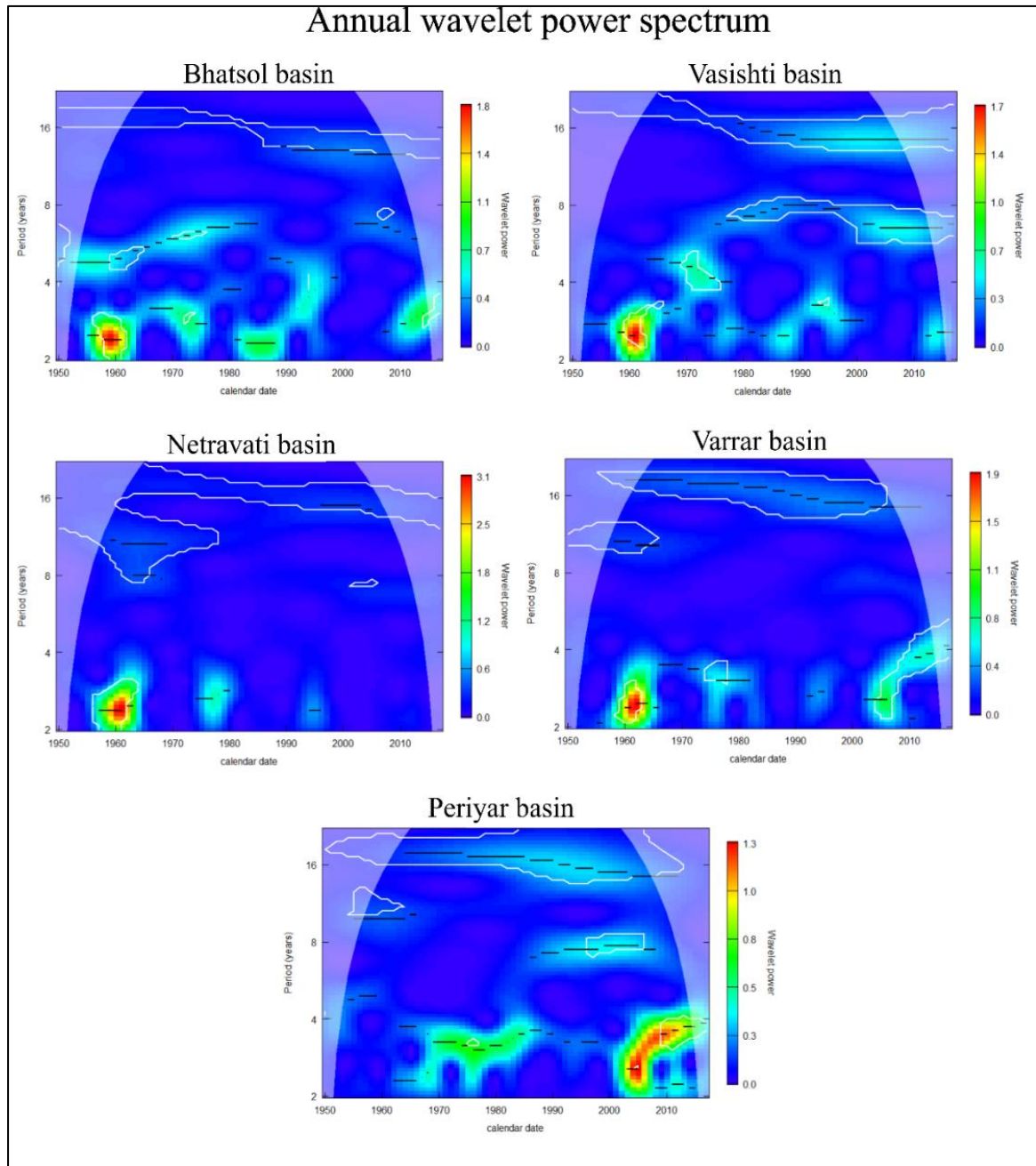


**Fig. 4.8** Wavelet power spectrum of annual rainfall.



Early decade from 1955 to 1965 exhibited very strong spectra of 2-4-year bands, the power of which later diminished to mild oscillations during the 1970s and to the weak band during the 1990s. The 2-4-year periodicity resumed later from 2000 to 2017. A mild interdecadal oscillation within the 16-year band was visible throughout the period for the Varrar basin. The Periyar basin indicated 2-4-year modulations from 1960 to 1990 which strengthened from 2000 onwards (Fig. 4.8). Moderate power band of 16 year periodicity was visible throughout the period, which strengthened its power from 1980 onwards. Later decades also depicted a moderate 8-year band commencing from 1980 onwards. The oscillations for annual rainfall varied in space and time, even though the five basins belonged to the same agro-climatic zone.

#### **4.3.4.2 Winter rainfall wavelet spectrum**

Bhatsol basin exhibited 2.5-5-year oscillations from 1950 to 1960 (significant at 5%), 1978 to 1982 and 2000 to 2010 for winter rainfall ( $R_{WN}$ ) as presented in Fig. 4.9. A significant high power 2-8-year oscillation enclosed in white line (at 5% significance level) from 1990 to 2000 (and beyond) was observed corresponding to the large excess and scanty rainfall events during this period. Moderate yet significant 16-year interdecadal oscillations were also noticed for  $R_{WN}$  in the basin. The wavelet spectra for  $R_{WN}$  in the Vasishti basin do not display substantial oscillations owing to the meagre winter rainfall totals distributed in the basin from 1950 to 2017, except for the strong 2-4-year spectra from 2007 to 2017. Like the Vasishti basin, the Netravati basin also depicted a significant 2-4-year high power spectra from the mid-2000s to 2017. The high-power spectra could be attributed to the intermittent occurrence of large excess or scanty rainfall totals during this period (Fig. 4.9).

Varrar basin exhibited  $R_{WN}$  spectra sporadically across the time frame. Strong oscillations of the 2-3-year band were observed in the early 1950s, 1980~1990 and from 2000 to 2017 for winter rainfall (Fig. 4.9). Moderate powers oscillations of 4-8-year bands were observed during 1955~1965 and 1980~1990. Interdecadal spectra of 8-16-year periods of mild power were noticed throughout the time frame. The winter rainfall ( $R_{WN}$ ) portrayed some 2-4-year periodicities with moderate power from 1950 to 1970 in the Periyar basin. Significant high-power oscillations from 4-year extending to 8-year bands observed from 1980 to 2000 were synchronous with large excess events during these decades. Winter rainfall exhibited discontinuous short periodicities as the distribution of

winter rainfall is very meagre in the west coast basins except for Periyar and Varrar basins (Fig. 4.9).

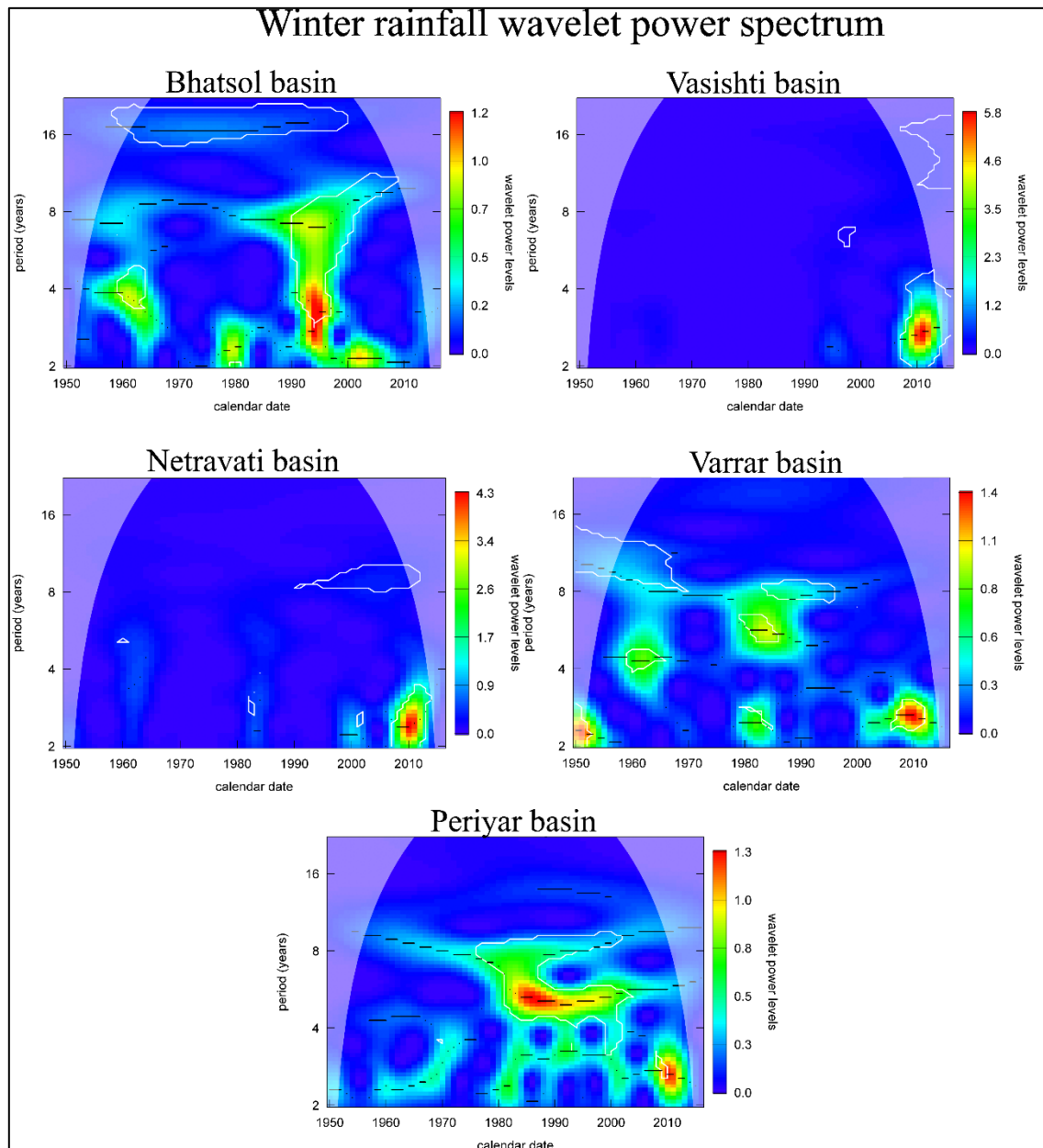


**Fig. 4.9. Wavelet power spectrum of winter rainfall.**

#### 4.3.4.3 Pre-monsoon wavelet spectrum

The pre-monsoon ( $R_{PRM}$ ) spectra indicated discontinuous short spectra in the range of 2-4-year as well as 4-8-year bands among the basins (Fig. 4.10). Similar to the winter rainfall spectra, the Bhatsol basin exhibited short 2-4 -year oscillations corresponding to the heavy rainfall totals during the decade 1950 to 1960, 1970 to 1975 and from 2000 to

2010. A high-power spike in the wavelet spectra (2-8-year band) was observed during 1990 corresponding to the large excess pre-monsoon rainfall with a departure of 521%. The Vasishti basin displayed strong periodicities of 2-4-year as well as 4-8-year bands during the early decade from 1950 to 1970 capturing the large excess rainfall events (Fig. 4.10). The spectra diminished from 1970, with a moderate spike in 1990, the later decade from 2000 to 2010 indicated 2-4-year band spectra for the pre-monsoon rainfall. Bhatsol basins, the later decade from 2000 to 2010 were noted with strong oscillations (2-4-year).

The pre-monsoon wavelet spectra in the Varrar basin captured the above normal rainfall events during the early years from 1950 to 1960 displayed in the 2-8-year bands (Fig. 4.10). Very short weak spectra were dispersed from 1970 to 1990, however strong oscillations of 2-4-year were visible for  $R_{PRM}$  after the year 2000 extending up to 2010 and little beyond. Similar observations were obtained for Periyar basin with moderate power 2-5-year oscillations during 1950 to 1960 and 1970 to 1980, which strengthened from 2000 to 2010. Large excess events from 1955 to 1965 were well captured by the 4 – 8-year band wavelet spectra for the pre-monsoon rainfall in the Netravati basin. Similar to Vasishti and

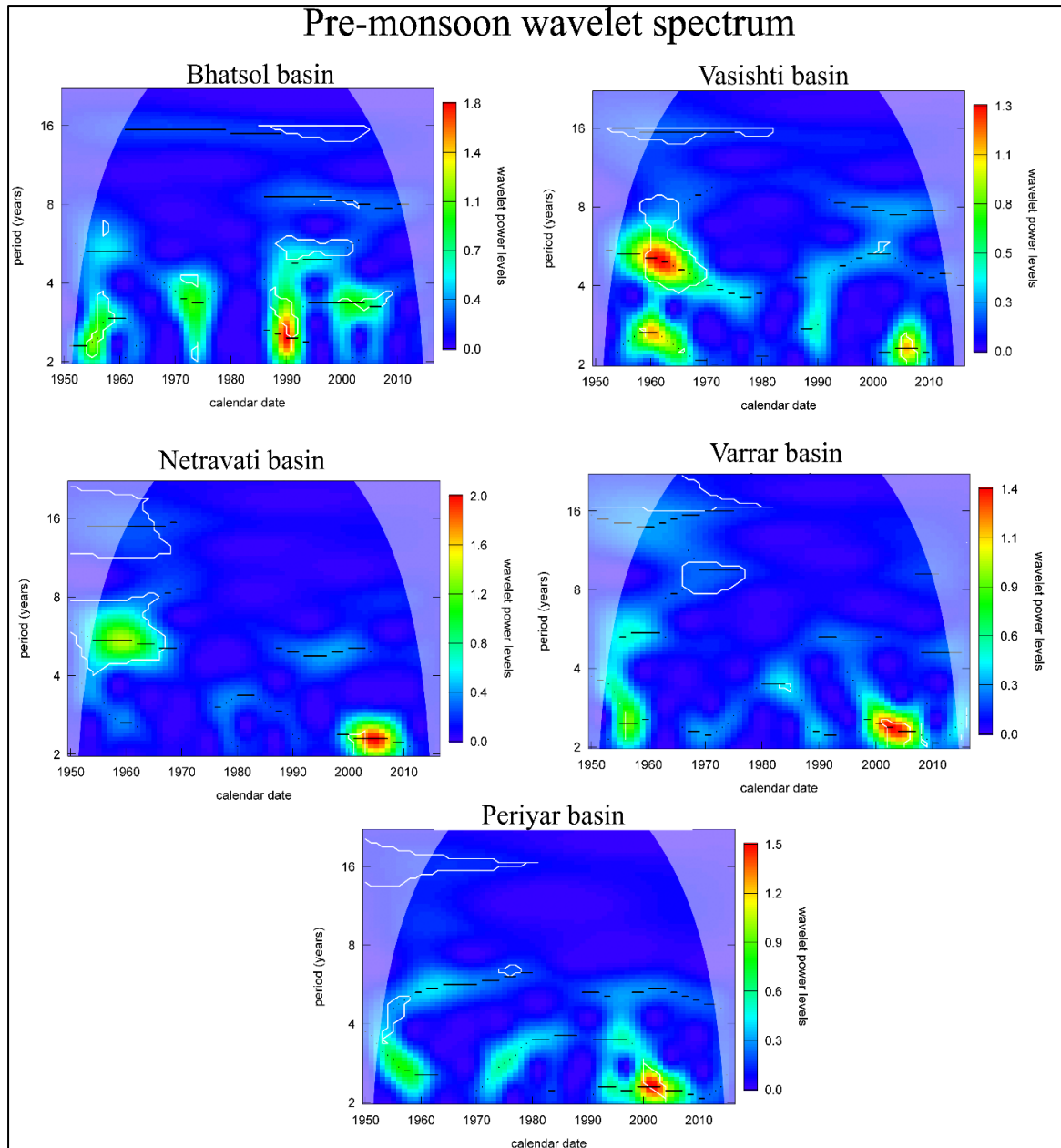


**Fig. 4.10. Wavelet power spectrum of pre-monsoon rainfall.**

#### **4.3.4.4 Southwest monsoon wavelet spectrum**

The wavelet spectra for southwest monsoon rainfall ( $R_{sw}$ ) displayed close resemblance to the annual rainfall spectrum, provided the share of former in the annual rainfall budget as given in Fig. 4.11. Bhatsol basin exhibited short high-power spectra of 2-3.5-year periodicities during 1950 to 1965, which further continued in short 2-4-year oscillations with moderate power during 1970s, 1980s up to 1990s after which the spectra diminished. A mild power of 4-8-year oscillations were visible from 1950 to 1990. A weak

interdecadal oscillation of 16-year band was observed from 1984 onwards. Dominant oscillations for the  $R_{SW}$  in the Bhatsol basin were 2-4-year periods during the early decades which weakened after the 1990s, but re-appeared after late-2000s

The southwest monsoon rainfall in the Vasishti basin displayed short periodicities of 2-4-year oscillations during early decades with a powerful spectrum from 1956 to 1965, which further weakened from 1970 to 1990 (Fig. 4.11). However, the periodicities appeared with moderate power from 1990 to 2000 and from 2010 and beyond, in the 2-4-year band. A moderate power 4-8-year band was visible throughout the time frame. Interdecadal oscillations of the 12-16-year band were noted from 1980 onwards. The early years from 1955 to 1965 displayed strong 2-4-year oscillations for  $R_{SW}$  in the Netravati basin. A moderate spike in the spectra was observed during the mid-1970s. Significant but mild spectra in the 16years was visible for the  $R_{SW}$  spectrum. Alike the Netravati basin, the Varrar basin also displayed very few inter-annual spectral periodicities except for the strong 2-4-year oscillation around the years 1955 to 1965, which further weakened and gained strength from 2000 onwards. A 16-year weak spectral band was noted for the  $R_{SW}$  in the basin. Short periodicities of 2-4-year oscillations were observed for  $R_{SW}$  in the Periyar basin during the early years from 1960 to 1980, which weakened after 1980. However, very strong spectrum in the 2-4- year band were obtained for the  $R_{SW}$  in the basin from 2000 onwards. Mild interdecadal oscillations in the 8-16-year band was observed from 1980 onwards (Fig. 4.11).

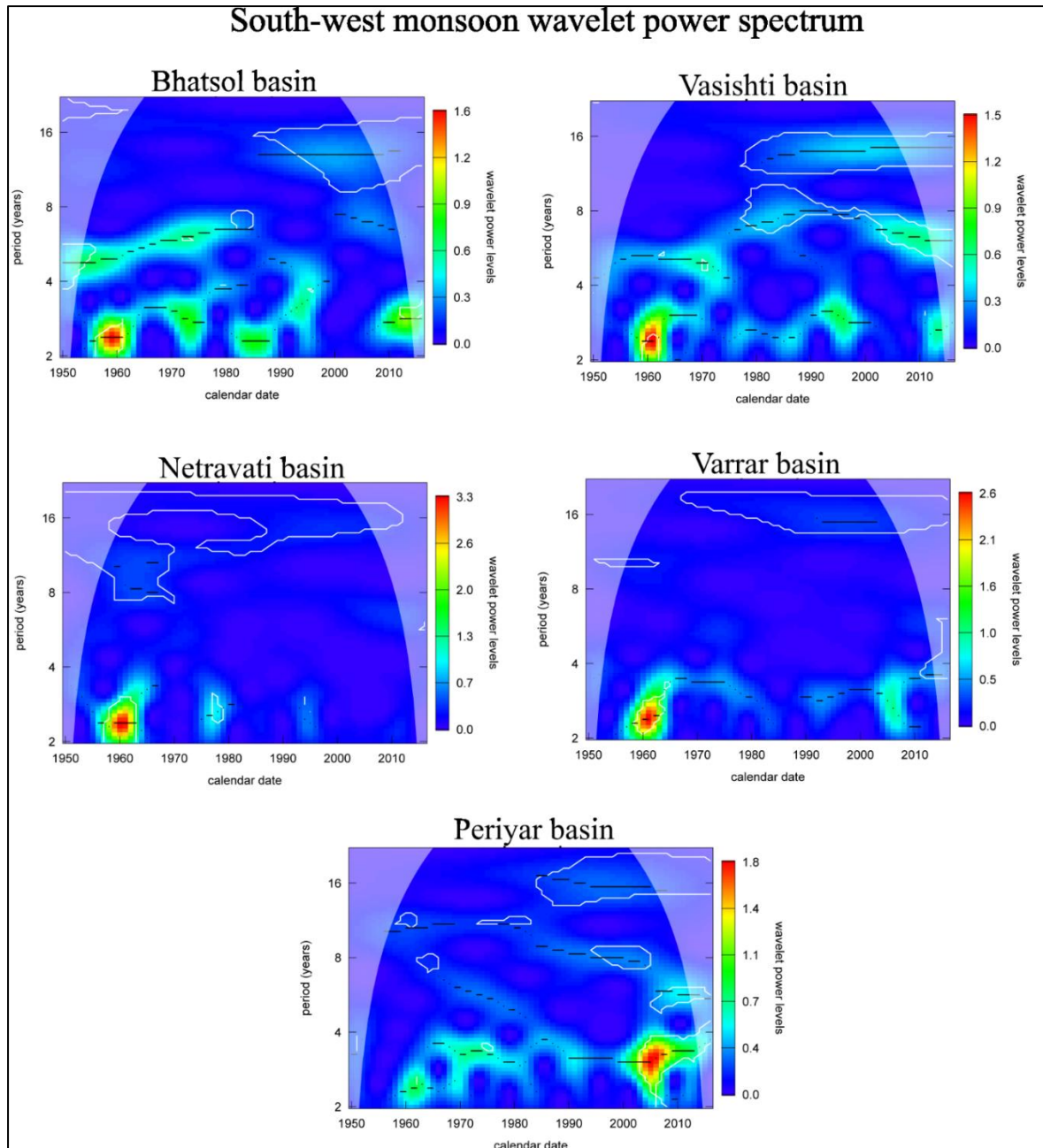


**Fig. 4.11. Wavelet power spectrum of southwest monsoon rainfall.**

#### **4.3.4.5 Post-monsoon wavelet spectrum**

The high fluctuations in the rainfall distribution and the presence of extreme rainfall totals were portrayed by 2-4-year, 4-8-year and 8-16-year bands for the post-monsoon rainfall ( $R_{POM}$ ) spectra among the west coast basins as presented in Fig. 4.12. The post-monsoon rainfall ( $R_{POM}$ ) displayed strong significant (area enclosed in the white line is significant at 5% level) oscillations in the 2-6-year bands from 1950 to 1965 in the Bhatsol

basin. A high power spectrum was seen from 1985 to 2000 in the variability of 2-4-year oscillations, which depicted a spike again from 2008 to 2011. A mild inter-decadal oscillation in the 10-16-year was observed in the spectra from 1990 onwards.

Early decades from 1950 to 1970 exhibited oscillations in the 2-4-year and 4-8-year period for  $R_{POM}$  in the Vasishti basin (Fig. 4.12). The spectrum resumed from 1980 onwards with strong 2-4-year variability and strong 3-6-year oscillations in the late 2000s. A significant but moderate power of 8-16-year band was observed throughout the period. The presence of interdecadal oscillations could be attributed to decadal variability in the post-monsoon rainfall distribution in the basin. Bhatsol and Vasishti basins exhibited greater variability in post-monsoon rainfall of large excess or scanty seasonal totals compared with Netravati, Varrar and Periyar basins. The Netravati basin indicated occasional periodicity for post-monsoon rainfall with a 4-6-year spectrum from 1950 to 1960 and 2-4-year bands from 1960 to 1980 and the late 1980s. A significantly strong power periodicity in the 3-6-year band was observed from 2000 onwards particularly from 2008 to 2010.

The Varrar basin exhibited strong 2-4-year oscillation in short periods from 1960 to 1980 and the late 1990s (Fig. 4.12). However, the post-monsoon rainfall in the basin displayed significant and strong periodicities in the 4-8-year period throughout the time frame analysed from 1950 to 2017. A mild 16-year band was visible throughout the period. Periyar basin displayed moderate 2-4-year modes for  $R_{POM}$  during the 1960s to 1970 and mid-1980s and beyond 2010. However, very strong spectra in the 4-8-year band were obtained from 1990 onwards, with a spike in power during 2006-2010. A mild 16-year band was visible in the wavelet spectrum of  $R_{POM}$  in the basin.

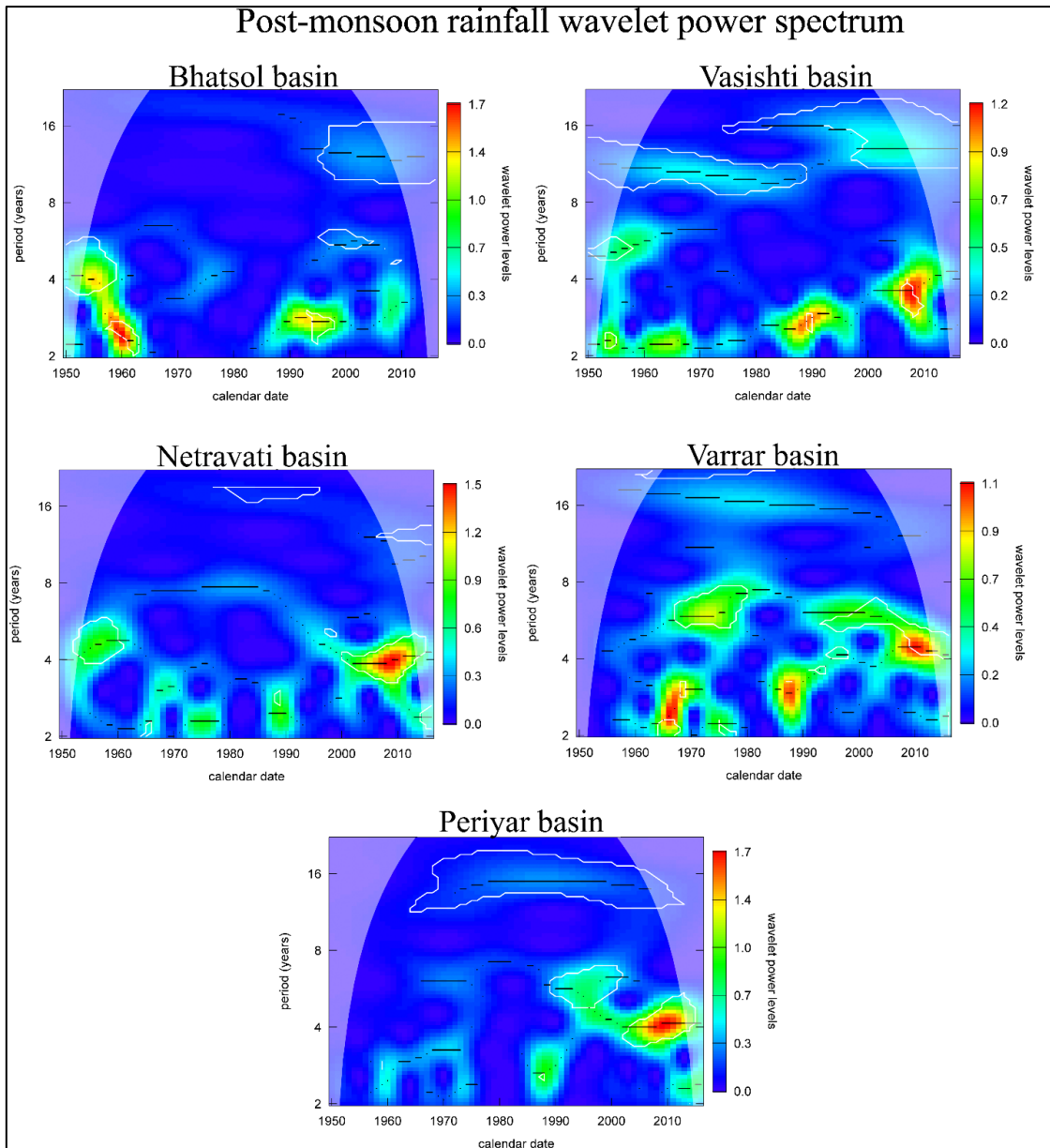


**Fig. 4.12. Wavelet power spectrum of post-monsoon rainfall**



#### 4.4 CLOSURE

The departure analysis of basin-averaged annual and seasonal rainfall was conducted in this chapter. The inter-annual, as well as decadal variability in the rainfall regimes, were examined. In addition, the wavelet power spectrum for annual and seasonal rainfall was investigated to understand periodicities associated with regional rainfall patterns. Furthermore, the presence of 2-4, 4-8 and 16-year oscillations were observed in the west coast basins though the presence of continuous strong spectra was lacking both spatially as well as temporally.

- The annual rainfall departures displayed decadal variability among the west coast basins. Though a general conclusion could not be attained, the decades 1980~1989 and 2000~2009 were the common driest decade among the basins. Periyar, Varrar and Netravati basins depicted a shift in the  $R_{AN}$  departures with a rising frequency of dry years after 1980. Vasishti and Bhatsol basins also indicated such a distribution though positive  $R_{AN}$  departures also occurred during the later years.
- Bhatsol, Vasishti and Netravati depicted strong similarity between annual ( $R_{AN}$ ) and southwest monsoon rainfall departures. However, the existence of dissimilarities in the annual and  $R_{SW}$  departures were visible for the Periyar basin, wherein the post-monsoon rainfall also contributes a fair share to the  $R_{AN}$  budget. The presence of large excess or scanty rainfall years was mainly confined to winter, pre-monsoon and post-monsoon rainfall.
- Sparse occurrence of excess or large excess winter rainfall ( $R_{WN}$ ) among the long period of deficit, scanty or no rainfall years was indicated as the character of winter rainfall departures mainly in the Bhatsol, Vasishti and Netravati basins. As the contribution of  $R_{WN}$  to the annual rainfall budget is very meagre, the spatio-temporal variations in departures of winter rainfall does not primarily affect the regional water balance. Anomalous  $R_{WN}$  departure values exceeding 100% could be attributed to no rainfall, extremely high-intensity rainfall, or low data quality. Also, the presence of large numbers of zero rainfall years (mostly in Netravati, Vasishti and Bhatsol basins) affected the calculated normal  $R_{WN}$  values to a meagre value.
- Pre-monsoon rainfall demonstrated uniformity in the temporal variation of rainfall departures among the west coast basins. Decadal to multi-decadal variability in the departures revealed wet early decades from 1950 to 1970, indicated by prominent

positive departures, followed by dry phase with negative departures during 1980~1999. Later decades from 2000 to 2017 also exhibited short variability, with dry phase during the first half (2000 to 2009), while second half indicated wet phase (2010 to 2017).

- The southwest monsoon rainfall ( $R_{SW}$ ) or Indian summer monsoon from July to September was found to display annual as well as decadal to multidecadal variations (Ravedkar et al. 2019). The west coast basins also exhibited annual to decadal variability in the  $R_{sw}$  regimes. The  $R_{sw}$  departures of five basins were in-phase during the early years from 1950 to 1960 indicated by principal wet years. From 1970 to 1990, prominent dry phase was visible among the basins. Vasishti and Bhatsol basins displayed greater wet years after 2000, while Varrar, Periyar and Netravati indicated vice-versa.
- The west coast basins demonstrated uniformity in the temporal distribution of post-monsoon rainfall. The early years between 1950 to 1960 and the decade from 1990 to 2000 were wet years with greater positive rainfall departures. The decade from 1980 to 1990 was a dry decade common to all the basins with predominant negative departures. Occurrences of large excess and scanty years were relatively higher in the Vasishti and Bhatsol basins for the post-monsoon rainfall departures.
- The dominant cycles for the annual rainfall ( $R_{AN}$ ) among the west coast basins were displayed in the 2-4-year bands. The early decade from 1955 to 1965 exhibited strong 2-4-year oscillations common to the study area, but the Periyar basin. Visible 2-4-year spectra with varying power were observed for  $R_{AN}$  in the studyarea. Interdecadal oscillations of the 8-16-year period were obtained with moderate power among all the basins, which mainly strengthened from 1980 onwards. Short spectra of inter-annual oscillations in 4-8-year bands were observed for  $R_{AN}$  distributed in the Bhastol and Vasishti basins. The presence of 2-4-year, 4-8-year and 8-16-years bands indicate the role of teleconnections in the region, though there exists spatial as well as temporal variations in their distribution.
- The distribution of winter rainfall ( $R_{WN}$ ) is unreliable and irregular among the west coast basins. Subsequently follows the wavelet spectra for  $R_{WN}$ . Netravati and Vasishti basins exhibited very short 2-4-year oscillations from mid-2000 onwards, while Periyar, Varrar and Bhatsol basins displayed strong 2-4-year oscillations irregularly distributed from 1950 to 2017. Strong 4-8-year spectra were visible for

$R_{WN}$  from 1990 onwards in the above mentioned three basins. The sporadic and erratic distribution of winter rainfall among the basins were evident from the percentage departures, confirming the irregularity in the spatial distribution of spectra in the region.

- The pre-monsoon rainfall ( $R_{PRM}$ ) spectra displayed short and dis-continuous temporal oscillations capturing the concurrent rainfall events for the spectral bands. As evident from annual as well as winter rainfall spectra, dominant cycle of oscillations were noted for the 2-4-year as well as 4-8-year bands for the  $R_{PRM}$  spectra. West coast basins exhibited common periods of oscillations in the 2-8-year bands during early decades from 1950 to 1970 and later, from 2000 to 2010 mainly in the 2-4-year region. Strong interdecadal oscillations were lacking for  $R_{PRM}$  wavelet spectra, except for the weak colour band observed for the 16-year band among the basins during early decades.
- Inter-annual periodicities of 2-4-years and 4-8-years were predominantly exhibited by Bhatsol, Vasishti and Periyar basins with varying wavelet power for southwest monsoon rainfall. While Netravati and Varrar basins presented few short periodicities of 2-4-year band confined to early decades. Statistically significant inter-decadal oscillations of 12-16-year period were evident among all the basins with moderate wavelet power though. The inter-annual and inter-decadal variability in the distribution of southwest monsoon rainfall (or in other words Indian summer monsoon) is evident from the periodicities obtained from the wavelet spectra. Inter-annual as well as inter-decadal modulations of southwest monsoon rainfall by El Nino SSTs (El Nino Sea Surface Temperature), Indian Ocean Dipole (IOD) and Pacific SSTs (Pacific Sea Surface Temperature) were reported earlier (Revadekar et al. 2019; Halder et al. 2022). Though located on the west coast of India, the basin indicated spatial as well as temporal variations in the wavelet power spectrum for annual as well as seasonal rainfall.
- Presence of 2-4-year, 4-8-year as well as 8-16-year periodicities in the post-monsoon rainfall wavelet spectra indicated the modulations of the seasonal rainfall by teleconnections on inter-annual as well as interdecadal scale. During El Nino years (La Nina), the northeast monsoon (NEM) or post-monsoon rainfall has increased (decreased) and caused positive (negative) anomalies in the southern peninsular region of India (Sreekala et al. 2011; Yadav 2012). Apart from ENSO oscillations,

inter-annual variability in the post-monsoon rainfall was attributed to Indian ocean dipole (IOD) and Equatorial Indian Ocean Oscillation (EQUINOO) by various researchers (Sreekala et al. 2011). Multi-decadal variations in post-monsoon rainfall could be explained in relation to ENSO oscillations (Rajeevan et al. 2012).



**TREND ANALYSIS OF RAINFALL AND GROUNDWATER LEVELS**

---

---

**5.1 INTRODUCTION**

It has been estimated that nearly two billion people worldwide rely on groundwater as their primary source of water (Giordano 2009). Though surface water has been exploited for ages, freshwater demands for the domestic and agricultural sector has also been met from groundwater. The agricultural sector boom emphasized the withdrawal of groundwater through uncontrolled public and private abstraction, making it imperative for decision-makers to prompt adequate management and conservation strategies. Past literature reported the changing patterns in Indian rainfall over varying time scales (Thomas and Prasannakumar 2016; Kothawale and Rajeevan 2017). Rainfall trend detection has gained momentum over the decades, given the scientific community's emphasis on climate change. Changing rainfall affects the water resources management directly or indirectly and thereby impairs the region's groundwater levels (GWLs). Long-term assessment of temporal variations of groundwater levels assists in understanding the response of the system to external forcing, namely – climatic and anthropogenic stressors. A comprehensive study of the rainfall and groundwater levels is crucial for the identification of strategies for water resource management in specific regions.

Significant trends (both decreasing and increasing) for annual and southwest monsoon rainfall over India have been reported by Guhathakurta and Rajeevan (2008), Rajeevan et al. (2008), Mondal et al. (2015), Thomas and Prasannakumar (2016), and Kothawale and Rajeevan (2017). A substantial number of studies have employed a non-parametric Mann-Kendall test for trend detection of long-term groundwater levels (Daneshvar Vousoughi et al. 2013; Panda et al. 2007; Shamsudduha et al. 2009; Tabari et al. 2012; Yan et al. 2015; Tirogo et al. 2016). Furthermore, an investigation of groundwater levels documented severe declining trends in agricultural regions (Sishodia et al. 2019). Additionally, studies also reported seasonal variations (both increasing and decreasing) in the GWL trends among major cities in India (Mohanavelu et al. 2020). However, hydrological time series is primarily nonlinear and non-stationary (Unnikrishnan and

Jothiprakash 2015). The conventional trend detection methods do not provide information on the shape of the trends. Recently, spectral methods have been employed in extracting the trend trajectories of hydro-meteorological time series (Sang et al. 2014; Unnikrishnan and Jothiprakash 2015; Aswathaiah and Nandagiri 2020). In this chapter, trend detection of rainfall (at annual and seasonal scales) and seasonal groundwater levels by employing modified Mann-Kendall (mMK) and Sen’s slope estimator (SE) is presented. In addition, the test power analysis on the non-parametric mMK hypothesis testing is examined in this study. Furthermore, the extraction of trend trajectories by Singular spectrum analysis (SSA) is also discussed in this chapter.

## 5.2 METHODOLOGY

### 5.2.1 Mann-Kendall (MK) Test

Mann-Kendall test (MK) is a non-parametric statistical test known for its generous application in trend detection studies of hydrological time series (Mudbhatkal et al. 2017). It is assumed that the Mann-Kendall trend test is a distribution-free rank-based test. The null hypothesis ( $H_0$ ) for the Mann-Kendall test assumes no trend in the time series, provided the data is independent and randomly distributed. The null hypothesis is tested against the alternative hypothesis ( $H_a$ ), which assumes that there is a trend (Mann 1945; Kendall 1975). For time series data  $x_1, x_2, x_3, \dots, x_n$ , the Mann-Kendall statistic ( $S$ ) is calculated as:

$$S = \sum_{k=1}^{n-1} \sum_{i=k+1}^n \text{sign}(x_i - x_k) \quad (5.1)$$

$$\text{Where, } \text{sign}(x_i - x_k) = \begin{cases} +1 & \text{if } \text{sign}(x_i - x_k) > 0 \\ 0 & \text{if } \text{sign}(x_i - x_k) = 0 \\ -1 & \text{if } \text{sign}(x_i - x_k) < 0 \end{cases}$$

It is reported that if  $n > 10$ , the statistic follows a normal distribution. For  $n > 10$ , the mean and variance for statistic  $S$  are as follows:

$$E[S] = 0 \quad (5.2)$$

$$\text{Var}(S) = \frac{n(n-1)(2n+5) - \sum_{i=1}^m t_i(t_i-1)(2t_i+5)}{18} \quad (5.3)$$

where  $n$  is the number of data points,  $m$  is the number of tied groups, and  $t_i$  denotes the number of ties of extent  $i$ .

The standard test statistic  $Z$  is calculated as follows:

$$Z = \begin{cases} \frac{S-1}{\sqrt{\text{Var}(S)}} & \text{for } S > 0 \\ 0 & \text{for } S = 0 \\ \frac{S+1}{\sqrt{\text{Var}(S)}} & \text{for } S < 0 \end{cases} \quad (5.4)$$

Suppose the  $|Z|$  value is greater than the theoretical value of  $Z_{\alpha/2}$ ; in that case, the null hypothesis is rejected, and the alternate hypothesis of a trend is accepted for a predefined significance level of  $\alpha$ . The sign of the  $Z$  value determines the trend direction (increasing or decreasing trend).

Auto-correlation affects the trend detection by MK test, and hydrological time series may contain autocorrelated data records. In the modified Mann-Kendall test, Hamed and Rao (1998) considered the effect of autocorrelation in a time series by calculating the autocorrelation between the ranks of the data after removing the apparent trend. The variance is adjusted as follows:

$$\text{Var}[S] = \frac{1}{18} [n(n-1)(2n+5)] \frac{n}{n_S^*} \quad (5.5)$$

$$\text{Where } \frac{n}{n_S^*} = 1 + \frac{2}{n(n-1)(n-2)} \sum_{i=1}^{n-1} (n-i)(n-i-1)(n-i-2)\rho_S(i) \quad (5.6)$$



Where  $n$  is the number of observations and  $\rho_S(i)$  is the autocorrelation function of the ranks of the observations (Hamed and Rao 1998). This study's significance level is fixed at 5% to examine the statistical significance and the direction of historical rainfall and groundwater level trends.

### 5.2.2 Sen's Slope Estimator (SE)

The magnitude of the trend (i.e., change in slope per unit time) is determined using Sen's slope estimator (Sen 1968) for rainfall and seasonal groundwater level data. To obtain the slope estimate  $Q$ , the slopes of all data value pairs are first calculated as follows:

$$Q_i = \frac{x_j - x_k}{j - k}, \text{ where } i = 1, 2, \dots, N, j > k. \quad (5.7)$$

The  $N$  values of  $Q_i$  estimates are ranked from smallest to largest, and Sen's estimator (SE) is computed as the median of all values and given as:

$$Q = Q_{\left[\frac{(N+1)}{2}\right]} \quad \text{if } N \text{ is odd,} \quad (5.8)$$

or

$$Q = 1/2 \left( Q_{\left[\frac{N}{2}\right]} + Q_{\left[\frac{N+2}{2}\right]} \right) \quad \text{if } N \text{ is even.} \quad (5.9)$$

### 5.2.3 Power Analysis of mMK Test

The cumulative distribution function (CDF) of generalized extreme value distribution (GEV) (Totaro et al., 2020) can be defined as:

$$F(z, \theta_{st}) = \exp \left\{ - \left[ 1 + \varepsilon \left( \frac{z - \zeta}{\sigma} \right) \right]^{-1/\varepsilon} \right\} \quad \varepsilon \neq 0$$

$$\exp \left\{ - \exp \left[ - \left( \frac{z - \zeta}{\sigma} \right) \right]^{-1/\varepsilon} \right\} \quad \varepsilon = 0, \text{ for } \sigma > 0 \quad (5.10)$$

Where  $\zeta$ ,  $\sigma$ , and  $\varepsilon$  are the position, scale, and shape GEV parameters, respectively, where  $\theta_{st} = [\zeta, \sigma, \varepsilon]$  is a general case for stationarity. Gumbel ( $\varepsilon = 0$ ), Fréchet ( $\varepsilon > 0$ ), and

Weibull ( $\varepsilon < 0$ ) distributions are exceptional cases of GEV distribution which could be accounted for implications of non-stationarity. The traditional GEV distributions could be expressed in terms of non-stationary ( $\theta_{ns}$ ) by accounting for the function of time or any other covariates in their parameters as:

$$\theta_{st \rightarrow \theta_{ns}} = [\zeta_t, \sigma_t, \varepsilon_t] \quad (5.11)$$

In this study, only a deterministic linear dependence on the time  $t$  of the position parameter  $\zeta$  has been introduced as per Totaro et al . 2020, leading Eq. (5.10) to be expressed as follows:

$$F(z, \theta_{st}) = \exp \left\{ - \left[ 1 + \varepsilon \left( \frac{z - \zeta_t}{\sigma} \right) \right]^{-1/\varepsilon} \right\} \quad \varepsilon \neq 0$$

$$\exp \left\{ - \exp \left[ - \left( \frac{z - \zeta_t}{\sigma} \right) \right]^{-1/\varepsilon} \right\} \quad \varepsilon = 0, \text{ for } \sigma > 0 \quad (5.12)$$

With  $\zeta_t = \zeta_0 + \zeta_1 t$  and  $\theta_{ns} = [\zeta_0, \zeta_1, \sigma_t, \varepsilon_t]$ .

In the present work, maximum likelihood (ML) estimated the GEV parameters from sample data. Any hypothesis test encompasses two types of errors: type I, which is the probability of acceptance of a trend when there is none, and type II (represented as  $\beta$ ) error when rejecting an actual trend. The choice of predefined significance level alpha ( $\alpha$ ) determines the probability of type I error. The power of the hypothesis test is defined as the probability of rejecting a null hypothesis when it is false (when an actual trend exists), which is given as  $1 - \beta$ . When conducting a hypothesis test from a data sample with the false null hypothesis, test power is determined by:

$$Power = \frac{N_{rej}}{N} \quad (5.13)$$

$N$  – is the total number of simulations, and  $N_{rej}$  is the number of rejections of the null hypothesis (Yue et al. 2002). A conventional value adopted for hypothesis testing is  $\alpha = 0.05$  and  $\beta = 0.2$ , wherein the threshold power value =  $0.8$  ( $1 - \beta$ ) is acceptable. The power

of non-parametric mMK is examined using the following steps (Totaro et al. 2020; Yue et al. 2002;):

1. The Monte Carlo (MC) simulations with  $N = 2000$  for each length  $L$  are generated using GEV synthetic series with ML estimated sample data parameters using eqns 3.19 and 3.20 as a parent distribution, where  $\zeta_1 \neq 0$ .
2. The mMK test is conducted on the 2000 MC simulations for different GEV parent distributions.
3. Power is calculated as:

$$Power = \frac{N_{rej}}{N}$$

Where  $N$  – is the total number of simulations and  $N_{rej}$  is the number of rejections of the null hypothesis (Yue et al. 2002).

#### 5.2.4 Singular Spectrum Analysis (SSA)

The singular spectrum analysis (SSA) technique decomposes the complex time series into several components: trend, seasonality, periodicity, and noise. The data-adaptive basis functions (Eigenvalues of trajectory matrix) used in SSA signal decomposition and reconstruction make it a robust tool for analyzing nonlinear dynamics, unlike the conventional spectral methods. SSA employs two stages: a) decomposition and b) reconstruction. During the first stage, SSA-decomposition, a univariate time series is converted to a multi-variate form by mapping into a trajectory matrix – a Hankel matrix (Elsner and Tsonis 1996). If  $X = x_1, x_2, x_2, \dots \dots \dots x_N$  is the time series of length  $N$ , then the trajectory matrix  $Y$  can be written as

$$Y = \begin{bmatrix} x_1 & x_2 & x_3 & \cdots & x_L \\ x_2 & x_3 & x_4 & \cdots & x_{L+1} \\ \cdots & \cdots & \cdots & \cdots & \cdots \\ x_K & x_{K+1} & x_{K+2} & \cdots & x_N \end{bmatrix} \quad (5.14)$$

Where  $L$  = window length,  $K$  = lag parameter,  $K = N - L + 1$ , and  $N$  = time series length. The next step in SSA is the singular value decomposition (SVD) of the lagged covariance matrix,  $Z = Y^T Y$ . SVD yields  $Y$  in the form of  $Y = UDV^T$ , where  $U(L \times L)$  and  $V(K \times L)$  are the left and right singular vectors, and  $D$  is a diagonal matrix of square roots

of eigenvalues of the covariance matrix  $Z$ . SVD produces the trajectory matrix  $Y$  in terms of the sum of  $D$  matrix as follows:

$$Y = \sum_{i=1}^d Y_i \quad (5.15)$$

$$Y_i = U_i \sqrt{\lambda_i} V_i^T \quad (5.16)$$

Where  $\lambda_i$  is the eigenvalues of  $Z$  with  $i = 1, 2, 3, \dots, d$ , where  $d = \max(i: \sqrt{\lambda_i} > 0)$ . The set of  $(\sqrt{\lambda_i}, U_i, V_i^T)$  is called the  $i^{\text{th}}$  eigentriples. The second stage is the SSA reconstruction, which involves selecting appropriate eigenvalues and corresponding eigenvectors from SVD and then Hankelization (averaging along components of matrices) of  $(K \times L)$  matrix from selected components of the SVD leading to the reconstruction of the time-series. The method of leading eigenfunction (Alexandrov and Golyandina 2006) is applied for grouping the eigentriples during the time series reconstruction for trend extraction (Elsner and Tsonis1996). The principal components (PCs) ( $a_k$ ) are produced based on the selected leading eigenfunctions as

$$a_{ik} = \sum_{j=1}^k x_{i+j-1} e_{jk} \quad (5.17)$$

where  $e_{jk}$  is the  $j^{\text{th}}$  component of the  $k^{\text{th}}$  eigenvector. The PCs are then ranked according to eigen fraction (the ratio of the corresponding eigenvalue to the sum of total eigenvalues). In the final stage of SSA, the original time series of record  $N$  is reconstructed from the trajectory matrix by diagonal averaging the selected matrices during the grouping stage. PCs and corresponding eigenvectors are employed to reconstruct the time series for trend extraction, thereby eliminating the noise (Unnikrishnan and Jothiprakash, 2015). The reconstructed components (R) of the original time series are obtained as

$$R_{i+j-1} = \sum_{K=1}^L a_{ik} e_{jk} \quad (5.18)$$

## 5.3 RESULTS AND DISCUSSIONS

### 5.3.1 mMK and SE Rainfall Trends

The long-term trends (1950 ~2017) of gridded, as well as basin-averaged rainfall time series at annual and seasonal scales, were analyzed using the Sen's slope estimator (SE), while the statistical significance was examined by the modified Mann-Kendall trend test (mMK). The basin-wise and grid-wise trends for annual and seasonal rainfall are given in Table 5.1 and Table. 5.2. About 124 grids indicated declining trends with negative slopes for annual rainfall ( $R_{AN}$ ), out of which 34 rainfall grids portrayed significant decline at a 5% significance level. Increasing trends were observed for 44 grids, with statistical significance observed at nine grids. For convenience, the basins are referred to without the "others" phrase throughout this chapter. As observed from Fig. 5.1, the significant declining  $R_{AN}$  trends are primarily located in the Varrar basin. Among 22 grids in Varrar, declining trends were observed at 19, out of which 12 exhibited statistical significance. Statistically significant, declining  $R_{AN}$  trends were observed for five grids in the Periyar basin, seven in Netravati and Vasishi basins, and two in the Bhatsol basin. Significant increasing  $R_{AN}$  trends were obtained for one grid each in the Periyar and Netravati basins, while five grids in the Vasishti and two in the Bhatsol basin. Furthermore, basin-wise trends for  $R_{AN}$  revealed a significant decline of -8.6mm/year, i.e., a decrease of 3.8% of average  $R_{AN}$  per decade observed for the Varrar basin (5% significance level). A reduction of -3.87mm/year, -5.09mm/year, and -0.24mm/year were obtained for  $R_{AN}$  trends in the Periyar, Netravati, and Bhatsol basins. While an increase of +1.05mm/year for  $R_{AN}$  was indicated in the Vasishti basin, as given in Table 5.1.

Examination of winter rainfall ( $R_{WN}$ ) trends indicated a more significant number of increasing trends at 109 grids, with six grids exhibiting statistically significant results. The slopes for increasing  $R_{WN}$  were very meagre, though identified as statistically significant. The declining trends for  $R_{WN}$  were observed for 59 grids, with statistically significant trends at four grids (Table 5.2 and Fig. 5.1). Four grids in the Vasishti basin and two in the Netravati indicated significant rising trends for  $R_{WN}$ . Nevertheless, the slope obtained is meagre. A significant decline in the  $R_{WN}$  was observed at two grids each in the Periyar and Varrar basins. The basin-wise  $R_{WN}$  trends portrayed a significant increase of +0.01mm/year, i.e., an increase of 5.8% of average  $R_{WN}$  per decade in the Vasishti basin. The decadal departures for  $R_{WN}$  also supplement the above results with excess winter rainfall observed after the year 1990 in the basin, as discussed in Chapter 4. A decrease of

-0.16mm/year, -0.04mm/year for the Periyar and Varrar basins, while an increase of +0.02mm/year was obtained for the Netravati basin, as given in Table 5.1.

Pre-monsoon rainfall ( $R_{PRM}$ ) displayed declining trends at 141 grids, with statistical significance portrayed by 21 grids. On the other hand, just 27 grids among the west coast basins indicated rising  $R_{PRM}$  trends, and statistical significance was observed at none, as given in Table 5.2. A significant decline of 4.5% of the average  $R_{PRM}$  per decade (-1.15mm/year) was observed in the Varrar basin. Pre-monsoon rainfall indicated a decrease of -1.22mm/year, -0.57mm/year, -0.42mm/year, and -0.05mm/year for the Periyar, Netravati, Vasishti, and Bhatsol basins.

Similar to the annual rainfall trends, the southwest monsoon ( $R_{SW}$ ) rainfall displayed declining trends at 121 grids out of 168. Statistical significance was obtained at 33 grids, as presented in Table 5.2 and Fig. 5.1. While increasing  $R_{SW}$  trends were indicated by 47 grids, 11 grids exhibited statistical significance for  $R_{SW}$ . As observed for  $R_{AN}$  trends, the Varrar basin exhibited significant declining trends for 14 grids out of 22 grids in the basin. Seven grids exhibited statistical  $R_{SW}$  decline in the Periyar basin, six in the Netravati, three in Vasishti, and two in the Bhatsol basin. A significant increase in  $R_{SW}$  was obtained at two grids in Netravati, five in Vasishti, and three in the Bhastol basins. As observed from Table 5.1, a significant decrease of -2.48mm/year (-1.9% decrease of average  $R_{SW}$  / decade), -6.57mm/year (-4.2% decrease of average  $R_{SW}$  /decade), and -5.34mm/year (-1.7% decrease of average  $R_{SW}$  decrease at 5% significance level was identified in the Periyar, Varrar, and Netravati basins respectively.

A decrease of -0.53mm/year was indicated by the Bhatsol basin, while an increase of +2.37mm/year for  $R_{SW}$  was observed in the Vasishti basin. Increasing  $R_{SW}$  could be attributed to the increase in the annual rainfall for the Vasishti basin (Table 5.1). Alike annual rainfall trends, the  $R_{SW}$  trends also indicated declining trends in the Periyar, Varrar, and Netravati basins, indicating a propensity to droughts in the future.

Post-monsoon rainfall ( $R_{POM}$ ) indicated declining trends in 89 grids out of 168 grids, of which 16 exhibited statistical significance. Vasishti basin showed a significant decline in 6 grids, followed by four in Varrar and Netravati and two in the Periyar basin. A significant increase was observed in two grids in Bhatsol and one in the Periyar basin. 79 grids indicated a rise in post-monsoon rainfall, with statistical significance confined to just three grids, as given in Table 5.2. Though basin-wise  $R_{POM}$  trends indicated a decrease among the west coast basins, none were significant. A decreasing  $R_{POM}$  of -0.36mm/year,

-0.55mm/year, -0.44mm/year, -0.72mm/year were identified in Periyar, Varrar, Netravati, and Vasishti basins, respectively, as presented in Table 5.1. While an insignificant increasing  $R_{POM}$  of +0.2mm/year was observed in the Bhatsol basin. The mMK and SE trends obtained for rainfall grids are given in Fig. 5.1. Significant increasing trends are represented by upward arrows and significant decreasing trends by downward arrows.

**Table 5.1 Basin-wise mMK and SE trends of annual and seasonal rainfall**

<b>Sub-basins</b>	<b><math>R_{AN}</math> (mm/year)</b>	<b><math>R_{WN}</math> (mm/year)</b>	<b><math>R_{PRM}</math> (mm/year)</b>	<b><math>R_{SW}</math> (mm/year)</b>	<b><math>R_{POM}</math> (mm/year)</b>
Periyar	-3.87	-0.16	-1.22	<b>-2.48</b>	-0.36
Varrar	<b>-8.60</b>	-0.04	<b>-1.15</b>	<b>-6.57</b>	-0.55
Netravati	-5.09	0.02	-0.57	<b>-5.34</b>	-0.44
Vasishti	1.05	<b>0.01</b>	-0.42	2.37	-0.72
Bhatsol	-0.24	0.02	-0.05	-0.53	0.20

Note: Bold indicates significant trends at a 5% significance level.

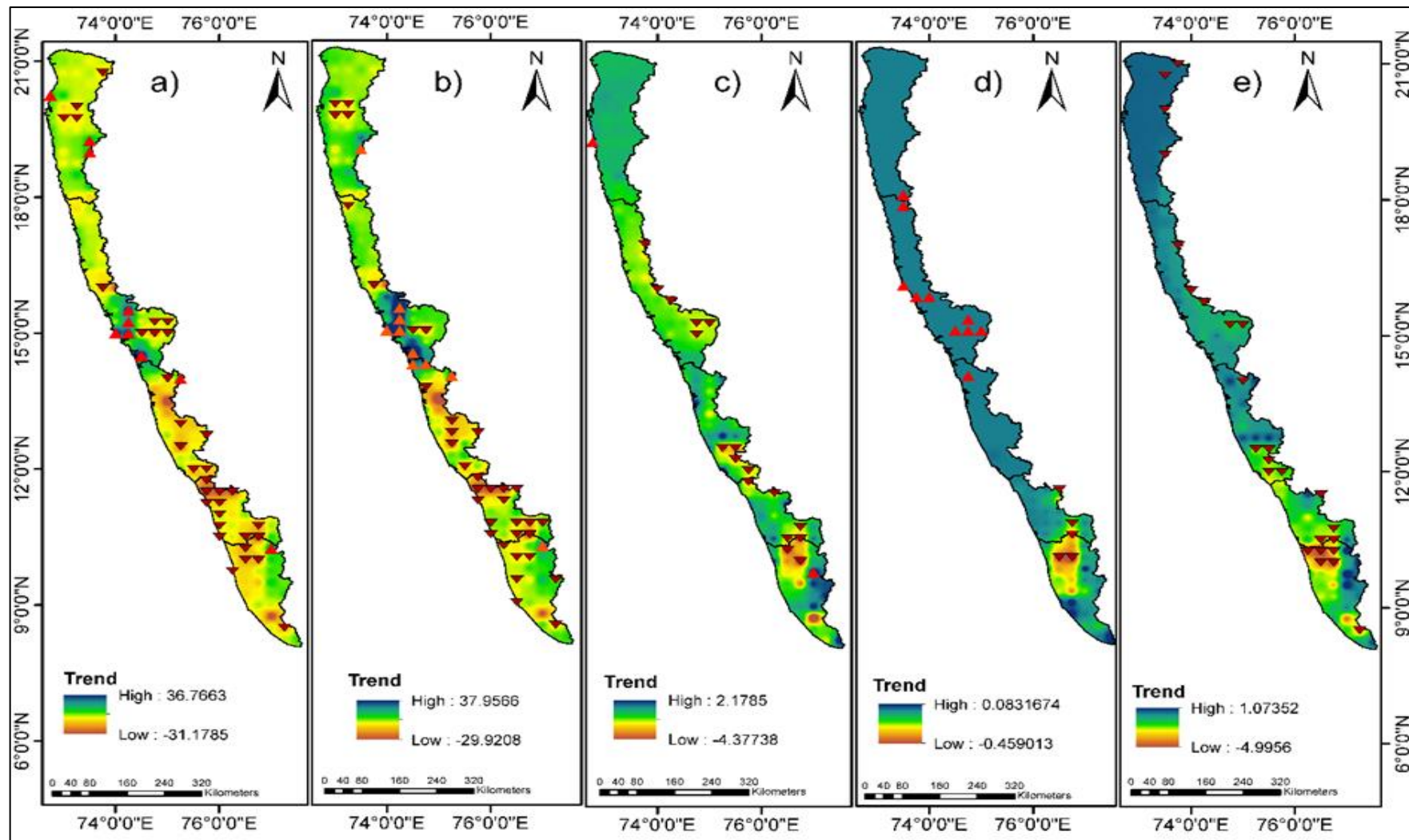


**Fig. 5.1** Rainfall trends for a) annual, b) southwest monsoon, c) pre-monsoon, d) winter and e) post-monsoon by mMK and SE



**Table 5.2 Grid-wise Mmk and SE trends of annual and seasonal rainfall**

<b>IMD-grid</b>	<b>Sub-basin</b>	<b>R<sub>AN</sub></b> <b>(mm/year)</b>	<b>R<sub>WN</sub></b> <b>(mm/year)</b>	<b>R<sub>PRM</sub></b> <b>(mm/year)</b>	<b>R<sub>SW</sub></b> <b>(mm/year)</b>	<b>R<sub>POM</sub></b> <b>(mm/year)</b>
101	Periyar	-2.5	-0.02	-0.8	-1.2	-0.9
102	Periyar	2.2	0.07	0.0	0.2	1.5
103	Periyar	-3.0	-0.14	-1.4	-1.0	-0.2
104	Periyar	<b>-11.9</b>	<b>-0.08</b>	<b>-3.0</b>	-7.6	-0.3
105	Periyar	-5.2	0.01	-0.4	-6.0	0.4
106	Periyar	-24.4	-0.01	-2.8	-17.7	-3.9
107	Periyar	-4.1	0.05	-0.9	-3.8	0.6
108	Periyar	-0.4	0.05	-0.4	-2.3	0.7
109	Periyar	-2.2	-0.01	0.1	-3.5	2.0
110	Periyar	-7.6	-0.15	-1.7	-5.3	-0.4
111	Periyar	-4.7	-0.31	-1.3	-3.1	0.3
112	Periyar	1.9	-0.11	-0.3	-0.4	0.8
113	Periyar	3.3	0.01	0.1	0.3	1.3
114	Periyar	-7.1	-0.11	-1.2	-5.6	-0.4
115	Periyar	-10.5	-0.24	-2.4	-5.9	-2.3
116	Periyar	7.4	0.00	0.9	5.0	1.4
117	Periyar	0.2	0.00	-0.2	-1.7	0.9
118	Periyar	-4.4	0.00	-0.7	-2.6	0.1
119	Periyar	-7.3	-0.19	-1.5	-4.0	-1.2
120	Periyar	-2.3	-0.23	-1.8	0.1	-1.4
121	Periyar	3.9	0.09	1.2	0.3	<b>2.5</b>
122	Periyar	-5.4	-0.07	-1.9	-4.1	1.0
123	Periyar	<b>-13.4</b>	<b>-0.36</b>	<b>-3.0</b>	-8.1	-2.0
124	Periyar	<b>-19.6</b>	<b>-0.47</b>	<b>-4.4</b>	-10.4	<b>-3.8</b>
125	Periyar	4.2	-0.01	-0.7	3.4	0.0
126	Periyar	2.5	0.00	0.6	1.6	0.3
127	Periyar	<b>-7.4</b>	<b>-0.03</b>	<b>-3.4</b>	-4.5	0.1
128	Periyar	<b>-14.4</b>	<b>-0.18</b>	<b>-4.7</b>	-7.6	<b>-3.6</b>
129	Periyar	-5.7	-0.25	-1.7	-2.2	-2.1
130	Periyar	<b>14.7</b>	<b>0.00</b>	<b>1.2</b>	12.5	-0.1
131	Varrar	<b>-8.2</b>	<b>0.00</b>	<b>-1.9</b>	-5.6	0.3
132	Varrar	-3.3	0.00	-0.9	-2.5	0.8
133	Varrar	<b>-9.2</b>	<b>-0.07</b>	<b>-1.3</b>	-7.2	<b>-1.3</b>
134	Varrar	<b>-27.4</b>	<b>-0.30</b>	<b>-2.5</b>	-22.4	<b>-3.2</b>
135	Varrar	4.0	0.00	0.2	1.8	0.6
136	Varrar	-4.8	0.00	-1.6	-2.4	-0.4

Note: Bold indicates significant trends at a 5% significance level.

IMD-grid	Sub-basin	R <sub>AN</sub> (mm/year)	R <sub>WN</sub> (mm/year)	R <sub>PRM</sub> (mm/year)	R <sub>SW</sub> (mm/year)	R <sub>POM</sub> (mm/year)
137	Varrar	-2.6	0.00	-1.0	-1.0	0.1
138	Varrar	<b>-7.4</b>	<b>0.00</b>	<b>-1.6</b>	-4.9	-1.1
139	Varrar	<b>-14.3</b>	<b>-0.17</b>	<b>-1.6</b>	-11.9	-1.5
140	Varrar	-1.5	0.00	-0.7	-1.2	0.2
141	Varrar	<b>-2.0</b>	<b>0.00</b>	<b>-1.0</b>	-1.9	0.3
142	Varrar	-6.6	0.00	-2.0	-3.4	-1.2
143	Varrar	0.6	0.00	-0.7	1.4	-0.3
144	Varrar	<b>-5.7</b>	<b>0.00</b>	<b>-1.5</b>	-4.7	0.9
145	Varrar	<b>-7.1</b>	<b>0.00</b>	<b>-0.9</b>	-5.2	0.0
146	Varrar	-6.8	-0.05	-0.4	-6.0	-0.6
147	Varrar	3.5	-0.13	-0.8	2.7	1.2
148	Varrar	<b>-24.1</b>	<b>-0.01</b>	<b>-1.7</b>	-19.8	-1.2
149	Varrar	<b>-24.8</b>	<b>0.00</b>	<b>-0.8</b>	-21.9	-0.9
150	Varrar	<b>-25.3</b>	<b>0.00</b>	<b>0.2</b>	-23.1	<b>-1.7</b>
151	Varrar	<b>-5.6</b>	<b>-0.08</b>	<b>-0.7</b>	-3.5	-0.6
152	Netravati	-6.2	0.00	-2.0	-3.8	0.2
153	Varrar	<b>-17.0</b>	<b>0.00</b>	<b>-1.8</b>	-11.8	<b>-2.3</b>
154	Netravati	0.0	0.00	-1.2	0.5	1.5
155	Netravati	<b>-14.5</b>	<b>0.00</b>	<b>-1.8</b>	-11.8	-0.6
156	Netravati	<b>-5.1</b>	<b>0.00</b>	<b>-1.1</b>	-3.3	<b>-1.2</b>
157	Netravati	-4.1	0.02	-1.0	-2.4	-1.3
158	Netravati	-2.6	0.00	-1.8	-0.3	<b>-2.1</b>
159	Netravati	<b>-6.0</b>	<b>0.01</b>	<b>-0.5</b>	-5.3	0.5
160	Netravati	<b>-21.3</b>	<b>0.00</b>	<b>-2.1</b>	-17.3	<b>-3.1</b>
161	Netravati	-4.9	0.00	-1.6	-1.0	<b>-2.9</b>
162	Netravati	-2.0	0.00	0.1	-4.1	0.3
163	Netravati	<b>-11.6</b>	<b>0.00</b>	<b>0.4</b>	-13.6	1.3
164	Netravati	-8.2	0.00	0.4	-11.0	0.6
165	Netravati	<b>-6.0</b>	<b>0.00</b>	<b>0.0</b>	-5.7	0.1
166	Netravati	-1.6	0.00	-0.8	-0.7	-0.7
167	Netravati	-6.3	0.00	-1.0	-5.8	-0.6
168	Netravati	<b>-9.9</b>	<b>0.00</b>	<b>-0.2</b>	-11.0	0.2
169	Netravati	-9.3	0.00	-0.3	-8.1	-0.6
170	Netravati	-2.2	0.00	-0.3	-1.7	0.2
171	Netravati	-14.2	0.00	-0.7	-13.0	-1.4
172	Netravati	-9.1	0.00	-0.4	-11.0	1.3
173	Netravati	-30.4	0.00	0.1	-28.3	-0.5

Note: Bold indicates significant trends at a 5% significance level.

IMD-grid	Sub-basin	R <sub>AN</sub> (mm/year)	R <sub>WN</sub> (mm/year)	R <sub>PRM</sub> (mm/year)	R <sub>SW</sub> (mm/year)	R <sub>POM</sub> (mm/year)
174	Netravati	-12.7	0.00	-0.2	-14.4	0.6
175	Netravati	-9.6	0.00	-0.1	-9.0	-1.1
176	Netravati	1.2	0.00	-0.4	3.5	-1.1
177	Netravati	-1.1	0.00	0.4	-2.0	0.7
178	Netravati	-9.4	0.00	-0.7	-6.6	-0.7
179	Netravati	<b>6.1</b>	<b>0.00</b>	<b>0.3</b>	4.6	0.6
180	Netravati	6.6	0.00	-0.1	6.7	-0.1
181	Netravati	7.9	0.00	-0.2	6.8	0.1
182	Vasishti	<b>33.4</b>	<b>0.00</b>	<b>-0.5</b>	35.7	0.2
183	Vasishti	5.5	0.00	-0.4	4.2	0.1
184	Vasishti	-2.3	0.00	-0.4	-1.7	0.0
185	Vasishti	8.1	0.00	-0.3	9.1	-0.5
186	Vasishti	-4.7	0.00	-0.1	-5.4	-0.5
187	Vasishti	<b>24.3</b>	<b>0.00</b>	<b>-0.2</b>	24.9	0.1
188	Vasishti	<b>23.3</b>	<b>0.00</b>	<b>-0.8</b>	26.6	-0.9
189	Vasishti	<b>-14.3</b>	<b>0.00</b>	<b>0.0</b>	-13.3	-0.7
190	Vasishti	<b>-16.7</b>	<b>0.00</b>	<b>-0.7</b>	-15.1	<b>-1.2</b>
191	Vasishti	<b>-3.2</b>	<b>0.00</b>	<b>-0.5</b>	-2.0	-1.0
192	Vasishti	-2.8	0.00	-0.5	-1.7	-0.5
193	Vasishti	<b>12.8</b>	<b>0.00</b>	<b>-0.6</b>	14.0	-0.4
194	Vasishti	-3.9	0.00	-0.6	-2.9	-0.5
195	Vasishti	<b>-3.4</b>	<b>0.00</b>	<b>-1.2</b>	-1.1	<b>-1.3</b>
196	Vasishti	<b>-3.3</b>	<b>0.00</b>	<b>-0.9</b>	-1.0	<b>-1.0</b>
197	Vasishti	-0.1	0.00	-0.3	0.1	-0.5
198	Vasishti	-1.8	0.00	-0.3	1.7	-0.7
199	Vasishti	<b>27.5</b>	<b>0.00</b>	<b>-0.6</b>	29.7	-0.7
200	Vasishti	-6.6	0.00	-0.4	-5.2	-1.0
201	Vasishti	-2.0	0.00	-0.6	-1.2	-0.9
202	Vasishti	-4.0	0.00	0.0	-3.7	-0.5
203	Vasishti	8.1	0.00	-0.5	9.7	-0.7
204	Vasishti	14.1	0.00	-1.1	16.7	<b>-1.2</b>
205	Vasishti	-2.0	0.00	-0.1	-1.1	-0.2
206	Vasishti	<b>-10.8</b>	<b>0.00</b>	<b>-0.1</b>	-10.4	-0.6
207	Vasishti	-19.9	0.00	-1.1	-17.4	<b>-1.5</b>
208	Vasishti	-4.4	0.00	0.0	-4.7	-0.7
209	Vasishti	-6.0	0.00	-0.3	-5.9	-1.0
210	Vasishti	-1.3	0.00	-0.1	-1.1	-0.5

Note: Bold indicates significant trends at a 5% significance level.

IMD-grid	Sub-basin	R <sub>AN</sub> (mm/year)	R <sub>WN</sub> (mm/year)	R <sub>PM</sub> (mm/year)	R <sub>SW</sub> (mm/year)	R <sub>POM</sub> (mm/year)
211	Vasishti	-5.6	0.00	-0.4	-4.4	-0.7
212	Vasishti	-2.1	0.00	-0.2	-1.5	-0.8
213	Vasishti	-6.5	0.00	-0.5	-4.8	-1.2
214	Vasishti	4.8	0.00	0.0	4.4	-0.5
215	Vasishti	-2.4	0.00	-0.2	-2.5	-0.8
216	Vasishti	-2.9	0.00	-0.7	-1.4	<b>-1.1</b>
217	Vasishti	2.2	0.00	-0.1	1.7	-0.4
218	Vasishti	-2.1	0.00	-0.3	-2.2	-0.6
219	Vasishti	-3.3	0.00	-0.1	-3.1	-0.2
220	Vasishti	-3.6	0.00	-0.1	-3.0	-0.6
221	Vasishti	<b>-8.1</b>	<b>0.00</b>	<b>0.0</b>	-7.4	-0.8
222	Vasishti	-0.6	0.00	-0.3	-0.5	-0.5
223	Bhastol	-2.7	0.00	0.0	-3.2	0.3
224	Bhastol	-6.7	0.00	-0.1	-6.5	-0.4
225	Bhastol	-7.6	0.00	-0.3	-7.4	-0.3
226	Bhastol	0.0	0.00	0.0	-0.4	0.0
227	Bhastol	0.4	0.00	0.0	0.3	-0.4
228	Bhastol	5.7	0.00	-0.4	6.1	-0.1
229	Bhastol	1.2	0.00	0.0	1.0	0.0
230	Bhastol	7.0	0.00	0.0	6.2	0.4
231	Bhastol	-3.4	0.00	0.0	-3.9	0.2
232	Bhastol	-2.3	0.00	0.0	-2.0	0.2
233	Bhastol	5.0	0.00	0.0	4.7	0.3
234	Bhastol	-4.9	0.00	0.0	-6.0	0.1
235	Bhastol	1.4	0.00	0.0	0.8	0.2
236	Bhastol	<b>7.0</b>	<b>0.00</b>	<b>-0.2</b>	6.0	0.3
237	Bhastol	4.7	0.00	0.0	4.9	<b>0.4</b>
238	Bhastol	-0.2	0.00	0.0	0.1	0.0
239	Bhastol	1.5	0.00	0.0	0.7	0.0
240	Bhastol	<b>10.6</b>	<b>0.00</b>	<b>-0.1</b>	10.6	0.1
241	Bhastol	3.4	0.00	0.0	3.2	0.5
242	Bhastol	-2.9	0.00	0.0	-2.8	0.1
243	Bhastol	-3.9	0.00	0.0	-4.5	0.3
244	Bhastol	-2.2	0.00	0.0	-1.8	0.3
245	Bhastol	1.6	0.00	0.0	0.9	0.3
246	Bhastol	-7.8	0.00	0.0	-8.6	0.0
247	Bhastol	-6.5	0.00	0.0	-6.9	0.2
248	Bhastol	-1.5	0.00	0.0	-1.3	0.1

Note: Bold indicates significant trends at a 5% significance level.

IMD-grid	Sub-basin	R <sub>AN</sub> (mm/year)	R <sub>WN</sub> (mm/year)	R <sub>PM</sub> (mm/year)	R <sub>SW</sub> (mm/year)	R <sub>POM</sub> (mm/year)
249	Bhastol	2.7	0.00	0.0	2.4	0.3
250	Bhastol	-6.4	0.00	0.0	-7.2	0.3
251	Bhastol	<b>-7.2</b>	<b>0.00</b>	<b>0.0</b>	-8.1	0.3
252	Bhastol	1.6	0.00	-0.1	1.9	0.0
253	Bhastol	6.4	0.00	0.0	5.6	0.3
254	Bhastol	6.2	0.00	0.0	5.5	<b>0.5</b>
255	Bhastol	-2.1	0.00	0.0	-1.6	0.2
256	Bhastol	-2.7	0.00	0.0	-3.0	0.2
257	Bhastol	-1.4	0.00	0.0	-2.0	0.2
258	Bhastol	-1.8	0.00	0.0	-2.1	0.3
259	Bhastol	-3.0	0.00	0.0	-3.2	0.3
260	Bhastol	-4.5	0.00	0.0	-4.0	0.1
261	Bristol	-4.3	0.00	0.0	-4.2	0.0
262	Bhastol	-1.5	0.00	0.0	-1.6	0.2
263	Bhastol	<b>-6.9</b>	<b>0.00</b>	<b>-0.1</b>	-6.1	0.2
264	Bhastol	0.3	0.00	0.0	0.4	0.0
265	Bhastol	-1.1	0.00	0.0	-1.1	0.0
266	Bhastol	-2.3	0.00	0.0	-2.0	0.0
267	Bhastol	-4.8	0.00	0.0	-4.5	0.0
268	Bhastol	-3.3	0.00	0.0	-3.1	0.1

Note: Bold indicates significant trends at a 5% significance level.

### 5.3.2 Power of mMK Test

The power of the modified Mann-Kendall (mMK) test was analyzed to examine the influence of parent distribution parameters on the power of the Mann-Kendall test, which is assumed to be a distribution-free test. The Monte Carlo simulation experiments were conducted for  $N = 2000$  for series length  $L$  (which in this study is rainfall series length = 68), using generalized extreme value distributions (GEV) for non-stationarity in the position parameter ( $\zeta$ ) using a linear trend ( $\zeta_t$ ) dependent on time  $t$ . For brevity, the power analysis of the annual rainfall series is discussed in this section.

The numerical investigation of the test power was performed using different GEV parameter sets obtained from the maximum likelihood (ML) estimated GEV parameter values for the annual rainfall series. The position parameter was given a constant value of  $\zeta_0 = 2500$ . The linear trend  $\zeta_t$  ranged from -30 to +30 with a step size of 2. The values selected for the scale parameter are  $\sigma = (200, 400, 600, 800, 1000, 1200)$ , and for the shape parameter  $\epsilon$ , the values fixed are  $(0.4, 0.2, 0, -0.2, -0.4)$ . The predefined significance level  $\alpha$  was equal to 0.05, and the length  $L$  was set to 68 (dataset length). A power of 0.8 is

considered an acceptable threshold value (Totaro et al. 2020) under the null hypothesis of no trend.

The test power for different generation sets of  $\sigma$  and  $\varepsilon$  for  $L=68$  and a fixed range of  $\zeta_1$  is given in Fig 5.2 (a-e). The power ranges from the predefined significance level of  $\alpha = 0.05$  (at  $\zeta_1=0$ ) to 1 for increasing values of the trend coefficient ( $\zeta_1$ ) under the null hypothesis of stationarity for all the generated GEV non-stationary sets. For a given trend, the test power collapses (slopes gentle) for higher values of  $\sigma$  and  $\varepsilon$ . For a given value of  $\varepsilon$  and  $\zeta_1$ , the power varies with  $\sigma$ . The power curve slopes more gently for heavy-tailed distribution ( $\varepsilon = +0.4$ ) for the given values of  $\zeta_1$  and  $\sigma$  and reaches a threshold value of 0.8 for higher values of  $\zeta_1$ , as given in Fig. 5.2 (e). The ML-estimated GEV parameters for the annual rainfall series for the entire study area are given in Table 5.3. For similar values of  $\zeta_1=23\text{mm/year}$ , the test power shows considerable difference based on  $\varepsilon$  and  $\sigma$ , as seen for *grd\_187* and *grd\_173*. Higher  $\sigma = 1333$  and  $\varepsilon = 0.38$  for *grd\_173* caused a drop in test power below 0.7 for  $\zeta_1=23\text{mm/year}$  (Fig. 5.2 c&e). Strong trends of practical significance could be accepted under the null hypothesis of stationarity due to parent distribution parameters owing to a lower power than the threshold value of 0.8. This inference is depicted for *grd\_173* and *grd\_178* (Table 5.3). Similar observations were discerned for a few other grids where distribution parameters influence the test power for a considerable value of  $\zeta_1$ .

The effect of series length on test power was analyzed for a constant  $\varepsilon = -0.4$  and  $\sigma = 400$ , as given in Fig. 5.2f. The test power considerably drops below the threshold of 0.8 for smaller sample lengths ( $L = 30$ ) for a given trend coefficient  $\zeta_1$ . For the present study, rainfall series have a good length, substantiating a threshold test power of 0.8 by the mMK for most grid trends. This study's groundwater level (GWL) series have a smaller length (1996 ~ 2017), causing a drop in test power. However, extreme events are primarily associated with rainfall compared to GWLs; numerical investigations on test power and the attainment of associated power to the threshold of 0.8 for rainfall series account for more importance under changing climatic scenarios. The above observations, therefore, ascertain the effects of parent distributions on the non-parametric mMK test's test power and the test power's inability to reach a threshold value of 0.8 in many grids with a significant trend coefficient. The investigations on test power indicated the probability of rejecting non-stationarity in the assessment of trend detection based on sample size and heavy-tailed distributions for a given trend coefficient. Owing to the lowering of test power below 0.8

for specific grids as investigated in this study, rather than solely relying on trends identified by statistical tests, it is advisable to incorporate subsidiary methods to ascertain the trend detection studies as in the case of singular spectrum analysis (SSA) in this study

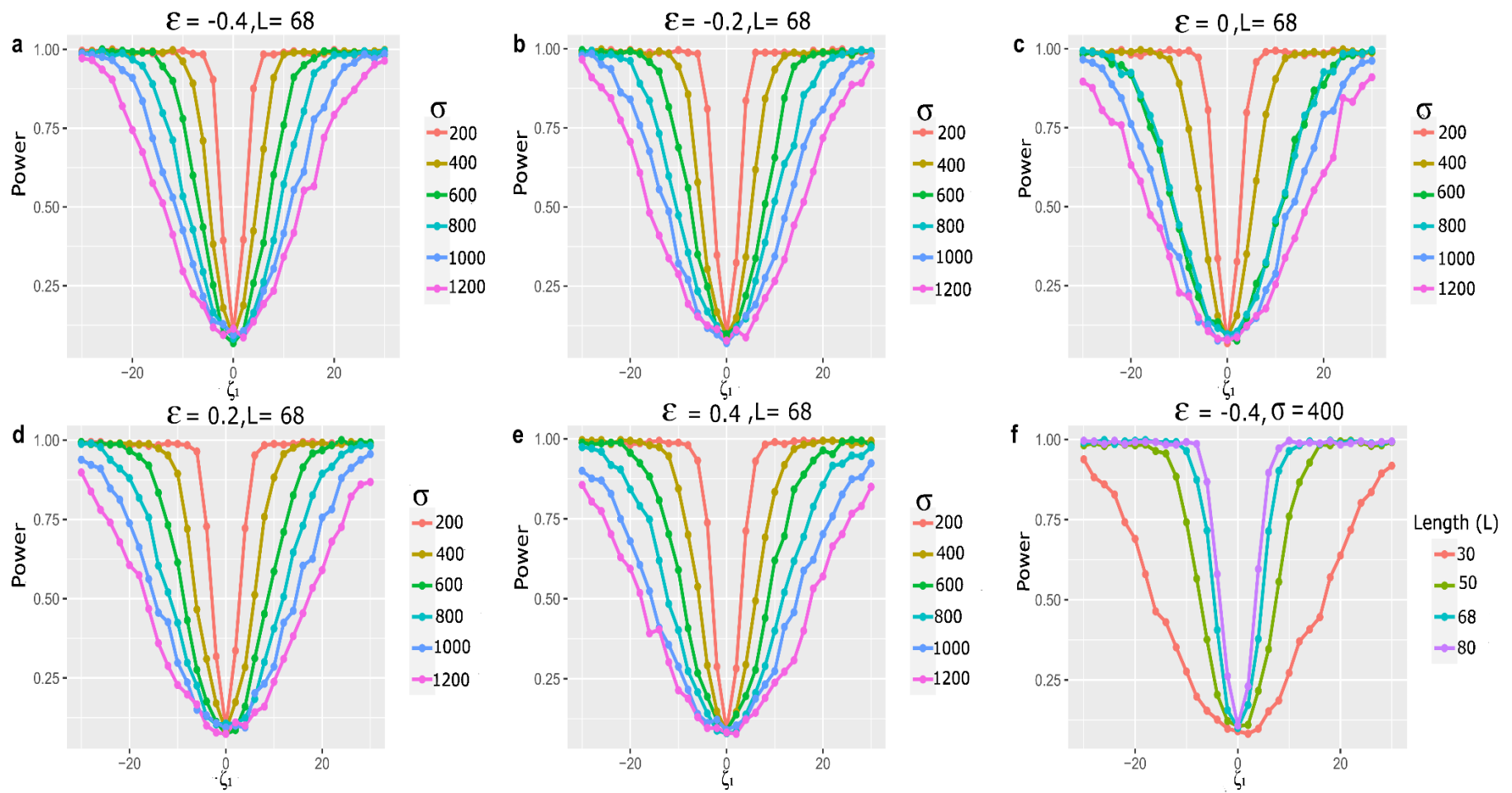


**Fig. 5.2** Test power analysis of mMK with varying position, scale, and shape parameters



**Table 5.3 ML estimated GEV parameters for annual rainfall time series**

Grids	$\zeta_0$	$\zeta_1$	$\sigma$	$\varepsilon$
grd_101	1171.3	-3.94	285.55	-0.11
grd_102	512.0	1.02	255.11	-0.10
grd_103	1587.5	-1.95	365.77	-0.31
<b>grd_104</b>	<b>1875.6</b>	<b>-10.89</b>	<b>468.87</b>	<b>-0.27</b>
grd_105	2175.1	-9.44	646.46	-0.38
grd_106	1714.5	-6.05	774.68	0.25
grd_107	2248.4	-3.71	412.97	-0.25
grd_108	2508.8	-4.81	719.74	-0.52
grd_109	1854.8	1.95	639.28	-0.46
grd_110	2501.1	-4.33	499.35	-0.17
grd_111	2603.5	-3.20	652.12	-0.19
grd_112	1087.7	-0.92	353.92	-0.07
grd_113	642.6	2.19	256.62	-0.08
grd_114	2949.2	-7.66	573.59	-0.35
grd_115	3134.6	1.46	999.70	-0.46
grd_116	1559.3	10.04	676.24	-0.31
grd_117	895.8	-4.29	267.09	0.01
<b>grd_118</b>	<b>2837.9</b>	<b>-5.14</b>	<b>545.74</b>	<b>-0.15</b>
grd_119	3131.7	-5.35	684.73	-0.36
grd_120	2815.1	0.98	799.80	-0.34
grd_121	1379.8	1.19	511.68	-0.17
grd_122	2980.4	-4.85	583.97	-0.28
<b>grd_123</b>	<b>3468.4</b>	<b>-12.88</b>	<b>624.92</b>	<b>-0.26</b>
<b>grd_124</b>	<b>3726.3</b>	<b>-19.05</b>	<b>792.81</b>	<b>-0.08</b>
grd_125	1994.1	1.63	766.43	-0.02
grd_126	651.5	-2.32	190.05	0.33
grd_127	2962.7	-4.41	696.53	-0.44
<b>grd_128</b>	<b>3036.9</b>	<b>-7.73</b>	<b>706.80</b>	<b>-0.23</b>
grd_129	2797.6	-1.97	989.51	-0.22
<b>grd_130</b>	<b>929.7</b>	<b>13.43</b>	<b>451.65</b>	<b>-0.07</b>
<b>grd_131</b>	<b>2913.3</b>	<b>-7.58</b>	<b>649.21</b>	<b>-0.33</b>
grd_132	2565.4	-3.90	559.73	-0.23
<b>grd_133</b>	<b>2203.8</b>	<b>-10.05</b>	<b>390.07</b>	<b>-0.07</b>
<b>grd_134</b>	<b>3183.4</b>	<b>-31.42</b>	<b>699.27</b>	<b>-0.32</b>
grd_135	478.6	1.81	266.90	0.01
<b>grd_136</b>	<b>2597.0</b>	<b>-7.01</b>	<b>490.57</b>	<b>-0.14</b>
grd_137	2329.1	-4.31	481.34	-0.16
grd_138	1742.3	-3.03	471.90	-0.24
<b>grd_139</b>	<b>2006.6</b>	<b>-16.11</b>	<b>371.69</b>	<b>-0.27</b>

Note: Bold indicates significant trends at 5% significance level.

Grids	$\zeta_0$	$\zeta_1$	$\sigma$	$\varepsilon$
grd_140	721.3	-3.97	193.27	0.06
<b>grd_141</b>	<b>2680.8</b>	<b>-5.39</b>	<b>500.36</b>	<b>-0.13</b>
grd_142	2344.8	-5.36	592.11	-0.18
grd_143	1443.1	-1.32	390.50	-0.17
<b>grd_144</b>	<b>3106.6</b>	<b>-7.74</b>	<b>568.91</b>	<b>-0.13</b>
<b>grd_145</b>	<b>2741.6</b>	<b>-8.44</b>	<b>502.49</b>	<b>-0.14</b>
grd_146	2530.3	-7.67	557.59	-0.26
grd_147	1042.6	2.60	447.94	-0.36
<b>grd_148</b>	<b>3812.5</b>	<b>-26.03</b>	<b>700.38</b>	<b>-0.05</b>
<b>grd_149</b>	<b>2777.0</b>	<b>-9.49</b>	<b>686.16</b>	<b>-0.03</b>
<b>grd_150</b>	<b>3346.9</b>	<b>-22.40</b>	<b>985.93</b>	<b>-0.21</b>
grd_151	1372.0	1.06	488.12	-0.48
<b>grd_152</b>	<b>3409.6</b>	<b>-6.56</b>	<b>538.27</b>	<b>-0.11</b>
grd_153	3101.2	-16.93	597.86	-0.22
grd_154	3163.9	0.07	545.93	-0.14
<b>grd_155</b>	<b>3765.9</b>	<b>-11.91</b>	<b>712.97</b>	<b>-0.11</b>
<b>grd_156</b>	<b>2027.3</b>	<b>-4.25</b>	<b>477.76</b>	<b>-0.13</b>
grd_157	4517.6	-2.67	934.83	-0.23
grd_158	3441.2	-0.99	842.50	-0.08
grd_159	3438.7	-2.02	484.75	0.00
<b>grd_160</b>	<b>4745.6</b>	<b>-19.28</b>	<b>782.65</b>	<b>-0.17</b>
grd_161	3682.0	-4.63	687.43	-0.23
grd_162	3795.4	-1.87	544.24	-0.04
grd_163	4311.5	-12.79	639.58	-0.08
grd_164	3333.2	-4.71	975.66	-0.13
<b>grd_165</b>	<b>1743.5</b>	<b>-6.33</b>	<b>389.39</b>	<b>-0.11</b>
grd_166	3510.6	-2.86	530.97	-0.07
grd_167	3958.5	-3.81	542.45	-0.01
<b>grd_168</b>	<b>4064.9</b>	<b>-7.98</b>	<b>534.48</b>	<b>-0.01</b>
grd_169	2412.8	-9.95	508.53	0.04
grd_170	4117.6	-0.88	827.34	-0.25
grd_171	4156.3	-14.77	972.08	-0.17
grd_172	4875.6	-9.22	855.48	-0.09
grd_173	4238.1	-23.45	1333.30	0.38
grd_174	4535.4	-1.64	1040.62	-0.04
grd_175	3966.4	-1.91	1068.66	-0.13
grd_176	4073.3	-0.02	594.84	-0.02
grd_177	2994.3	-2.35	949.59	-0.30
<b>grd_178</b>	<b>2074.7</b>	<b>-9.55</b>	<b>448.70</b>	<b>0.37</b>
<b>grd_179</b>	<b>923.2</b>	<b>2.24</b>	<b>286.13</b>	<b>0.21</b>
grd_180	3604.0	8.20	718.84	-0.16

Note: Bold indicates significant trends at 5% significance level.

Grids	$\zeta_0$	$\zeta_1$	$\sigma$	$\varepsilon$
grd_181	2773.7	5.81	649.26	-0.04
<b>grd_182</b>	<b>3043.5</b>	<b>25.80</b>	<b>1064.67</b>	<b>-0.01</b>
grd_183	2381.2	1.71	618.53	-0.20
grd_184	3354.0	-1.58	498.97	-0.07
grd_185	2890.4	1.53	723.24	-0.10
grd_186	2089.4	-4.67	455.50	-0.07
<b>grd_187</b>	<b>2427.6</b>	<b>23.78</b>	<b>1069.04</b>	<b>-0.05</b>
<b>grd_188</b>	<b>3034.1</b>	<b>11.86</b>	<b>969.39</b>	<b>0.20</b>
<b>grd_189</b>	<b>2594.1</b>	<b>-13.22</b>	<b>463.44</b>	<b>0.06</b>
<b>grd_190</b>	<b>2020.2</b>	<b>-16.40</b>	<b>392.45</b>	<b>-0.07</b>
<b>grd_191</b>	<b>1035.5</b>	<b>-3.84</b>	<b>212.20</b>	<b>0.13</b>
grd_192	3360.1	0.11	859.12	-0.22
<b>grd_193</b>	<b>2730.3</b>	<b>9.76</b>	<b>753.81</b>	<b>-0.15</b>
grd_194	1793.0	-3.08	401.24	0.09
<b>grd_195</b>	<b>1138.6</b>	<b>-5.96</b>	<b>199.53</b>	<b>0.19</b>
<b>grd_196</b>	<b>801.8</b>	<b>-4.20</b>	<b>150.62</b>	<b>0.00</b>
grd_197	2707.6	0.50	480.44	-0.22
grd_198	3846.4	2.71	1059.18	-0.30
<b>grd_199</b>	<b>2128.5</b>	<b>27.36</b>	<b>967.09</b>	<b>-0.27</b>
grd_200	1795.1	-9.69	414.10	0.06
grd_201	968.5	-2.79	199.74	-0.05
grd_202	3027.5	0.44	654.45	-0.38
grd_203	2956.7	12.26	1155.99	-0.23
grd_204	1922.2	10.22	871.83	-0.05
grd_205	2819.7	0.17	608.67	-0.23
<b>grd_206</b>	<b>3612.8</b>	<b>-14.30</b>	<b>848.42</b>	<b>-0.40</b>
grd_207	2296.9	-23.76	694.95	-0.19
grd_208	3339.4	-4.34	691.40	-0.27
grd_209	3446.7	-8.41	680.36	-0.44
grd_210	3654.7	3.85	926.75	-0.43
grd_211	4727.7	2.40	1368.70	-0.28
grd_212	3481.2	-1.38	774.78	-0.49
grd_213	2766.2	-5.37	764.10	-0.22
grd_214	2648.5	6.89	683.10	-0.43
grd_215	3069.2	1.24	647.54	-0.34
grd_216	1743.8	-2.33	383.38	-0.01
grd_217	2780.9	2.70	629.79	-0.29

Note: Bold indicates significant trends at 5% significance level.

Grids	$\zeta_0$	$\zeta_1$	$\sigma$	$\varepsilon$
grd_218	2849.5	-3.14	519.55	-0.26
grd_219	3145.7	-2.94	616.04	-0.18
grd_220	3418.6	-6.03	675.38	-0.15
grd_221	3657.8	-6.80	687.18	-0.34
grd_222	3668.4	2.66	768.91	-0.36
grd_223	3056.5	-3.98	612.14	-0.13
grd_224	3797.9	-8.72	755.00	-0.36
grd_225	4785.3	-5.85	1284.57	-0.39
grd_226	3022.8	-0.30	628.58	-0.15
grd_227	3392.8	0.69	638.59	-0.28
grd_228	2431.1	2.02	697.23	0.04
grd_229	3038.3	1.45	704.74	-0.29
grd_230	3297.5	6.62	792.73	-0.28
grd_231	2877.2	-4.17	779.02	-0.37
grd_232	3467.0	-3.18	784.04	-0.07
grd_233	1930.3	2.98	492.84	-0.21
grd_234	2879.6	-5.90	628.96	-0.29
grd_235	3208.3	0.50	713.15	-0.25
<b>grd_236</b>	<b>1415.9</b>	<b>4.24</b>	<b>380.06</b>	<b>0.29</b>
grd_237	1939.5	5.19	575.64	-0.19
grd_238	2275.1	-0.09	469.13	-0.10
grd_239	2342.2	0.65	650.51	-0.25
<b>grd_240</b>	<b>1321.1</b>	<b>9.72</b>	<b>538.52</b>	<b>-0.09</b>
grd_241	2108.9	2.18	458.16	-0.18
grd_242	2497.4	-3.14	522.39	-0.15
grd_243	2468.7	-3.34	537.29	-0.10
grd_244	2490.2	-1.72	599.94	-0.24
grd_245	1987.4	0.60	552.79	-0.18
<b>grd_246</b>	<b>2768.4</b>	<b>-8.61</b>	<b>574.62</b>	<b>-0.14</b>
<b>grd_247</b>	<b>2780.7</b>	<b>-6.36</b>	<b>539.07</b>	<b>-0.12</b>
grd_248	2847.1	-1.71	780.66	-0.28
grd_249	1737.7	2.09	512.08	-0.09
grd_250	2448.9	-5.41	505.70	-0.03
<b>grd_251</b>	<b>2465.7</b>	<b>-7.01</b>	<b>484.39</b>	<b>-0.14</b>
grd_252	1562.6	0.02	439.87	0.01
<b>grd_253</b>	<b>1474.2</b>	<b>5.06</b>	<b>383.25</b>	<b>0.06</b>
grd_254	1672.9	7.26	506.33	0.01
grd_255	1962.6	-0.79	489.86	-0.17
grd_256	1719.9	-1.81	493.15	-0.21
grd_257	1907.2	-0.06	564.96	-0.17

Note: Bold indicates significant trends at 5% significance level.

<b>Grids</b>	$\zeta_0$	$\zeta_1$	$\sigma$	$\epsilon$
grd_258	1858.0	0.25	517.67	-0.15
grd_259	1760.2	-1.12	480.05	-0.14
grd_260	1650.0	-0.49	480.89	-0.06
grd_261	1826.0	-3.05	452.33	-0.06
grd_262	1799.0	-2.60	635.89	-0.14
<b>grd_263</b>	<b>1286.2</b>	<b>-0.95</b>	<b>482.55</b>	<b>-0.16</b>
grd_264	1193.2	2.31	418.32	0.01
grd_265	1224.1	0.21	377.93	0.03
grd_266	1302.6	0.40	452.13	-0.10
grd_267	1357.6	-0.98	427.90	-0.09
grd_268	1071.8	-1.30	301.19	0.02

Note: Bold indicates significant trends at 5% significance level.

### 5.3.3 SSA- Rainfall Trends

Having analyzed the effect of parent distribution on the test power of modified Mann-Kendall (mMK), the trends with practical importance may not be considered significant by mMK due to parent distribution parameters. Hence it is essential to extract the trend-trajectory and change points, if any. The singular spectrum analysis (SSA) was conducted to examine the trend trajectory for both annual and seasonal rainfall and is discussed in this section. However, this section discusses SSA-extracted sample grid trends for brevity. The SSA extracted trends for total of 168 grids for annual rainfall are given in Appendix 2. The window length (L) was adopted as 34 ( $L = N/2$ ). The leading eigenvectors with slowly varying components were chosen to reconstruct the time series. The annual rainfall ( $R_{AN}$ ) trends extracted by SSA for sample grids is given in Fig. 5.3 As discussed in the power analysis section, some of the grids with a practical slope were not identified by mMK, which could be accredited to parent distribution parameters. Therefore, extraction of trend trajectory would enable understanding the temporal variations for slopes identified as insignificant.

The  $R_{AN}$  trend for grid 106 (Periyar Basin) was identified as an insignificant trend (Table 5.2) by mMK. However, the SSA-trend for grid 106 indicated a monotonic trend sloping downward from 1960 onwards with an approximate slope of 29mm/year (from SSA) from Fig. 5.3. This is comparable to the Sen's slope value of 24.11mm/year (Table 5.2). Grid 116 exhibited first decreasing slope from 1950 to 1960 and non-monotonic rising slopes from 1960 to 1980 and from 1990 to 2017 (Fig 5.3), complementing the SE trends. The SSA extracted a downward slope for grid 142 (Varrar basin) with different slopes for

the periods 1950 to 1965, 1970 to 1990 and 1990 to 2017 following the rainfall regimes. Grid 135 exhibited nearly a flat slope from 1950 to 1975, a mild rise from 1970 to 1980, followed by a flat slope from 1980 to 2000 and a rising limb after 2000. The Sen's slope (SE) identified an increasing slope of +3.99mm/year for the grid, which is identical to the SSA trend for the rising limb between 700mm and 1000mm over a period of 68 years, i.e., + 4.4mm/year as the increase in rainfall was visible only in the later years.

Grid173 (Netravati basin) exhibited a continuous downward slope up to 2010, after which a mild rise is visible from the SSA- trend trajectory. Though Sen's slope identified a profound slope of 31.4mm/year, mMK failed to identify it as significant, which could be attributed to the parent distribution parameters for the data as given in Table 5.3. Similarly, the SSA identified a monotonously increasing slope from 1960 to 2013 in the grid 180. The SE value was obtained as +6.5mm/year, while from SSA, we can decipher a slope of + 5.88mm/year for the rising curve.

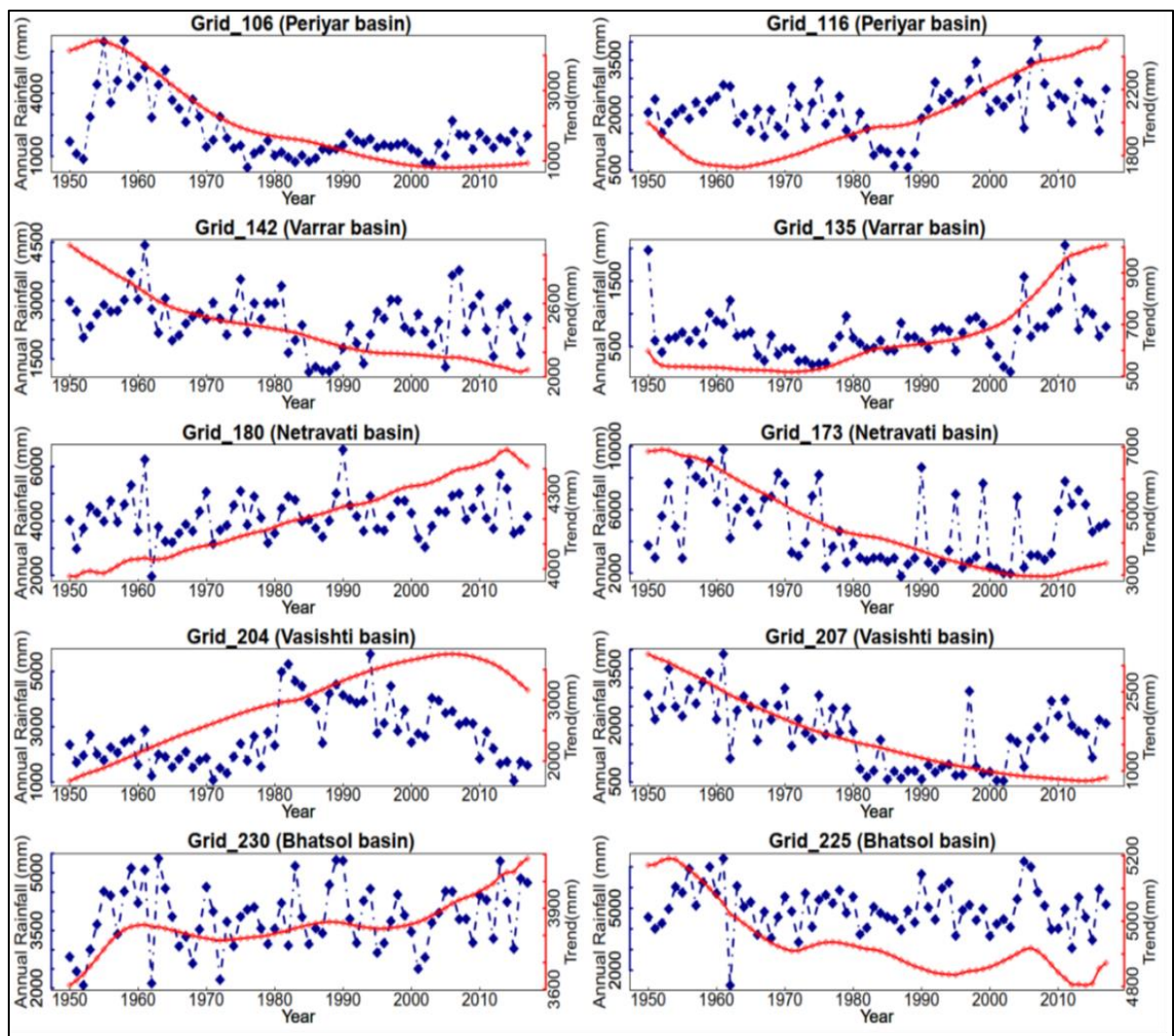


**Fig. 5.3 SSA extracted annual rainfall trends at selected sample grids**

Grid 207 (Vasishti basin) exhibited a steep downward slope till 2000, after which the slope flattened, as shown in Fig. 5.3. However, the mMK identified the slope as insignificant though an appreciable slope of -19.9mm/year from SE analysis and an approximate slope of 22mm/year from SSA which was identified for the grid (Table 5.2). A similar observation could be obtained for Grid 204, where an upward slope from 1950 to 2000 was observed. SE value obtained was +14.11mm/year, and the SSA slope was approximately +17.64mm/year. Grid 225 (Bhatsol basin) exhibited a non-monotonic and non-linear trend with downward and upward slopes for a short period throughout the data record. A similar non-linear trajectory was captured for  $R_{AN}$  at grid 230.

Trends for winter rainfall ( $R_{WN}$ ) extracted using SSA for sample grids are given in Fig. 5.4 As discussed in chapter 4, Netravati, Vasishti, and Bhatsol basins receive meager amounts of  $R_{WN}$  and indicated non-linear trends with almost flat slopes during early decades, while the abrupt rise in the later years. The erratic distribution of  $R_{WN}$  could be observed from the trend lines extracted with non-monotonous nature by SSA. Grid 129 (Periyar) exhibited highly non-linear declining trends, while grid 134 (Varrar) exhibited a continuous downward slope. Grids 102 (Periyar) and 150 (Varrar) indicated rising slopes, although years with scanty rainfall could impact the values of the rising slopes. Grids 161 and 177 (Netravati), 211 and 190 (Vasishti), also 238 and 228 (Bhatsol) basins have indicated zero slopes by Sen's slope estimator. Even though mMK identified grids 177 and 190 as significant (Table 5.2), their trend trajectories show flat slopes except for a rise after 2000. Examination of the trend lines implied that the grids identified with statistical significance exhibited very meagre or zero slope values by the SE method for  $R_{WN}$  which is in accordance with SSA trends obtained. The identification of statistical significance could be attributed to the significant rainfall totals that have occurred during the later years in these grids.

The pre-monsoon ( $R_{PRM}$ ) trends indicated a similar trajectory as that of  $R_{WN}$  with non-monotonic and non-linear trends following the uneven rainfall distribution during the data record as given in Fig.5.5. Grid 120 (Periyar) exhibited downward up to 2000 and upward curve from 2000 onwards. Grids 131 (Varrar) and 152 (Netravati) displayed steep downward slopes. However, after 2000, the slopes flattened due to some above-normal rainfall events. The SE extracted slopes for grids 131, and 152 were -1.87mm/year and -1.97mm/year, which complies with the SSA slopes of -2.2m/year and -2.9mm/year, respectively. Grids 188 (Vasishti) and 260 (Bhatsol) indicated downward slopes with greater scanty rainfall years, which is visible from their trend-lines and also from the

meagre SE values from Table 5.2. Sen's slope indicated mild increasing slopes for 130, 150 and 163, though the trend trajectory indicated highly non-linear and non-monotonic trajectories. Grid 202 is the only grid in the Vasishti basin with an increasing SE value for pre-monsoon, a negligible trend (Table 5.2). The trend trajectories agree with the meagre SE slope value of +0.0017mm/year for grid 202. Grid 234 indicated a flat slope due to scanty rainfall totals up to 1990 and then a rising curve due to above-normal events as given in Fig. 5.5.

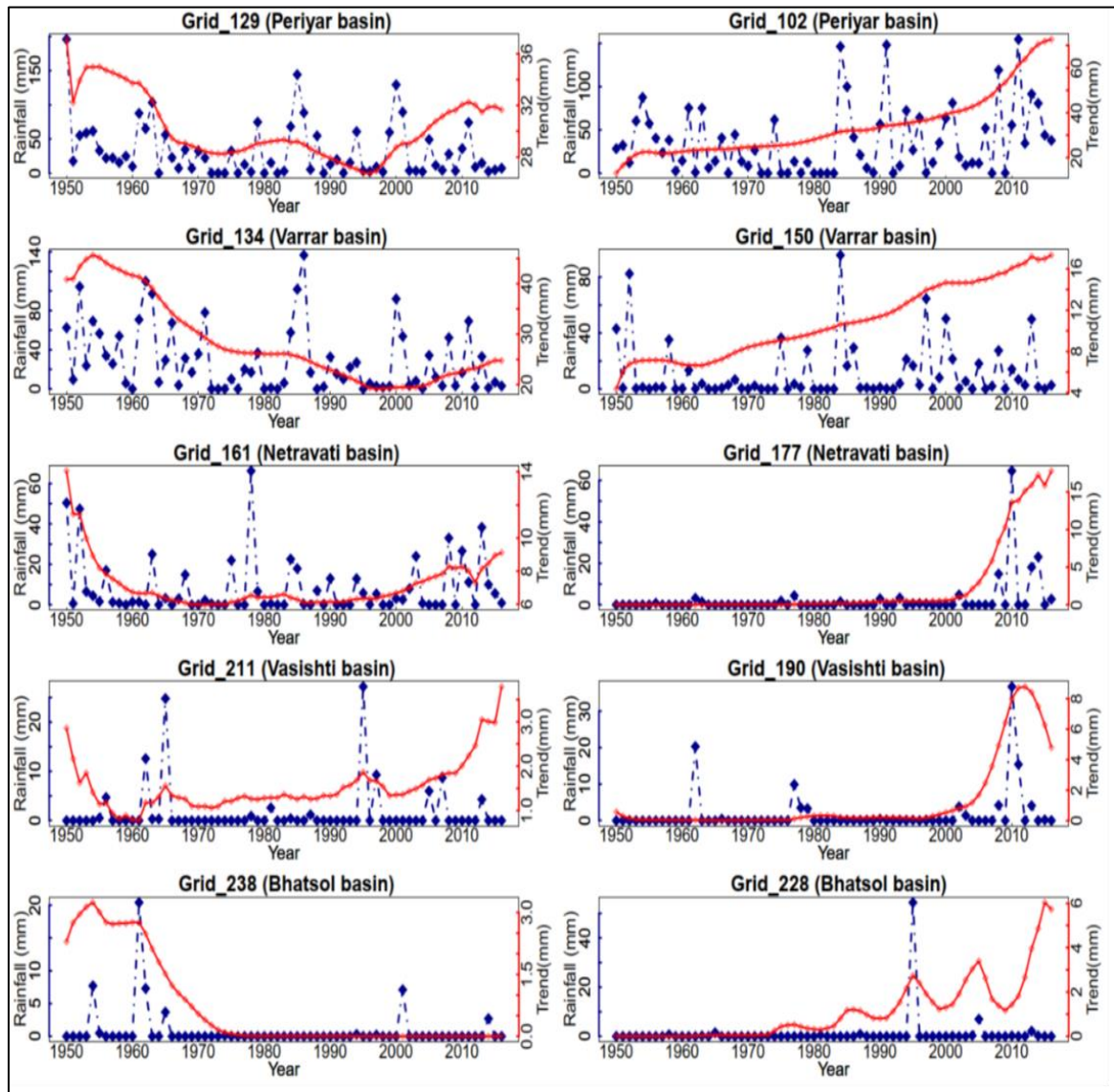


**Fig. 5.4 SSA extracted winter rainfall trends at sample grids**



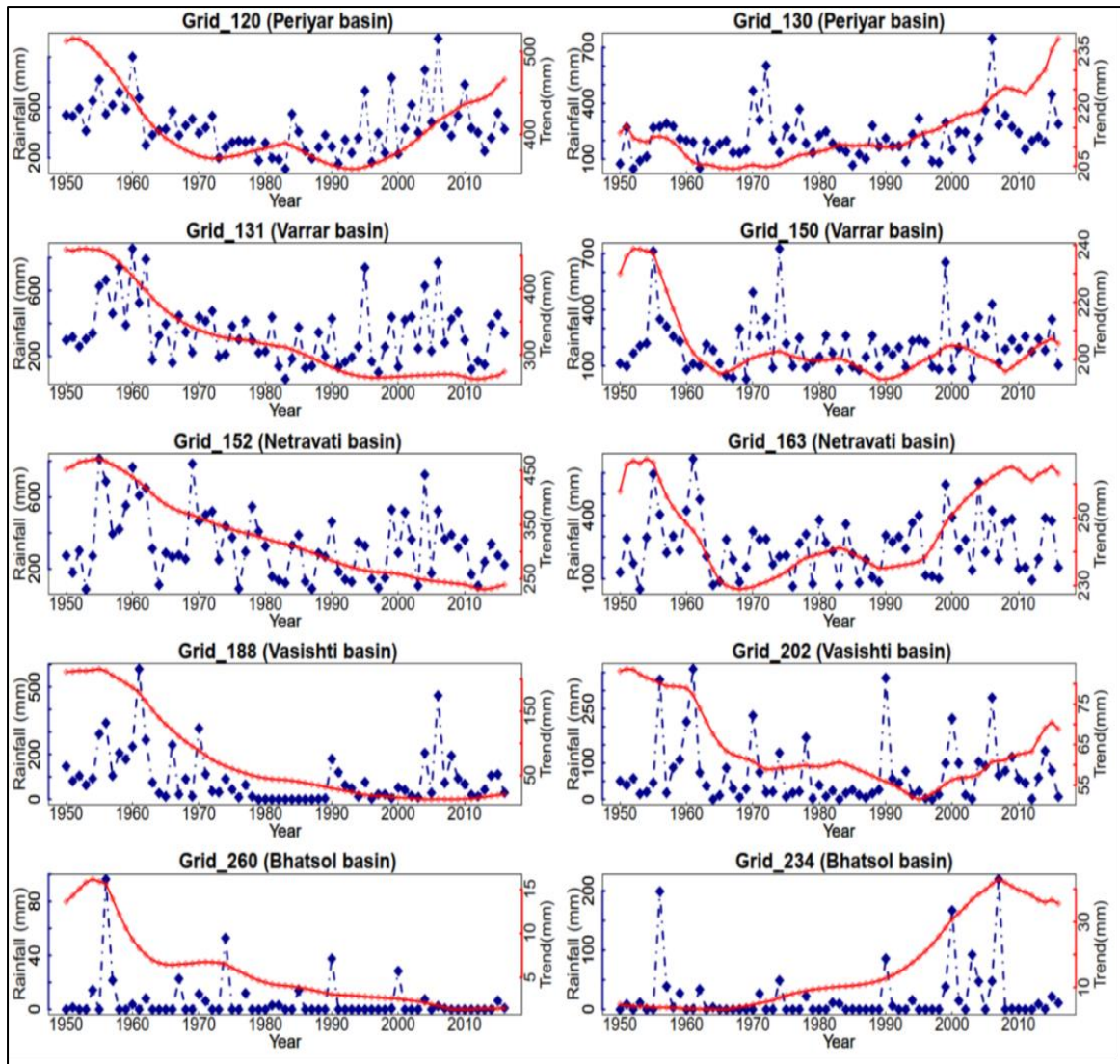


**Fig. 5.5 SSA extracted pre-monsoon rainfall trends at sample grids**

The trajectories for southwest monsoon trends ( $R_{sw}$ ) displayed prominent declining trends for grid 106 (Periyar) and grid 149 (Varrar) as given in Fig.5.6. However, as discussed in the mMK test power analysis section, grid 106 was identified as insignificant  $R_{sw}$  trend even though a substantial slope of  $-17.65\text{mm/year}$  was indicated in Table 5.2, as well as a slope of  $-22\text{mm/year}$  was obtained from SSA. The substantial slope of  $-21.9\text{mm/year}$  identified by SE for grid 149 is supplementing the monotonous trajectory of  $-22\text{mm/year}$  extracted by SSA. An upward climb was observed for grid 130 (Periyar) with a SE value of  $+12.5\text{mm/year}$ , while the SSA slope was estimated to an approximate value of  $+11.76\text{mm/year}$ . Grid 147 (Varrar) displayed an unevenly mild slope up to 2000, followed by a rise. Grids 173 and 176 (Netravati) exhibited monotonic downward and upward slopes respectively. Though identified with a considerable slope of  $-28.25\text{mm/year}$  by Sen's slope and approximately  $-29.8\text{mm/year}$  from SSA trends for grid 173, the parental

distribution could be attributed to the acceptance of the null hypothesis of no significant trend by mMK. SE identified a slope of  $-17.36\text{mm/year}$  and  $+16.7\text{mm/year}$  for 207 and 203 in Fig. 5.6 respectively. Examining their SSA trends, monotonous slopes of appreciable values are visible for the RSW series, even though considered statistically insignificant (Table 5.2). Bhatsoil grids 224 and 228 exhibited undulating decreasing and increasing slopes respectively.

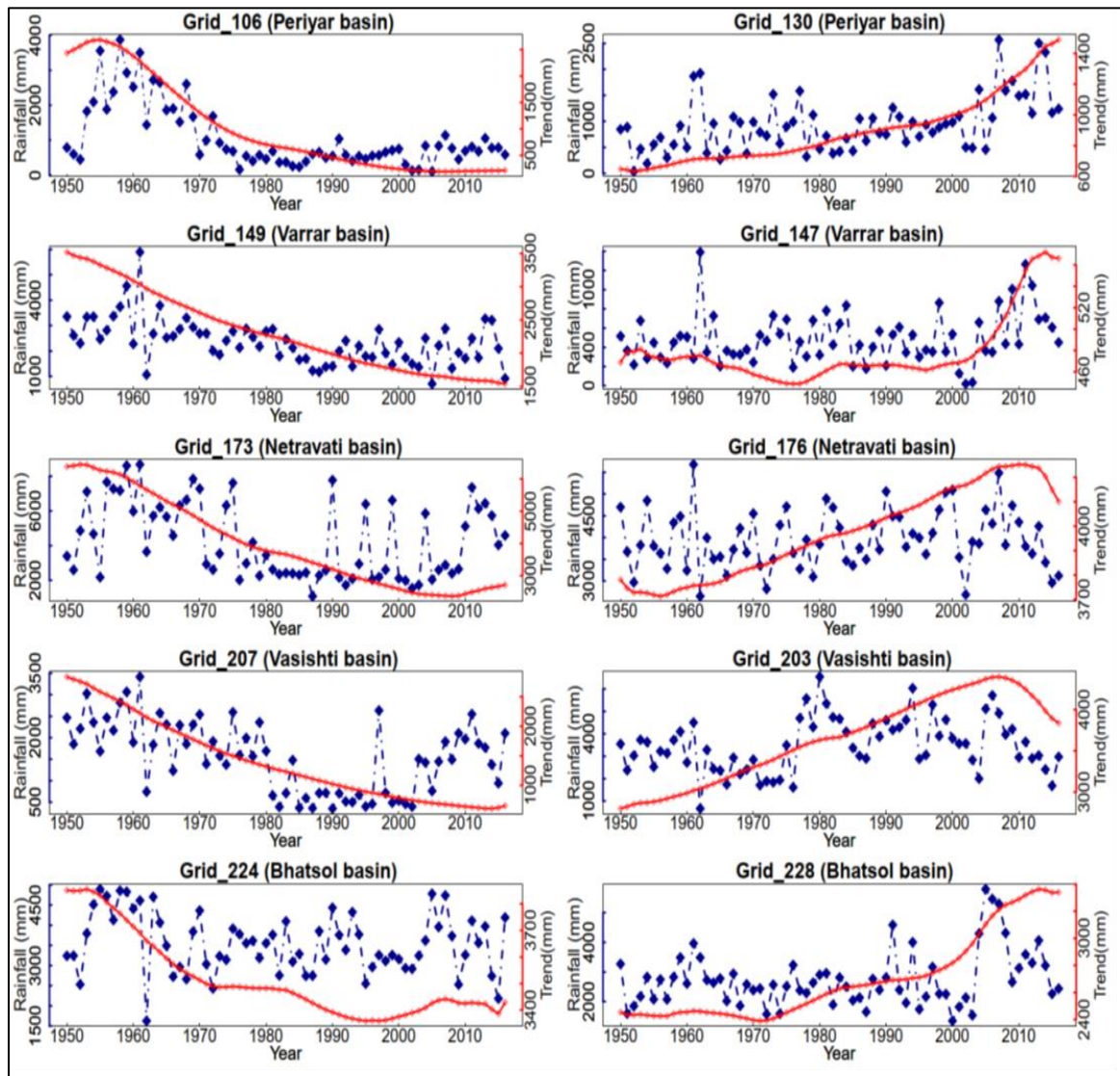


**Fig. 5.6 SSA extracted southwest monsoon rainfall trends at sample grids**

A steady declining slope of approximately  $-3\text{mm/year}$  for grid 124 and  $-1.8\text{mm/year}$  for grid 134 was exhibited by post-monsoon rainfall ( $R_{\text{POM}}$ ) using SSA as in Fig. 5.7. The SSA obtained non-linear and non-monotonic decreasing trajectories for grids 171, 213 and 224. Undulating rising curves were indicated by grids 121, 132, 154, 182, and 241 for the  $R_{\text{POM}}$  trends. As observed in the rainfall and departure analysis from chapter 4, the post-

monsoon rainfall exhibited temporal variability as indicated by non-linear and non-monotonous trend trajectories.

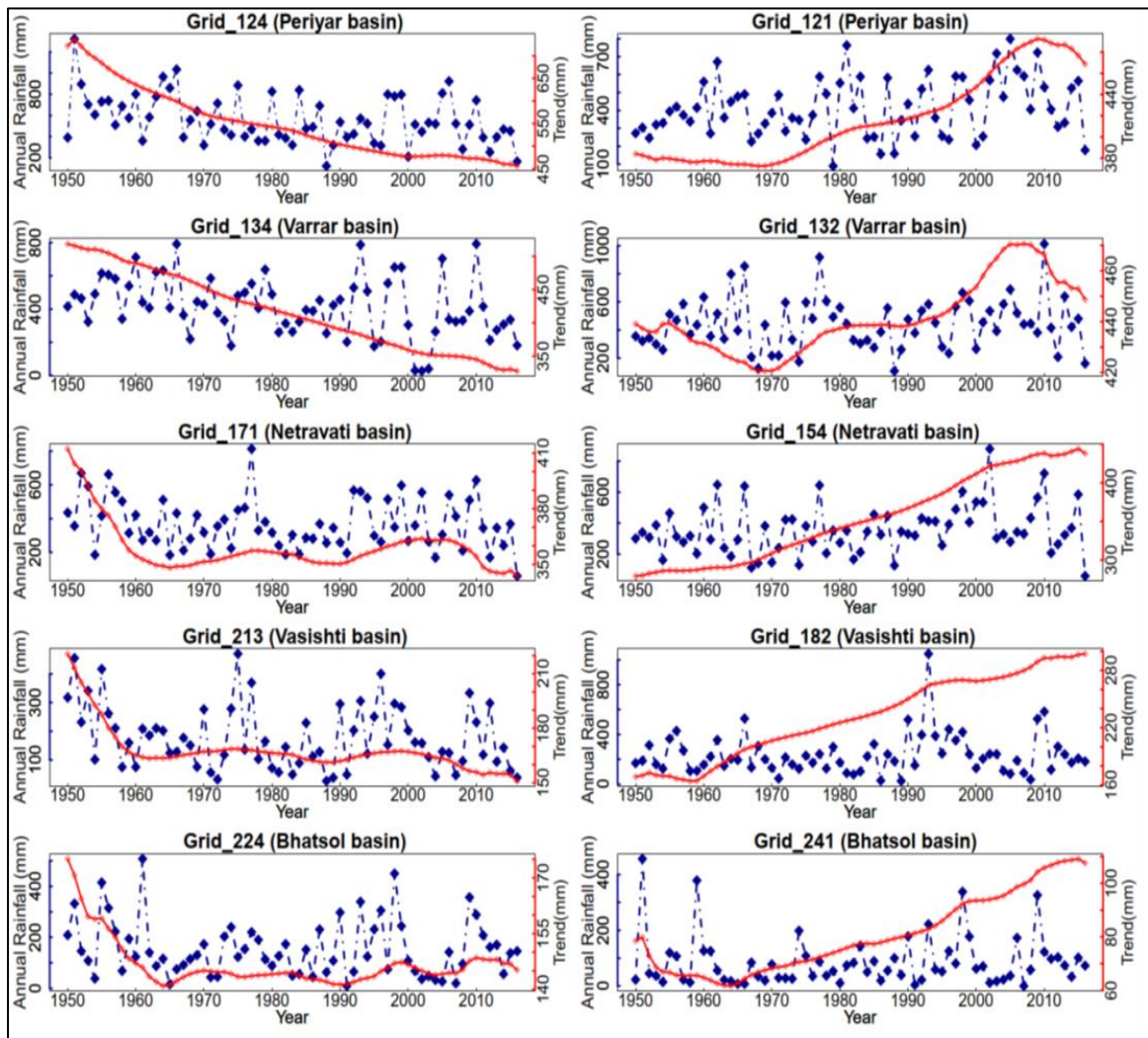


**Fig. 5.7 SSA extracted post-monsoon rainfall trends at sample grids**

### 5.3.4 mMK and SE Groundwater Level Trends

Investigation of groundwater level (GWL) trends of 418 wells located in the west coast basins was conducted using the Sen's slope estimator (SE) and their statistical significance was examined by the modified Mann-Kendall test (mMK). Trend detection aims to analyze the responses of GWLs to external stressors mainly climatic and anthropogenic. The GWL dataset from 1996 to 2017 was analyzed for winter, pre-monsoon, monsoon and post-monsoon seasons obtained from Central Ground Water Board (CGWB). The basin-wise distribution of average GWL trends is given in Table 5.4. The season wise GWL trends are presented in Fig. 5.8. The results indicated that only a subset of wells portrayed significant trends. Significant declines in the GWLs were observed at an average slope of  $-0.05\text{m/year}$  (18.3% wells) in Bhatsol,  $-0.06\text{m/year}$  (17.2% wells) in

Vasishti , -0.07m/year (11.5% wells) in Netravati, -0.06m/year (8.4% wells) in Varrar and -0.03m/year (6.6% wells) in the Periyar basins for the winter season. While 10% wells displayed significant increasing GWL trends at an average slope of +0.05m/year in the Bhatsol basin, 15.2% of wells at +0.07m/year in the Vasishti basin, 10.1% of wells at +0.02m/year in the Netravati basin, 10.4% wells at +0.03m/year in the Varrar basin and 11.5% well at an average slope of +0.05m/year in the Periyar basin for the winter season as given in Table 5.4. For the pre-monsoon season, significant decline at an average slope of -0.11m/year (21% wells) in Bhastol basin, -0.1m/year (23.4% wells) in Vasishti basin, -0.13m/year (9.6% wells) in Netravati basin, -0.09m/year (13.3% wells) in Varrar basin and -0.04m/year (7.7% wells) in the Periyar basin was observed. However, the season also witnessed rising trends as well. Significant rise at an average slope of +0.12m/year (8.7% wells) in Bhatsol, +0.1m/year (4.7% wells) in Vasishti, +0.09m/year (12% wells) in Netravati, +0.07m/year (12.21% wells) in Varrar and +0.06m/year (10.3% wells) in the Periyar basin were obtained. Significant decline of -1.34m/year (17.3% wells) in Bhatsol, -0.046m/year (7.8% wells) in Vasishti, -0.08m/year (10.6% wells) in Netravati, -0.07m/year (16% wells) in Varrar and -0.05m/year (10.3% wells) in the Periyar basins were indicated by mMK test. Significant rise at an average slope of +0.05m/year (4.3% wells) in Bhatsol, +0.05m/year (8.6% wells) in Netravati, -0.05m/year (4.7% wells) in Varrar and +0.08m/year (6.7% wells) in the Periyar basin were exhibited by mMK trends for the monsoon season.

Significant decline of -0.05m/year (10% wells) in Bhatsol, -0.06m/year (15.6% wells) in Vasishti, -0.09m/year (3.3% wells) in Netravati, -0.06m/year (10.4% wells) in Varrar and -0.05m/year (13.9% wells) in the Periyar basins were obtained for the post-monsoon season. A significant rise of 0.1m/year (1.7% wells) in Bhatsol, 0.05m/year (6.3% wells) in Vasishti, -0.06m/year (6.6% wells) in Netravati, -0.02m/year (3.8% wells) in Varrar and -0.1m/year (3.3% wells) in the Periyar basins was indicated by the post-monsoon GWLs. Both significant decline and rise were exhibited by the GWLs in the study area nevertheless, the percentage of insignificant trends was prominent as seen in Table 5.4. Also, the Sen's slope trend values obtained were mild i.e. between +0.05m/year to -0.05m/year for majority of observation wells, except a sub-set of wells. This could be attributed to the short data length of GWLs and also the above and below-normal rainfall years that occurred throughout the time frame. It could be observed from Fig. 5.8 that the wells belonging to the slope class between -0.05m/year and +0.05/year are greater in number. The mMK and SE trends for 418 wells are given in Appendix 3.

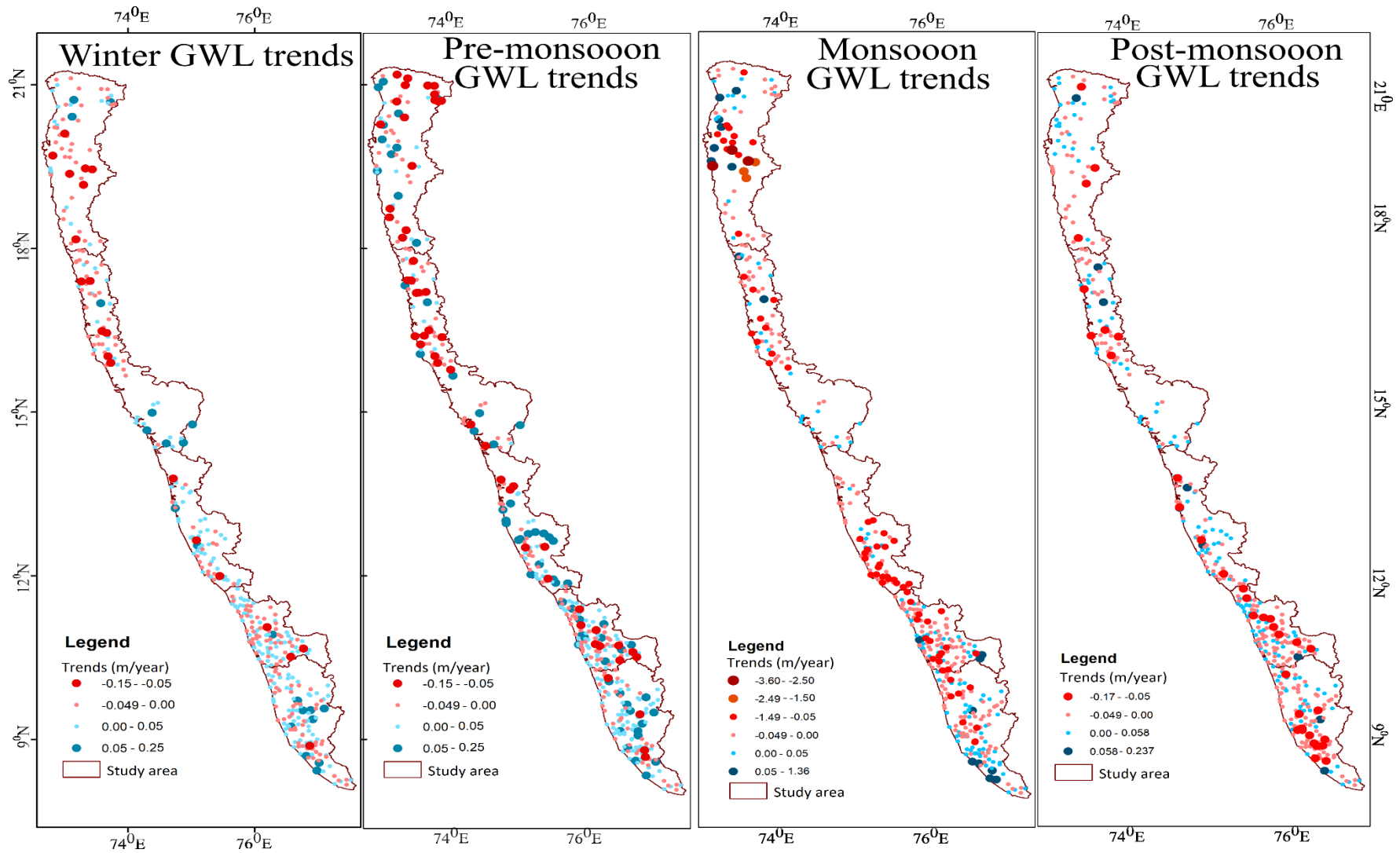


**Fig. 5.8. mMK and SE trends of seasonal groundwater levels (GWLs)**

**Table 5.4 Seasonal groundwater level (GWLs) trends by mMK and SE**

Basins	Trends	Winter		Pre-monsoon		Monsoon		Post-monsoon	
		Mean slope /year (m/year)	Proportion of wells (%)	Mean slope /year (m/year)	Proportion of wells (%)	Mean slope /year (m/year)	Proportion of wells (%)	Mean slope /year (m/year)	Proportion of wells (%)
<b>Bhatsol Basin</b> <b>Total Wells: 61</b>	Significant declining	-0.05	18.33	-0.11	21.00	-1.34	17.33	-0.05	10.00
	Significant rising	0.05	10.00	0.12	8.67	0.05	4.33	0.10	1.67
	Insignificant trends	0.00	71.67	-0.01	70.33	-0.03	78.33	-0.01	88.33
<b>Vasishti Basin</b> <b>Total Wells: 65</b>	Significant declining	-0.06	17.19	-0.10	23.44	-0.05	7.81	-0.06	15.63
	Significant rising	0.07	15.19	0.10	4.69	-	0.00	0.05	6.25
	Insignificant trends	0.01	67.60	-0.03	71.88	-0.02	92.19	0.02	78.19
<b>Netravati Basin</b> <b>Total Wells: 62</b>	Significant declining	-0.07	11.48	-0.13	9.60	-0.08	10.60	-0.09	3.28
	Significant rising	0.02	10.11	0.09	12.00	0.05	8.60	0.06	6.56
	Insignificant trends	0.02	78.41	-0.02	78.68	-0.01	80.78	-0.01	90.16
<b>Varrar Basin</b> <b>Total Wells: 104</b>	Significant declining	-0.06	8.39	-0.09	13.26	-0.07	15.98	-0.06	10.38
	Significant rising	0.03	10.38	0.07	12.21	0.05	4.72	0.02	3.77
	Insignificant trends	0.01	81.32	-0.01	74.52	-0.01	79.30	-0.01	85.87
<b>Periyar Basin</b> <b>Total Wells: 126</b>	Significant declining	-0.03	6.56	-0.04	7.74	-0.05	10.30	0.05	13.93
	Significant rising	0.05	11.48	0.06	10.30	0.08	6.74	0.10	3.28
	Insignificant trends	0.01	81.96	0.01	82.00	0.01	82.96	-0.02	82.83
<b>Total wells: 418</b>	Significant declining	-0.05	11.06	-0.09	13.68	-0.32	12.28	-0.04	11.03
	Significant rising	0.04	11.27	0.09	9.81	0.05	5.05	0.07	4.08
	Insignificant trends	0.01	76.77	-0.01	75.60	-0.01	81.70	0.00	83.95

### 5.3.5 SSA – PMGWL Trends

The mMK and SE analysis obtained the significance, direction and magnitude of the regional groundwater levels (GWLs) of the west coast basins. Since wells are huge in number, the discussion on the application of SSA in trend extraction is presented in this section only for post-monsoon GWLs. The trajectories of the PMGWL trends were examined using the SSA method. Since only a subset of wells indicated significant trends from the sample pool, it is essential to evaluate the trend lines even for wells with insignificant trends. The representative samples for rising and falling trends for each basin are discussed here. The SSA extracted trends (1996~2017) for representative wells (meters below ground level) are shown in Fig. 5.9.

The SSA extracted groundwater level (GWL) trend for Well W1135 (Periyar basin) shows that from 2001 to 2017, the GWL trend indicated a nonlinear decline from -6.5m to -10.0m below ground level (bgl). The well W1199 exhibited a linear rise in GWL trend from -1.0m to -0.6m up to 2014.

For the Varrar basin, the GWL trend (W1402) also showed a continuous decline for the entire duration, with a steep decline towards the end of the time series. However, continuous rising trends were indicated for the well W1460 in the same basin from 2000 onwards. Well W1069 (Netravati basin) exhibited a decreasing trend altogether from 1996 (-3.8m) to -6.0m with a sharp decline towards the end. In contrast, well 1059 experienced a non-linear trend with a downward slope till 2000 and then an increasing trend from 2000 to 2013.

A continuous declining GWL from -1m to more than -2.5m was indicated by well W1126 (Vasishti basin), while the well W1714 in the same basin experienced a continuously increasing trend. In the Bhatsol basin, the SSA captured the falling GWL trends in the well W1038 from 1998 to the last couple of years. The GWL trend for the well W1002 showed monotonously increasing trend from 1998 till the end, with specific change points. Also, it is visible that the GWL trends are mostly nonlinear and sometimes exhibit short-term rise and fall in the trajectory over the study period.

The SSA well captured the non-linearity in the PMGWL trends established by SE and mMK test. Even for statistically insignificant trends (wells 1069, 1059, 1038), the trend line indicates considerable GWL fluctuations, which otherwise could not have been obtained from the mMK and SE analysis. Though declining PMGWL trends were more

prominent, wells with rising trends were also identified during the trend detection studies. Significant increasing trends obtained for  $R_{AN}$  and  $R_{SW}$  (Table 5.2) could be the reason for the same apart from other factors.

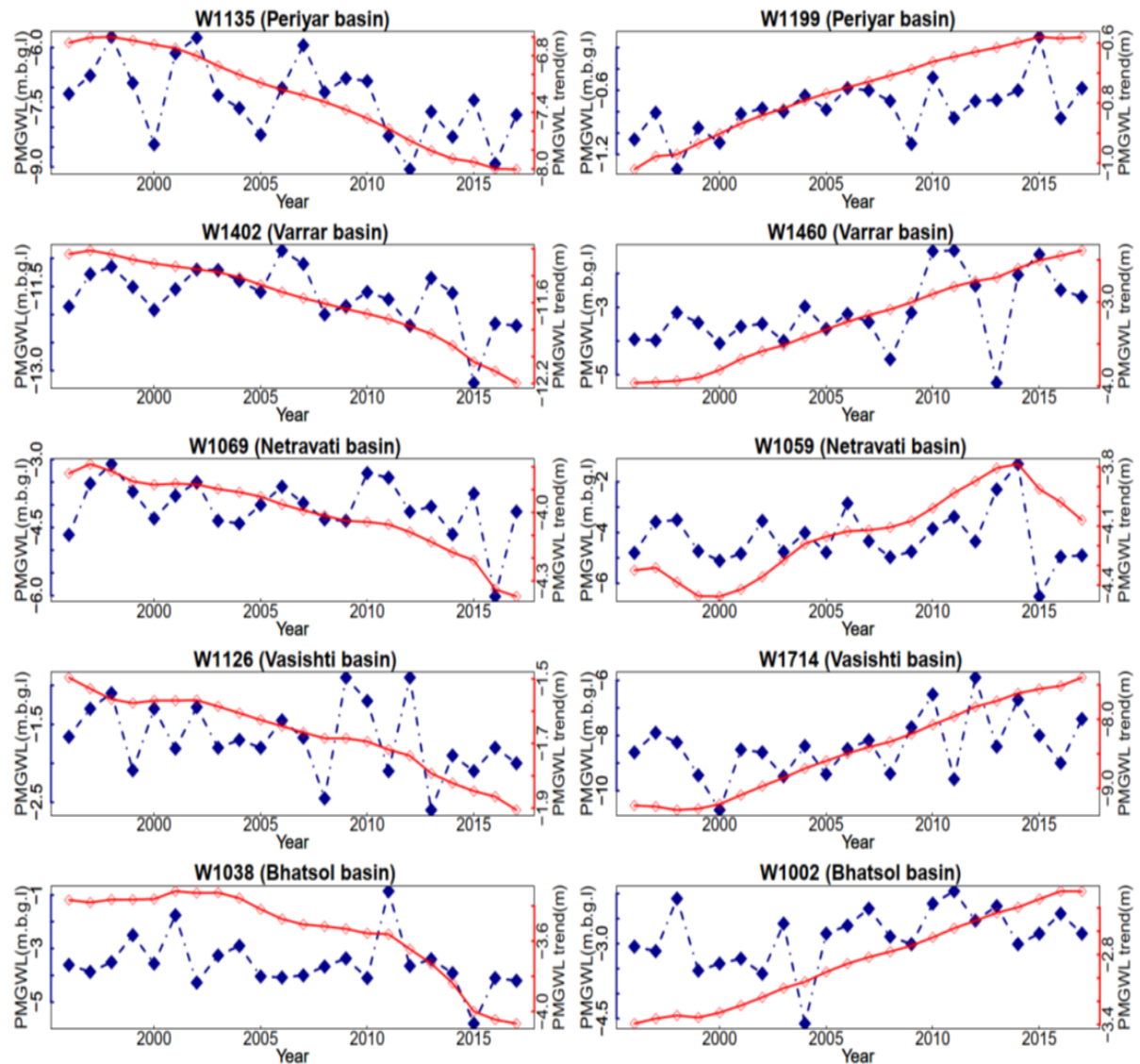


**Fig. 5.9** SSA extracted post-monsoons GWL (PMGWL) trends for sample wells

## 5.4 CLOSURE

An examination of historical trends of rainfall and groundwater levels at annual and seasonal scales was presented in this chapter. The widely used modified Mann-Kendall (mMK) and Sen's slope estimator (SE) were employed for trend detection studies. The test power analysis of mMK revealed the influence of parent distribution parameters on attainment of the threshold power of mMK. In addition to magnitude, direction and



significance, an investigation of trend trajectory was carried out by the singular spectrum analysis (SSA). The following conclusions were formulated from these analyses:

- Annual rainfall ( $R_{AN}$ ) trends indicated prominent declining trends among the west coast basins. Thirty-three grids indicated significant declining trend while nine grids indicated significant increasing trends. A significant decline of -3.8% of the average  $R_{AN}$  per decade was indicated in the Varrar basin. The basin also indicated the highest number of grids with significant decreasing  $R_{AN}$  trends i.e. 12 grids.
- A significant increase of +5.89% of average  $R_{WN}$  per decade was indicated by the Vasishti basin for winter rainfall. Increasing  $R_{WN}$  trends were observed at 109 grids with meagre slopes in the Vasishti basin.
- Prominent declining trends were observed in the pre-monsoon season both grid-wise and basin-wise. A significant decline of 4.5% of average  $R_{PRM}$  per decade (-1.2mm/year) was observed in the Varrar basin for the pre-monsoon rainfall.
- The southwest monsoon rainfall ( $R_{SW}$ ) trends were identical to the annual rainfall ( $R_{AN}$ ), given the former's bulk share to the  $R_{AN}$  totals. The southern basins namely Periyar, Varrar and Netravati portrayed significant decline at -1.9%, -4.2% and -1.7% decline of average  $R_{SW}$  per decade respectively.
- Post-monsoon rainfall indicated both declining and increasing trends, however 16 grids exhibited statistical significance, particularly the grids in the Vasishti basin.
- The influence of parent distribution parameters on the test power of the mMK test was investigated. Shape and scale parameters affect the test power of non-parametric mMK test, otherwise assumed to be distribution free rank based test.
- An average significant decline of -0.05m/year i.e. 1.1m in 22years was observed in 11% wells and a significant rise of +0.044m/year i.e. a total of 0.97m in 11.3% wells in the west coast basins for the winter season.
- Pre-monsoon GWLs exhibited both declines as well a rise. A significant slope of -0.094m/year in 13.65 % of wells and +0.088m/year in 9.8% of wells was obtained. Though pre-monsoon trends indicated a significant rise in a section of wells, the presence of such rising trends could be attributed to above normal pre-monsoon events that occurred after the year 2000 in the basins.
- Significant trends by mMK for the monsoon and post-monsoon GWLs indicated greater number of falls than rises. An average significant fall of -0.032m/year i.e.

7m decline in 12.3% wells was observed for monsoon, while -0.042m/year i.e. 0.92m fall in 11% wells was indicated during the post-monsoon season.

- Furthermore, wells identified with slopes between +0.05m/year and -0.05m/year dominated the results for all seasons.
- Groundwater levels being a non-linear multifactorial entity, the GWL trends indicated the response of GWLs to climatic and human stressors. In general, only a subset of wells was identified with significant rising and falling groundwater level (GWL) trends by the modified Mann-Kendall (mMK) test. About 75% and more wells indicated insignificant trends for all the seasons; post-monsoon season scored the top position with 84% of wells. This could be attributed to short dataset length or due to changing wet and dry phase of rainfall.
- The SSA methodology efficiently captured non-linear trends for even insignificant trends as well, that bear sufficient trend slope of practical significance. The grids such as 106, 173, etc. were identified as statistically insignificant, however, SSA extracted trends indicated monotonic declines in the rainfall totals for these grids. SSA thus aids in examining the trend trajectories for practically significant slopes which could be accepted under the null hypothesis of no trend owing to parent distribution parameters.



# GROUNDWATER LEVEL PREDICTIONS

## 6.1 INTRODUCTION

Groundwater is one of the world's largest fresh water reservoirs, maintaining global water and food security by catering to domestic, agricultural, and industrial water demands (Malakar et al. 2021). Escalation in the rainfall variability owing to an increase in extremes like droughts and floods, deterioration of surface water quality, urbanization, increased private well construction, spike the need for strategic use and conservation of available groundwater resources. Extensive groundwater depletion is reported worldwide owing to rising agricultural and population demands (Taylor et al. 2013; Famiglietti 2014; Rodell et al. 2018), which could worsen given the wavering precipitation patterns. Despite the crucial significance of groundwater on socio-economic stability, insufficient monitoring and management exist, leading to over-usage and declining aquifer levels, particularly in developing countries (Famiglietti 2014). Groundwater modelling is an efficient tool for simulating non-linear complex groundwater dynamics and future predictions (Mohapatra et al. 2021). The potential of physically-based numerical models on groundwater predictions is well documented. However, the requisite of extensive data makes it challenging in data scarce regions. Over the last few decades, data-driven models have manifested a rising interest among the scientific community concerning applications in the field of hydrology. This chapter presents the implementation of artificial neural networks and support vector machines on groundwater level predictions in the west coast basins.

## 6.2 METHODOLOGY

### 6.2.1 Artificial Neural Networks (ANN)

Artificial neural networks (ANN) is a supervised machine learning method developed after the biological nervous system. The fundamental processing unit of an ANN model is called a neuron that is arranged as an input layer, a hidden layer, and an output layer. The connection linking the neurons between the layers is termed as connection weight. The predictor variables are fed to the input layer, and the hidden layer executes the data processing, and the output layer generates the output. An activation function processes

the biases and weighted sum of the inputs of preceding neurons to the successor (Yoon et al. 2011). In this study, a feed-forward neural network with backpropagation (Svozil et al. 1997) is developed with a single hidden layer (ASCE 2000; Maier and Dandy 2000). The activation function consists of the log-sigmoid function in the hidden layer and a linear output in the output layer. The ANN model could be mathematically represented as:

$$Y_j = f \left( \sum_{i=1}^N W_{ji} X_i + b_j \right) \quad 6.1$$

Where  $X_i$  is the value at the  $i^{\text{th}}$  node in the previous layer,  $Y_j$  is the value at the  $j^{\text{th}}$  node in the present layer,  $W_{ji}$  is the connection weights between  $Y_j$  and  $X_i$ ,  $b_j$  is the bias at the  $j^{\text{th}}$  node,  $N$  is the total number of nodes in the previous layer and  $f$  is the activation function.

### 6.2.2 Support Vector Machines (SVM)

Support Vector Machines (SVM) is a data learning method for executing classification and regression problems (Yoon et al. 2011; Mohapatra et al. 2021). The fundamental equations of SVM for regression are developed from Vapnik's theory (Vapnik et al. 1997). Let  $\{(X_1 Y_1) \dots (X_N Y_N)\}$  be the training datasets of length  $N$ ,  $X_k \in R^m$ ,  $Y_k \in R$ , where  $X$  is the input vector of  $m$  components, and  $Y$  is the target value. The following denotes the SVM estimator for regression:

$$f(X) = W \cdot \phi(X) + b \quad 6.2$$

Where  $W$  is the weight vector and  $b$  is the bias.  $\phi$  represents the non-linear transfer function that maps the input vectors to a higher dimension for linear regression. The optimization problem to obtain the solution for Eqtn. 6.2 is given as:

$$\begin{aligned} &\text{Minimize} && \frac{1}{2} \|W\|^2 + C \sum_{k=1}^N (\xi_k - \xi_k^*) \\ &W, b, \xi_k, \xi_k^* && \\ &\text{Subject to} && \begin{cases} Y_k - W^T \phi(X_k) - b \leq \varepsilon + \xi_k \\ W^T \phi(X_k) + b - Y_k \leq \varepsilon + \xi_k^* \\ \xi_k, \xi_k^* \geq 0 \end{cases} \quad k = 1, 2, \dots, N \end{aligned} \quad 6.3$$

Where  $C$  denotes the regularization constant,  $\varepsilon$  is the error tolerance range of the function, and  $\xi_k, \xi_k^*$  are the slack variables. The radial basis function (RBF) kernel was used in this study as the transformation function.

### 6.2.3 Model Training, Testing and Performance Evaluation

This study subdivided the seasonal groundwater level data from the Central Ground Water Board (CGWB) dataset for 22 years from 1996 to 2017 into training and testing sets. Antecedent rainfall, mean, maximum, and minimum temperature, and groundwater draft were taken as predictors for the models. Daily gridded rainfall ( $0.25^\circ \times 0.25^\circ$ ) and temperature ( $1^\circ \times 1^\circ$ ) from the India Meteorological Department (IMD) were averaged for monthly and seasonal scales. The groundwater draft was estimated from a population water demand of 135lites per capita per day, accounting for the block and taluk-wise (administrative units) population census data (Census of India, 1991, 2001, 2011). The irrigation demand was estimated from Central Ground Water Board (CGWB) published reports (CGWB, Govt. of India). The ANN and SVM models were developed for individual wells to ascertain the feasibility of applying machine learning models to predict non-linear groundwater levels (GWL). The models were trained using 75% of the dataset from 1996 to 2012 and the remaining 25% from 2012 to 2017 for testing. Model type-1 used both climatic variables and draft as predictors, while only climatic variables were taken as input for model type-2. The root mean square error (RMSE) and coefficient of determination ( $R^2$ ) were evaluated to check the model performance.

Normalization of varying scale time series data is essential to avoid unequal weightage assignment in the models. Max-min normalization was adopted to normalize all the time series data given as:

$$x_{norm} = \frac{x - x_{min}}{x_{max} - x_{min}} \quad 6.4$$

The root mean square error (RMSE) and  $R^2$  (coefficient of determination) was calculated for each model. Root mean square error (RMSE) is a quadratic measure that determines the error between target and model output values given as:

$$RMSE = \left( \frac{1}{N} \sum_{i=1}^N (y_i - x_i)^2 \right)^{\frac{1}{2}} \quad 6.5$$

Where  $y_i$  and  $x_i$  are the predicted and observed values.

The coefficient of determination is the measure that provides information about the goodness of fit of a model and is given by:

$$R^2 = 1 - \frac{\sum (y_i - \hat{y})^2}{\sum (y_i - \bar{y})^2} \quad 6.6$$

Where  $y_i$ ,  $\hat{y}$  and  $\bar{y}$  are the actual value, residuals, and mean. The data pre-processing and simulation models were processed using R-statistical software and associated packages.

## 6.3 RESULTS AND DISCUSSIONS

### 6.3.1 ANN-GWL Predictions

The artificial neural network (ANN) algorithm generated 418 models of type I and type II each. The predictors for the type I model are abstraction and meteorological variables, while for the type II model, only meteorological variables were considered. Model-1 is termed ANN-1, and model-2 is termed ANN-2. The performance statistics of ANN-1 and ANN-2 models for testing (2012-2017) phase by evaluating the observed and predicted groundwater levels for 418 models are presented in Tables 6.1& 6.2. It can be observed that about 24.16% of models exhibited an RMSE<0.1m, 69.14% showed an RMSE between 0.1m to 0.2m, 6.22% of models indicated an RMSE between 0.2m to 0.3m, and only 0.48% were observed with an RMSE between 0.3m to 0.4m, during the testing phase by ANN1 models. About 37.8% of models accounted for an  $R^2$  (coefficient of determination) >0.8, 22.72% of models indicated an  $R^2$  between 0.7 to 0.8, 18.66% of models portrayed  $R^2$  between 0.7 to 0.6, and 20.81% models were observed with an  $R^2$  <0.6. Overall, ANN1 models simulated the groundwater levels satisfactorily, with 93.30% of models exhibiting an RMSE<0.2m and 60.53% of models with an  $R^2$ >0.7.

The performance of ANN2 models for the individual sites indicated good statistics. However relatively lower than ANN1 models (Table 6.1& 6.2). About 24.88% of models exhibited an RMSE<0.1m, 68.89% exhibited an RMSE between 0.1m to 0.2m, and 6.22%

indicated an RMSE between 0.2m to 0.3m during the testing phase by ANN2 models. About 34.45% of models accounted for an  $R^2$  (coefficient of determination)  $>0.8$ , 23.68% of models were observed with an  $R^2$  between 0.7 to 0.8, 17.46% of models were reported with an  $R^2$  between 0.7 to 0.6 and 24.40% models accounted for an  $R^2 <0.6$ . Overall, ANN2 models simulated the groundwater levels satisfactorily, with 93.77% of models exhibiting an  $RMSE < 0.2m$  and 58.13% accounting for an  $R^2 > 0.7$ . Though the performance statistics of ANN2 models were lower than ANN1 models, their margin is relatively small, with approximately a 2% difference in  $R^2 > 0.7$ . At the same time, both have similar RMSE statistics for the testing predictions.

**Table 6.1 RMSE metrics of ANN and SVM models for testing phase**

<b>RMSE-testing</b>				
<b>Range</b>	<b>ANN1</b>	<b>ANN2</b>	<b>SVM1</b>	<b>SVM2</b>
<0.1m	24.16	24.88	26.56	25.84
0.1m -0.2m	69.14	68.9	67.94	68.42
0.2m-0.3m	6.22	6.22	5.5	5.74
0.3m-0.4m	0.48	0	0	0

Note: Values given in the table denote the percentage.

**Table 6.2  $R^2$  metrics of ANN and SVM models for testing phase**

<b><math>R^2</math>-testing</b>				
<b>Range</b>	<b>ANN1</b>	<b>ANN2</b>	<b>SVM1</b>	<b>SVM2</b>
$>0.8$	37.8	34.45	36.36	33.01
0.8-0.7	22.73	23.68	20.57	22.25
0.6-0.7	18.66	17.46	18.9	15.79
$<0.6$	20.81	24.4	24.16	28.95

Note: Values given in the table denote the percentage.



### 6.3.2 SVM-GWL Model Predictions

The support vector machines (SVM) models were developed for individual wells to examine the performance of the SVM algorithm in applying to a significant number of wells with spatial heterogeneity among the west coast basins. Four hundred eighteen models (for 418 wells) were developed for model type 1 and 2. Model-1 is termed SVM-1, and model-2 is denoted as SVM-2. The performance statistics of SVM-1 and SVM-2 models for testing (2012-2017) phase by evaluating the observed and predicted groundwater levels for 418 wells are presented in Table 6.1 and Table 6.2. It can be observed that about 26.55% of models exhibited an RMSE<0.1m, 67.94% of models indicated an RMSE between 0.1m to 0.2m, and about 5.5% models were identified with an RMSE between 0.2m to 0.3m during the testing phase by SVM1 models. Approximately 36.36% of models accounted for an  $R^2$  (coefficient of determination) >0.8, 20.57% of models showed an  $R^2$  between 0.7 to 0.8, 18.89% displayed an  $R^2$  between 0.7 to 0.6, and 24.16% models accounted for an  $R^2$  <0.6. Overall, SVM1 models simulated the groundwater levels satisfactorily, with 94.49% of models indicated with an RMSE<0.2m and 56.93% of models reported with an  $R^2$  >0.7.

The performance of SVM2 models for the individual wells obtained is relatively lower than SVM1 models (Table 6.1&6.2). About 25.84% of models exhibited an RMSE<0.1m, 68.42% indicated an RMSE between 0.1m to 0.2m, and 5.74% showed an RMSE between 0.2m to 0.3m during the testing phase by SVM2 models. About 33.01% of models accounted for an  $R^2$  (coefficient of determination) >0.8, 22.25% accounted for an  $R^2$  between 0.7 to 0.8, 15.79% displayed an  $R^2$  value between 0.7 to 0.6, and 28.95% models accounted for an  $R^2$  <0.6. Overall, SVM2 models simulated the groundwater levels satisfactorily, with 94.25% of models identified with an RMSE<0.2m and 55.26% of models noted with an  $R^2$  >0.7. Though the performance statistics of SVM2 models were lower than SVM1 models, their margin is relatively small, with approximately 2% difference in  $R^2$  >0.7, while similar RMSE metrics were noted.

### 6.3.3 Basin-wise ANN Model Performance

The basin-wise performance metrics of ANN1 models in percentage during the testing period from 2012 to 2017 are presented in Table 6.3. The distribution of coefficient of determination  $R^2$  and root mean squared error (RMSE) distributed across the west coast basins are presented as violin plots in Fig. 6.1 and Fig. 6.2. About 73.76% of models in the

Bhatsol basin, 71.66% of models in Vasishti basin, 68.86% models in Netravati basin, 60.46% models in Varrar and 43.94% models in the Periyar basin exhibited an  $R^2 > 0.7$  for the ANN1 models. Besides, the proportion of ANN1 models identified with an  $R^2 > 0.6$  is greater than 79% among the west coast basins but Periyar basin.

Regarding ANN2 models, an  $R^2$  value greater than 0.7 was indicated by 71.42% of models in the Bhatsol basin, 66.13% of models in Vasishti, 65.66% of models in Netravati, 56.77% of models in Varrar and 45% models in the Periyar basin as presented in Table 6.4. ANN1 and ANN2 models have exhibited promising results relevant to  $R^2$  metrics among the west coast basins, except the Periyar basin, with relatively lower metrics.

**Table 6.3 Basin-wise  $R^2$  (testing phase) metrics of ANN1 models**

Sub-basin	$R^2$ (testing) - ANN1				
	>0.9	0.8-0.9	0.7-0.8	0.6-0.7	<0.6
Bhatsol	18.03	39.34	16.39	13.11	13.11
Vasishti	11.94	34.32	25.4	7.5	20.9
Netravati	18.03	24.6	26.23	16.4	14.75
Varrar	10.4	28.3	21.76	21.7	17.92
Periyar	4.9	15.44	23.6	26	30.08

Note: Values given in the table denote the percentage.

**Table 6.4 Basin-wise  $R^2$  (testing phase) metrics of ANN2 models**

Sub-basin	$R^2$ (testing)- ANN2				
	>0.9	>0.8	0.7-0.8	0.6-0.7	<0.6
Bhatsol	15.87	34.92	20.63	14.29	14.29
Vasishti	21	29	16.13	17.8	16.1
Netravati	15.63	28.13	21.9	15.63	18.8
Varrar	8.7	18.27	29.8	18.27	25
Periyar	3.2	16.8	25	19.2	36

Note: Values given in the table denote the percentage.

The root mean squared error (RMSE) observed for ANN1 models indicated that about 93.44% of models in the Bhatsol basin, 89.54% in the Vasishti basin, 96.74% in the Netravati basin, 94.4% of models in the Varrar basin and 92.7% models in the Periyar basin were observed with an RMSE <0.2m as given in Table 6.5. About 96.82% of ANN2 models in the Bhatsol basin, 93.55% of models in Vasishti, 96.94 % in Netravati, 90.4% in Varrar, and 93.6% of models in Periyar exhibited an RMSE<0.2m as given in Table 6.6. Both ANN1 and ANN2 models displayed RMSE proportions alike. Irrespective of the type I and type II ANN models, the Periyar basin exhibited greater than 93% of models with an RMSE less than 0.2m, compared to lower R<sup>2</sup> metrics.

**Table 6.5 Basin-wise RMSE (testing phase) metrics of ANN1 models**

<b>RMSE - ANN1</b>				
<b>Sub-basin</b>	<b>&lt;0.1m</b>	<b>0.1m-0.2m</b>	<b>0.2m-0.3m</b>	<b>&gt;0.3m</b>
Bhatsol	18.04	75.4	6.55	-
Vasishti	16.41	73.13	8.95	1.5
Netravati	41	55.74	3.27	-
Varrar	23.6	70.8	5.6	-
Periyar	23.6	69.1	6.5	0.8

Note: Values given in the table denote the percentage.

**Table 6.6 Basin-wise RMSE (testing phase) metrics of ANN2 models**

<b>RMSE - ANN2</b>				
<b>Sub-basin</b>	<b>&lt;0.1m</b>	<b>0.1m-0.2m</b>	<b>0.2m-0.3m</b>	<b>&gt;0.3m</b>
Bhatsol	23.81	73.01	3.17	-
Vasishti	24.2	69.35	6.45	-
Netravati	35.94	61	3.12	-
Varrar	23.1	67.3	9.6	-
Periyar	21.6	72	6.4	-

Note: Values given in the table denote the percentage.

### 6.3.4 Basin-wise SVM Model Performance

The basin-wise  $R^2$  values indicated by the SVM 1 models for groundwater level prediction during the testing period from 2012 to 2017 are presented in Table 6.7. It could be observed that about 71.42% of models in the Bhatsol basin, 69.21% of models in the Vasishti basin, 66.15% of models in the Netravati basin, 54.1% models in Varrar and 40.95% of models in the Periyar basin exhibited an  $R^2 > 0.7$  for the SVM1 models. Besides, the proportion of SVM1 models identified with an  $R^2 > 0.6$  is greater than 80% among Bhatsol, Vasishti, and Netravati basins and over 70% in the Varrar basin. However, a relatively lower percentage of models (40.95%) exhibited an  $R^2 > 0.6$  in the Periyar basin.

On observing the  $R^2$  values obtained for SVM2 models as given in Table 6.8, an  $R^2$  value  $> 0.7$  was portrayed by 64.6% of models in the Bhastol, 63.65% in the Vasishti basin, 65.15% in Netravati basin, 60.41% in Varrar basin and 39.2% models in the Periyar basin. In line with the SVM1 results, SVM2 models identified with an  $R^2$  value  $> 0.6$  were 81.54%, 81.83%, and 81.83% models in Bhatsol, Vasishti, and Netravati basins, respectively, and 72.9% in Varrar basin. About 55% of models in the Periyar basin indicated an  $R^2 > 0.6$ .

**Table 6.7 Basin-wise  $R^2$  (testing phase) metrics of SVM1 models**

Sub-basin	$R^2$ - SVM1				
	$>0.9$	<b>0.8-0.9</b>	<b>0.7-0.8</b>	<b>0.6-0.7</b>	<b>&lt;0.6</b>
Bhatsol	7.93	39.68	23.81	14.3	14.3
Vasishti	12.3	33.84	23.07	18.46	12.31
Netravati	16.92	25.8	23.43	16.92	16.92
Varrar	9.21	27.55	17.34	19.4	26.53
Periyar	6.3	16.54	18.11	22	37

Note: Values given in the table denote the percentage.

**Table 6.8 Basin-wise R<sup>2</sup> (testing phase) metrics of SVM2 models**

<b>R2 - SVM2</b>					
<b>Sub-basin</b>	<b>&gt;0.9</b>	<b>0.8-0.9</b>	<b>0.7-0.8</b>	<b>0.6-0.7</b>	<b>&lt;0.6</b>
Bhatsol	7.71	36.92	20	17	18.46
Vasishti	13.63	27.3	22.72	18.18	18.18
Netravati	16.67	25.76	22.72	16.67	18.18
Varrar	8.33	28.12	23.96	12.5	30.21
Periyar	2.4	15.2	21.6	16	44.8

Note: Values given in the table denote the percentage.

The root mean squared error (RMSE) observed for SVM1 models indicated that about 96.82 % of models in the Bhatsol basin, 95.37% in the Vasishti basin, 93.84% in the Netravati basin, 94.4% of models in Varrar basin and 92.7% models in the Periyar basin were observed with an RMSE <0.2m as given in Table 6.9. About 96.91% of SVM2 models in the Bhatsol basin, 90.91% of models in Vasishti, 92.42 % in Netravati, 93.83% in Varrar, and 96% of models in Periyar exhibited an RMSE<0.2m as given in Table 6.10. Both SVM1 and SVM2 models displayed RMSE proportions alike.

**Table 6.9 Basin-wise RMSE (testing phase) metrics of SVM1 models**

<b>RMSE - SVM1</b>			
<b>Sub-basin</b>	<b>&lt;0.1m</b>	<b>0.1m - 0.2m</b>	<b>0.2m - 0.3m</b>
Bhatsol	12.7	84.12	3.17
Vasishti	21.53	73.84	4.61
Netravati	38.46	55.38	6.15
Varrar	26.53	66.32	7.14
Periyar	29.92	64.57	5.5

Note: Values given in the table denote the percentage.

**Table 6.10 Basin-wise RMSE (testing phase) metrics of SVM2 models**

<b>RMSE - SVM2</b>			
<b>Sub-basin</b>	<b>&lt;0.1m</b>	<b>0.1m - 0.2m</b>	<b>0.2m - 0.3m</b>
Bhatsol	12.3	84.61	3.07
Vasishti	24.24	66.67	9
Netravati	40.91	51.51	7.57
Varrar	23	70.83	6.25
Periyar	28	68	4.8

Note: Values given in the table denote the percentage.

The basin-wise distribution of  $R^2$  and RMSE values represented as violin plots for ANN and SVM models are presented in Fig. 6.1 and Fig.6.2. The basin-wise distribution map of ANN and SVM models for  $R^2$  during the testing phase is given in Fig. 6.3. As discussed earlier both ANN and SVM models performed alike in predicting the groundwater levels during the testing phase from 2012 to 2017. The performance of ANN and SVM models indicated promising results with respect to RMSE values among five west coast basins, with greater than 90% of models exhibiting an RMSE  $<0.2m$ .

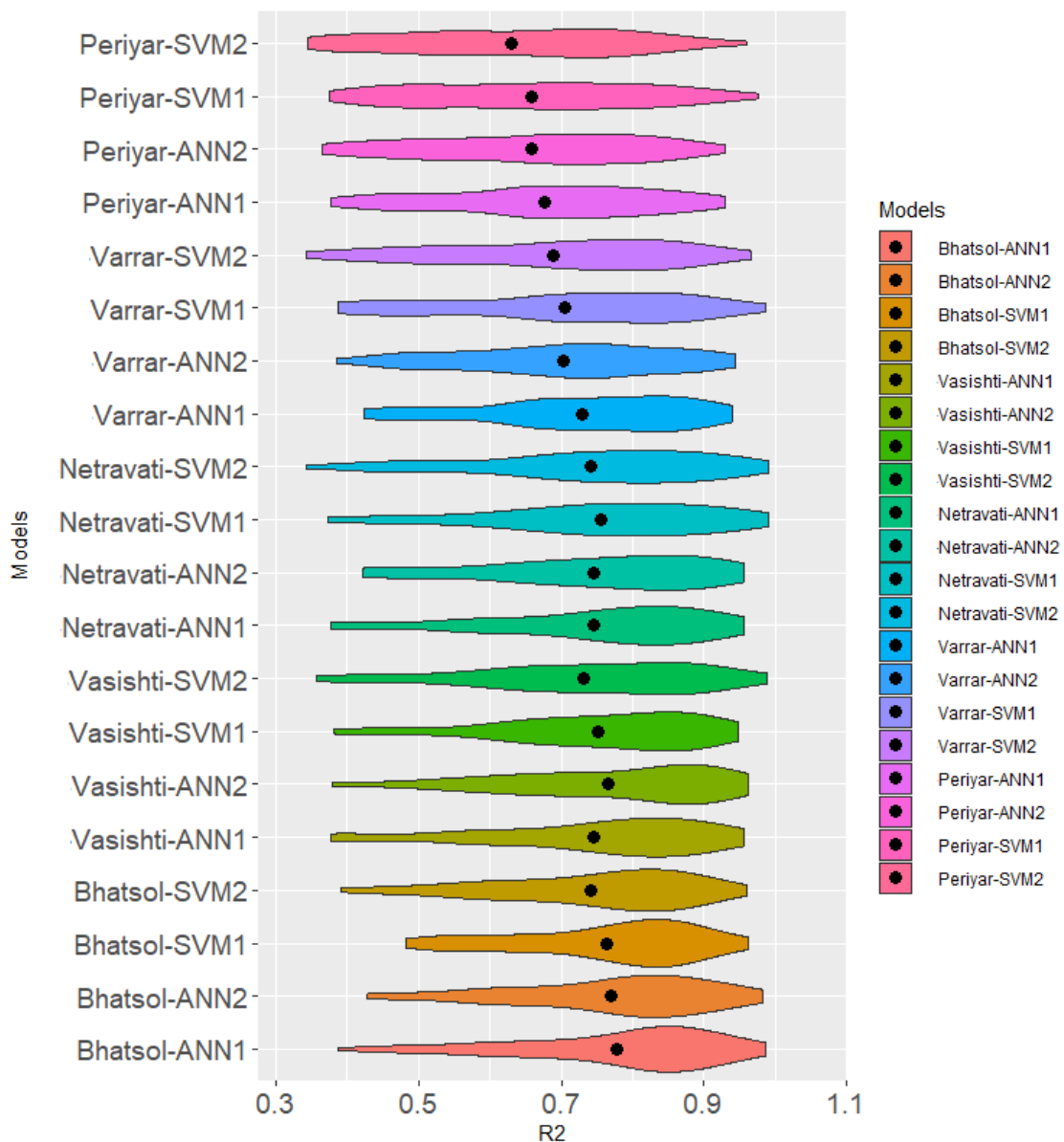


**Fig. 6.1 Basin-wise violin plots for  $R^2$  of ANN and SVM models**

Overall, ANN1 models performed relatively better in terms of RMSE and  $R^2$ . From Fig. 6.1, it could be observed that the distribution of models with higher values of  $R^2$  is indicated in Bhatsol, Vasishti, and Netravati basins. While the distribution widens towards lower  $R^2$  values for Periyar and Varrar basins. Similar conclusions could be made from Fig. 6.3, where the groundwater models for the wells present in the Bhatsol, Vasihti, and Netravati basins represented higher values of  $R^2$  compared to the southern basins of Periyar and Varrar. The RMSE and  $R^2$  values obtained during training and testing phase is given in Appendix 4 and Appendix 5 for ANN and SVM models.

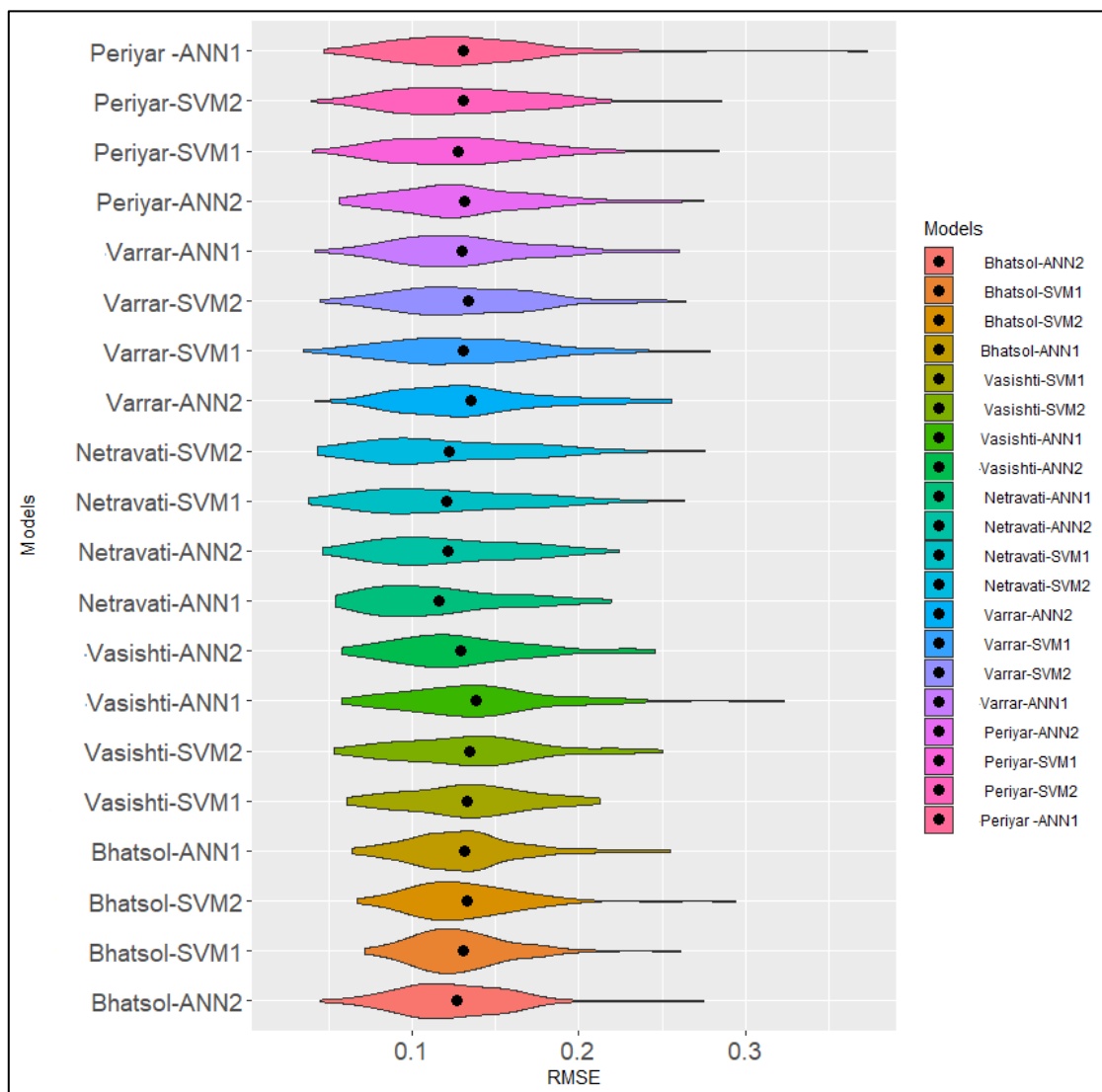


**Fig. 6.2 Basin-wise violin plots for RMSE of ANN and SVM models**

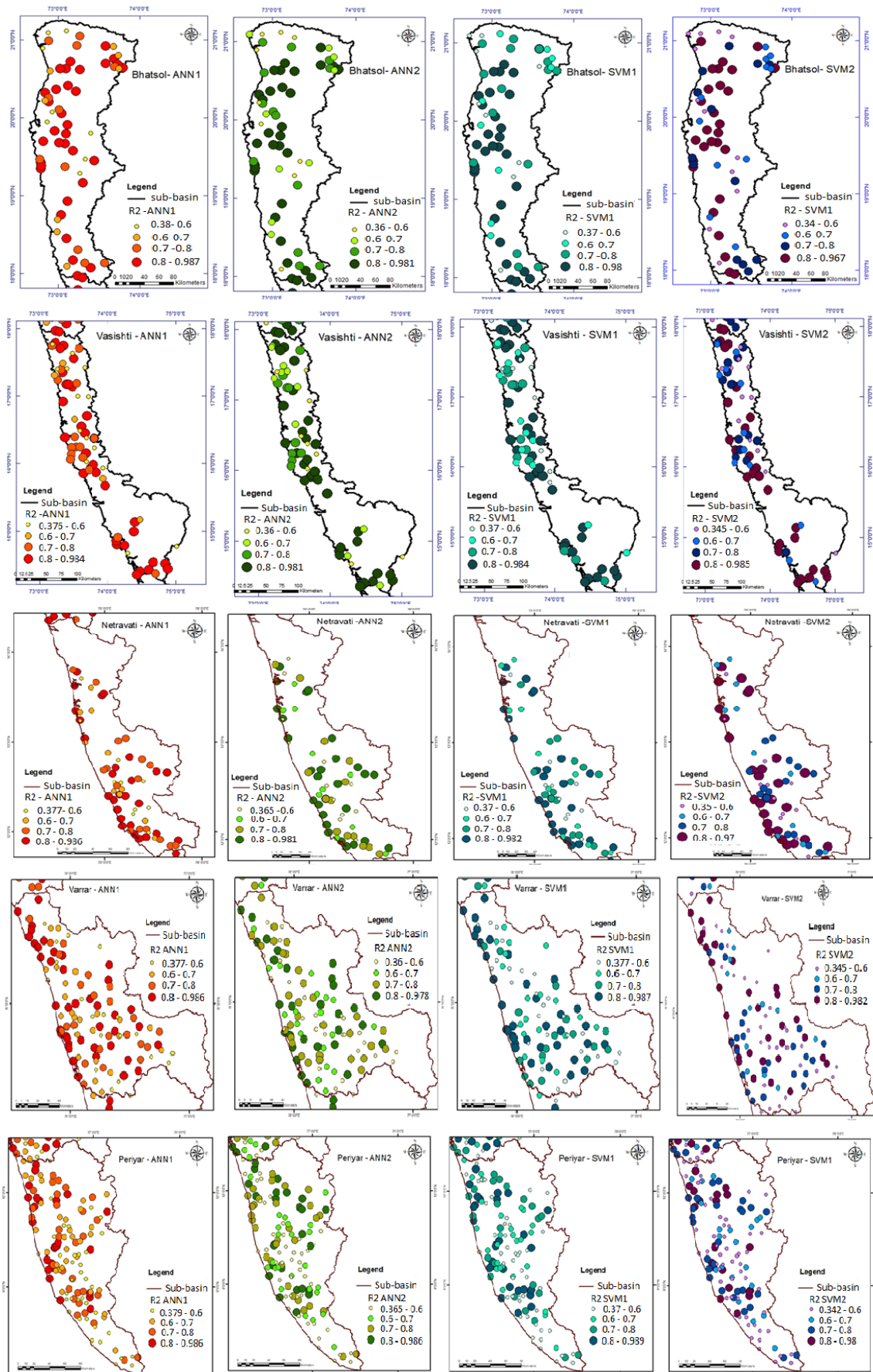


**Fig. 6.3. Basin-wise distribution map of R<sup>2</sup> testing for ANN and SVM models**



## 6.4 CLOSURE

- Groundwater level models were developed for individual wells (418 wells) in the west coast basins using ANN and SVM algorithms, each of Type 1 and Type2 architecture. The RMSE values ranging from 0.04m to 0.37m and  $R^2$  ranging from 0.986 to 0.377 were obtained for the testing phase by the ANN1 models. The ANN2 models indicated an RMSE between 0.042 to 0.275m and an  $R^2$  between 0.365 to 0.981 during the testing predictions.
- SVM 1 exhibited RMSE values ranging from 0.035m to 0.28m and  $R^2$  ranging from 0.98 to 0.37 for the testing phase. SVM2 models exhibited an RMSE between 0.039 to 0.285m and an  $R^2$  between 0.35 to 0.97 during the test period from 2012 to 2017.
- About 93.30% of ANN1 models, 93.77% of ANN2 models, 94.49% of SVM1 models, and 94.25% of SVM2 models exhibited an RMSE<0.2m out of a total of 418 models each. About 60.53% ANN1, 58.13% ANN2 models, 56.93% SVM1 models, and 55.26% SVM2 models exhibited an  $R^2 >0.7$ , indicating the accountability of both ANN and SVM approach in predicting the groundwater levels (GWLs).
- The performance statistics qualified the ANN1 model as the best model among the four in predicting groundwater levels (GWLs) in the west coast basins. Though groundwater draft is an indispensable predictor for modelling GWL, ANN2 models also exhibited reasonably good performance for GWL prediction with only meteorological predictors. Similar inferences could be obtained between the SVM1 and SVM2 models with a relatively lower margin between their performances.
- The developed ANN and SVM models could predict the GWLs over spatially heterogenous in-situ datasets under varying hydrogeology, topography, and meteorological conditions. However, the models could not generalize a portion of wells, wherein about 20.81% ANN1 models, 24.40% ANN2 models, 24.16% SVM1 models, and approximately 28.95% SVM2 models displayed an  $R^2$  value<0.6, which could be attributed to uncertainty in input datasets or data quality.
- The models generalized well in terms of RMSE with only a meagre percentage of models, i.e., 6.7% ANN1 models, 6.22% ANN2 models, 5.5% SVM1 Models, and 5.74% SVM2 models associated with an RMSE>0.2m.
- Spatial assessment of the performance of machine learning models revealed Bhatsol, Vasishti, and Netravati basins had a greater percentage of models with

$R^2 > 0.8$  compared to Varrar and Periyar basins. The spatial pattern in performance metrics was evident in both ANN and SVM models.

- The spatial variations in model performances could be attributed to rainfall patterns, uncertainty in datasets, surface topography, and hydrogeological settings. However, the ANN and SVM models proved efficient in capturing the groundwater level patterns on a constrained dataset with only four seasonal values available annually over a varying meteorological and hydrogeological study area for a limited dataset length of 22 years.



### CONCLUSIONS

---

The present study aimed at a comprehensive understanding of the rainfall and groundwater levels in the west coast basins of India. Temporal distribution and periodicities of rainfall were conducted to understand the variabilities and underlying patterns in the region. The historical trends of rainfall and groundwater levels were examined by the modified Mann-Kendall (mMK) test and singular spectrum analysis (SSA). The influence of parent distribution on the modified Mann-Kendall test was investigated. The feasibility of machine learning approaches namely artificial neural networks (ANN) and support vector machine (SVM) in simulating the heterogeneously distributed groundwater levels was analyzed.

The conclusions formulated from the present investigation are presented in this chapter. The key findings from the study are organized sequentially and chapter-wise for convenience. Furthermore, the limitation of the present study and the scope for future research are also documented.

#### 7.1 SPATIOTEMPORAL ANALYSIS OF RAINFALL

The departure analysis of basin-averaged annual and seasonal rainfall was conducted to examine the inter-annual as well as decadal variability in the rainfall regimes along the west coast of India. In addition, the wavelet power spectrum for annual and seasonal rainfall was investigated to understand the periodicities associated with regional rainfall patterns.

- The annual rainfall departures displayed decadal variability among the west coast basins. The decades from 1980 to 1989 and from 2000 to 2009 were observed as the driest decade common among the west coast basins. An increase in the frequency of dry years was noted after 1980 for Periyar, Varrar, and Netravati basins.
- Departures for southwest monsoon rainfall portrayed that the five basins were in-phase during the early years from 1950 to 1960 associated with principal wet years.

From 1970 to 1990, a prominent dry phase was visible among the basins. The Vasishti and Bhatsol basins displayed relative rise in wet years after 2000, while Varrar, Periyar, and Netravati indicated vice-versa.

- The pre- and post-monsoon rainfall departures exhibited decadal wet and dry epochs uniformly among the west coast basins. Anomalous departure values for winter rainfall were obtained owing to the irregular rainfall and presence of large excess and scanty years. Decadal to multidecadal variability was noticed for annual and seasonal rainfall departures among the west coast basins.
- The dominant cycles observed for the annual rainfall ( $R_{AN}$ ) among the west coast basins were displayed in the 2-4-year, 4-8-year and 8-16-year bands. Interdecadal oscillations of the 8-16-year period were obtained with moderate power among all the basins, which mainly strengthened from 1980 onwards.
- Inter-annual periodicities of 2-4-years and 4-8-years were predominantly exhibited by Bhatsol, Vasishti, and Periyar basins with varying wavelet power for southwest monsoon rainfall. While Netravati and Varrar basins presented few short periodicities of 2-4-year band confined to early decades. However, statistically significant inter-decadal oscillations of 12-16-year period were evident among all the basins with moderate wavelet power. The inter-annual and inter-decadal variability in the distribution of southwest monsoon rainfall (or in other words Indian summer monsoon) is evident from the periodicities obtained from the wavelet spectra.
- Inter-annual as well as inter-decadal modulations of southwest monsoon rainfall by El Nino SSTs (El Nino Sea Surface Temperature), Indian Ocean Dipole (IOD) and Pacific SSTs (Pacific Sea Surface Temperature) were reported earlier (Revadekar et al. 2019; Halder et al. 2022). Though located on the west coast of India, the basins indicated spatial and temporal variations in the wavelet power spectrum for annual and seasonal rainfall.
- Winter and pre-monsoon rainfall portrayed spectral bands mainly in the 2-4-year and 4-8-year periods among the basins. While post-monsoon rainfall indicated 2-4-year, 4-8-year and 8-16-year periodicities as well. Inter-annual, as well as inter-decadal periodicities in the post-monsoon rainfall, could be attributed to ENSO, Indian Ocean Dipole (IOD), and Equatorial Indian Ocean Oscillation (EQUINOO) modulations (Sreekala et al. 2011; Rajeevan et al. 2012).

- From the wavelet analysis, it can be concluded that the oscillations varied both temporally and spatially. Like rainfall distribution, wavelet spectra also varied from south to north. Interannual and interdecadal oscillations observed in the spectra reveal the role of teleconnections in the region.

## 7.2 TREND ANALYSIS OF RAINFALL AND GROUNDWATER LEVELS

Time series data of rainfall and groundwater levels were analyzed for historical trends. Grid-wise, as well as basin-wise trends of annual and seasonal rainfall series from 1950 to 2017, were conducted. Seasonal groundwater level trends for 418 wells were also carried out. The widely used modified Mann-Kendall (mMK) and Sen's slope estimator were employed for trend detection studies. The test power analysis of mMK to examine the influence of parent distribution parameters on trend detection studies was implemented. Furthermore, singular spectrum analysis (SSA) was employed to extract trend trajectory.

- Annual rainfall trends indicated prominent declining trends among the west coast basins. Thirty-three grids indicated a significant declining trend while nine grids indicated significant increasing trends. A significant decline of -3.8% of the average  $R_{AN}$  per decade was indicated in the Varrar basin. The basin also indicated the highest number of grids with significant decreasing  $R_{AN}$  trends i.e. 12 grids.
- The winter rainfall exhibited an increase among 109 grids with the Vasishti basin observed with a significant increase of +5.89% of average  $R_{WN}$  per decade. A greater number of increasing  $R_{WN}$  trends with meagre slopes were observed. However, winter rainfall does not contribute a lion's share to the total annual rainfall budget and rising winter rainfall trends may not suffice the regional water demands.
- The southwest monsoon rainfall ( $R_{SW}$ ) trends were identical to the annual rainfall ( $R_{AN}$ ), given the former's bulk share to the  $R_{AN}$  totals. The southern basins namely Periyar, Varrar, and Netravati portrayed significant decline at -1.9%, -4.2%, and -1.7% decline of average  $R_{SW}$  per decade respectively.
- Rainfall trends indicated falling trends for annual and southwest monsoon rainfall which could adversely affect the region's groundwater reserves.
- Significant trends by mMK for the monsoon and post-monsoon GWLs indicated a greater number of falls than rises. An average significant fall of -0.032m/year i.e.

7m decline in 12.3% wells was observed for monsoon, while -0.042m/year i.e. 0.92m fall in 11% wells was indicated during the post-monsoon season.

- Furthermore, wells identified with slopes between +0.05m/year and -0.05m/year dominated the results for all seasons.
- The test power analysis of the mMK enumerated the importance of power analysis on the sample data parameters and compared the obtained value to the acceptable threshold value (in this study threshold was taken as 0.8). The investigation on mMK test power revealed the influence of parent distribution parameters on the significant testing by mMK.
- The SSA methodology efficiently captured the non-linear trends for even insignificant trends that bear sufficient trend slope of practical significance. SSA thus aids in examining the trend trajectories for practically significant slopes, even though the null hypothesis of no trend being accepted due to parent distribution type.

### **7.3 GROUNDWATER LEVEL PREDICTIONS**

The artificial neural network (ANN) and support vector machines (SVM) were incorporated to examine the feasibility of machine learning models in predicting groundwater levels in the west coast basins.

- The machine learning models namely ANN1, ANN2, SVM1, and SVM2 performed well in predicting the groundwater levels during the test period from 2012 to 2017. All four models showcased promising results in terms of RMSE with more than 93% of models in each category associated with an  $RMSE < 0.2m$ .
- About 60.53% ANN1, 58.13% ANN2 models, 56.93% SVM1 models, and 55.26% SVM2 models exhibited an  $R^2 > 0.7$ , indicating the accountability of both ANN and SVM approach in predicting the groundwater levels (GWLs). The performance statistics qualified the ANN1 model as the best model relatively among the models in predicting groundwater levels (GWLs) in the west coast basins.
- Spatial assessment of the performance of machine learning models revealed that Bhatsol, Vasishti, and Netravati basins had a greater percentage of models with  $R^2 > 0.8$  compared to Varrar and Periyar basins.

#### **7.4 LIMITATIONS AND SCOPE FOR FUTURE RESEARCH**

- The present study performed a comprehensive analysis of the historical trends and spatio-temporal variations of rainfall and groundwater levels. The study could be further extended to future climatic scenarios as well.
- The site-specific predictor variables could be incorporated in the groundwater level prediction studies, apart from meteorological and abstraction predictors implemented in the current study.
- The groundwater levels used for the present investigation were constrained to the seasonal dataset. Implementation of weekly / monthly datasets could impart further inferences.





# APPENDIX 1

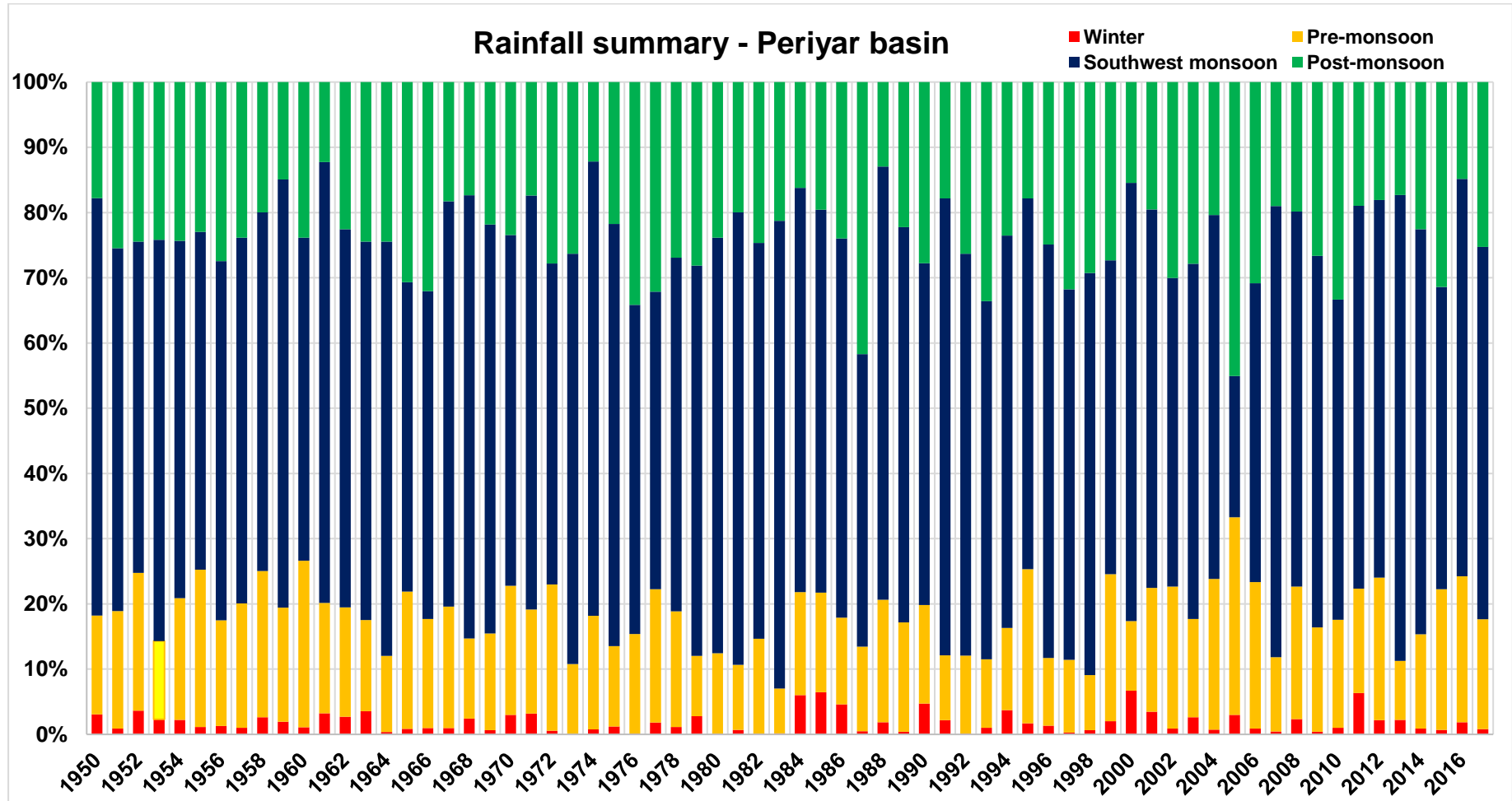


Fig. A. 1.1 Season-wise rainfall summary of Periyar basin from 1950 to 2017

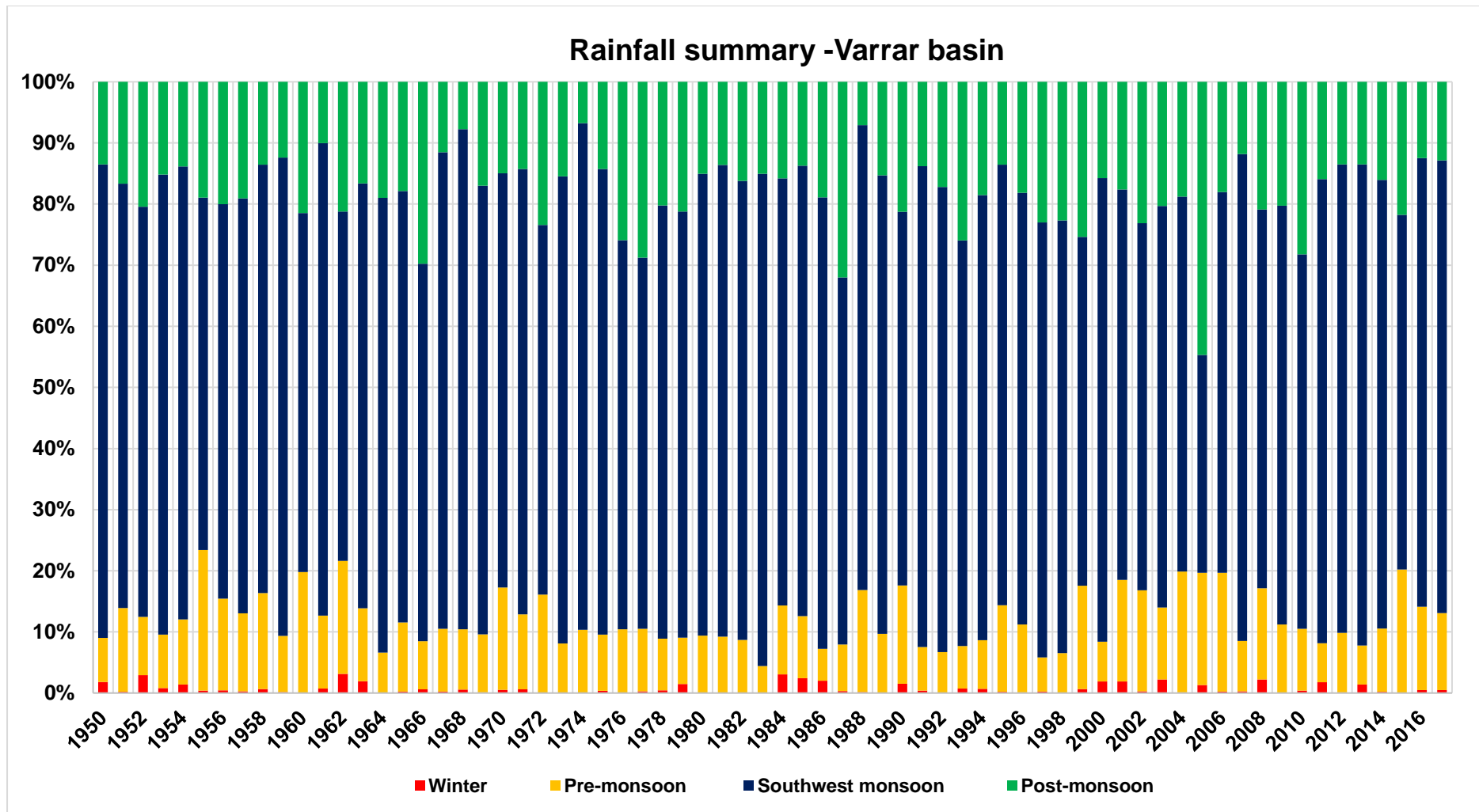


Fig. A. 1.2 Season-wise rainfall summary of Varrar basin from 1950 to 2017

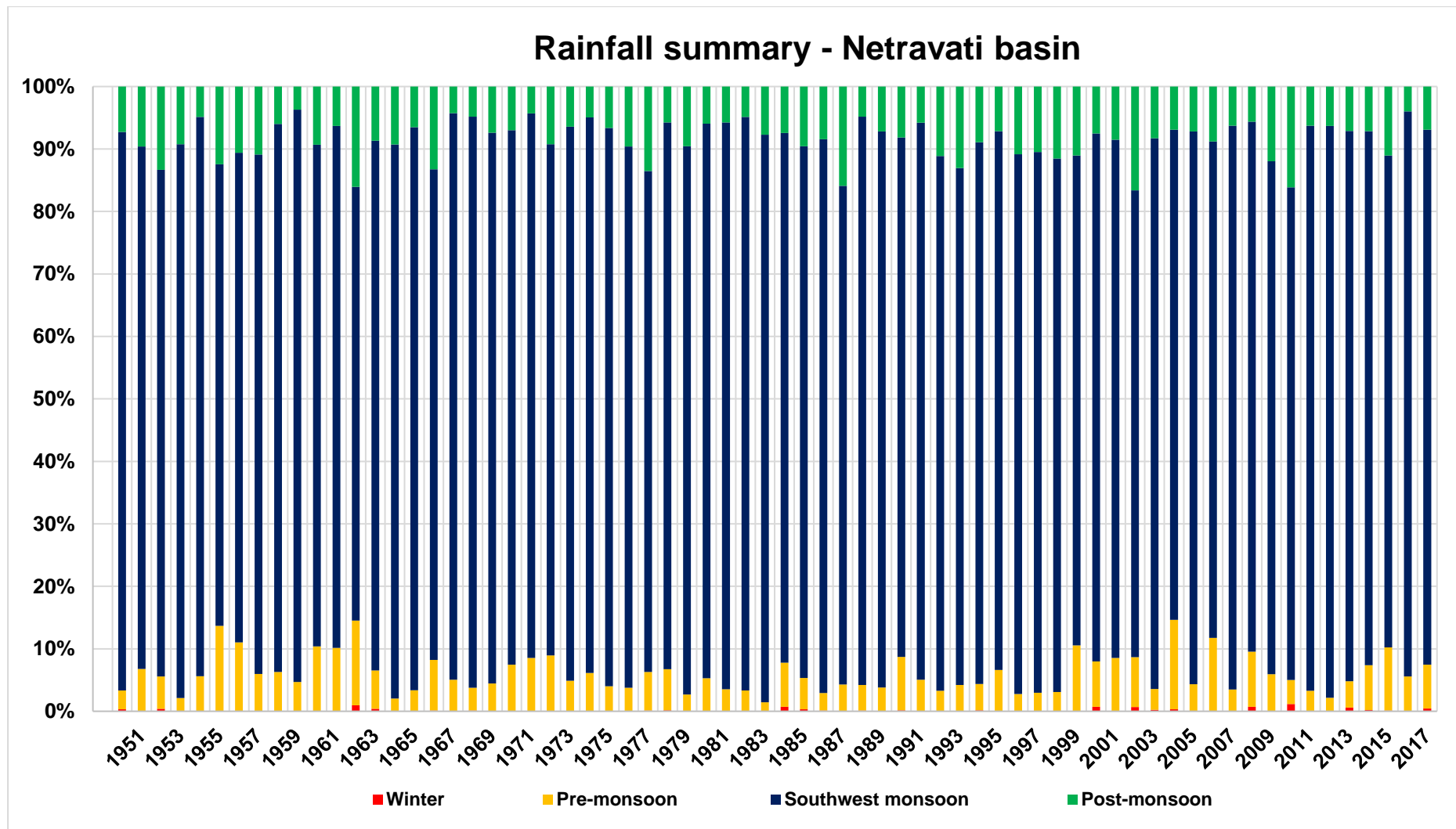


Fig. A. 1.3 Season-wise rainfall summary of Netravati basin from 1950 to 2017

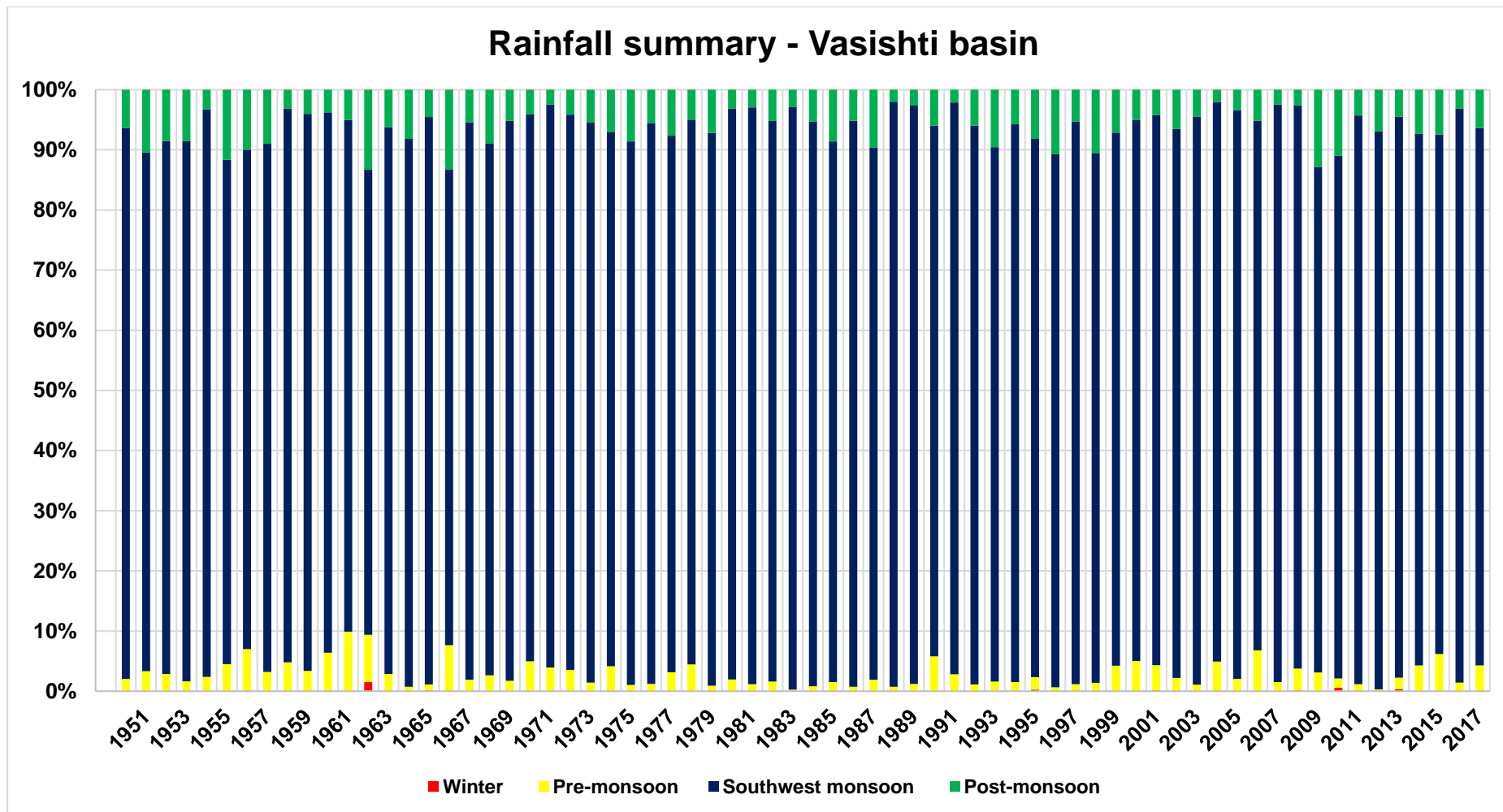


Fig. A. 1.4 Season-wise rainfall summary of Vasishti basin from 1950 to 2017

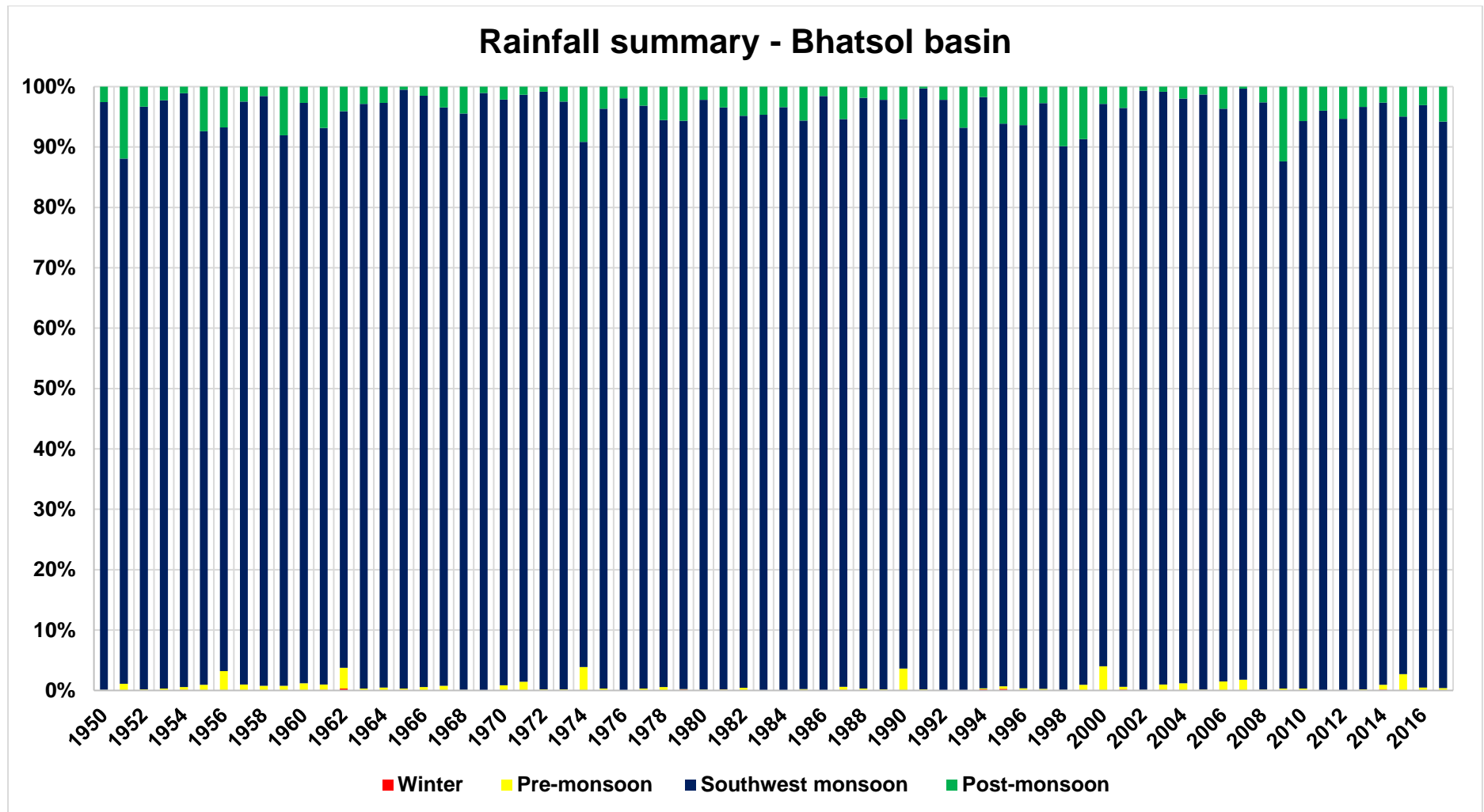


Fig. A. 1.5 Season-wise rainfall summary of Bhatsol basin from 1950 to 2017



## APPENDIX 2

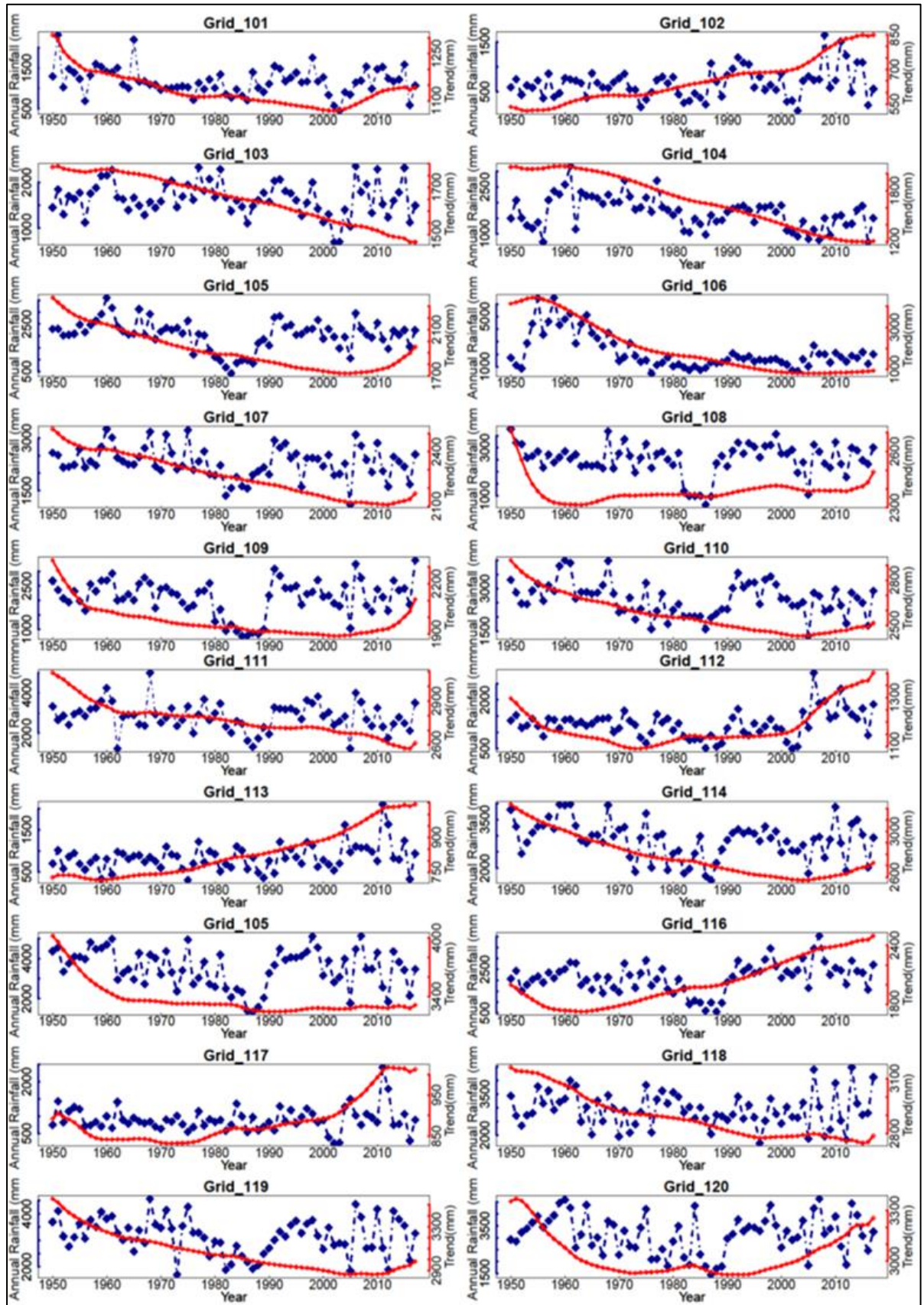


Fig. A.2.1 SSA-extracted annual rainfall trends for grids 101 to 120



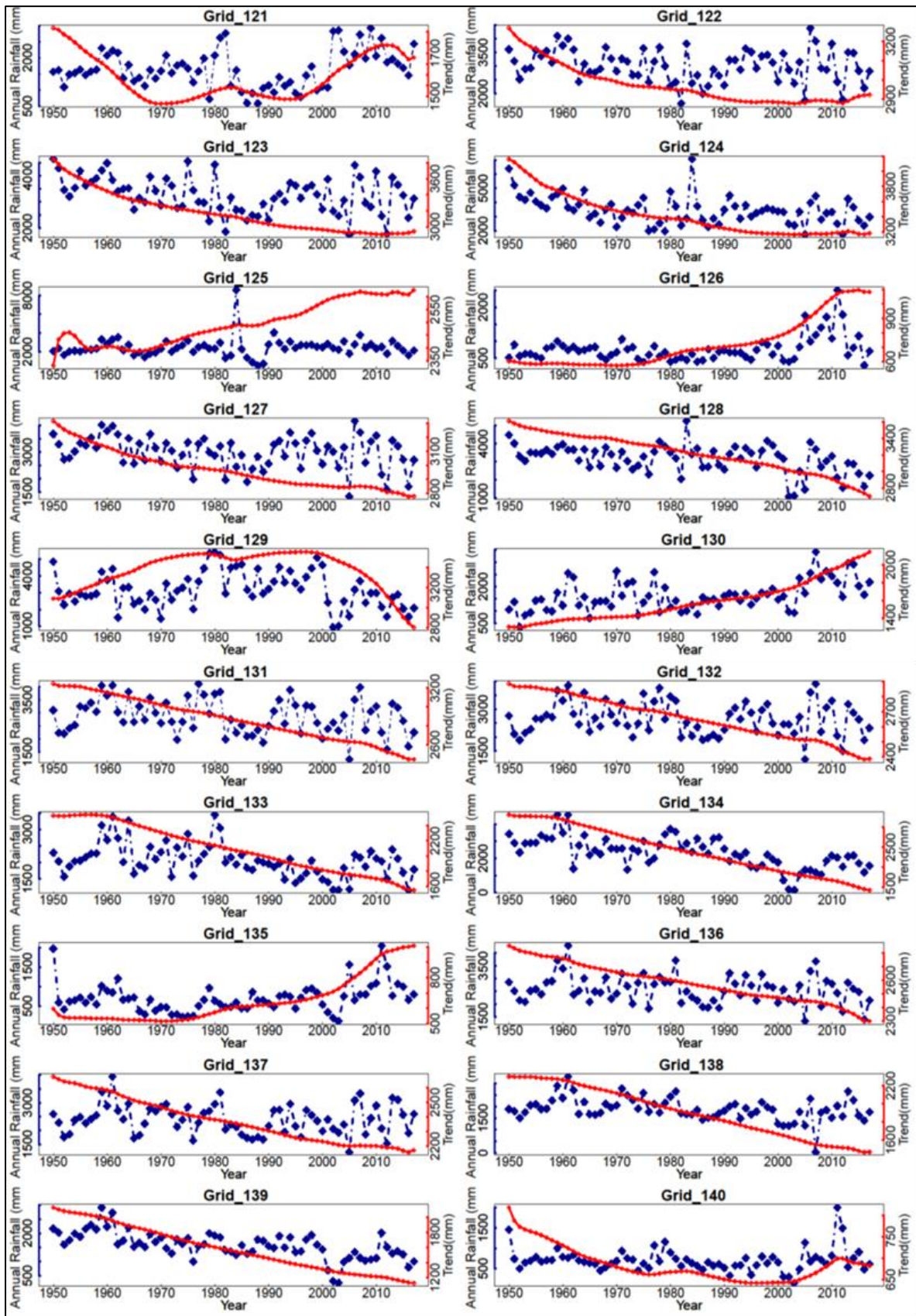


Fig. A.2.2 SSA-extracted annual rainfall trends for grids 121 to 140

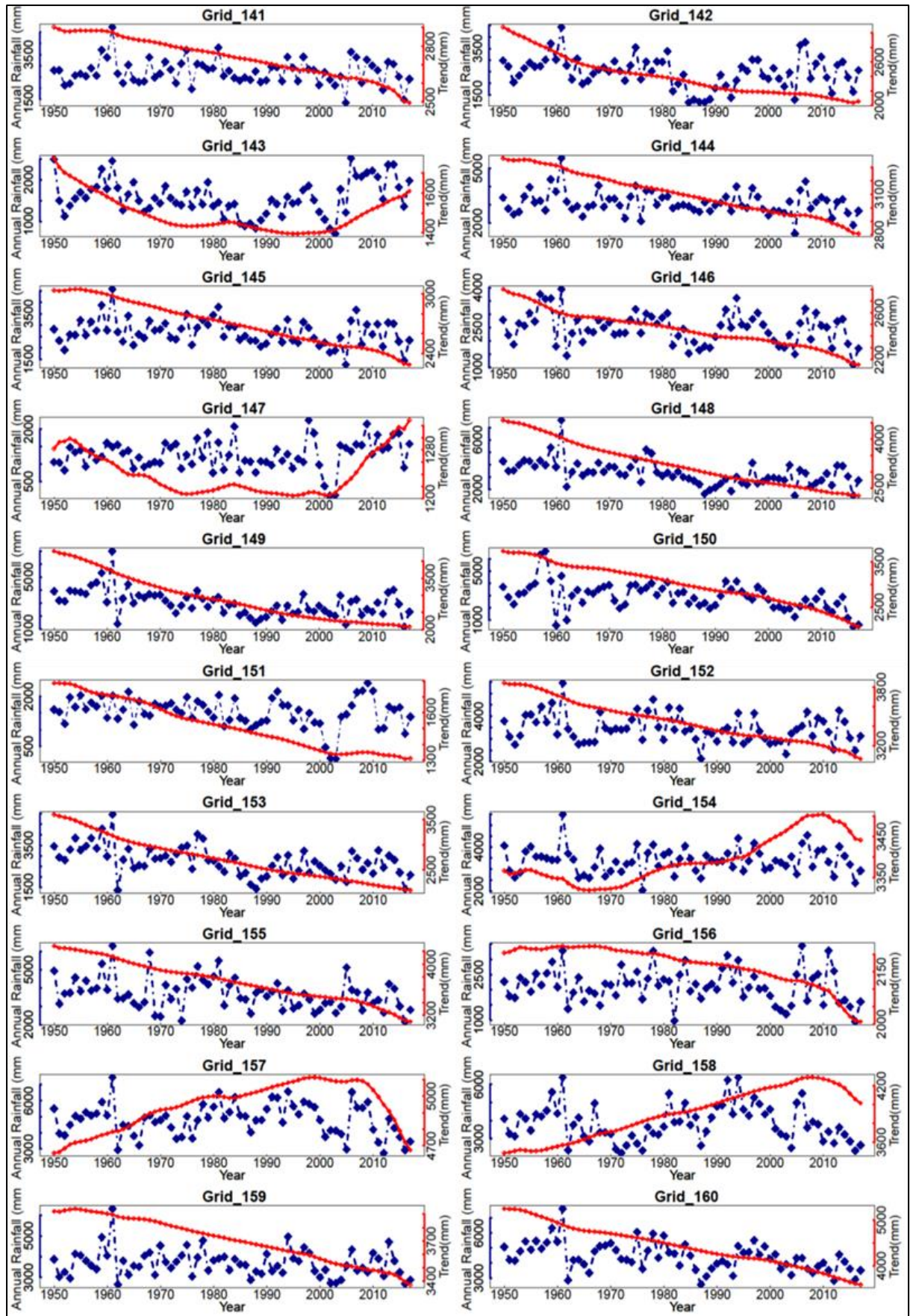


Fig. A.2.3 SSA-extracted annual rainfall trends for grids 141 to 160

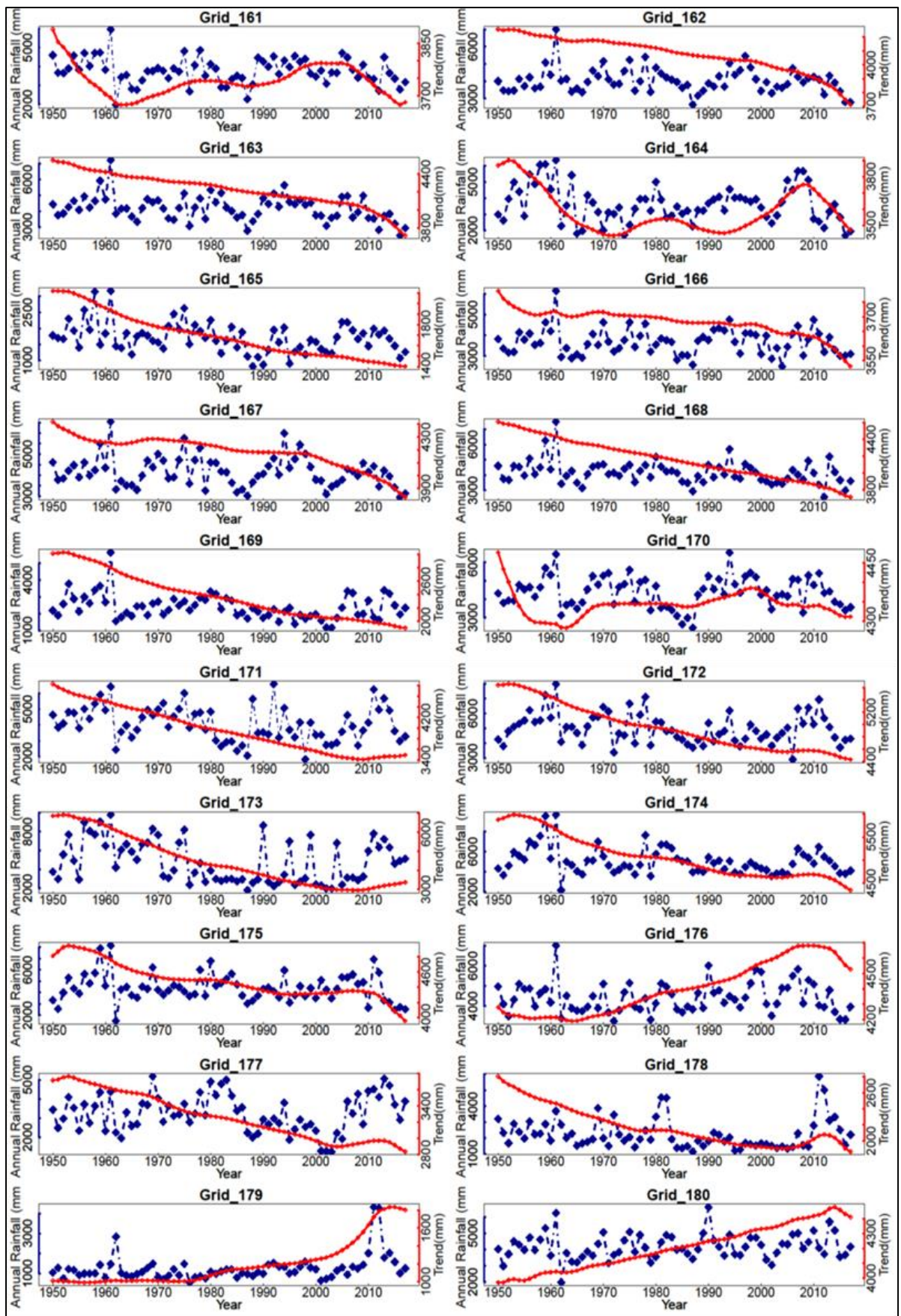


Fig. A.2.4 SSA-extracted annual rainfall trends for grids 161 to 180

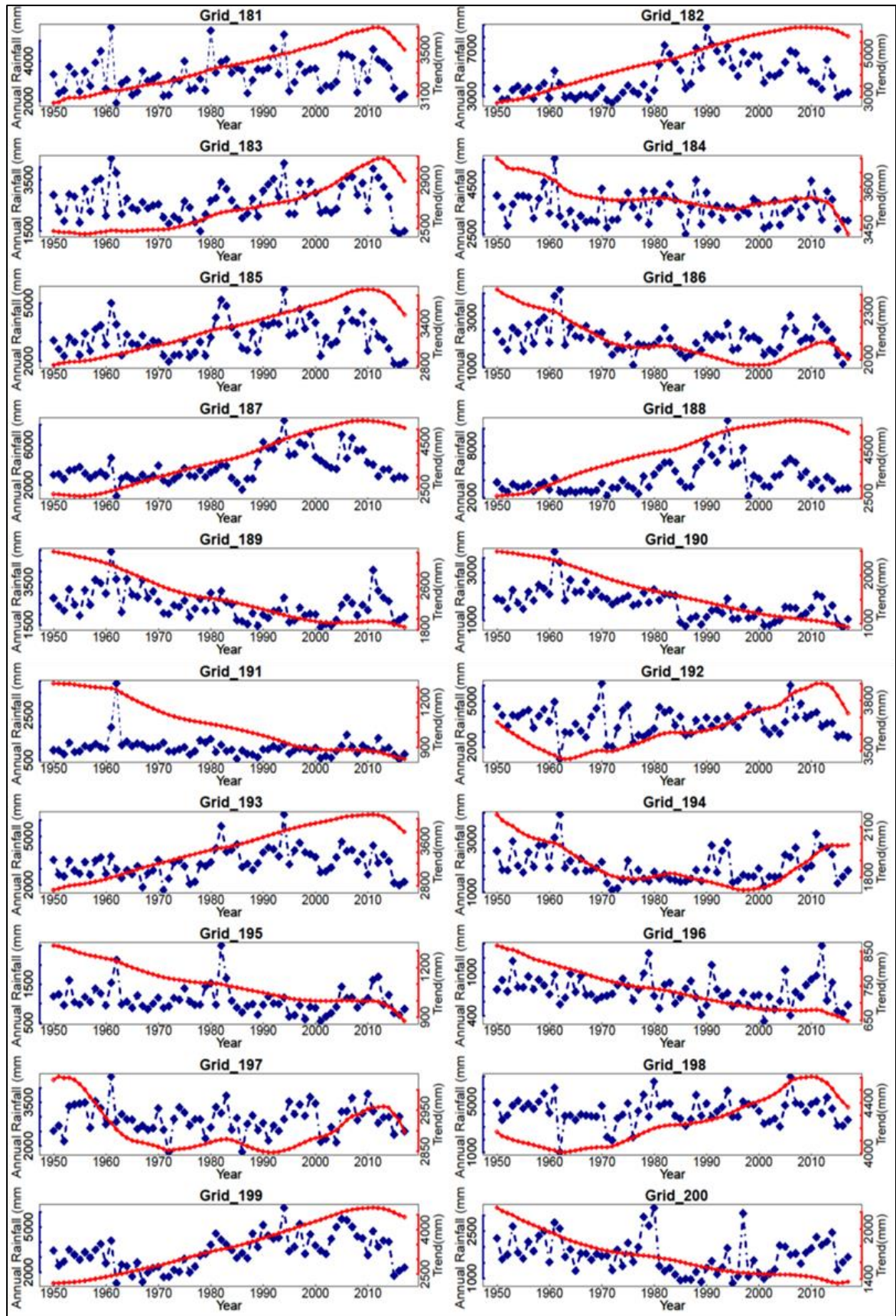


Fig. A.2.5 SSA-extracted annual rainfall trends for grids 181 to 200

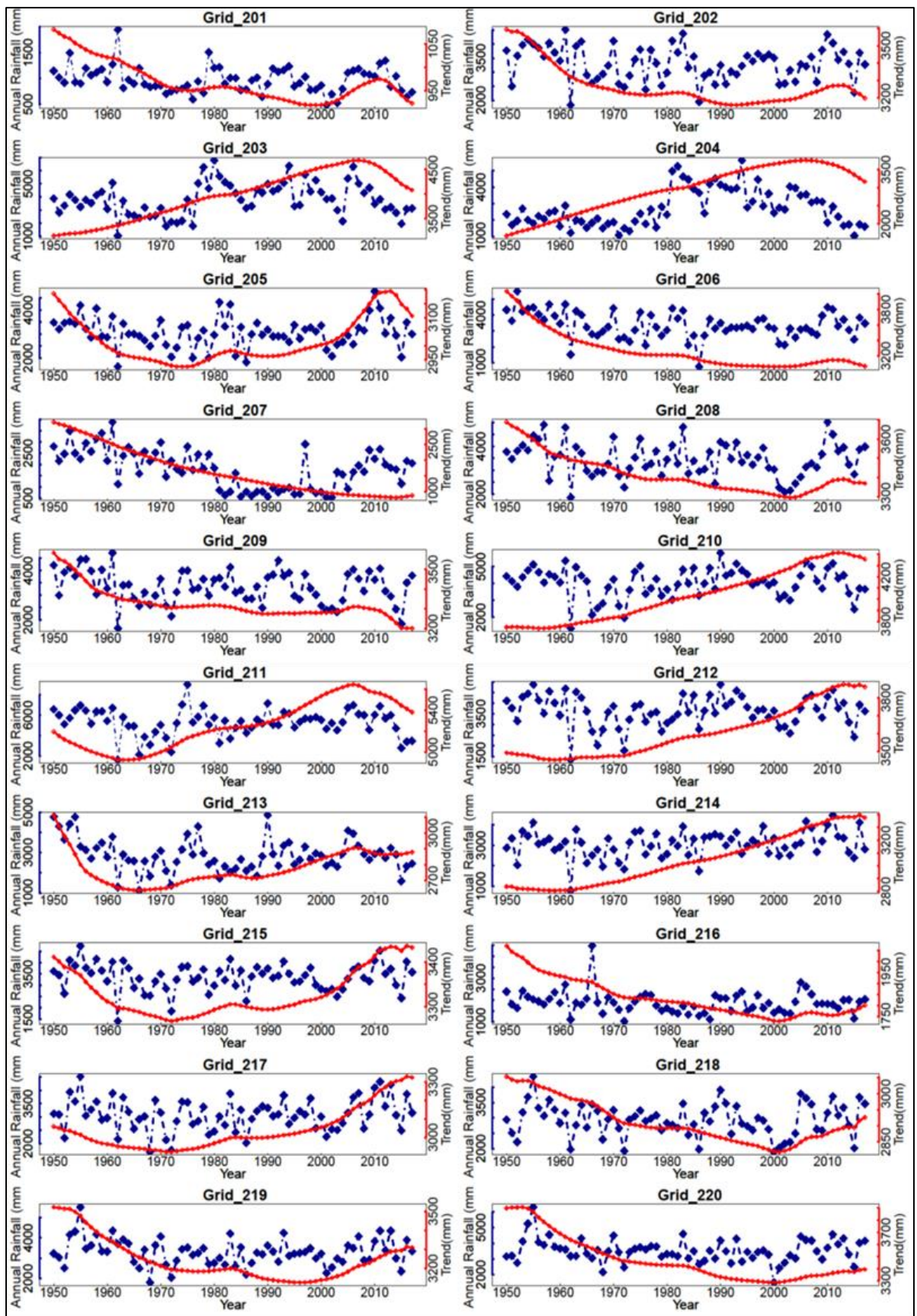


Fig. A.2.6 SSA-extracted annual rainfall trends for grids 201 to 220

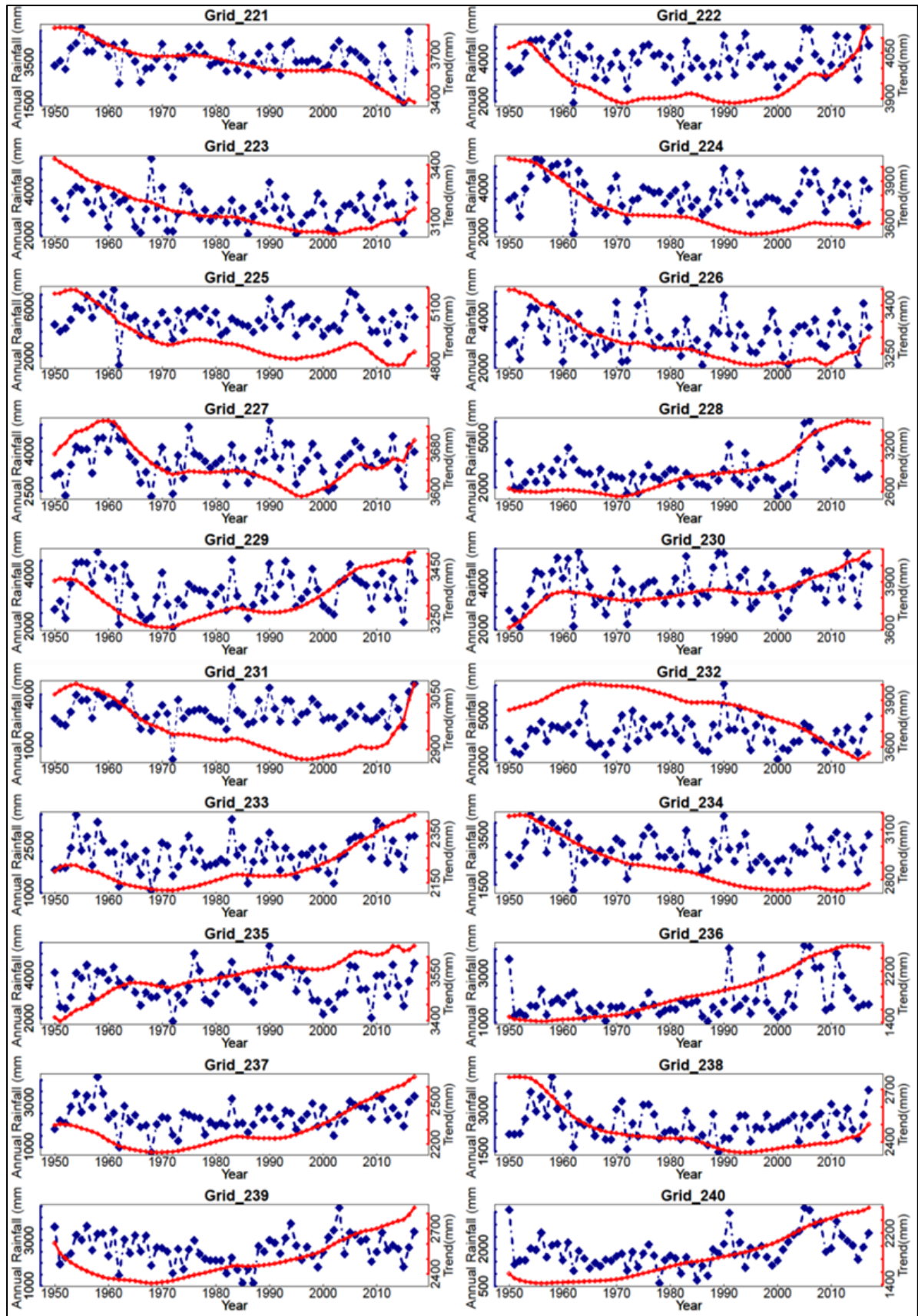


Fig. A.2.7 SSA-extracted annual rainfall trends for grids 221 to 240

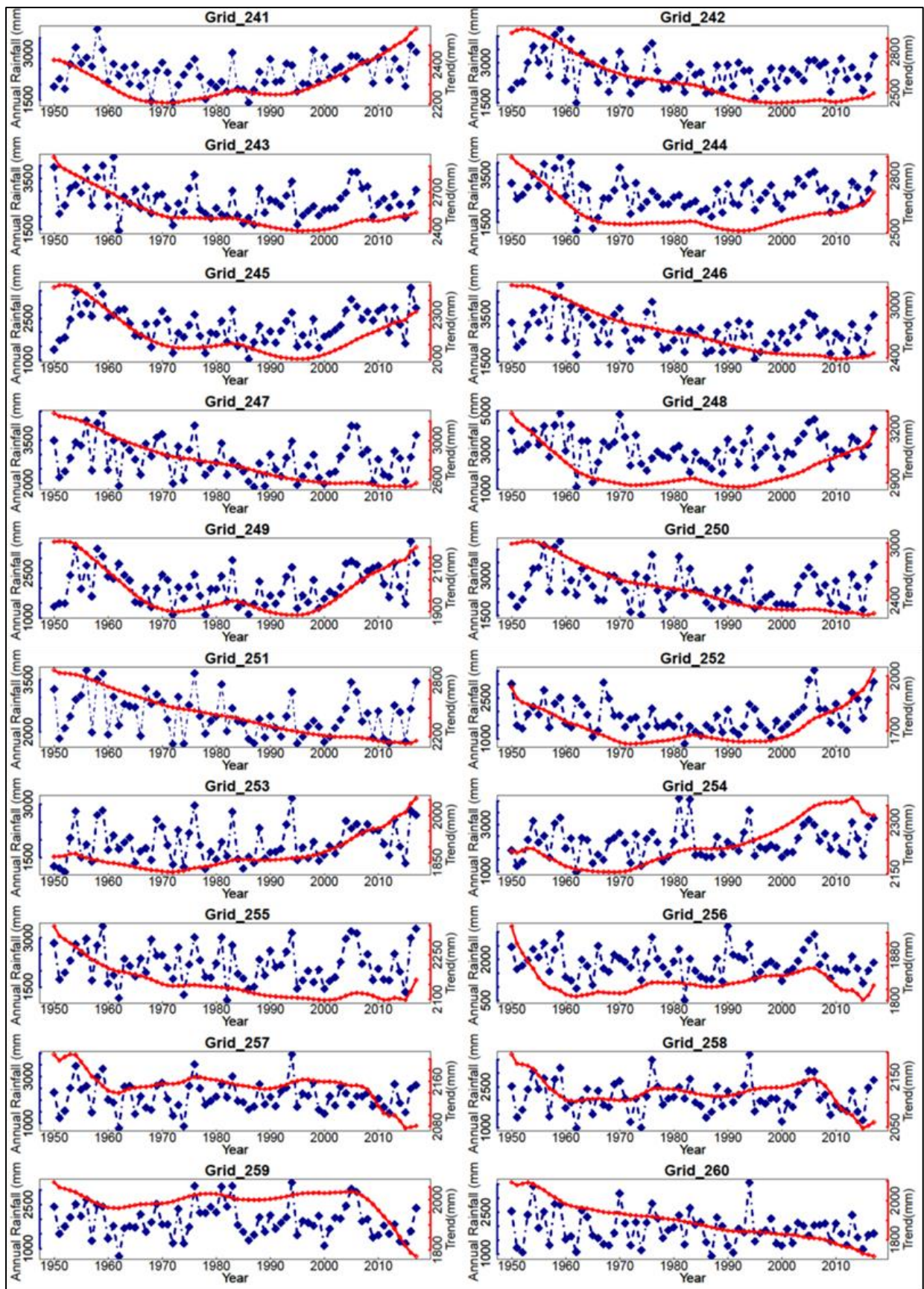
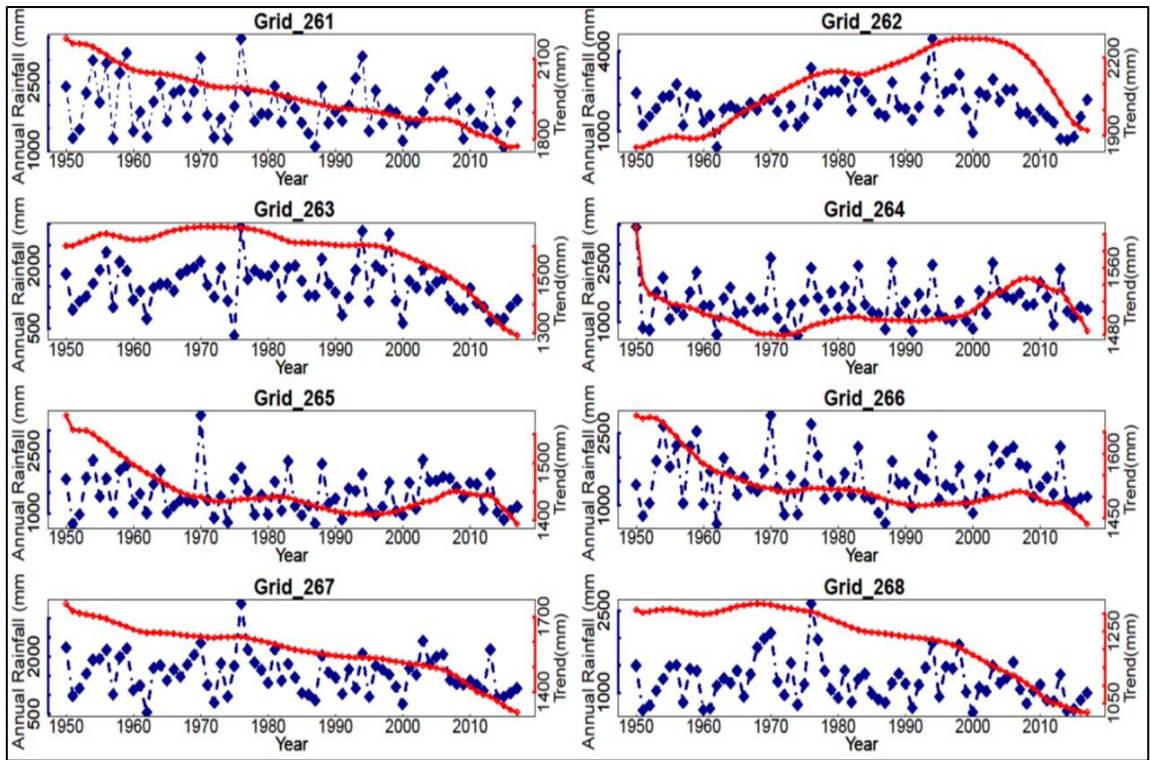


Fig. A.2.8 SSA-extracted annual rainfall trends for grids 241 to 260



**Fig. A.2.9 SSA-extracted annual rainfall trends for grids 261 to 268**





### APPENDIX 3

**Table A.3.1 mMK and SE trends of groundwater levels**

Well id	Winter trends (m/year)	Pre-monsoon trends (m/year)	Monsoon trends (m/year)	Post-monsoon trends (m/year)
W02171	-0.023	-0.023	-0.023	-0.023
W02177	0.014	0.014	0.014	0.014
W02178	0.016	0.016	0.016	0.016
W02179	-0.014	-0.014	-0.014	-0.014
W02181	-0.012	-0.012	-0.012	-0.012
W02185	0.031	0.031	0.031	0.031
W02186	0.000	0.000	0.000	0.000
W02935	-0.001	<b>0.020</b>	0.014	-0.021
W02944	-0.003	0.028	0.040	-0.059
W02945	-0.008	0.022	<b>-0.020</b>	<b>-0.064</b>
W02947	-0.007	0.034	<b>-0.033</b>	-0.098
W02948	-0.024	0.044	<b>-0.036</b>	<b>-0.085</b>
W02951	-0.014	-0.012	-0.016	-0.010
<b>W02961</b>	<b>0.021</b>	0.046	0.000	0.011
W02963	0.002	0.012	-0.009	0.001
W02975	0.007	-0.003	-0.008	-0.003
W02976	-0.004	<b>-0.033</b>	0.003	-0.004
<b>W02977</b>	<b>0.019</b>	<b>0.039</b>	<b>0.014</b>	0.008
<b>W02978</b>	<b>0.054</b>	0.100	-0.006	-0.024
W02979	0.013	0.023	0.006	-0.005
W02982	0.015	0.010	0.003	-0.003
W02983	0.005	0.010	-0.004	-0.003
W02997	0.007	0.011	-0.003	<b>-0.038</b>
W03000	0.005	0.007	-0.010	-0.003
W03001	-0.022	-0.024	<b>-0.024</b>	<b>-0.036</b>
W03007	-0.008	-0.005	<b>-0.009</b>	0.005
<b>W03009</b>	<b>-0.036</b>	<b>-0.058</b>	<b>-0.140</b>	<b>-0.060</b>
<b>W03018</b>	<b>0.019</b>	<b>0.052</b>	0.018	0.008
W03020	0.004	0.022	-0.007	<b>-0.019</b>
W03021	0.001	0.019	-0.014	-0.009
W03026	0.020	0.015	0.020	0.041
W03027	0.007	<b>-0.035</b>	-0.047	-0.003
W03030	0.002	0.006	0.006	0.002
W03031	0.016	0.000	<b>-0.063</b>	-0.045
W03038	-0.011	<b>0.050</b>	-0.062	0.026
<b>W03039</b>	<b>0.024</b>	<b>0.020</b>	-0.006	0.008
W03042	-0.003	0.009	-0.021	0.000
W03044	0.017	0.061	-0.014	-0.001

Note: Bold indicates significant trends at 5% significance level.

Well id	Winter trends (m/year)	Pre-monsoon trends (m/year)	Monsoon trends (m/year)	Post-monsoon trends (m/year)
W03047	-0.007	0.021	-0.044	-0.011
<b>W03051</b>	<b>-0.032</b>	-0.033	0.000	-0.026
W03052	0.004	-0.006	-0.090	-0.029
W03055	0.016	<b>0.025</b>	<b>-0.026</b>	0.015
W03059	0.003	0.005	0.005	-0.003
W03061	-0.015	-0.009	<b>-0.027</b>	<b>-0.037</b>
W03081	-0.005	0.015	<b>-0.017</b>	<b>-0.016</b>
W03083	-0.001	0.029	-0.029	-0.049
<b>W03087</b>	<b>0.062</b>	<b>0.088</b>	<b>0.028</b>	0.018
<b>W03094</b>	<b>-0.025</b>	-0.015	0.007	0.007
<b>W03099</b>	<b>0.036</b>	<b>0.102</b>	0.013	0.016
W03100	0.005	<b>0.025</b>	-0.016	-0.024
W03104	0.009	<b>0.046</b>	0.003	-0.007
W03107	0.001	0.047	-0.004	-0.005
W03112	-0.003	0.001	-0.008	-0.004
W03115	0.006	0.003	-0.010	<b>-0.019</b>
W03116	0.014	0.032	0.009	0.001
W03131	0.003	-0.018	-0.022	-0.027
<b>W03134</b>	<b>-0.120</b>	-0.091	<b>-0.061</b>	-0.017
<b>W03139</b>	<b>0.014</b>	0.001	<b>-0.025</b>	0.010
W03140	0.015	<b>0.095</b>	<b>-0.070</b>	-0.004
W03149	0.034	<b>0.216</b>	<b>-0.056</b>	-0.013
<b>W03151</b>	<b>-0.013</b>	0.004	-0.077	-0.014
<b>W03152</b>	<b>-0.016</b>	-0.017	<b>-0.151</b>	-0.016
<b>W03161</b>	<b>0.022</b>	<b>0.116</b>	-0.089	0.013
<b>W03162</b>	<b>0.029</b>	<b>0.051</b>	<b>-0.072</b>	0.005
W03164	-0.012	0.033	<b>-0.060</b>	-0.016
W03166	0.007	-0.001	<b>-0.032</b>	-0.007
W03169	0.011	0.064	<b>-0.075</b>	0.018
W03171	0.007	0.020	-0.011	-0.007
W03172	0.002	0.006	-0.012	0.000
W03175	-0.009	0.004	-0.003	0.006
W03176	0.033	<b>0.046</b>	<b>-0.151</b>	-0.080
W03177	-0.014	-0.022	<b>-0.078</b>	-0.016
W03182	-0.033	0.021	-0.127	-0.037
W03187	0.003	-0.004	-0.003	0.010
<b>W03192</b>	<b>0.016</b>	-0.001	0.007	0.000
W03196	-0.009	0.025	<b>-0.093</b>	-0.025
W03206	-0.001	-0.006	-0.009	0.003
W03210	0.002	0.014	<b>-0.109</b>	-0.011
W03211	0.016	0.024	0.018	-0.003
W03212	0.012	0.017	-0.080	0.006
W03213	0.011	<b>0.021</b>	-0.091	0.007

Note: Bold indicates significant trends at 5% significance level.

Well id	Winter trends (m/year)	Pre-monsoon trends (m/year)	Monsoon trends (m/year)	Post-monsoon trends (m/year)
W03216	0.006	-0.005	-0.044	0.010
<b>W03219</b>	<b>-0.142</b>	-0.028	-0.023	<b>-0.060</b>
W03230	0.092	-0.068	<b>0.050</b>	<b>0.089</b>
<b>W03231</b>	<b>0.017</b>	<b>0.089</b>	-0.092	-0.008
<b>W03232</b>	<b>0.042</b>	<b>0.062</b>	-0.024	<b>0.022</b>
W03235	0.011	0.012	-0.011	0.012
W03238	0.000	-0.017	-0.023	-0.025
W03239	-0.005	-0.012	-0.022	-0.001
<b>W03240</b>	<b>-0.037</b>	0.004	-0.020	<b>-0.035</b>
W03243	-0.044	-0.081	-0.039	<b>-0.053</b>
W03244	0.009	<b>-0.010</b>	-0.027	<b>-0.086</b>
W03246	-0.013	0.030	0.006	-0.017
W03248	0.005	0.020	0.017	-0.005
W03249	-0.005	-0.013	<b>-0.044</b>	-0.031
<b>W03252</b>	<b>0.033</b>	0.029	0.021	<b>0.033</b>
W03256	0.032	<b>0.036</b>	<b>0.048</b>	0.009
W03257	-0.063	-0.014	-0.022	<b>-0.102</b>
W03259	-0.009	<b>0.037</b>	-0.017	-0.029
W03261	0.001	0.011	0.040	-0.028
W03262	0.009	0.023	0.020	-0.058
W03273	0.011	0.047	0.000	-0.040
W03275	-0.011	0.000	0.000	-0.020
W03282	0.014	<b>0.034</b>	0.049	-0.011
W03283	-0.001	0.002	0.026	-0.007
W03284	0.001	<b>-0.017</b>	0.009	<b>-0.041</b>
W03288	0.000	<b>0.142</b>	0.002	-0.007
W03292	0.006	-0.002	0.004	<b>-0.020</b>
W03299	0.004	-0.017	0.010	-0.008
<b>W03308</b>	<b>-0.031</b>	0.013	-0.053	-0.055
W03326	0.029	0.039	-0.020	-0.040
W03331	-0.003	0.018	-0.001	-0.005
W03332	0.060	-0.068	-0.032	-0.056
<b>W03335</b>	<b>0.015</b>	0.014	0.003	-0.007
W03337	-0.011	-0.035	-0.029	<b>-0.055</b>
W03338	0.008	-0.002	<b>-0.074</b>	-0.023
W03340	0.017	<b>0.043</b>	-0.040	0.015
W03343	0.077	<b>0.055</b>	0.007	0.027
W03347	0.025	0.033	<b>-0.028</b>	-0.015
W03348	-0.004	0.018	0.045	0.042
W03349	0.015	<b>0.092</b>	-0.018	-0.033
W03352	-0.003	0.000	0.011	0.000
W03358	-0.020	0.003	0.058	0.010
W03363	0.020	0.038	0.026	0.000

Note: Bold indicates significant trends at 5% significance level.

Well id	Winter trends (m/year)	Pre-monsoon trends (m/year)	Monsoon trends (m/year)	Post-monsoon trends (m/year)
W03373	0.006	0.018	0.024	0.014
<b>W03377</b>	<b>0.082</b>	-0.035	-0.017	0.034
<b>W03379</b>	<b>0.042</b>	<b>0.133</b>	-0.024	0.058
W03381	0.013	0.002	<b>-0.046</b>	-0.025
<b>W03383</b>	<b>0.034</b>	0.007	0.010	0.024
W03385	0.007	<b>-0.012</b>	-0.019	0.014
W03386	-0.014	-0.016	<b>-0.035</b>	<b>-0.020</b>
W03387	-0.004	-0.002	-0.012	0.017
W03388	-0.011	-0.024	-0.022	-0.009
<b>W03389</b>	<b>-0.045</b>	0.016	<b>-0.137</b>	-0.014
W03390	-0.027	0.003	-0.010	0.019
W03391	-0.017	<b>-0.065</b>	<b>-0.043</b>	-0.011
<b>W03393</b>	<b>0.032</b>	0.020	0.007	0.014
W03396	0.025	<b>0.016</b>	-0.003	0.009
W03397	0.000	-0.017	<b>-0.032</b>	-0.025
W03400	-0.046	-0.030	0.026	0.001
W03404	0.009	-0.013	0.027	-0.022
W03406	0.001	-0.010	-0.007	0.008
W03409	0.024	<b>0.110</b>	-0.015	-0.013
W03410	-0.011	-0.013	<b>-0.053</b>	-0.069
W03415	-0.005	-0.004	-0.003	-0.014
W03416	0.022	0.001	-0.016	0.002
W03417	0.013	0.002	0.004	0.022
W03418	0.018	0.002	<b>-0.096</b>	-0.053
<b>W03419</b>	<b>0.035</b>	<b>0.077</b>	-0.005	<b>0.042</b>
W03422	-0.006	-0.015	0.008	-0.006
W03423	0.000	<b>-0.025</b>	<b>-0.094</b>	<b>-0.071</b>
W03430	-0.003	-0.035	-0.006	0.004
W03431	0.000	-0.011	0.012	0.013
W03432	-0.003	-0.009	0.013	-0.018
W03433	0.001	-0.003	-0.016	-0.016
W03434	-0.003	0.001	<b>-0.088</b>	-0.065
W03435	0.003	0.038	-0.003	0.005
<b>W03438</b>	<b>-0.046</b>	<b>-0.060</b>	-0.003	0.002
W03440	0.007	<b>0.092</b>	<b>-0.081</b>	-0.019
W03441	-0.002	0.016	-0.016	-0.002
W03442	-0.013	-0.004	-0.009	-0.018
W03443	-0.011	0.003	-0.177	-0.018
W03447	0.006	0.037	0.022	0.036
W03450	-0.029	-0.040	0.007	-0.028
<b>W03453</b>	<b>-0.035</b>	-0.055	-0.013	<b>-0.040</b>
W03454	0.018	-0.041	-0.047	-0.032
W03457	-0.021	0.007	-0.057	-0.036

Note: Bold indicates significant trends at 5% significance level.

Well id	Winter trends (m/year)	Pre-monsoon trends (m/year)	Monsoon trends (m/year)	Post-monsoon trends (m/year)
<b>W03461</b>	<b>0.032</b>	<b>0.061</b>	-0.009	-0.002
W03462	0.000	0.004	-0.011	-0.014
W03467	0.003	0.015	-0.022	-0.049
W03469	0.063	<b>0.187</b>	0.017	-0.073
<b>W03470</b>	<b>-0.133</b>	<b>-0.110</b>	-0.037	<b>-0.122</b>
W03474	-0.002	0.009	-0.016	-0.048
W03478	-0.008	-0.008	0.004	-0.004
W03479	-0.001	<b>0.023</b>	<b>0.021</b>	<b>0.024</b>
<b>W03483</b>	<b>-0.039</b>	<b>0.062</b>	0.010	0.011
W03484	-0.009	<b>-0.027</b>	0.004	0.010
W03487	0.012	<b>0.052</b>	-0.010	<b>0.017</b>
W03489	0.011	0.020	-0.015	-0.007
W03495	0.029	0.050	<b>0.100</b>	0.006
W03501	-0.016	-0.015	-0.042	-0.033
W03504	-0.012	<b>0.028</b>	-0.042	-0.064
<b>W03505</b>	<b>-0.012</b>	<b>-0.040</b>	-0.024	<b>-0.026</b>
W03512	-0.004	0.023	0.000	-0.006
W03523	-0.003	-0.026	0.014	-0.011
W03526	0.041	0.020	<b>0.101</b>	0.015
<b>W03527</b>	<b>-0.111</b>	<b>-0.248</b>	<b>-0.156</b>	<b>-0.175</b>
W03530	0.010	<b>-0.084</b>	0.063	-0.032
W03531	0.022	-0.029	0.014	-0.002
W03532	0.005	0.038	0.013	0.004
W03536	-0.013	0.052	-0.008	-0.001
W03537	-0.022	-0.078	-0.023	<b>-0.054</b>
W03541	0.013	0.071	0.015	-0.010
W03542	-0.006	0.008	-0.003	<b>-0.031</b>
W03545	0.000	-0.003	-0.013	-0.020
W03548	0.015	<b>0.038</b>	-0.034	0.015
<b>W03553</b>	<b>0.037</b>	0.025	0.034	0.014
<b>W03555</b>	<b>-0.091</b>	-0.065	-0.013	0.074
W03556	0.004	-0.006	-0.015	-0.019
W03558	0.015	-0.019	-0.038	-0.014
W03559	0.023	0.017	-0.031	0.006
<b>W03560</b>	<b>-0.042</b>	<b>-0.046</b>	<b>-0.065</b>	-0.022
W03562	0.004	0.000	-0.012	-0.008
W03563	-0.005	0.007	0.035	-0.027
W03565	0.006	-0.014	0.007	-0.017
W03570	-0.031	<b>-0.085</b>	-0.027	0.030
W03571	-0.008	-0.028	-0.014	0.000
<b>W03572</b>	<b>0.034</b>	<b>-0.286</b>	<b>0.039</b>	0.053
W03574	0.004	-0.012	<b>-0.017</b>	-0.020
W03575	-0.013	-0.025	0.007	-0.002

Note: Bold indicates significant trends at 5% significance level.

Well id	Winter trends (m/year)	Pre-monsoon trends (m/year)	Monsoon trends (m/year)	Post-monsoon trends (m/year)
W03577	0.000	<b>-0.017</b>	-0.008	<b>0.012</b>
W03578	0.008	0.010	-0.035	-0.014
W03579	0.007	0.030	-0.024	0.010
W03584	-0.005	0.007	<b>-0.080</b>	-0.008
W03587	-0.009	0.006	-0.004	-0.045
W03589	0.004	0.017	-0.018	-0.018
W03592	0.012	<b>0.077</b>	0.034	0.015
W03594	0.015	<b>0.073</b>	-0.003	-0.006
<b>W03599</b>	<b>0.029</b>	0.000	-0.026	-0.048
W03607	0.045	0.010	-0.088	<b>0.059</b>
W03610	-0.006	0.015	-0.004	-0.023
W03619	0.010	<b>0.026</b>	0.018	0.015
<b>W03620</b>	<b>0.077</b>	<b>0.134</b>	0.039	<b>0.086</b>
W03624	0.017	0.007	-0.008	-0.001
W03628	0.008	-0.005	-0.003	0.000
W03631	0.058	0.065	0.110	-0.011
W03635	-0.020	0.005	-0.021	<b>-0.085</b>
W03645	-0.021	-0.023	0.010	-0.015
W03648	0.053	<b>0.047</b>	<b>0.097</b>	-0.005
<b>W03653</b>	<b>0.155</b>	<b>0.201</b>	<b>0.224</b>	<b>0.238</b>
<b>W03656</b>	<b>0.028</b>	0.039	<b>0.081</b>	0.011
W03663	0.044	0.009	0.024	0.033
W03674	0.003	-0.003	0.019	-0.011
W03676	-0.044	-0.005	0.004	-0.010
<b>W03677</b>	<b>-0.042</b>	<b>-0.064</b>	0.001	-0.003
W03679	-0.026	-0.017	0.045	-0.050
W03683	0.028	0.040	-0.013	-0.030
W03686	0.046	0.023	<b>0.101</b>	0.022
<b>W03691</b>	<b>-0.028</b>	<b>0.058</b>	0.031	-0.035
W03693	-0.041	-0.006	0.037	-0.073
W03697	-0.003	-0.033	-0.008	-0.012
W03703	-0.001	-0.012	-0.040	-0.001
W03705	0.001	-0.006	-0.018	0.013
W03706	-0.003	0.009	-0.014	-0.007
<b>W03707</b>	<b>0.020</b>	0.027	-0.025	-0.004
W03710	0.009	0.033	0.018	0.034
W03714	0.006	-0.028	<b>-0.066</b>	-0.008
W03716	-0.025	-0.027	<b>-0.035</b>	<b>-0.035</b>
W03718	-0.008	0.010	-0.087	0.000
W03727	-0.005	-0.010	-0.012	0.022
W03734	0.004	0.029	<b>-0.026</b>	-0.033
<b>W03736</b>	<b>0.019</b>	<b>0.063</b>	-0.018	<b>-0.035</b>
<b>W03737</b>	<b>0.026</b>	<b>0.039</b>	-0.023	0.007

Note: Bold indicates significant trends at 5% significance level.

Well id	Winter trends (m/year)	Pre-monsoon trends (m/year)	Monsoon trends (m/year)	Post-monsoon trends (m/year)
W03741	0.001	0.019	-0.008	0.007
<b>W03748</b>	<b>0.010</b>	0.000	<b>-0.057</b>	-0.017
W03751	0.010	0.016	-0.003	0.014
W03754	0.000	0.003	-0.012	-0.015
W03756	-0.007	-0.002	<b>-0.089</b>	-0.018
W03757	0.002	-0.005	0.027	0.028
W03758	0.004	<b>-0.039</b>	0.026	0.030
W03761	0.013	0.010	-0.074	-0.045
W03762	0.000	-0.006	-0.063	-0.015
W03763	0.012	-0.056	<b>0.008</b>	0.000
<b>W05338</b>	<b>-0.042</b>	-0.002	0.007	0.010
W05339	0.008	0.017	<b>-0.078</b>	0.010
W05346	0.042	<b>0.105</b>	-0.065	0.027
W05462	0.007	0.032	0.000	0.004
W05464	0.002	-0.003	-0.002	0.018
W05465	-0.040	-0.040	-0.030	-0.071
<b>W05469</b>	<b>0.253</b>	0.206	0.009	0.046
W05473	0.009	<b>-0.138</b>	<b>-0.016</b>	0.000
W05474	0.071	0.076	-0.040	0.003
<b>W05477</b>	<b>0.015</b>	-0.006	0.004	0.002
<b>W05480</b>	<b>0.099</b>	0.059	0.020	0.047
W05686	0.036	0.033	-0.043	-0.008
<b>W05688</b>	<b>-0.031</b>	<b>-0.212</b>	-0.047	-0.029
<b>W05690</b>	<b>0.021</b>	<b>-0.057</b>	0.006	0.008
W05860	0.025	-0.011	0.001	-0.002
W05861	0.024	<b>0.062</b>	-0.004	-0.025
W05863	0.047	<b>0.099</b>	-0.022	0.018
W05864	-0.005	-0.011	0.024	0.032
W06067	-0.090	<b>-0.134</b>	-0.045	<b>-0.114</b>
W06069	0.006	-0.029	-0.023	-0.004
<b>W06070</b>	<b>0.042</b>	<b>0.149</b>	-0.013	0.048
W06072	0.052	0.071	-0.037	0.074
<b>W06076</b>	<b>0.022</b>	-0.031	0.025	0.022
<b>W06078</b>	<b>0.044</b>	0.000	0.008	0.033
W06081	0.035	-0.047	-0.021	-0.003
W06083	0.020	-0.006	-0.015	-0.023
W06085	0.018	-0.021	-0.016	0.001
W06195	0.010	0.050	0.029	0.001
W06200	-0.022	0.059	-0.070	0.008
W06384	-0.003	-0.040	-0.008	-0.041
<b>W06389</b>	<b>0.026</b>	<b>-0.047</b>	0.007	0.019
W06392	0.059	<b>0.146</b>	0.047	0.036

Note: Bold indicates significant trends at 5% significance level



Well id	Winter trends (m/year)	Pre-monsoon trends (m/year)	Monsoon trends (m/year)	Post-monsoon trends (m/year)
W06542	0.024	0.028	<b>-0.075</b>	-0.015
W06543	0.014	<b>0.079</b>	-0.007	<b>0.048</b>
<b>W06547</b>	<b>0.021</b>	<b>0.076</b>	-0.006	0.018
W06551	-0.044	-0.081	-0.051	-0.047
W06705	0.043	-0.126	0.022	<b>0.102</b>
W06707	-0.010	-0.063	-0.004	-0.022
W06708	0.002	-0.040	0.000	-0.001
W06710	0.028	-0.054	-0.036	-0.019
<b>W06712</b>	<b>0.027</b>	<b>-0.023</b>	0.014	<b>0.026</b>
<b>W06713</b>	<b>0.073</b>	<b>0.047</b>	0.000	<b>0.047</b>
<b>W06745</b>	<b>-0.070</b>	0.002	0.212	<b>-0.040</b>
W06747	-0.024	-0.016	0.907	-0.031
W06748	-0.008	0.057	-0.696	0.027
<b>W06751</b>	<b>-0.025</b>	-0.001	-1.059	-0.003
W06752	-0.029	-0.035	-1.785	-0.018
W06753	-0.016	0.008	-0.483	0.000
<b>W06754</b>	<b>-0.053</b>	-0.039	1.271	0.011
<b>W06756</b>	<b>-0.078</b>	<b>-0.116</b>	<b>-2.840</b>	-0.037
W06758	-0.006	0.066	1.181	0.017
<b>W06762</b>	<b>-0.062</b>	-0.010	<b>-2.310</b>	<b>-0.051</b>
W06763	-0.009	-0.011	<b>-3.600</b>	-0.037
W06764	-0.009	-0.004	<b>-0.938</b>	0.025
W06765	0.018	-0.010	1.360	0.000
W06766	0.002	0.015	0.152	-0.020
W06767	0.005	0.054	<b>-2.765</b>	-0.035
W07387	-0.022	<b>-0.079</b>	-0.019	-0.035
W07390	-0.013	0.003	-0.010	0.013
W07394	0.011	0.021	0.004	-0.027
W07401	0.031	<b>0.123</b>	<b>-0.018</b>	0.000
W07402	-0.021	0.014	-0.006	-0.003
W07403	0.023	0.016	0.013	0.034
W07404	-0.040	-0.006	-0.013	-0.034
<b>W07407</b>	<b>-0.153</b>	-0.065	-0.072	-0.011
W07409	-0.012	-0.012	-0.008	0.010
W07410	0.003	<b>-0.050</b>	-0.006	-0.038
<b>W07416</b>	<b>-0.033</b>	-0.004	-0.004	-0.018
W07418	0.000	0.003	0.024	0.020
W07420	-0.007	0.000	-0.010	0.019
<b>W07421</b>	<b>0.033</b>	0.009	-0.056	0.005
W07424	0.015	-0.088	-0.020	-0.006
W07425	0.012	0.042	<b>-0.055</b>	0.010
<b>W07490</b>	<b>-0.081</b>	-0.105	-0.112	<b>-0.144</b>

Note: Bold indicates significant trends at 5% significance level

Well id	Winter trends (m/year)	Pre-monsoon trends (m/year)	Monsoon trends (m/year)	Post-monsoon trends (m/year)
W07494	-0.048	<b>-0.110</b>	0.028	-0.022
W07495	0.014	-0.041	-0.020	-0.025
W07496	-0.022	-0.076	-0.028	<b>-0.060</b>
W07496	-0.022	-0.076	-0.028	<b>-0.060</b>
<b>W07497</b>	<b>-0.051</b>	-0.044	0.000	-0.017
W07498	0.016	0.000	-0.014	<b>-0.022</b>
W07500	-0.037	<b>-0.048</b>	0.000	-0.014
W07501	-0.002	<b>0.135</b>	-0.002	0.025
<b>W07504</b>	<b>-0.025</b>	<b>-0.050</b>	-0.001	-0.008
W07505	-0.009	-0.030	0.000	<b>-0.016</b>
W07506	-0.005	-0.037	0.002	-0.005
<b>W07507</b>	<b>-0.045</b>	-0.030	-0.069	-0.021
W07551	-0.020	-0.008	-0.997	0.011
W07554	-0.003	<b>0.137</b>	-0.665	0.009
W07561	-0.019	0.000	-1.180	0.002
<b>W07563</b>	<b>-0.065</b>	0.045	<b>-2.148</b>	<b>-0.053</b>
<b>W07565</b>	<b>-0.053</b>	<b>-0.042</b>	-0.967	-0.043
W07568	-0.012	0.058	-1.091	-0.031
W07569	-0.010	0.028	-0.454	-0.007
W08005	-0.017	0.000	0.005	0.001
<b>W08010</b>	<b>0.024</b>	<b>0.149</b>	-0.013	0.020
<b>W08011</b>	<b>0.030</b>	<b>0.070</b>	0.025	0.040
W08143	-0.009	<b>-0.142</b>	0.000	0.018
W08148	0.017	<b>-0.188</b>	-0.008	0.006
W08151	-0.010	-0.068	-0.001	-0.006
W08153	0.008	-0.030	-0.003	-0.002
W08154	-0.001	-0.093	-0.013	-0.007
<b>W08191</b>	<b>0.026</b>	0.006	0.031	0.028
<b>W08712</b>	<b>0.063</b>	0.000	<b>0.080</b>	<b>0.109</b>
W08713	0.038	<b>-0.180</b>	0.008	0.031
W08869	-0.011	<b>-0.087</b>	-0.043	-0.024
W08871	-0.001	-0.041	-0.015	0.003
W08879	-0.039	<b>-0.113</b>	0.029	<b>-0.056</b>
W08908	-0.003	<b>-0.120</b>	<b>-0.052</b>	-0.007
W08947	-0.012	-0.060	-0.001	-0.003
W08948	-0.004	<b>-0.133</b>	0.010	0.012
W08952	0.006	0.005	-0.021	-0.044
<b>W08954</b>	<b>-0.029</b>	<b>0.072</b>	<b>0.027</b>	0.009
<b>W08955</b>	<b>0.072</b>	<b>0.096</b>	0.024	0.031
W08996	-0.007	-0.066	0.000	-0.002
<b>W09000</b>	<b>0.095</b>	<b>0.227</b>	0.006	0.046
W09001	-0.025	<b>-0.048</b>	-0.010	-0.012
W09004	0.020	0.004	-0.027	0.025

Note: Bold indicates significant trends at 5% significance level

Well id	Winter trends (m/year)	Pre-monsoon trends (m/year)	Monsoon trends (m/year)	Post-monsoon trends (m/year)
W09005	-0.009	-0.093	0.018	0.029
W09007	-0.017	-0.042	0.017	-0.007
W09008	0.017	0.012	0.064	0.027
W17573	0.000	-0.067	<b>-0.012</b>	-0.045
<b>W17576</b>	<b>-0.075</b>	<b>-0.100</b>	<b>-0.051</b>	<b>-0.065</b>
<b>W17578</b>	<b>-0.036</b>	<b>-0.100</b>	0.001	-0.007
W17580	-0.016	-0.009	0.003	-0.008
W17583	-0.040	0.053	-0.019	-0.032
W17587	0.010	-0.011	<b>-0.021</b>	-0.017
W17597	-0.050	-0.042	-0.028	<b>-0.025</b>
W17600	-0.017	-0.040	0.063	0.005
W17602	-0.007	0.006	-0.008	-0.009
W17603	-0.010	0.017	0.009	-0.018
<b>W17604</b>	<b>-0.035</b>	-0.048	<b>-0.035</b>	0.001
W17606	-0.031	0.007	-0.015	0.010
W17608	0.000	<b>-0.145</b>	-0.017	0.006
W17609	0.007	<b>-0.057</b>	0.026	<b>0.124</b>
<b>W17610</b>	<b>-0.037</b>	-0.076	-0.005	-0.021
<b>W17617</b>	<b>-0.036</b>	-0.011	-0.005	<b>-0.019</b>
W17619	0.016	0.058	-0.012	0.033
W17620	-0.009	-0.123	-0.151	0.030
W17621	-0.020	-0.007	0.000	-0.073
W17622	-0.013	-0.026	-0.008	<b>-0.022</b>
W17624	-0.025	-0.072	-0.011	-0.008
<b>W17625</b>	<b>0.156</b>	0.106	0.310	0.150
W17653	0.000	<b>-0.085</b>	<b>-0.080</b>	0.016
<b>W17655</b>	<b>-0.038</b>	-0.014	-0.021	<b>-0.013</b>
W17656	-0.009	0.065	0.007	-0.007
W17657	0.010	-0.024	-0.009	0.002
W17658	-0.026	<b>-0.120</b>	-0.051	<b>-0.117</b>
W17659	-0.003	-0.004	-0.023	-0.014
W17661	-0.012	0.000	-0.007	0.002
W17663	0.001	0.024	-0.026	-0.009
<b>W17664</b>	<b>-0.075</b>	<b>-0.112</b>	-0.052	<b>-0.105</b>
W17666	-0.040	-0.060	-0.097	-0.015
W17667	-0.076	-0.095	0.000	<b>0.054</b>
W17668	0.036	0.030	0.027	0.038

Note: Bold indicates significant trends at 5% significance level.

## APPENDIX 4

**Table A 4.1 R<sup>2</sup> and RMSE of ANN models during training and testing phase**

well	ANN1				ANN2			
	RMSE- Trainin g	R2- Trainin g	RMSE - Testin g	R2- Testin g	RMSE- Trainin g	R2- Trainin g	RMSE - Testin g	R2- Testin g
W02171	0.16	0.49	0.17	0.50	0.16	0.48	0.17	0.51
W02177	0.12	0.59	0.14	0.50	0.12	0.58	0.14	0.51
W02178	0.12	0.64	0.13	0.74	0.12	0.63	0.13	0.72
W02179	0.24	0.30	0.21	0.38	0.24	0.29	0.21	0.42
W02181	0.10	0.60	0.08	0.65	0.10	0.59	0.08	0.65
W02185	0.14	0.41	0.16	0.79	0.14	0.40	0.16	0.74
W02186	0.13	0.50	0.12	0.46	0.13	0.49	0.12	0.48
W02935	0.18	0.46	0.12	0.38	0.14	0.61	0.15	0.40
W02944	0.18	0.58	0.16	0.67	0.18	0.63	0.15	0.66
W02945	0.12	0.76	0.16	0.62	0.13	0.70	0.15	0.67
W02947	0.16	0.70	0.16	0.63	0.17	0.67	0.15	0.71
W02948	0.22	0.44	0.18	0.79	0.21	0.55	0.16	0.84
W02951	0.17	0.55	0.12	0.70	0.16	0.54	0.13	0.58
W02961	0.15	0.57	0.14	0.56	0.16	0.46	0.16	0.55
W02963	0.11	0.74	0.13	0.81	0.11	0.73	0.11	0.73
W02975	0.11	0.87	0.12	0.83	0.11	0.89	0.12	0.78
W02976	0.11	0.72	0.15	0.69	0.11	0.69	0.17	0.71
W02977	0.15	0.80	0.17	0.87	0.18	0.72	0.19	0.66
W02978	0.14	0.66	0.12	0.66	0.14	0.67	0.12	0.54
W02979	0.11	0.84	0.10	0.90	0.13	0.75	0.13	0.80
W02982	0.11	0.90	0.08	0.92	0.11	0.86	0.09	0.91
W02983	0.14	0.75	0.12	0.76	0.14	0.71	0.13	0.65
W02997	0.09	0.89	0.13	0.75	0.10	0.90	0.14	0.76
W03000	0.11	0.80	0.11	0.75	0.10	0.85	0.10	0.70
W03001	0.14	0.76	0.09	0.85	0.14	0.75	0.11	0.78
W03007	0.10	0.78	0.09	0.87	0.11	0.76	0.08	0.82
W03009	0.16	0.66	0.18	0.65	0.21	0.43	0.12	0.55
W03018	0.14	0.54	0.10	0.64	0.11	0.63	0.22	0.59
W03020	0.17	0.49	0.08	0.76	0.14	0.57	0.13	0.59
W03021	0.14	0.69	0.08	0.82	0.15	0.53	0.08	0.77
W03026	0.10	0.65	0.08	0.78	0.14	0.73	0.10	0.74
W03027	0.11	0.54	0.07	0.74	0.10	0.69	0.09	0.77
W03030	0.16	0.74	0.17	0.72	0.12	0.66	0.06	0.73
W03031	0.12	0.83	0.10	0.80	0.13	0.73	0.16	0.82
W03038	0.12	0.65	0.11	0.65	0.11	0.84	0.10	0.78
W03039	0.14	0.76	0.11	0.87	0.15	0.52	0.14	0.39
W03042	0.09	0.84	0.06	0.90	0.12	0.66	0.12	0.58

well	ANN1				ANN2			
	RMSE-Trainin g	R2-Trainin g	RMSE-Testin g	R2-Testin g	RMSE-Trainin g	R2-Trainin g	RMSE-Testin g	R2-Testin g
W03044	0.13	0.69	0.09	0.82	0.15	0.73	0.12	0.80
W03047	0.14	0.62	0.09	0.76	0.08	0.83	0.07	0.89
W03051	0.10	0.49	0.13	0.76	0.13	0.64	0.08	0.83
W03052	0.21	0.41	0.15	0.54	0.14	0.58	0.08	0.82
W03055	0.12	0.59	0.10	0.63	0.10	0.54	0.13	0.70
W03059	0.11	0.59	0.10	0.67	0.19	0.44	0.14	0.56
W03061	0.11	0.80	0.10	0.87	0.12	0.63	0.10	0.64
W03081	0.18	0.55	0.21	0.65	0.13	0.53	0.12	0.52
W03083	0.13	0.82	0.14	0.66	0.12	0.76	0.09	0.82
W03087	0.10	0.49	0.12	0.48	0.15	0.53	0.11	0.72
W03094	0.13	0.64	0.15	0.68	0.15	0.64	0.23	0.66
W03099	0.16	0.72	0.15	0.57	0.14	0.74	0.17	0.65
W03100	0.11	0.89	0.13	0.79	0.08	0.53	0.07	0.54
W03104	0.13	0.84	0.15	0.69	0.15	0.53	0.12	0.82
W03107	0.18	0.46	0.10	0.51	0.16	0.69	0.16	0.79
W03112	0.07	0.90	0.12	0.72	0.12	0.93	0.13	0.81
W03115	0.10	0.82	0.11	0.87	0.11	0.85	0.10	0.86
W03116	0.13	0.70	0.17	0.65	0.15	0.57	0.12	0.75
W03131	0.08	0.95	0.07	0.95	0.08	0.88	0.11	0.71
W03134	0.15	0.34	0.08	0.59	0.11	0.79	0.11	0.87
W03139	0.13	0.69	0.13	0.69	0.13	0.69	0.13	0.70
W03140	0.10	0.91	0.08	0.87	0.08	0.93	0.08	0.94
W03149	0.15	0.78	0.11	0.76	0.15	0.35	0.08	0.59
W03151	0.07	0.89	0.08	0.84	0.13	0.74	0.11	0.71
W03152	0.13	0.74	0.17	0.56	0.11	0.88	0.11	0.85
W03161	0.09	0.91	0.09	0.85	0.15	0.76	0.15	0.74
W03162	0.15	0.61	0.13	0.47	0.07	0.90	0.08	0.80
W03164	0.10	0.81	0.12	0.77	0.13	0.72	0.17	0.56
W03166	0.08	0.87	0.07	0.70	0.20	0.45	0.13	0.60
W03169	0.14	0.78	0.10	0.88	0.09	0.92	0.09	0.84
W03171	0.12	0.82	0.15	0.66	0.14	0.70	0.14	0.44
W03172	0.10	0.84	0.06	0.93	0.10	0.84	0.12	0.72
W03175	0.17	0.64	0.17	0.71	0.08	0.80	0.07	0.70
W03176	0.08	0.83	0.08	0.72	0.13	0.83	0.10	0.85
W03177	0.16	0.76	0.07	0.92	0.12	0.80	0.14	0.69
W03182	0.11	0.83	0.13	0.76	0.09	0.82	0.06	0.94
W03187	0.06	0.96	0.08	0.86	0.16	0.65	0.18	0.66
W03192	0.08	0.83	0.11	0.82	0.09	0.84	0.08	0.76
W03196	0.10	0.90	0.09	0.90	0.13	0.80	0.07	0.92
W03206	0.17	0.44	0.09	0.67	0.12	0.79	0.13	0.74
W03210	0.11	0.93	0.12	0.76	0.06	0.95	0.07	0.88
W03211	0.23	0.39	0.18	0.43	0.07	0.85	0.11	0.80

well	ANN1				ANN2			
	RMSE- Trainin g	R2- Trainin g	RMSE - Testin g	R2- Testin g	RMSE- Trainin g	R2- Trainin g	RMSE - Testin g	R2- Testin g
W03212	0.10	0.79	0.05	0.83	0.10	0.90	0.09	0.89
W03213	0.19	0.71	0.14	0.70	0.14	0.34	0.18	0.42
W03216	0.11	0.64	0.09	0.69	0.10	0.90	0.15	0.63
W03216	0.12	0.81	0.11	0.93	0.21	0.50	0.18	0.46
W03219	0.09	0.96	0.09	0.92	0.11	0.78	0.05	0.90
W03230	0.16	0.44	0.21	0.42	0.17	0.71	0.14	0.67
W03231	0.10	0.90	0.12	0.80	0.11	0.59	0.08	0.72
W03232	0.12	0.78	0.12	0.73	0.11	0.83	0.11	0.92
W03235	0.10	0.75	0.07	0.87	0.09	0.91	0.10	0.90
W03238	0.06	0.99	0.11	0.80	0.10	0.92	0.10	0.85
W03239	0.08	0.96	0.08	0.94	0.12	0.83	0.12	0.75
W03240	0.16	0.58	0.09	0.67	0.10	0.78	0.08	0.85
W03243	0.16	0.64	0.10	0.93	0.06	0.96	0.10	0.83
W03244	0.10	0.74	0.13	0.50	0.11	0.90	0.08	0.93
W03246	0.11	0.79	0.13	0.75	0.19	0.43	0.10	0.67
W03248	0.10	0.68	0.12	0.77	0.16	0.63	0.13	0.86
W03249	0.09	0.57	0.11	0.67	0.09	0.76	0.13	0.55
W03252	0.20	0.44	0.08	0.92	0.12	0.75	0.14	0.69
W03256	0.09	0.62	0.16	0.42	0.09	0.71	0.11	0.82
W03257	0.13	0.50	0.11	0.59	0.08	0.63	0.12	0.66
W03259	0.16	0.28	0.08	0.40	0.19	0.45	0.08	0.86
W03261	0.09	0.78	0.09	0.79	0.08	0.57	0.19	0.50
W03262	0.13	0.83	0.17	0.78	0.12	0.58	0.12	0.49
W03273	0.12	0.62	0.08	0.68	0.10	0.72	0.10	0.80
W03275	0.09	0.44	0.05	0.51	0.13	0.81	0.17	0.84
W03282	0.17	0.59	0.09	0.87	0.12	0.63	0.09	0.63
W03283	0.08	0.60	0.16	0.45	0.09	0.62	0.06	0.44
W03284	0.13	0.79	0.14	0.78	0.20	0.33	0.06	0.93
W03288	0.17	0.46	0.20	0.55	0.08	0.63	0.15	0.53
W03292	0.13	0.76	0.12	0.82	0.12	0.74	0.14	0.79
W03299	0.16	0.28	0.10	0.42	0.13	0.74	0.11	0.83
W03308	0.10	0.74	0.12	0.55	0.14	0.28	0.09	0.50
W03326	0.19	0.36	0.18	0.65	0.11	0.45	0.13	0.42
W03331	0.14	0.65	0.16	0.78	0.10	0.69	0.12	0.50
W03332	0.15	0.66	0.13	0.80	0.21	0.38	0.20	0.55
W03335	0.11	0.89	0.12	0.90	0.14	0.67	0.18	0.79
W03337	0.12	0.90	0.14	0.86	0.21	0.59	0.13	0.90
W03338	0.11	0.75	0.06	0.87	0.11	0.85	0.11	0.93
W03340	0.15	0.68	0.11	0.76	0.12	0.83	0.16	0.75
W03343	0.16	0.73	0.22	0.68	0.11	0.73	0.09	0.72
W03347	0.13	0.47	0.14	0.58	0.15	0.70	0.15	0.65
W03348	0.18	0.61	0.14	0.78	0.17	0.69	0.20	0.67

well	ANN1				ANN2			
	RMSE-Trainin g	R2-Trainin g	RMSE-Testin g	R2-Testin g	RMSE-Trainin g	R2-Trainin g	RMSE-Testin g	R2-Testin g
W03349	0.14	0.77	0.13	0.68	0.11	0.33	0.14	0.58
W03352	0.14	0.39	0.18	0.40	0.19	0.56	0.18	0.68
W03358	0.10	0.34	0.26	0.44	0.16	0.69	0.12	0.75
W03363	0.14	0.47	0.05	0.65	0.14	0.40	0.18	0.48
W03373	0.16	0.49	0.13	0.67	0.09	0.43	0.27	0.63
W03377	0.12	0.72	0.17	0.65	0.14	0.43	0.07	0.66
W03379	0.16	0.78	0.13	0.74	0.16	0.48	0.13	0.55
W03381	0.15	0.74	0.22	0.63	0.17	0.57	0.18	0.63
W03383	0.14	0.63	0.13	0.68	0.15	0.76	0.13	0.75
W03385	0.09	0.86	0.11	0.89	0.16	0.71	0.21	0.60
W03386	0.12	0.61	0.16	0.46	0.14	0.64	0.10	0.77
W03387	0.11	0.88	0.15	0.85	0.10	0.80	0.10	0.87
W03388	0.12	0.79	0.10	0.85	0.13	0.57	0.16	0.46
W03389	0.13	0.92	0.13	0.73	0.13	0.80	0.23	0.44
W03390	0.14	0.91	0.19	0.83	0.13	0.73	0.08	0.93
W03391	0.11	0.67	0.08	0.77	0.12	0.83	0.13	0.73
W03393	0.12	0.58	0.17	0.47	0.15	0.88	0.19	0.77
W03396	0.08	0.95	0.11	0.94	0.11	0.63	0.09	0.70
W03397	0.10	0.91	0.23	0.51	0.10	0.93	0.11	0.90
W03400	0.10	0.81	0.16	0.68	0.11	0.84	0.24	0.49
W03404	0.12	0.45	0.12	0.55	0.10	0.79	0.16	0.64
W03406	0.10	0.72	0.10	0.88	0.12	0.51	0.12	0.54
W03409	0.10	0.82	0.10	0.83	0.11	0.63	0.09	0.90
W03410	0.13	0.79	0.18	0.65	0.10	0.84	0.08	0.86
W03415	0.12	0.86	0.12	0.85	0.14	0.78	0.20	0.63
W03416	0.13	0.80	0.14	0.82	0.11	0.84	0.16	0.69
W03417	0.12	0.88	0.13	0.81	0.12	0.78	0.15	0.75
W03418	0.15	0.68	0.16	0.52	0.11	0.86	0.13	0.78
W03419	0.12	0.80	0.09	0.85	0.14	0.71	0.17	0.56
W03422	0.09	0.64	0.09	0.76	0.10	0.63	0.09	0.87
W03423	0.10	0.85	0.09	0.83	0.11	0.78	0.10	0.80
W03430	0.12	0.91	0.13	0.91	0.12	0.88	0.13	0.88
W03431	0.09	0.90	0.10	0.88	0.11	0.86	0.09	0.86
W03432	0.14	0.81	0.14	0.80	0.14	0.73	0.13	0.73
W03433	0.08	0.92	0.06	0.94	0.09	0.90	0.14	0.72
W03434	0.14	0.75	0.15	0.69	0.14	0.72	0.15	0.71
W03435	0.10	0.72	0.06	0.75	0.10	0.71	0.09	0.74
W03438	0.10	0.69	0.18	0.64	0.10	0.64	0.17	0.58
W03440	0.12	0.70	0.10	0.64	0.12	0.73	0.12	0.64
W03441	0.06	0.66	0.15	0.69	0.06	0.63	0.13	0.73
W03442	0.06	1.00	0.20	0.70	0.07	0.96	0.19	0.67
W03443	0.15	0.74	0.19	0.65	0.14	0.75	0.20	0.59

well	ANN1				ANN2			
	RMSE-Trainin g	R2-Trainin g	RMSE-Testin g	R2-Testin g	RMSE-Trainin g	R2-Trainin g	RMSE-Testin g	R2-Testin g
W03447	0.10	0.87	0.09	0.84	0.12	0.78	0.13	0.75
W03450	0.12	0.88	0.14	0.88	0.13	0.83	0.22	0.71
W03453	0.09	0.47	0.14	0.45	0.10	0.53	0.13	0.51
W03454	0.11	0.55	0.18	0.53	0.10	0.63	0.18	0.51
W03457	0.08	0.82	0.17	0.44	0.10	0.71	0.09	0.89
W03461	0.11	0.83	0.10	0.90	0.10	0.68	0.04	0.94
W03462	0.11	0.54	0.06	0.86	0.15	0.53	0.13	0.64
W03467	0.16	0.57	0.13	0.67	0.22	0.25	0.14	0.68
W03469	0.14	0.72	0.12	0.44	0.12	0.66	0.16	0.61
W03470	0.11	0.70	0.14	0.70	0.12	0.83	0.13	0.83
W03474	0.12	0.84	0.14	0.83	0.10	0.78	0.11	0.74
W03478	0.10	0.78	0.12	0.76	0.07	0.60	0.10	0.90
W03479	0.07	0.54	0.10	0.91	0.10	0.70	0.12	0.81
W03483	0.10	0.74	0.12	0.83	0.13	0.81	0.09	0.93
W03484	0.09	0.75	0.11	0.92	0.18	0.78	0.17	0.77
W03487	0.16	0.87	0.18	0.78	0.10	0.89	0.25	0.39
W03489	0.11	0.92	0.08	0.94	0.09	0.35	0.13	0.66
W03495	0.10	0.35	0.13	0.65	0.13	0.53	0.12	0.72
W03501	0.13	0.49	0.14	0.69	0.13	0.71	0.14	0.66
W03504	0.12	0.69	0.13	0.74	0.10	0.83	0.15	0.80
W03505	0.08	0.88	0.15	0.79	0.30	0.58	0.24	0.44
W03512	0.12	0.79	0.11	0.81	0.15	0.77	0.13	0.73
W03523	0.15	0.71	0.11	0.82	0.14	0.73	0.10	0.83
W03526	0.15	0.51	0.18	0.48	0.16	0.47	0.17	0.47
W03527	0.17	0.61	0.16	0.66	0.17	0.63	0.17	0.80
W03530	0.23	0.34	0.25	0.47	0.30	0.33	0.23	0.49
W03531	0.19	0.72	0.17	0.77	0.19	0.67	0.15	0.74
W03532	0.20	0.54	0.20	0.54	0.23	0.53	0.20	0.52
W03536	0.14	0.64	0.08	0.73	0.15	0.63	0.09	0.49
W03537	0.16	0.54	0.14	0.55	0.18	0.60	0.14	0.53
W03541	0.13	0.82	0.14	0.78	0.15	0.77	0.12	0.76
W03542	0.10	0.74	0.19	0.67	0.10	0.66	0.19	0.63
W03545	0.07	0.93	0.11	0.70	0.09	0.87	0.13	0.65
W03548	0.14	0.71	0.14	0.74	0.15	0.69	0.14	0.75
W03553	0.16	0.69	0.08	0.90	0.21	0.64	0.09	0.90
W03555	0.17	0.74	0.11	0.84	0.20	0.63	0.14	0.73
W03556	0.13	0.61	0.11	0.73	0.12	0.63	0.11	0.77
W03558	0.13	0.64	0.10	0.73	0.13	0.63	0.09	0.77
W03559	0.18	0.70	0.16	0.50	0.22	0.71	0.17	0.47
W03560	0.11	0.82	0.19	0.76	0.12	0.74	0.20	0.67
W03562	0.11	0.82	0.11	0.88	0.13	0.78	0.09	0.87
W03563	0.19	0.59	0.14	0.64	0.19	0.63	0.15	0.48



well	ANN1				ANN2			
	RMSE-Trainin g	R2-Trainin g	RMSE-Testin g	R2-Testin g	RMSE-Trainin g	R2-Trainin g	RMSE-Testin g	R2-Testin g
W03565	0.17	0.74	0.04	0.98	0.19	0.70	0.07	0.94
W03570	0.14	0.64	0.16	0.65	0.17	0.60	0.18	0.54
W03571	0.16	0.79	0.09	0.85	0.13	0.70	0.12	0.77
W03572	0.16	0.64	0.16	0.54	0.15	0.53	0.16	0.60
W03574	0.09	0.54	0.06	0.42	0.12	0.56	0.06	0.49
W03575	0.12	0.88	0.07	0.90	0.10	0.85	0.08	0.87
W03577	0.11	0.79	0.12	0.68	0.14	0.73	0.15	0.53
W03578	0.08	0.90	0.08	0.88	0.10	0.88	0.09	0.82
W03579	0.10	0.66	0.10	0.66	0.10	0.66	0.09	0.69
W03584	0.17	0.70	0.24	0.49	0.20	0.69	0.25	0.37
W03587	0.10	0.55	0.12	0.38	0.10	0.53	0.12	0.40
W03589	0.14	0.64	0.11	0.66	0.13	0.61	0.12	0.53
W03592	0.14	0.54	0.16	0.45	0.16	0.43	0.18	0.43
W03594	0.17	0.24	0.07	0.56	0.13	0.25	0.07	0.44
W03599	0.21	0.41	0.18	0.65	0.21	0.34	0.18	0.63
W03607	0.21	0.54	0.13	0.73	0.10	0.50	0.09	0.41
W03610	0.11	0.78	0.06	0.91	0.17	0.64	0.14	0.68
W03619	0.12	0.34	0.08	0.66	0.10	0.73	0.06	0.88
W03620	0.22	0.36	0.19	0.59	0.08	0.46	0.10	0.40
W03624	0.14	0.74	0.09	0.93	0.18	0.48	0.14	0.53
W03628	0.16	0.51	0.15	0.47	0.14	0.73	0.10	0.86
W03631	0.16	0.64	0.37	0.72	0.21	0.33	0.18	0.85
W03635	0.12	0.59	0.14	0.50	0.10	0.65	0.14	0.48
W03645	0.12	0.64	0.13	0.74	0.13	0.63	0.12	0.72
W03648	0.24	0.30	0.17	0.44	0.24	0.29	0.18	0.37
W03653	0.13	0.50	0.12	0.46	0.21	0.37	0.17	0.43
W03656	0.16	0.49	0.17	0.50	0.15	0.53	0.17	0.42
W03663	0.24	0.30	0.21	0.38	0.15	0.33	0.09	0.46
W03674	0.10	0.60	0.08	0.65	0.18	0.33	0.20	0.48
W03676	0.20	0.41	0.15	0.49	0.10	0.49	0.08	0.72
W03677	0.11	0.72	0.08	0.88	0.12	0.68	0.11	0.74
W03679	0.13	0.49	0.13	0.60	0.12	0.44	0.11	0.68
W03683	0.14	0.41	0.16	0.79	0.12	0.53	0.16	0.78
W03686	0.10	0.23	0.22	0.41	0.19	0.26	0.26	0.37
W03691	0.16	0.63	0.13	0.70	0.14	0.58	0.13	0.60
W03693	0.17	0.42	0.11	0.75	0.17	0.41	0.11	0.65
W03697	0.12	0.63	0.12	0.56	0.12	0.63	0.12	0.51
W03703	0.11	0.74	0.07	0.87	0.10	0.74	0.08	0.85
W03705	0.08	0.91	0.08	0.89	0.09	0.91	0.08	0.89
W03706	0.08	0.93	0.11	0.88	0.09	0.94	0.11	0.87
W03707	0.09	0.84	0.08	0.67	0.09	0.78	0.09	0.66
W03710	0.17	0.54	0.11	0.69	0.15	0.43	0.10	0.74

well	ANN1				ANN2			
	RMSE-Trainin g	R2-Trainin g	RMSE-Testin g	R2-Testin g	RMSE-Trainin g	R2-Trainin g	RMSE-Testin g	R2-Testin g
W03714	0.17	0.46	0.14	0.65	0.17	0.56	0.13	0.61
W03716	0.08	0.76	0.26	0.45	0.09	0.67	0.26	0.40
W03718	0.18	0.57	0.19	0.46	0.17	0.55	0.14	0.48
W03727	0.11	0.85	0.10	0.82	0.11	0.86	0.09	0.88
W03734	0.10	0.91	0.09	0.91	0.11	0.86	0.10	0.90
W03736	0.14	0.93	0.14	0.61	0.16	0.88	0.13	0.60
W03737	0.13	0.79	0.12	0.68	0.11	0.81	0.12	0.70
W03741	0.12	0.82	0.11	0.85	0.12	0.83	0.11	0.84
W03748	0.09	0.86	0.09	0.80	0.09	0.86	0.11	0.74
W03751	0.08	0.98	0.13	0.85	0.07	0.97	0.13	0.85
W03754	0.12	0.88	0.15	0.76	0.13	0.88	0.13	0.85
W03756	0.12	0.78	0.11	0.60	0.11	0.77	0.11	0.58
W03757	0.11	0.76	0.09	0.77	0.09	0.79	0.12	0.66
W03758	0.10	0.94	0.17	0.64	0.05	0.85	0.18	0.59
W03761	0.16	0.80	0.12	0.82	0.15	0.80	0.13	0.75
W03762	0.11	0.77	0.11	0.75	0.13	0.75	0.13	0.65
W03763	0.12	0.89	0.13	0.92	0.12	0.93	0.14	0.93
W05338	0.13	0.65	0.12	0.68	0.13	0.67	0.12	0.66
W05339	0.10	0.74	0.09	0.79	0.10	0.78	0.08	0.85
W05346	0.10	0.84	0.11	0.87	0.11	0.90	0.11	0.85
W05462	0.10	0.93	0.07	0.97	0.20	0.38	0.22	0.64
W05464	0.18	0.59	0.20	0.74	0.11	0.91	0.06	0.95
W05465	0.09	0.85	0.15	0.83	0.17	0.58	0.13	0.75
W05469	0.17	0.62	0.15	0.58	0.09	0.83	0.17	0.81
W05473	0.14	0.54	0.14	0.84	0.16	0.70	0.16	0.56
W05474	0.13	0.77	0.07	0.93	0.14	0.48	0.22	0.62
W05477	0.15	0.64	0.07	0.89	0.13	0.78	0.07	0.92
W05480	0.12	0.91	0.14	0.83	0.13	0.65	0.07	0.89
W05686	0.11	0.89	0.10	0.89	0.13	0.92	0.10	0.96
W05688	0.11	0.86	0.11	0.93	0.11	0.87	0.11	0.87
W05690	0.10	0.76	0.11	0.73	0.12	0.83	0.13	0.89
W05860	0.12	0.69	0.10	0.83	0.10	0.68	0.12	0.66
W05861	0.09	0.94	0.08	0.91	0.10	0.76	0.10	0.82
W05863	0.11	0.84	0.13	0.78	0.09	0.93	0.08	0.91
W05864	0.13	0.84	0.17	0.79	0.12	0.83	0.14	0.80
W06067	0.14	0.69	0.10	0.87	0.13	0.83	0.17	0.76
W06069	0.08	0.96	0.06	0.95	0.15	0.68	0.20	0.91
W06070	0.14	0.68	0.15	0.67	0.15	0.48	0.14	0.45
W06072	0.10	0.74	0.19	0.40	0.06	0.93	0.05	0.95
W06076	0.10	0.76	0.11	0.85	0.14	0.67	0.15	0.66
W06078	0.10	0.84	0.09	0.94	0.11	0.87	0.19	0.44
W06081	0.11	0.84	0.11	0.94	0.10	0.80	0.12	0.84

well	ANN1				ANN2			
	RMSE-Trainin g	R2-Trainin g	RMSE-Testin g	R2-Testin g	RMSE-Trainin g	R2-Trainin g	RMSE-Testin g	R2-Testin g
W06083	0.13	0.86	0.20	0.64	0.12	0.76	0.08	0.93
W06085	0.15	0.66	0.10	0.89	0.12	0.80	0.09	0.87
W06195	0.21	0.57	0.22	0.40	0.14	0.75	0.23	0.65
W06200	0.12	0.74	0.11	0.75	0.14	0.73	0.09	0.89
W06384	0.13	0.84	0.13	0.89	0.20	0.45	0.21	0.43
W06389	0.12	0.81	0.14	0.76	0.10	0.76	0.10	0.76
W06392	0.18	0.43	0.17	0.42	0.12	0.83	0.12	0.89
W06542	0.09	0.84	0.11	0.79	0.14	0.63	0.11	0.88
W06543	0.10	0.54	0.08	0.63	0.15	0.54	0.09	0.60
W06547	0.10	0.89	0.08	0.90	0.10	0.83	0.11	0.80
W06551	0.15	0.58	0.16	0.57	0.12	0.63	0.10	0.54
W06705	0.16	0.57	0.17	0.63	0.10	0.86	0.09	0.89
W06707	0.10	0.89	0.17	0.80	0.17	0.63	0.16	0.82
W06708	0.15	0.54	0.12	0.51	0.15	0.57	0.16	0.51
W06710	0.15	0.75	0.17	0.65	0.14	0.58	0.17	0.63
W06712	0.12	0.87	0.12	0.90	0.10	0.90	0.19	0.78
W06713	0.09	0.97	0.11	0.90	0.15	0.55	0.13	0.50
W06745	0.19	0.66	0.19	0.70	0.12	0.82	0.18	0.64
W06747	0.16	0.44	0.17	0.59	0.13	0.79	0.09	0.93
W06748	0.20	0.59	0.17	0.48	0.10	0.95	0.11	0.91
W06751	0.12	0.87	0.12	0.92	0.17	0.70	0.19	0.69
W06752	0.19	0.67	0.16	0.59	0.17	0.45	0.16	0.61
W06753	0.21	0.46	0.20	0.39	0.20	0.58	0.17	0.47
W06754	0.11	0.86	0.10	0.88	0.13	0.03	0.13	0.94
W06756	0.11	0.50	0.18	0.47	0.16	0.72	0.16	0.59
W06758	0.12	0.88	0.13	0.83	0.11	0.83	0.10	0.85
W06762	0.14	0.84	0.11	0.83	0.12	0.45	0.24	0.43
W06763	0.10	0.94	0.10	0.93	0.12	0.86	0.12	0.79
W06764	0.08	0.98	0.12	0.91	0.14	0.83	0.11	0.78
W06765	0.13	0.79	0.13	0.78	0.10	0.92	0.11	0.89
W06766	0.14	0.85	0.14	0.89	0.08	0.98	0.11	0.90
W06767	0.11	0.91	0.11	0.84	0.12	0.78	0.13	0.75
W07387	0.13	0.59	0.11	0.69	0.14	0.81	0.11	0.88
W07390	0.12	0.84	0.11	0.77	0.11	0.91	0.13	0.80
W07394	0.10	0.94	0.11	0.91	0.11	0.71	0.12	0.63
W07401	0.12	0.94	0.14	0.85	0.12	0.77	0.11	0.77
W07402	0.13	0.73	0.11	0.73	0.10	0.91	0.09	0.93
W07403	0.11	0.63	0.19	0.52	0.15	0.84	0.14	0.83
W07404	0.15	0.84	0.23	0.85	0.12	0.88	0.15	0.81
W07407	0.22	0.42	0.14	0.39	0.13	0.76	0.11	0.72
W07409	0.09	0.96	0.23	0.74	0.11	0.78	0.18	0.40
W07410	0.10	0.87	0.16	0.87	0.14	0.82	0.13	0.86

well	ANN1				ANN2			
	RMSE- Trainin g	R2- Trainin g	RMSE - Testin g	R2- Testin g	RMSE- Trainin g	R2- Trainin g	RMSE - Testin g	R2- Testin g
W07416	0.11	0.89	0.12	0.94	0.19	0.53	0.15	0.56
W07418	0.13	0.73	0.14	0.82	0.10	0.95	0.18	0.73
W07420	0.10	0.93	0.12	0.90	0.11	0.86	0.12	0.83
W07421	0.12	0.60	0.08	0.62	0.12	0.84	0.07	0.94
W07424	0.12	0.77	0.09	0.83	0.13	0.76	0.12	0.87
W07425	0.13	0.73	0.17	0.38	0.10	0.95	0.11	0.88
W07490	0.22	0.46	0.32	0.40	0.11	0.70	0.07	0.65
W07494	0.15	0.48	0.14	0.70	0.11	0.70	0.12	0.74
W07495	0.15	0.75	0.18	0.59	0.12	0.81	0.17	0.38
W07496	0.14	0.76	0.14	0.77	0.17	0.43	0.25	0.57
W07496	0.13	0.85	0.14	0.84	0.15	0.55	0.14	0.71
W07497	0.13	0.80	0.12	0.81	0.14	0.75	0.19	0.52
W07498	0.12	0.89	0.13	0.86	0.13	0.77	0.14	0.84
W07500	0.12	0.88	0.13	0.88	0.13	0.81	0.12	0.83
W07501	0.11	0.59	0.06	0.72	0.12	0.92	0.10	0.91
W07504	0.22	0.59	0.13	0.78	0.15	0.86	0.10	0.93
W07505	0.14	0.50	0.12	0.76	0.11	0.58	0.06	0.74
W07506	0.09	0.96	0.16	0.78	0.21	0.58	0.12	0.85
W07507	0.12	0.83	0.10	0.80	0.18	0.57	0.13	0.73
W07551	0.14	0.84	0.17	0.83	0.09	0.94	0.13	0.85
W07554	0.10	0.94	0.11	0.82	0.13	0.80	0.10	0.86
W07561	0.09	0.95	0.11	0.89	0.11	0.86	0.16	0.73
W07563	0.11	0.93	0.14	0.83	0.11	0.89	0.11	0.83
W07565	0.10	0.87	0.14	0.76	0.09	0.94	0.10	0.86
W07568	0.12	0.91	0.13	0.83	0.12	0.89	0.16	0.68
W07569	0.10	0.92	0.11	0.87	0.10	0.86	0.14	0.75
W08005	0.09	0.74	0.06	0.83	0.10	0.95	0.13	0.85
W08010	0.10	0.78	0.08	0.80	0.09	0.94	0.10	0.84
W08011	0.07	0.70	0.13	0.51	0.09	0.83	0.07	0.85
W08143	0.10	0.87	0.13	0.85	0.10	0.81	0.08	0.77
W08148	0.08	0.79	0.13	0.76	0.07	0.66	0.13	0.49
W08151	0.14	0.81	0.11	0.87	0.10	0.84	0.15	0.78
W08153	0.14	0.80	0.13	0.69	0.07	0.83	0.15	0.78
W08154	0.06	0.58	0.25	0.60	0.12	0.85	0.08	0.88
W08191	0.11	0.91	0.13	0.80	0.14	0.72	0.14	0.67
W08712	0.12	0.84	0.08	0.98	0.06	0.67	0.27	0.67
W08713	0.11	0.90	0.08	0.95	0.11	0.89	0.13	0.81
W08869	0.09	0.82	0.14	0.57	0.11	0.87	0.09	0.93
W08871	0.10	0.68	0.16	0.47	0.10	0.88	0.09	0.94
W08879	0.11	0.81	0.16	0.73	0.10	0.81	0.16	0.56
W08908	0.10	0.78	0.14	0.73	0.09	0.73	0.16	0.46
W08947	0.14	0.74	0.06	0.99	0.12	0.55	0.12	0.60

well	ANN1				ANN2			
	RMSE-Trainin g	R2-Trainin g	RMSE-Testin g	R2-Testin g	RMSE-Trainin g	R2-Trainin g	RMSE-Testin g	R2-Testin g
W08948	0.05	0.75	0.15	0.65	0.12	0.83	0.17	0.76
W08952	0.12	0.89	0.10	0.85	0.11	0.73	0.13	0.58
W08954	0.16	0.81	0.13	0.93	0.13	0.68	0.07	0.97
W08955	0.09	0.93	0.09	0.81	0.05	0.71	0.16	0.65
W08996	0.23	0.55	0.15	0.93	0.11	0.88	0.10	0.84
W09000	0.09	0.91	0.08	0.85	0.13	0.87	0.04	0.98
W09001	0.12	0.86	0.12	0.87	0.10	0.87	0.09	0.81
W09004	0.13	0.70	0.14	0.81	0.20	0.61	0.11	0.92
W09005	0.15	0.61	0.24	0.61	0.11	0.88	0.09	0.93
W09007	0.12	0.60	0.09	0.85	0.11	0.86	0.14	0.84
W09008	0.11	0.77	0.21	0.65	0.13	0.69	0.11	0.83
W17573	0.13	0.69	0.15	0.68	0.14	0.53	0.14	0.58
W17576	0.08	0.86	0.14	0.89	0.12	0.55	0.10	0.83
W17578	0.12	0.72	0.16	0.70	0.10	0.81	0.11	0.74
W17580	0.13	0.68	0.12	0.60	0.14	0.68	0.16	0.67
W17583	0.10	0.97	0.14	0.83	0.08	0.85	0.14	0.86
W17587	0.17	0.72	0.11	0.85	0.14	0.65	0.16	0.78
W17597	0.09	0.81	0.16	0.59	0.13	0.63	0.12	0.58
W17600	0.12	0.67	0.21	0.59	0.11	0.95	0.12	0.87
W17602	0.13	0.84	0.12	0.78	0.15	0.78	0.12	0.85
W17603	0.12	0.84	0.08	0.96	0.10	0.74	0.19	0.64
W17604	0.08	0.86	0.09	0.80	0.12	0.53	0.16	0.69
W17606	0.11	0.79	0.15	0.69	0.12	0.83	0.15	0.65
W17608	0.13	0.66	0.14	0.77	0.12	0.83	0.08	0.94
W17609	0.16	0.52	0.17	0.53	0.09	0.84	0.11	0.77
W17610	0.14	0.81	0.14	0.91	0.11	0.81	0.13	0.69
W17617	0.12	0.80	0.10	0.90	0.12	0.68	0.15	0.69
W17619	0.15	0.49	0.10	0.63	0.13	0.81	0.12	0.94
W17620	0.17	0.71	0.11	0.84	0.12	0.75	0.10	0.89
W17621	0.11	0.87	0.15	0.80	0.15	0.98	0.12	0.66
W17622	0.14	0.76	0.13	0.89	0.17	0.75	0.14	0.77
W17624	0.11	0.80	0.15	0.72	0.12	0.86	0.15	0.77
W17625	0.17	0.51	0.21	0.38	0.16	0.73	0.11	0.88
W17653	0.11	0.38	0.16	0.60	0.09	0.82	0.17	0.68
W17655	0.14	0.61	0.16	0.38	0.14	0.77	0.11	0.84
W17656	0.14	0.78	0.11	0.85	0.08	0.86	0.06	0.90
W17657	0.09	0.87	0.07	0.86	0.11	0.91	0.15	0.91
W17658	0.10	0.93	0.14	0.86	0.09	0.65	0.23	0.45
W17659	0.09	0.67	0.20	0.57	0.12	0.84	0.09	0.90
W17661	0.11	0.86	0.08	0.93	0.14	0.73	0.09	0.84
W17663	0.14	0.75	0.09	0.85	0.16	0.63	0.18	0.54
W17664	0.15	0.69	0.18	0.55	0.15	0.75	0.11	0.80

well	ANN1				ANN2			
	RMSE- Trainin g	R2- Trainin g	RMSE - Testin g	R2- Testin g	RMSE- Trainin g	R2- Trainin g	RMSE - Testin g	R2- Testin g
W17666	0.16	0.72	0.12	0.77	0.16	0.70	0.13	0.94
W17667	0.15	0.70	0.22	0.76	0.18	0.68	0.13	0.78
W17668	0.21	0.56	0.14	0.73	0.14	0.60	0.16	0.53



## APPENDIX 5

**Table A 5.1 R<sup>2</sup> and RMSE of SVM models during training and testing phase**

well	SVM1				SVM2			
	RMSE- Training	R2- Training	RMSE- Testing	R2- Testing	RMSE- Training	R2- Training	RMSE- Testing	R2- Testing
W02171	0.16	0.49	0.17	0.50	0.16	0.48	0.17	0.51
W02177	0.12	0.59	0.14	0.50	0.12	0.58	0.14	0.51
W02178	0.12	0.64	0.13	0.74	0.12	0.63	0.13	0.72
W02179	0.24	0.30	0.21	0.38	0.24	0.29	0.21	0.42
W02181	0.10	0.60	0.08	0.65	0.10	0.59	0.08	0.65
W02185	0.14	0.41	0.16	0.79	0.14	0.40	0.16	0.74
W02186	0.13	0.50	0.12	0.46	0.13	0.49	0.12	0.48
W02935	0.17	0.39	0.12	0.41	0.16	0.44	0.12	0.39
W02944	0.18	0.57	0.16	0.60	0.19	0.51	0.16	0.56
W02945	0.13	0.76	0.11	0.66	0.13	0.71	0.11	0.64
W02947	0.16	0.68	0.14	0.61	0.16	0.63	0.14	0.66
W02948	0.20	0.47	0.17	0.87	0.22	0.51	0.15	0.89
W02951	0.17	0.47	0.12	0.65	0.17	0.48	0.13	0.53
W02961	0.17	0.44	0.17	0.45	0.20	0.27	0.16	0.46
W02963	0.12	0.75	0.12	0.78	0.12	0.74	0.12	0.74
W02975	0.11	0.88	0.11	0.84	0.11	0.86	0.12	0.78
W02976	0.11	0.72	0.17	0.67	0.11	0.67	0.19	0.60
W02977	0.17	0.69	0.11	0.83	0.19	0.62	0.13	0.75
W02978	0.14	0.63	0.11	0.64	0.14	0.62	0.11	0.58
W02979	0.13	0.79	0.08	0.93	0.13	0.77	0.08	0.89
W02982	0.12	0.84	0.06	0.98	0.12	0.82	0.07	0.96
W02983	0.12	0.72	0.12	0.73	0.12	0.71	0.11	0.74
W02997	0.11	0.87	0.12	0.81	0.11	0.87	0.12	0.78
W03000	0.11	0.74	0.09	0.75	0.10	0.76	0.09	0.72
W03001	0.14	0.74	0.10	0.86	0.14	0.70	0.11	0.80
W03007	0.14	0.58	0.06	0.92	0.14	0.57	0.07	0.90
W03008	0.21	0.20	0.10	0.51	0.21	0.20	0.10	0.50
W03009	0.13	0.67	0.19	0.62	0.13	0.65	0.20	0.59
W03011	0.17	0.14	0.07	0.38	0.17	0.13	0.07	0.34
W03013	0.15	0.15	0.12	0.52	0.17	0.37	0.12	0.61
W03018	0.17	0.36	0.11	0.60	0.16	0.43	0.08	0.83
W03020	0.17	0.44	0.09	0.79	0.14	0.65	0.09	0.73
W03021	0.14	0.65	0.09	0.76	0.11	0.63	0.09	0.75
W03026	0.12	0.56	0.09	0.75	0.13	0.43	0.07	0.70
W03027	0.13	0.44	0.06	0.78	0.16	0.50	0.16	0.77
W03030	0.17	0.54	0.17	0.73	0.13	0.75	0.09	0.81
W03031	0.14	0.76	0.10	0.80	0.16	0.33	0.15	0.36



well	SVM1				SVM2			
	RMSE- Training	R2- Training	RMSE- Testing	R2- Testing	RMSE- Training	R2- Training	RMSE- Testing	R2- Testing
W03035	0.16	3.04	0.14	0.41	0.14	0.52	0.11	0.68
W03038	0.14	0.49	0.11	0.69	0.14	0.73	0.10	0.85
W03039	0.14	0.75	0.09	0.88	0.09	0.79	0.09	0.81
W03042	0.08	0.86	0.08	0.86	0.13	0.62	0.10	0.82
W03044	0.13	0.65	0.09	0.83	0.14	0.48	0.09	0.80
W03047	0.14	0.54	0.09	0.81	0.12	0.38	0.14	0.77
W03051	0.11	0.39	0.14	0.76	0.18	0.45	0.14	0.54
W03052	0.19	0.47	0.13	0.58	0.10	0.54	0.08	0.62
W03055	0.12	0.65	0.08	0.66	0.13	0.47	0.12	0.46
W03059	0.12	0.47	0.12	0.40	0.12	0.75	0.09	0.79
W03061	0.13	0.75	0.08	0.87	0.14	0.48	0.10	0.52
W03075	0.14	0.51	0.10	0.49	0.16	0.58	0.10	0.64
W03081	0.16	0.64	0.11	0.68	0.14	0.74	0.17	0.51
W03083	0.14	0.76	0.15	0.66	0.11	0.40	0.07	0.45
W03087	0.10	0.43	0.07	0.38	0.15	0.48	0.13	0.74
W03094	0.14	0.54	0.14	0.74	0.14	0.58	0.08	0.75
W03099	0.16	0.64	0.09	0.71	0.12	0.88	0.15	0.71
W03100	0.12	0.88	0.17	0.66	0.14	0.76	0.11	0.77
W03104	0.13	0.78	0.14	0.64	0.16	0.55	0.10	0.67
W03107	0.16	0.56	0.10	0.70	0.07	0.85	0.11	0.69
W03112	0.08	0.86	0.11	0.77	0.14	0.66	0.14	0.73
W03115	0.15	0.64	0.12	0.82	0.13	0.51	0.11	0.53
W03116	0.12	0.60	0.12	0.59	0.08	0.93	0.08	0.95
W03131	0.08	0.94	0.08	0.97	0.15	0.28	0.09	0.54
W03134	0.14	0.29	0.09	0.59	0.13	0.67	0.10	0.69
W03139	0.14	0.67	0.10	0.69	0.11	0.86	0.09	0.84
W03140	0.12	0.86	0.09	0.87	0.10	0.68	0.28	0.34
W03149	0.17	0.74	0.08	0.78	0.17	0.73	0.08	0.77
W03151	0.08	0.81	0.08	0.85	0.08	0.80	0.08	0.85
W03152	0.16	0.73	0.15	0.59	0.14	0.71	0.16	0.53
W03155	0.19	0.39	0.14	0.58	0.19	0.37	0.15	0.56
W03161	0.10	0.84	0.08	0.86	0.10	0.83	0.08	0.85
W03162	0.15	0.61	0.13	0.47	0.15	0.59	0.13	0.46
W03164	0.10	0.74	0.12	0.76	0.10	0.74	0.12	0.74
W03166	0.08	0.77	0.06	0.70	0.08	0.76	0.06	0.70
W03169	0.14	0.74	0.08	0.88	0.14	0.73	0.08	0.85
W03171	0.11	0.75	0.15	0.66	0.12	0.72	0.15	0.65
W03172	0.10	0.79	0.05	0.97	0.12	0.73	0.05	0.97
W03175	0.16	0.64	0.19	0.68	0.15	0.63	0.18	0.68
W03176	0.10	0.76	0.08	0.72	0.10	0.75	0.07	0.73
W03177	0.15	0.74	0.06	0.94	0.14	0.73	0.06	0.93
W03182	0.10	0.76	0.13	0.75	0.13	0.72	0.13	0.74

well	SVM1				SVM2			
	RMSE- Training	R2- Training	RMSE- Testing	R2- Testing	RMSE- Training	R2- Training	RMSE- Testing	R2- Testing
W03187	0.07	0.92	0.05	0.96	0.07	0.90	0.05	0.95
W03192	0.07	0.82	0.12	0.80	0.08	0.80	0.11	0.80
W03196	0.10	0.82	0.09	0.89	0.10	0.83	0.09	0.86
W03197	0.17	0.24	0.18	0.37	0.16	0.23	0.18	0.40
W03206	0.14	0.24	0.04	0.74	0.16	0.23	0.04	0.73
W03210	0.13	0.84	0.12	0.70	0.11	0.86	0.12	0.71
W03211	0.20	0.46	0.16	0.48	0.20	0.43	0.16	0.48
W03212	0.11	0.64	0.06	0.80	0.11	0.63	0.05	0.83
W03213	0.18	0.64	0.13	0.74	0.18	0.58	0.13	0.74
W03216	0.10	0.54	0.10	0.74	0.10	0.53	0.10	0.73
W03216	0.10	0.82	0.12	0.91	0.11	0.80	0.12	0.91
W03219	0.10	0.94	0.08	0.96	0.11	0.90	0.09	0.94
W03230	0.19	0.29	0.22	0.41	0.16	0.29	0.23	0.45
W03231	0.11	0.88	0.11	0.83	0.11	0.89	0.10	0.84
W03232	0.11	0.80	0.12	0.78	0.11	0.78	0.12	0.79
W03235	0.11	0.74	0.08	0.88	0.10	0.70	0.08	0.87
W03238	0.07	0.94	0.10	0.87	0.07	0.93	0.10	0.87
W03239	0.09	0.92	0.10	0.93	0.10	0.89	0.10	0.91
W03240	0.15	0.49	0.07	0.83	0.15	0.43	0.07	0.88
W03243	0.15	0.59	0.14	0.88	0.15	0.53	0.15	0.82
W03244	0.12	0.54	0.12	0.77	0.11	0.57	0.13	0.63
W03246	0.13	0.68	0.14	0.77	0.13	0.64	0.14	0.70
W03248	0.10	0.64	0.14	0.80	0.10	0.63	0.13	0.78
W03249	0.09	0.59	0.13	0.58	0.10	0.55	0.13	0.56
W03252	0.19	0.54	0.07	0.91	0.19	0.38	0.08	0.81
W03256	0.09	0.46	0.18	0.45	0.10	0.43	0.17	0.52
W03257	0.14	0.34	0.14	0.44	0.09	0.70	0.11	0.73
W03261	0.09	0.71	0.09	0.80	0.14	0.80	0.17	0.73
W03262	0.13	0.85	0.17	0.80	0.12	0.53	0.08	0.71
W03273	0.11	0.59	0.08	0.65	0.09	0.40	0.05	0.43
W03275	0.09	0.40	0.05	0.48	0.17	0.53	0.11	0.87
W03282	0.10	0.54	0.09	0.93	0.09	0.49	0.17	0.42
W03283	0.08	0.57	0.16	0.47	0.13	0.69	0.15	0.80
W03284	0.12	0.74	0.14	0.81	0.14	0.68	0.14	0.74
W03292	0.13	0.73	0.14	0.75	0.14	0.16	0.10	0.40
W03299	0.14	0.17	0.10	0.43	0.12	0.40	0.13	0.36
W03308	0.12	0.54	0.14	0.42	0.12	0.50	0.14	0.38
W03326	0.18	0.26	0.18	0.62	0.20	0.33	0.18	0.55
W03331	0.15	0.59	0.19	0.69	0.15	0.53	0.20	0.67
W03332	0.19	0.54	0.16	0.84	0.20	0.45	0.16	0.82
W03335	0.13	0.80	0.12	0.93	0.14	0.75	0.15	0.84
W03337	0.10	0.86	0.14	0.88	0.12	0.82	0.17	0.73

well	SVM1				SVM2			
	RMSE- Training	R2- Training	RMSE- Testing	R2- Testing	RMSE- Training	R2- Training	RMSE- Testing	R2- Testing
W03338	0.11	0.72	0.09	0.68	0.11	0.71	0.10	0.58
W03340	0.15	0.62	0.11	0.68	0.15	0.61	0.11	0.67
W03343	0.18	0.65	0.18	0.54	0.18	0.62	0.18	0.60
W03347	0.12	0.33	0.15	0.48	0.12	0.29	0.15	0.52
W03348	0.17	0.58	0.16	0.75	0.18	0.54	0.18	0.69
W03349	0.15	0.70	0.13	0.65	0.17	0.61	0.11	0.67
W03352	0.15	0.33	0.21	0.54	0.15	0.23	0.21	0.56
W03358	0.11	0.33	0.28	0.60	0.11	0.23	0.29	0.58
W03363	0.11	0.34	0.04	0.69	0.11	0.33	0.04	0.59
W03373	0.16	0.40	0.14	0.57	0.17	0.38	0.15	0.55
W03377	0.16	0.74	0.16	0.60	0.16	0.73	0.13	0.71
W03379	0.17	0.70	0.14	0.69	0.16	0.69	0.19	0.66
W03381	0.16	0.70	0.12	0.69	0.15	0.49	0.15	0.41
W03383	0.15	0.50	0.15	0.40	0.11	0.75	0.12	0.85
W03385	0.18	0.81	0.15	0.86	0.13	0.52	0.17	0.39
W03386	0.13	0.54	0.16	0.43	0.12	0.81	0.15	0.82
W03387	0.11	0.85	0.14	0.84	0.14	0.66	0.11	0.73
W03388	0.14	0.67	0.11	0.74	0.14	0.75	0.13	0.66
W03389	0.14	0.74	0.12	0.68	0.16	0.85	0.18	0.84
W03390	0.17	0.84	0.18	0.85	0.14	0.53	0.11	0.69
W03391	0.12	0.52	0.10	0.69	0.11	0.89	0.08	0.90
W03396	0.10	0.92	0.09	0.91	0.11	0.88	0.12	0.89
W03397	0.10	0.91	0.13	0.89	0.12	0.50	0.19	0.37
W03400	0.11	0.77	0.21	0.39	0.12	0.77	0.13	0.50
W03406	0.11	0.57	0.18	0.42	0.14	0.72	0.16	0.66
W03409	0.12	0.76	0.13	0.54	0.11	0.85	0.11	0.91
W03410	0.13	0.76	0.16	0.69	0.16	0.73	0.13	0.85
W03415	0.11	0.86	0.08	0.96	0.11	0.87	0.12	0.78
W03416	0.14	0.74	0.14	0.83	0.17	0.58	0.15	0.54
W03417	0.11	0.88	0.12	0.79	0.14	0.53	0.17	0.34
W03418	0.18	0.69	0.13	0.50	0.11	0.48	0.11	0.86
W03419	0.13	0.62	0.17	0.39	0.12	0.73	0.08	0.83
W03422	0.11	0.46	0.11	0.84	0.13	0.84	0.09	0.92
W03423	0.11	0.78	0.08	0.87	0.10	0.83	0.10	0.85
W03430	0.12	0.87	0.09	0.93	0.13	0.79	0.10	0.78
W03431	0.11	0.85	0.09	0.86	0.09	0.90	0.05	0.97
W03432	0.11	0.80	0.10	0.81	0.15	0.67	0.16	0.50
W03433	0.08	0.94	0.06	0.97	0.11	0.53	0.04	0.81
W03434	0.16	0.67	0.15	0.57	0.14	0.64	0.09	0.72
W03435	0.12	0.57	0.03	0.85	0.07	0.97	0.18	0.72
W03438	0.12	0.52	0.22	0.39	0.16	0.57	0.17	0.53
W03440	0.13	0.68	0.09	0.73	0.12	0.77	0.12	0.72

well	SVM1				SVM2			
	RMSE- Training	R2- Training	RMSE- Testing	R2- Testing	RMSE- Training	R2- Training	RMSE- Testing	R2- Testing
W03442	0.08	0.97	0.18	0.69	0.15	0.80	0.16	0.87
W03443	0.17	0.66	0.19	0.67	0.11	0.33	0.16	0.61
W03445	0.14	0.78	0.16	0.55	0.16	0.38	0.17	0.53
W03450	0.14	0.83	0.15	0.87	0.11	0.76	0.15	0.58
W03453	0.12	0.18	0.15	0.69	0.16	0.73	0.09	0.91
W03454	0.13	0.45	0.17	0.53	0.24	0.23	0.10	0.39
W03457	0.10	0.76	0.14	0.62	0.13	0.57	0.17	0.61
W03461	0.17	0.74	0.07	0.88	0.13	0.77	0.18	0.45
W03468	0.22	0.24	0.10	0.41	0.12	0.73	0.12	0.75
W03470	0.12	0.61	0.15	0.67	0.14	0.81	0.11	0.95
W03474	0.13	0.82	0.18	0.50	0.15	0.81	0.15	0.75
W03478	0.14	0.74	0.11	0.80	0.10	0.88	0.11	0.87
W03484	0.08	0.81	0.12	0.94	0.14	0.57	0.16	0.45
W03487	0.20	0.81	0.12	0.80	0.11	0.77	0.18	0.81
W03489	0.11	0.87	0.11	0.86	0.20	0.58	0.23	0.40
W03504	0.14	0.55	0.15	0.54	0.11	0.82	0.12	0.73
W03505	0.10	0.84	0.17	0.80	0.12	0.71	0.11	0.83
W03510	0.20	0.55	0.23	0.41	0.15	0.43	0.17	0.48
W03512	0.11	0.83	0.11	0.80	0.17	0.53	0.16	0.83
W03523	0.13	0.66	0.11	0.87	0.23	0.33	0.23	0.44
W03526	0.14	0.44	0.17	0.46	0.16	0.73	0.15	0.70
W03527	0.15	0.56	0.17	0.75	0.21	0.44	0.22	0.50
W03530	0.23	0.34	0.23	0.43	0.13	0.50	0.07	0.75
W03531	0.16	0.63	0.14	0.76	0.14	0.55	0.15	0.52
W03532	0.20	0.45	0.22	0.51	0.12	0.78	0.13	0.73
W03536	0.10	0.54	0.06	0.85	0.11	0.61	0.23	0.64
W03537	0.14	0.54	0.15	0.53	0.12	0.74	0.12	0.65
W03541	0.11	0.82	0.12	0.78	0.15	0.63	0.12	0.71
W03542	0.11	0.74	0.21	0.64	0.15	0.56	0.11	0.83
W03545	0.12	0.75	0.12	0.68	0.18	0.58	0.13	0.75
W03548	0.15	0.62	0.14	0.69	0.11	0.45	0.12	0.73
W03553	0.15	0.64	0.10	0.87	0.11	0.58	0.10	0.71
W03555	0.18	0.64	0.12	0.83	0.16	0.58	0.14	0.48
W03556	0.11	0.44	0.12	0.73	0.14	0.70	0.21	0.59
W03558	0.11	0.59	0.10	0.75	0.14	0.70	0.09	0.83
W03559	0.16	0.63	0.15	0.42	0.16	0.58	0.13	0.57
W03560	0.12	0.79	0.20	0.72	0.14	0.68	0.07	0.95
W03562	0.14	0.69	0.08	0.88	0.15	0.53	0.18	0.54
W03563	0.16	0.59	0.12	0.63	0.12	0.73	0.09	0.84
W03565	0.14	0.74	0.06	0.99	0.15	0.50	0.18	0.55
W03570	0.15	0.59	0.17	0.64	0.10	0.34	0.07	0.52
W03571	0.12	0.80	0.07	0.94	0.12	0.74	0.08	0.87

well	SVM1				SVM2			
	RMSE- Training	R2- Training	RMSE- Testing	R2- Testing	RMSE- Training	R2- Training	RMSE- Testing	R2- Testing
W03572	0.15	0.44	0.19	0.55	0.14	0.63	0.13	0.53
W03574	0.10	0.43	0.07	0.44	0.09	0.78	0.08	0.85
W03575	0.13	0.72	0.07	0.92	0.11	0.53	0.10	0.67
W03577	0.14	0.67	0.11	0.72	0.12	0.30	0.13	0.36
W03578	0.10	0.76	0.07	0.88	0.14	0.54	0.11	0.52
W03579	0.10	0.76	0.10	0.68	0.16	0.38	0.19	0.39
W03584	0.17	0.73	0.21	0.42	0.13	0.13	0.06	0.52
W03587	0.12	0.38	0.12	0.51	0.21	0.33	0.19	0.61
W03589	0.13	0.58	0.11	0.55	0.12	0.36	0.09	0.40
W03594	0.14	0.14	0.06	0.53	0.17	0.60	0.13	0.68
W03595	0.21	0.31	0.19	0.63	0.15	0.63	0.07	0.85
W03604	0.11	0.38	0.09	0.40	0.13	0.18	0.09	0.42
W03607	0.17	0.64	0.14	0.69	0.15	0.63	0.10	0.86
W03610	0.12	0.64	0.07	0.86	0.16	0.27	0.19	0.38
W03619	0.13	0.23	0.09	0.55	0.20	0.26	0.17	0.91
W03620	0.20	0.26	0.25	0.47	0.11	0.50	0.14	0.50
W03624	0.15	0.67	0.08	0.92	0.14	0.51	0.15	0.60
W03628	0.16	0.28	0.15	0.51	0.18	0.30	0.17	0.40
W03631	0.20	0.38	0.22	0.92	0.21	0.20	0.19	0.39
W03635	0.11	0.51	0.15	0.50	0.14	0.23	0.18	0.36
W03645	0.14	0.52	0.15	0.57	0.16	0.43	0.18	0.37
W03648	0.18	0.31	0.17	0.45	0.15	0.16	0.11	0.36
W03653	0.14	0.34	0.14	0.42	0.23	0.30	0.21	0.60
W03656	0.15	0.43	0.17	0.42	0.11	0.41	0.09	0.58
W03659	0.15	0.17	0.11	0.44	0.12	0.63	0.12	0.77
W03663	0.23	0.31	0.21	0.54	0.13	0.39	0.15	0.41
W03674	0.11	0.42	0.08	0.68	0.13	0.45	0.18	0.71
W03676	0.16	0.38	0.13	0.50	0.12	0.23	0.27	0.41
W03677	0.13	0.59	0.10	0.88	0.21	0.33	0.17	0.49
W03679	0.13	0.40	0.14	0.54	0.15	0.52	0.14	0.68
W03683	0.13	0.46	0.17	0.74	0.13	0.50	0.11	0.66
W03690	0.21	0.36	0.18	0.48	0.13	0.58	0.13	0.50
W03691	0.14	0.60	0.14	0.70	0.12	0.64	0.15	0.49
W03693	0.14	0.47	0.10	0.71	0.08	0.89	0.10	0.84
W03697	0.13	0.59	0.13	0.48	0.10	0.91	0.15	0.76
W03703	0.12	0.63	0.15	0.55	0.08	0.76	0.07	0.71
W03705	0.08	0.92	0.09	0.88	0.15	0.35	0.13	0.62
W03706	0.10	0.84	0.15	0.74	0.16	0.49	0.16	0.35
W03707	0.09	0.77	0.07	0.73	0.10	0.61	0.26	0.41
W03710	0.15	0.44	0.14	0.69	0.18	0.50	0.11	0.46
W03711	0.19	0.62	0.09	0.43	0.13	0.78	0.09	0.83
W03716	0.09	0.69	0.28	0.50	0.11	0.73	0.08	0.91

well	SVM1				SVM2			
	RMSE- Training	R2- Training	RMSE- Testing	R2- Testing	RMSE- Training	R2- Training	RMSE- Testing	R2- Testing
W03718	0.18	0.51	0.11	0.48	0.14	0.25	0.15	0.64
W03727	0.13	0.78	0.09	0.84	0.12	0.72	0.11	0.64
W03734	0.10	0.91	0.10	0.90	0.14	0.75	0.11	0.83
W03736	0.17	0.26	0.15	0.64	0.09	0.82	0.09	0.80
W03737	0.12	0.75	0.11	0.64	0.07	0.97	0.17	0.73
W03741	0.14	0.74	0.11	0.84	0.13	0.84	0.14	0.79
W03748	0.09	0.82	0.09	0.84	0.12	0.70	0.11	0.54
W03751	0.07	0.94	0.17	0.74	0.10	0.65	0.09	0.84
W03754	0.13	0.85	0.15	0.76	0.05	0.85	0.19	0.54
W03756	0.11	0.69	0.11	0.56	0.15	0.76	0.12	0.71
W03757	0.06	0.66	0.07	0.80	0.13	0.73	0.14	0.71
W03758	0.08	0.87	0.19	0.60	0.14	0.85	0.17	0.83
W03761	0.14	0.78	0.12	0.72	0.13	0.63	0.13	0.60
W03762	0.13	0.70	0.13	0.73	0.10	0.73	0.09	0.76
W03763	0.13	0.87	0.17	0.88	0.12	0.84	0.11	0.83
W05338	0.13	0.64	0.13	0.65	0.21	0.23	0.25	0.67
W05339	0.12	0.74	0.09	0.79	0.12	0.91	0.06	0.99
W05346	0.10	0.87	0.10	0.84	0.18	0.48	0.15	0.63
W05347	0.20	0.34	0.26	0.63	0.10	0.81	0.18	0.82
W05462	0.10	0.92	0.07	0.99	0.19	0.53	0.14	0.65
W05464	0.17	0.54	0.15	0.68	0.17	0.53	0.21	0.76
W05465	0.10	0.84	0.20	0.82	0.13	0.78	0.05	0.92
W05469	0.19	0.59	0.13	0.72	0.15	0.58	0.08	0.88
W05473	0.15	0.54	0.15	0.91	0.13	0.86	0.10	0.99
W05474	0.13	0.74	0.06	0.94	0.10	0.85	0.09	0.90
W05477	0.10	0.84	0.08	0.88	0.13	0.78	0.14	0.87
W05480	0.12	0.88	0.12	0.85	0.10	0.66	0.13	0.65
W05686	0.13	0.85	0.11	0.89	0.10	0.74	0.10	0.81
W05688	0.10	0.89	0.10	0.95	0.08	0.88	0.08	0.89
W05690	0.10	0.69	0.13	0.75	0.12	0.81	0.15	0.75
W05860	0.10	0.75	0.10	0.82	0.10	0.74	0.18	0.78
W05861	0.08	0.91	0.08	0.90	0.15	0.58	0.20	0.93
W05863	0.12	0.82	0.13	0.77	0.15	0.23	0.10	0.66
W05864	0.10	0.75	0.18	0.79	0.06	0.93	0.06	0.95
W06067	0.16	0.74	0.18	0.92	0.15	0.63	0.15	0.65
W06068	0.20	0.24	0.10	0.63	0.12	0.83	0.18	0.44
W06069	0.05	0.95	0.06	0.98	0.11	0.73	0.13	0.81
W06070	0.15	0.64	0.15	0.63	0.13	0.73	0.08	0.93
W06072	0.13	0.81	0.18	0.49	0.13	0.76	0.08	0.88
W06076	0.10	0.81	0.13	0.81	0.14	0.77	0.22	0.63
W06078	0.12	0.74	0.09	0.79	0.14	0.64	0.09	0.88
W06081	0.10	0.78	0.09	0.84	0.20	0.53	0.20	0.48

well	SVM1				SVM2			
	RMSE- Training	R2- Training	RMSE- Testing	R2- Testing	RMSE- Training	R2- Training	RMSE- Testing	R2- Testing
W06083	0.14	0.81	0.20	0.65	0.10	0.68	0.08	0.73
W06085	0.15	0.74	0.08	0.92	0.13	0.83	0.12	0.89
W06195	0.20	0.54	0.22	0.40	0.15	0.68	0.10	0.90
W06200	0.10	0.74	0.08	0.76	0.17	0.39	0.10	0.55
W06384	0.13	0.84	0.13	0.88	0.11	0.82	0.11	0.79
W06389	0.14	0.74	0.13	0.85	0.12	0.84	0.08	0.90
W06392	0.16	0.44	0.09	0.62	0.15	0.68	0.17	0.78
W06542	0.11	0.82	0.12	0.78	0.17	0.53	0.17	0.53
W06547	0.10	0.89	0.08	0.92	0.16	0.53	0.17	0.68
W06550	0.16	0.72	0.18	0.74	0.10	0.88	0.19	0.81
W06551	0.17	0.54	0.17	0.56	0.16	0.53	0.14	0.45
W06705	0.16	0.54	0.16	0.72	0.13	0.77	0.17	0.64
W06707	0.10	0.90	0.19	0.82	0.13	0.80	0.08	0.94
W06708	0.15	0.54	0.14	0.49	0.08	0.95	0.10	0.92
W06710	0.13	0.77	0.17	0.66	0.19	0.64	0.19	0.69
W06712	0.13	0.83	0.12	0.84	0.14	0.44	0.19	0.45
W06713	0.09	0.94	0.14	0.87	0.19	0.59	0.12	0.62
W06745	0.18	0.69	0.19	0.69	0.13	0.81	0.13	0.96
W06747	0.15	0.40	0.18	0.54	0.19	0.68	0.15	0.55
W06748	0.19	0.60	0.12	0.65	0.12	0.74	0.12	0.84
W06751	0.12	0.85	0.12	0.96	0.12	0.75	0.12	0.82
W06752	0.17	0.73	0.15	0.55	0.13	0.39	0.25	0.45
W06754	0.11	0.80	0.11	0.85	0.15	0.73	0.10	0.80
W06755	0.12	0.76	0.12	0.84	0.15	0.76	0.12	0.79
W06756	0.13	0.42	0.26	0.48	0.11	0.86	0.12	0.83
W06758	0.14	0.80	0.10	0.82	0.09	0.94	0.11	0.90
W06762	0.14	0.82	0.10	0.84	0.15	0.69	0.14	0.73
W06763	0.10	0.90	0.11	0.88	0.15	0.79	0.11	0.85
W06764	0.09	0.97	0.12	0.91	0.16	0.79	0.12	0.79
W06765	0.13	0.73	0.14	0.75	0.13	0.61	0.12	0.63
W06766	0.13	0.83	0.12	0.85	0.16	0.56	0.17	0.39
W06767	0.13	0.86	0.13	0.82	0.14	0.76	0.11	0.74
W07387	0.13	0.62	0.13	0.65	0.13	0.86	0.11	0.90
W07390	0.14	0.76	0.10	0.79	0.15	0.77	0.15	0.76
W07394	0.11	0.89	0.09	0.93	0.14	0.82	0.13	0.79
W07396	0.13	0.84	0.15	0.84	0.15	0.64	0.11	0.75
W07401	0.13	0.85	0.13	0.83	0.10	0.54	0.17	0.52
W07402	0.14	0.67	0.10	0.77	0.18	0.75	0.16	0.78
W07403	0.11	0.55	0.18	0.55	0.19	0.33	0.14	0.53
W07404	0.16	0.83	0.17	0.82	0.13	0.91	0.16	0.72
W07407	0.18	0.40	0.13	0.53	0.12	0.85	0.12	0.84
W07409	0.11	0.95	0.19	0.73	0.13	0.83	0.10	0.90

well	SVM1				SVM2			
	RMSE- Training	R2- Training	RMSE- Testing	R2- Testing	RMSE- Training	R2- Training	RMSE- Testing	R2- Testing
W07410	0.11	0.88	0.15	0.89	0.13	0.69	0.14	0.83
W07416	0.11	0.88	0.13	0.94	0.11	0.92	0.12	0.88
W07418	0.13	0.72	0.15	0.81	0.12	0.53	0.06	0.60
W07420	0.11	0.92	0.14	0.88	0.13	0.63	0.14	0.76
W07421	0.09	0.54	0.06	0.62	0.11	0.75	0.16	0.42
W07424	0.13	0.64	0.11	0.80	0.17	0.61	0.21	0.62
W07425	0.11	0.74	0.16	0.42	0.15	0.43	0.14	0.72
W07490	0.17	0.60	0.21	0.62	0.14	0.75	0.19	0.52
W07494	0.15	0.44	0.14	0.76	0.14	0.73	0.15	0.80
W07495	0.14	0.75	0.18	0.64	0.14	0.75	0.13	0.80
W07496	0.13	0.80	0.14	0.80	0.14	0.86	0.12	0.88
W07497	0.14	0.77	0.13	0.83	0.14	0.85	0.13	0.86
W07498	0.13	0.87	0.13	0.86	0.13	0.42	0.05	0.62
W07500	0.13	0.88	0.12	0.90	0.18	0.47	0.16	0.70
W07501	0.13	0.44	0.06	0.66	0.17	0.45	0.13	0.67
W07504	0.20	0.47	0.17	0.68	0.11	0.86	0.16	0.75
W07505	0.17	0.49	0.12	0.71	0.13	0.71	0.10	0.82
W07506	0.09	0.95	0.16	0.79	0.14	0.81	0.14	0.82
W07507	0.13	0.76	0.09	0.81	0.13	0.82	0.12	0.83
W07551	0.12	0.88	0.14	0.85	0.11	0.89	0.10	0.89
W07554	0.12	0.86	0.10	0.86	0.21	0.75	0.13	0.66
W07561	0.10	0.91	0.13	0.86	0.12	0.81	0.15	0.76
W07563	0.19	0.87	0.12	0.75	0.13	0.87	0.15	0.81
W07565	0.10	0.88	0.15	0.73	0.11	0.85	0.10	0.87
W07568	0.12	0.90	0.13	0.83	0.10	0.70	0.07	0.83
W07569	0.10	0.90	0.10	0.86	0.12	0.71	0.08	0.81
W08005	0.10	0.70	0.07	0.83	0.08	0.63	0.13	0.50
W08010	0.12	0.73	0.08	0.78	0.11	0.76	0.17	0.69
W08011	0.07	0.66	0.13	0.54	0.09	0.75	0.15	0.69
W08143	0.10	0.80	0.15	0.76	0.13	0.76	0.09	0.85
W08148	0.09	0.74	0.16	0.76	0.15	0.66	0.16	0.63
W08151	0.15	0.66	0.12	0.77	0.06	0.53	0.29	0.63
W08153	0.14	0.67	0.14	0.65	0.12	0.80	0.16	0.69
W08191	0.12	0.83	0.17	0.64	0.12	0.78	0.11	0.89
W08712	0.11	0.82	0.08	0.95	0.12	0.83	0.10	0.90
W08713	0.12	0.84	0.10	0.86	0.10	0.72	0.15	0.56
W08869	0.09	0.76	0.14	0.61	0.09	0.64	0.16	0.47
W08871	0.06	0.67	0.15	0.51	0.14	0.47	0.11	0.59
W08873	0.13	0.50	0.12	0.57	0.10	0.84	0.16	0.74
W08879	0.10	0.87	0.15	0.76	0.13	0.68	0.13	0.58
W08908	0.11	0.75	0.11	0.71	0.14	0.71	0.09	0.92
W08947	0.15	0.59	0.12	0.80	0.06	0.65	0.17	0.63



well	SVM1				SVM2			
	RMSE- Training	R2- Training	RMSE- Testing	R2- Testing	RMSE- Training	R2- Training	RMSE- Testing	R2- Testing
W08948	0.06	0.71	0.15	0.67	0.12	0.75	0.12	0.75
W08952	0.12	0.82	0.17	0.51	0.14	0.83	0.11	0.90
W08954	0.16	0.81	0.17	0.89	0.12	0.78	0.10	0.74
W08955	0.12	0.80	0.11	0.64	0.23	0.53	0.12	0.89
W08996	0.20	0.61	0.13	0.88	0.12	0.80	0.07	0.88
W09000	0.12	0.81	0.09	0.77	0.11	0.83	0.13	0.82
W09001	0.11	0.84	0.11	0.85	0.16	0.63	0.13	0.78
W09004	0.15	0.59	0.14	0.80	0.19	0.53	0.14	0.57
W09005	0.16	0.63	0.21	0.54	0.11	0.53	0.09	0.84
W09007	0.12	0.47	0.09	0.84	0.11	0.76	0.11	0.75
W09008	0.10	0.79	0.11	0.75	0.15	0.60	0.17	0.57
W17573	0.14	0.67	0.17	0.61	0.10	0.78	0.15	0.86
W17576	0.09	0.82	0.14	0.88	0.15	0.55	0.20	0.67
W17579	0.13	0.66	0.18	0.80	0.13	0.57	0.13	0.55
W17580	0.13	0.58	0.13	0.55	0.13	0.88	0.14	0.81
W17583	0.10	0.94	0.13	0.84	0.17	0.68	0.13	0.86
W17587	0.16	0.74	0.12	0.90	0.12	0.44	0.14	0.39
W17596	0.12	0.48	0.12	0.38	0.10	0.72	0.18	0.56
W17597	0.05	0.73	0.19	0.48	0.12	0.58	0.18	0.74
W17600	0.12	0.62	0.19	0.69	0.12	0.82	0.14	0.65
W17602	0.13	0.78	0.13	0.72	0.14	0.83	0.09	0.92
W17603	0.13	0.84	0.11	0.88	0.10	0.82	0.11	0.71
W17604	0.10	0.82	0.10	0.75	0.11	0.79	0.13	0.70
W17606	0.12	0.80	0.15	0.67	0.12	0.69	0.16	0.69
W17608	0.12	0.70	0.14	0.75	0.15	0.91	0.15	0.63
W17609	0.15	0.62	0.16	0.64	0.15	0.77	0.12	0.95
W17610	0.15	0.84	0.12	0.93	0.19	0.46	0.25	0.36
W17617	0.12	0.74	0.11	0.88	0.13	0.69	0.13	0.83
W17619	0.15	0.52	0.08	0.64	0.14	0.53	0.08	0.65
W17620	0.17	0.67	0.15	0.72	0.17	0.66	0.15	0.71
W17621	0.13	0.84	0.16	0.72	0.13	0.83	0.16	0.74
W17622	0.14	0.76	0.12	0.89	0.15	0.73	0.11	0.91
W17624	0.11	0.82	0.16	0.72	0.11	0.82	0.18	0.66
W17653	0.10	0.34	0.19	0.44	0.18	0.50	0.23	0.36
W17655	0.14	0.56	0.14	0.43	0.15	0.50	0.14	0.42
W17656	0.15	0.71	0.10	0.86	0.15	0.70	0.10	0.83
W17657	0.08	0.84	0.08	0.87	0.08	0.83	0.07	0.85
W17658	0.10	0.92	0.14	0.85	0.12	0.88	0.15	0.86
W17659	0.10	0.64	0.21	0.56	0.10	0.56	0.23	0.44
W17661	0.12	0.85	0.09	0.91	0.13	0.82	0.10	0.87
W17663	0.10	0.79	0.08	0.89	0.13	0.77	0.09	0.84
W17664	0.15	0.66	0.17	0.64	0.15	0.64	0.17	0.63

well	SVM1				SVM2			
	RMSE- Training	R2- Training	RMSE- Testing	R2- Testing	RMSE- Training	R2- Training	RMSE- Testing	R2- Testing
W17666	0.15	0.78	0.11	0.84	0.15	0.74	0.11	0.81
W17667	0.15	0.74	0.15	0.91	0.16	0.70	0.15	0.86
W17668	0.18	0.61	0.15	0.75	0.20	0.57	0.15	0.74



## REFERENCES

- Alijani, B., O'Brien, J. and Yarnal, B. (2008). "Spatial analysis of precipitation intensity and concentration in Iran." *Theor. Appl. Climatol.* 94 (1–2): 107–124.
- ASCE Task Committee on Application of Artificial Neural Networks in Hydrology, 2000a. Artificial neural networks in hydrology I: preliminary concepts. *J. Hydrol. Eng.* 5, 115–123.
- ASCE Task Committee on Application of Artificial Neural Networks in Hydrology, 2000b. Artificial neural networks in hydrology II: hydrologic applications. *J. Hydrol. Eng.*, 5, 124–137.
- Asoka, A., Gleeson, T., Wada, Y., and Mishra, V., (2017). "Relative contribution of monsoon precipitation and pumping to changes in groundwater storage in India." *Nat. Geosci.*, 10, 109–117.
- Alexandrov, T., and Golyandina, N. (2006). "Automatic trend extraction and forecasting for a family of time series." In Proc., Int. Symp. On Forecasting. Medford, MA: International Institute of Forecasters.
- Aswathaiah, U and Nandagiri, L. (2020). "Extraction of nonlinear trends in time series of rainfall using singular spectrum analysis." *J. Hydrol. Eng., ASCE*, 25(12), 04020053.
- Banerjee, P., Prasad, R.K., Singh, V.S., (2009). "Forecasting of groundwater level in hard rock region using artificial neural network." *Environ. Geol.* 58 (6), 1239–1246.
- Beck, F., Bárdossy, A., Seidel, J., Müller, T., Fernandez Sanchis, E. and Hauser, A. (2015). "Statistical analysis of sub-daily precipitation extremes in Singapore." *J. Hydrol. Reg. Stud.*,3: 337–358.
- Bisht, D. S., Chatterjee, C., Raghuwanshi, N. S. and Sridhar, V. (2018). "Spatio-temporal

trends of rainfall across Indian river basins.” *Theor. Appl. Climatol.*, 132 (1–2): 419–436.

Bothale, R. V., and Katpatal, Y. B. (2016). “Trends and Anomalies in Extreme Climate Indices and Influence of El Niño and La Niña over Pranhita Catchment in Godavari Basin, India.” *J. Hydrol. Eng.*, 21 (2): 5015023.

Le Brocque, A. F., Kath, J. and Reardon-Smith, K. (2018). “Chronic groundwater decline: A multi-decadal analysis of groundwater trends under extreme climate cycles.” *J. Hydrol.* 561 (March): 976–986.

Caloiero, T., Coscarelli, R., E. Ferrari, E., and Mancini. M., (2011). “Trend detection of annual and seasonal rainfall in Calabria (Southern Italy).” *Int. J. Climatol.*, 31 (1): 44–56.

Chatterjee, R., Samadder, S., Mondal, D. and Adhikari, K. (2020). “ Analysis of spatio-temporal trend in groundwater elevation data from arsenic affected alluvial aquifers – Case study from Murshidabad district, West Bengal, Eastern India.” *J Earth Syst Sci .*, 129, 228.

Census Data of India (2011,2001,1991). Reports of the Office of the Registrar General and Census Commissioner, India, Ministry of Home Affairs, Govt. of India.

Chen, Z., Grasby, S. E. and Osadetz, K. G. (2004). “Relation between climate variability and groundwater levels in the upper carbonate aquifer, southern Manitoba, Canada.” *J. Hydrol.* 290 (1–2): 43–62.

Chen, L.H., Chen, C.T., Lin, D.W., (2011). “Application of integrated back-propagation network and self-organizing map for groundwater level forecasting.” *J. Water Res. Plan. Man.*, 137 (4), 352–365.

Chen, J. L., Wilson, C. R., Tapley, B. D., canlon, B. and Güntner, A. (2016). “Long-term groundwater storage change in Victoria, Australia from satellite gravity and in situ observations.” *Glob. Planet. Change*, 139 56–65.

CGWB, (2006). Dynamic Groundwater Resources of India. (as on March 2004). Central Ground Water Board (CGWB), Ministry of Water Resources, New Delhi, India.

CGWB, (2009). Dynamic Groundwater Resources of India. (as on March 2009). Central Ground Water Board (CGWB), Ministry of Water Resources, New Delhi, India.

CGWB, (2011). Dynamic Groundwater Resources of India. Central Ground Water Board (CGWB), Ministry of Water Resources, New Delhi, India.

CGWB, (2013). Dynamic Groundwater Resources of India. Central Ground Water Board (CGWB), Ministry of Water Resources, New Delhi, India.

CGWB (Central Ground Water Board). (2014). Report on the status of groundwater quality in coastal aquifers of India. Faridabad, India: CGWB.

CGWB, (2017). Dynamic Groundwater Resources of India. Central Ground Water Board (CGWB), Ministry of Water Resources, New Delhi, India.

CGWB (Central Ground Water Board). (2019). Dynamic groundwater resources of India, 2017. Faridabad, India: CGWB.

CGWB, (2020). Dynamic Groundwater Resources of India. Central Ground Water Board (CGWB), Ministry of Water Resources, New Delhi, India.

CGWB (Central Ground Water Board). (2018). Ground Water Year Book of India 2017-2018. Faridabad, India: CGWB.

CGWB (Central Ground Water Board). (2019a). Ground Water Year Book of Kerala (2018-2019). Thiruvananthapuram, India: CGWB.

CGWB (Central Ground Water Board). (2019b). Ground Water Year Book of Karnataka (2018-2019). Bengaluru, India: CGWB.

CGWB (Central Ground Water Board). (2019c). Ground Water Year Book of Maharashtra and Union Territory of Darda and Nager Haveli (2018-2019). Nagpur, India: CGWB.

- CWC (Central Water Commission). 2005. *Annual report (2008-2009)*, New Delhi: India.
- CWC (Central Water Commission). 2014. *Watershed Atlas of India*, New Delhi: India.
- CWC (Central Water Commission). 2016. *Annual report (2015-2016)*, New Delhi: India.
- Coscarelli, R., and Caloiero, T. (2012). “Analysis of daily and monthly rainfall concentration in Southern Italy (Calabria region).” *J. Hydrol.*, 416–417 145–156.
- Coulibaly, P., Anctil, F., Aravena, R. and Bobee, B., (2001). “Artificial neural network modeling of water table depth fluctuations.” *Water Resour. Res.*, 37 (4), 885–896.
- Daliakopoulos, I.N., Coulibaly, P and Tsanis, I.K. (2005). “Groundwater level forecasting using artificial neural networks.” *J. Hydrol.*, 309, 229–240.
- Dalin, C., Wada, Y., Kastner, T. and Puma, M.J. (2017). “Groundwater depletion embedded in international food trade.” *Nature* 543, 700–704.
- Daneshvar Vousoughi, F., Dinpashoh, Y., Aalami, M. T. and Jhajharia, D.(2013). “Trend analysis of groundwater using non-parametric methods (case study: Ardabil plain).” *Stoch. Environ. Res. Risk Assess.*, 27 (2): 547–559.
- De Luís, M., Raventós, J., González-Hidalgo, J. C., Sánchez, J. R., and Cortina, J. (2000). “Spatial analysis of rainfall trends in the region of valencia (East Spain).” *Int. J. Climatol.* 20 (12): 1451–1469.
- Elsner, J. B., and A. A. Tsonis. (1996). *Singular spectrum analysis—A new tool in time series analysis*. New York: Plenum.
- Eltahir, E. A. B., and Yeh, P. J. F. (1999). “On the asymmetric response of aquifer water level to floods and droughts in Illinois.” *Water Resour. Res.*, 35 (4), 1199–1217.
- Falga, R and Wang, C. (2022). “The rise of Indian summer monsoon precipitation extremes and its correlation with long-term changes of climate and anthropogenic factors.” *Scientific*

*Reports*, 12(1), 11985.

Famiglietti, J.S. (2014). “The global groundwater crisis.” *Nat. Clim. Change.*, 4, 945-948.

FAO FAO statistical yearbook 2013 - World food and agriculture 2013 FAO Rome

Giordano, M. (2009). “Global groundwater? Issues and solutions.” *Annu Rev Environ Resour.*, 34, 153–178.

Grinsted, A., Moore, J. C. and Jevrejeva, S. (2004). “Application of the cross wavelet transform and wavelet coherence to geophysical time series.” *Nonlinear Process. Geophys.* 11 (5/6), 561–566.

Guhathakurta, P., and Rajeevan, M. (2008). “Trends in the rainfall pattern over India.” *Int. J. Climatol.*, 28 (11): 1453–1469.

Guimaraes Santos, C. A., Galvao, C. O. and Trigo, R. M. (2003). “Rainfall data analysis using wavelet transform.” *IAHS-AISH Publ.* 278, 195–201.

Halder, S., Parekh, A., Chowdary, J. S. and Gnanaseelan, C. (2022). “Dynamical and moist thermodynamical processes associated with Western Ghats rainfall decadal variability.” *npj Climate and Atmospheric Science.*, 5:8.

Hamed, K. H., and A. Ramachandra Rao. (1998). “A modified Mann-Kendall trend test for autocorrelated data.” *J. Hydrol.* 204 (1): 182–196.

Holman, I. P., Rivas-Casado, M., Bloomfield, J. P. and J. J. Gurdak, J. J. (2011). “Identifying non-stationary groundwater level response to North Atlantic ocean-atmosphere teleconnection patterns using wavelet coherence.” *Hydrogeol. J.* 19 (6): 1269–1278.

Hora, T., Srinivasan, V., and Basu, N.B., (2019). “The Groundwater Recovery Paradox in South India.” *Geophys. Res. Lett.* 46, 9602–9611.

IPCC (Intergovernmental Panel on Climate Change). (2007). “Climate change 2007: Impacts, adaptation, and vulnerability.” Contribution of Working Group II to the fourth assessment report of the Intergovernmental Panel on Climate Change, M. L. Parry, O. F.



Canziani, J. P. Palutikof, P. J. van der Linden, and C. E. Hanson, eds., Cambridge University Press, Cambridge, U.K.

Jan, C. D., Chen, T. H. and Lo. W. C. (2007). “Effect of rainfall intensity and distribution on groundwater level fluctuations.” *J. Hydrol.* 332 (3–4): 348–360.

Jain, S. K., Nayak, P. C., Singh, Y. and Chandniha, S. K. (2017). “Trends in rainfall and peak flows for some river basins in India.” *Curr. Sci.* 112 (8): 1712–1726.

Jain, M., Fishman, R., Mondal, P., Galford, G. L., Bhattarai, N., Naeem, S., Lall, U., Balwinder-Singh and DeFries, R. S. (2021). “Groundwater depletion will reduce cropping intensity in India.” *Sci. Adv.*, 7(9),

Kang, S. and H. Lin, H. (2007). “Wavelet analysis of hydrological and water quality signals in an agricultural watershed.” *J. Hydrol.* 338 (1–2): 1–14.

Kendall, M. G. (1975). Rank correlation methods. London: Charles Griffin.

Khaki, M., Yusoff, I., Islami, N., (2015). “Simulation of groundwater level through artificial intelligence system.” *Environ. Earth Sci.*, 73 (12), 8357–8367.

Kothawale, D. R., and Rajeevan, M. (2017). “Monthly, Seasonal and Annual Rainfall Time Series for All-India, Homogeneous Regions and Meteorological Subdivisions: 1871-2016 Indian Institute of Tropical Meteorology (IITM) Earth System Science Organization (ESSO) Ministry of Earth Sciences, Indian *Inst. Trop. Meteorol. Earth 02*, 1871–2016.

Krishna, B., Satyaji Rao, Y.R. and Vijaya, T. (2008). “Modelling groundwater levels in an urban coastal aquifer using artificail neural networks.” *Hydrol. Process.*, 22, 1180–1188.

Krishna, B., Satyaji Rao, Y.R., Vijaya, T., (2008). “Modelling groundwater levels in an urban coastal aquifer using artificail neural networks.” *Hydrol. Process.* 22, 1180–1188.

Krishan, G., Rao, M. S., Loyal, R. S., Lohani, A. K., Tuli, N. K., Takshi, K. S., Kumar, C.

P., Semwal, P. and Kumar, S. (2014). “Groundwater Level Analyses of Punjab, India: a Quantitative Approach.” *Octa J. Environ. Res.*, 2 (3), 221–226.

Krishnakumar, K. N., Prasada Rao, G. S. L. H. V. and Gopakumar, C. S. (2009). “Rainfall trends in twentieth-century over Kerala, India.” *Atmos. Environ.*, 43 (11): 1940–1944.

Kumar, P., Chandniha, S. K., Lohani, A. K., Nema, A. K. and Krishan, G. (2018). “Trend Analysis of Groundwater Level Using Non-Parametric Tests in Alluvial Aquifers of Uttar Pradesh, India.” *Curr. World Environ.*, 13 (1), 44–54.

Kumar, P. and Foufoula-Georgiou, E. (1997). “Wavelet analysis for geophysical applications.” *Rev. Geophys.*, 35 (4): 385–412.

Kuss, A. J. M. and J. J. Gurdak. 2014. “Groundwater level response in U.S. principal aquifers to ENSO, NAO, PDO, and AMO.” *J. Hydrol. Elsevier B.V.* 519 (PB): 1939–1952.

Labat, D. (2005). “Recent advances in wavelet analyses: Part 1. A review of concepts.” *J. Hydrol.* 314 (1–4): 275–288.

Li, H., Y. Lu, C. Zheng, X. Zhang, B. Zhou, and J. Wu. 2020. “Seasonal and Inter-Annual Variability of Groundwater and Their Responses to Climate Change and Human Activities in Arid and Desert Areas: A Case Study in Yaoba Oasis, Northwest China.” *Water*, 12, 303.

Liang, L., Li, L. and Liu, Q. (2011). “Precipitation variability in Northeast China from 1961 to 2008.” *J. Hydrol.*, 404 (1–2): 67–76.

Maier, H.R. and Dandy, G.C. (2000). Neural networks for the prediction and forecasting of water resources variables: a review of modeling issues and applications. *Environ. Modell. Software* 15, 101–124.

Malakar, P., Sarkar, S., Mukherjee, A., Bhanja, S. and Sun, A. Y. (2021). “Use of machine learning and deep learning methods in groundwater.” Book Chapter., *Chapter 40., Global Groundwater.* 545-555.

Malakar, P., Mukherjee, A., Bhanja, S. N., Ganguly, A. R., Ray, R. K., Zahid, A., Sarkar, S., Saha, D., and Chattopadhyay, S. (2021). “Three decades of depth-dependent

groundwater response to climate variability and human regime in the transboundary Indus-Ganges-Brahmaputra-Meghna mega river basin aquifers.” *Adv. in Water Res.*, 149, 103856.

Mann H. B. (1945). “Nonparametric tests against trend.” *Econom. J. Econom. Soc.* 13 (3): 245–259.

Masih, I., Uhlenbrook, Maskey, S. and Smakhtin, V. (2011). “Streamflow trends and climate linkages in the Zagros Mountains, Iran.” *Clim. Change.*, 104 (2): 317–338.

Ministry of Water Resources. (2014). "Watershed Atlas of India." Central Water Commission and National Remote Sensing Centre, Govt. of India, 205pp.

Mishra, A. K., and V. P. Singh. 2010. “A review of drought concepts.” *J. Hydrol.* 391 (1): 202–216.

Mishra, V., Tiwari, A.D. and Kumar, R. (2022). “A framework to incorporate spatiotemporal variability of rainfall extremes in summer monsoon declaration in India.” *Environ. Res. Lett.*, 17 (2022) 094039.

Mohanavelu, A., Kasiviswanathan, K. S., Mohanasundaram, S., Ilampooranan, I., Jianxun He, Pingale, S. M., Soundharajan, B. S., and Diwan Mohaideen, D. M. M. (2020). “Trends and Non-Stationarity in Groundwater Level Changes in Rapidly Developing Indian Cities.” *Water*, 12(11), 32

Mohapatra, J. B., Jha, P., Jha, M., K., and Biswal, S. (2021). “Efficacy of machine learning techniques in predicting groundwater fluctuations in agro-ecological zones of India.” *Sci. Total Environ.*, 785 (2021) 147319 09.

Mohanty, S., Jha, M.K., Raul, S.K., Panda, R.K., Sudheer, K.P., (2015). “Using artificial neural network approach for simultaneous forecasting of weekly groundwater levels at multiple sites.” *Water Resour. Manag.* 29 (15), 5521–5532.

Mondal, A., Khare, D. and Kundu, S. (2015). “Spatial and temporal analysis of rainfall and temperature trend of India.” *Theor. Appl. Climatol.* 122 (1–2): 143–158.

Mudbhatkal, A., Raikar, R.V., Venkatesh, B. and Mahesha, A. (2017). “Impacts of climate change on varied River-Flow regimes of southern India.” *J. Hydrol. Eng.* 22 (9): 1–13.

Mukherjee, A., Ramachandran, P., (2018). “Prediction of GWL with the help of GRACE TWS for unevenly spaced time series data in India: analysis of comparative performances of SVR, ANN and LRM.” *J. Hydrol.* 558, 647–658.

Nageswararao, M.M., Sannan, M. C. and Mohanty, U. C. (2019). “Characteristics of various rainfall events over South Peninsular India during northeast monsoon using high-resolution gridded dataset (1901–2016).” *Theor. Appl. Climatol.*, 137, 2573–2593.

Nair, P.J., Chakraborty, A., Varikoden, H., Francis, P.A. and Kuttippurath, J. (2018). “The local and global climate forcings induced inhomogeneity of Indian rainfall”. *Scientific Reports*, 8, 6026.

Nayak, P.C., Satyajit Rao, Y.R., Sudheer, K.P., (2006). “Groundwater level forecasting in a shallow aquifer using artificial neural network approach.” *Water Resour. Manag.* 20, 77–90.

Ngongondo, C., Xu, C. Y., Gottschalk, L. and Alemaw, B. (2011). “Evaluation of spatial and temporal characteristics of rainfall in Malawi: A case of data-scarce region.” *Theor. Appl. Climatol.*, 106 (1–2): 79–93.

Nourani, V., Asghari Mogaddam, A., Nadiri, A.O., (2008). “An ANN-based model for spatiotemporal groundwater level forecasting.” *Hydrol. Process.* 22, 5054–5066.

Panda, D. K., Mishra, A., Jena, S. K., James, B. K. and Kumar, A, (2007). “The influence of drought and anthropogenic effects on groundwater levels in Orissa, India.” *J. Hydrol.* 343 (3–4): 140–153.

Panda, D. K., A. Mishra, A. and Kumar, A. (2012). “Quantification of trends in groundwater levels of Gujarat in western India.” *Hydrol. Sci. J.*, 57 (7): 1325–1336.

Partal, T., and Kahya, E. (2006). “Trend analysis in Turkish precipitation data.” *Hydrol. Process.* 20 (9): 2011–2026.

Pai, D. S., Sridhar, L., Rajeevan, M., Sreejith, O. P., Satbhai, N. S., and Mukhopadhyay, B. (2014). “Development of a new high spatial resolution ( $0.25^\circ \times 0.25^\circ$ ) long period (1901–2010) daily gridded rainfall data set over India and its comparison with existing data sets over the region.” *Mausam*, 65(1), 1–18.

Pathak, A.A. and Dodamani, B.M. (2019). Trend Analysis of Groundwater Levels and Assessment of Regional Groundwater Drought: Ghataprabha River Basin, India. *Nat Resour Res* 28, 631–643.

Perez-Valdivia, C., Sauchyn, D. and Vanstone, J. (2012). “Groundwater levels and teleconnection patterns in the Canadian Prairies.” *Water Resour. Res.* 48 (7).

Pophare, A. M., Lamsoge, B. R., Katpatal, Y, B. and Nawale, V. P. (2014). “Impact of over-exploitation on groundwater quality: A case study from WR-2 watershed, India.” *J. Earth Syst. Sci.* 123 (7), 1541–1566.

Preethi, B., Mujumdar, M., Kripalani, R.H., Prabhu, Amita, Krishnan, R., (2017). “Recent trends and tele-connections among South and East Asian summer monsoons in a warming environment.” *Clim. Dyn.* 48, 2489–2505.

Rajeevan, M., Bhate, J. and Jaswal, A. K. (2008). “Analysis of variability and trends of extreme rainfall events over India using 104 years of gridded daily rainfall data.” *Geophys. Res. Lett.* 35 (18): 1–6.

Rajeevan, M., Unnikrishnan, C. K., Jyoti Bhate, J., Niranjan Kumara, K and Sreekala, P. P. (2012). “Northeast monsoon over India: variability and prediction.” *Meteorol. Appl.* 19: 226–236.

Rajae, T., Ebrahimi, H., and Nourani, V. (2019). “A review of the artificial intelligence methods in groundwater level modeling.” *J. Hydrol.* 572, 336–351.

Ramos, N. F., Folch, A., Fernández-García, D., Lane, M., Thomas, M., Gathenya, J. M., Wara, C., Thomson, P., Custodio, E. and Hope, R. (2020). “Evidence of groundwater vulnerability to climate variability and economic growth in coastal Kenya.” *J. Hydrol.* 586 124920

Revadekar, J. V., Varikoden, H., Murumkar, P.K. and Ahmed, S.A. (2018). “Latitudinal variation in summer monsoon rainfall over Western Ghat of India and its association with global sea surface temperatures.” *Sci. Total Environ.*, 613-614, 88-97.

Rodell, M., Famiglietti, J.S., Wiese, D.N., Reager, J.T., Beaudoin, H.K. and Landerer,

F.W. (2018). “Emerging trends in global freshwater availability.” *Nature* 557 (7707), 651-659.

Roshni, T., Jha, M.K. and Drisya, J. (2020). “Neural network modeling for groundwater-level forecasting in coastal aquifers.” *Neural Comput. & Applic.* 32, 12737–12754.

Rust, W., Holman, I., Corstanje, R., Bloomfield, J. and Cuthbert, M. (2018). “A conceptual model for climatic teleconnection signal control on groundwater variability in Europe.” *Earth-Science Rev.* 177: 164–174.

Sahoo, S., Jha, M.K., (2013). “Groundwater-level prediction using multiple linear regression and artificial neural network techniques: a comparative assessment.” *Hydrogeol. J.* 21, 1865–1887.

Sang, Y. F., Z. Wang, and C. Liu. (2014). “Comparison of the MK test and EMD method for trend identification in hydrological time series.” *J. Hydrol.* 510 (Mar): 293–298.

Sen, P. K. (1968). “Estimates of the regression coefficient based on Kendall’s tau.” *J. Am. Stat. Assoc.* 63 (324): 1379–1389.

Shahid, S., and Hazarika, M. K. (2010). “Groundwater drought in the northwestern districts of Bangladesh.” *Water Resour. Manag.* 24 (10): 1989–2006.

Shaji, E., Nayagam, S.P., Kunhambu, V., Thambi, D.S., (2008). “Change in the groundwater scenario in Kerala over the last two decades.” *Golden Jubilee Memoir Geol. Soc. India.* 69, 67–85.

Shamsudduha, M., Chandler, R. E., Taylor, R. G. and Ahmed, K. M. (2009). “Recent trends in groundwater levels in a highly seasonal hydrological system: The Ganges-Brahmaputra-Meghna Delta.” *Hydrol. Earth Syst. Sci.*, 13 (12): 2373–2385.

Shanley, J. B., Chalmers, A. T., Mack, T. J., Smith, T. E. and Harte, P.T. (2016). “Groundwater Level Trends and Drivers in Two Northern New England Glacial Aquifers.”

*J. Am. Water Resour. Assoc.* 52 (5): 1012–1030.

Sheikh, M. M., Manzoor, N., Ashraf, J., Adnan, M., Collins, D., Hameed, S., Manton, M. J., Ahmed, A. U., Baidya, S. K., Borgaonkar, H. P., Islam, N., Jayasinghearachchi, D., Kothawale, D. R., Premalal, K. H. M. S., Revadekar, J. V., and Shrestha, M. L. (2015). “Trends in extreme daily rainfall and temperature indices over South Asia.” *Int. J. Climatol.*, 35 (7): 1625–1637.

Shirmohammadi, B., Vafakhah, M., Moosavi, V., Moghaddamnia, A., (2013). “Application of several data-driven techniques for predicting groundwater level.” *Water Resour. Manag.* 27 (2), 419–432.

Sishodia, R. P., Shukla, S., Graham, W. D., Wani, S. P. and Garg, K. K. (2016). “Bi-decadal groundwater level trends in a semi-arid south Indian region: Declines, causes, and management.” *J. Hydrol. Reg. Stud.*, 8. 43–58.

Smerdon, B. D., (2017). “A synopsis of climate change effects on groundwater recharge.” *J. Hydrol.*, 555: 125–128.

Sreekala, P.P., Rao, S. V. B. and Rajeevan, M. (2011). “Northeast monsoon rainfall variability over south peninsular India and its teleconnections.” *Theor Appl Climatol.*, 108,73–83.

Suryanarayana, C., Sudheer, C., Mahammood, V., Panigrahi, B.K., (2014). “An integrated wavelet-support vector machine for groundwater level prediction in Visakhapatnam, India.” *Neurocomputing* 145, 324–335.

Svozil, D., Kvasnička, V. and Pospíchal, J (1997). “Introduction to multi-layer feed-forward neural networks.” *Chemom. Intell. Lab. Syst.*, 39(1), 43–62.

Swain, S., Sahoo, S., Taloor, A. K., Mishra, S. K., and Pande, A. (2022). “Exploring recent groundwater level changes using Innovative Trend Analysis (ITA) technique over three districts of Jharkhand India.” *Groundwater for Sustainable Development*, 18, 100783.

Tabari, H., Nikbakht, J. and Shifteh Some'e, B. (2012). "Investigation of groundwater level fluctuations in the north of Iran." *Environ. Earth Sci.* 66 (1), 231–243.

Tabari, H., and Talaei, P. H. (2011). "Temporal variability of precipitation over Iran: 1966–2005." *J. Hydrol.*, 396 (3): 313–320.

Taylor, R.G., Scanlon, B., Do'nn, P., Rodell, M., Van Beek, R., and Wada, Y. (2013). "Ground water and climate change." *Nat. Clim. Change.*, 3, 322-329.

Thakur, G. S., and T. Thomas, T. (2011). "Analysis of groundwater levels for detection of a trend in Sagar district, Madhya Pradesh." *J. Geol. Soc. India* 77 (4), 303–308.

Thomas, J. and Prasannakumar, V. (2016). "Temporal analysis of rainfall (1871-2012) and drought characteristics over a tropical monsoon-dominated State (Kerala) of India." *J. Hydrol.*, 534, 266–280.

Thornthwaite, C. W. (1948). "An approach toward a rational classification of climate." *Geogr. Rev.*, 38(1), 55–94.

Tirogo, J., A. Jost, A. Biaou, D. Valdes-Lao, Y. Koussoubé, and P. Ribstein. (2016). "Climate variability and groundwater response: A case study in Burkina Faso (West Africa)." *Water*, 8 (5), 1–20.

Tiwari, V.M., Wahr, J., and Swenson, S., (2009). "Dwindling groundwater resources in northern India, from satellite gravity observations." *Geophys. Res. Lett.* 36, L18401.

Torrence, C., and Compo, G. P. (1998). "A Practical Guide to Wavelet Analysis." *Bull. Am. Meteorol. Soc.* 79 (1): 61–78.

Totaro, V., A. Gioia, and V. Iacobellis. (2020). "Numerical investigation on the power of parametric and nonparametric tests for trend detection in annual maximum series." *Hydrol. Earth Syst. Sci.*, 24, 473-488.



Trichakis, I.C., Nikolos, I.K., Karatzas, G.P., (2011). “Artificial Neural Network (ANN) Based modeling for karstic groundwater level simulation.” *Water Resour. Manag.* 25, 1143–1152.

Tsanis, I.K., Coulibaly, P., Daliakopoulos, I.N., (2014). “Improving groundwater level forecasting with a feed-forward neural network and linearly regressed projected precipitation.” *J. Hydroinform.* 10 (4), 317–330.

Unnikrishnan, P., and V. Jothiprakash. (2015). “Extraction of nonlinear rainfall trends using singular spectrum analysis.” *J. Hydrol. Eng., ASCE*, 20(12), 05015007.

Vapnik, V.N. (1995). “The Nature of Statistical Learning Theory.” Springer-Verlag, New York, USA. 314 p.

Vaux, H., (2011). “Groundwater under stress: The importance of management.” *Environ. Earth Sci.* 62 (1): 19–23.

Velasco, E. M., Gurdak, J. J., Dickinson, J. E., Ferré, T. P. A. and Corona, C. R. (2017). “Interannual to multi-decadal climate forcings on groundwater resources of the U.S. West Coast.” *J. Hydrol. Reg. Stud.*, (11). 250–265.

Vörösmarty, C., McIntyre, P., Gessner, M., Dudgeon, D., Prusevich, A., Green, P., Glidden, S., Bunn, S. E., Sullivan, C. A., Reidy Liermann, C. and Davies, P. M. (2010). “Global threats to human water security and river biodiversity.” *Nature*, 467, 555–561.

Weider, K., and Boutt, D. F. (2010). “Heterogeneous water table response to climate revealed by 60 years of groundwater data.” *Geophys. Res. Lett.* 37 (24): 10–15.

Whittemore, D. O., Butler, J. J. and Wilson, B. B. (2016). “Assessing the major drivers of water-level declines: new insights into the future of heavily stressed aquifers.” *Hydrol. Sci. J.*, 61 (1): 134–145.

Yadav, R. K. (2012). “Why is ENSO influencing Indian northeast monsoon in the recent decades?” *Int. J. Climatol.*, 33: 2163-2180.

Yan, S. F., Yu, S. E., Wu, Y. B., Pan, D. F., She, D. L. and Ji, J. (2015). “Seasonal Variations in Groundwater Level and Salinity in Coastal Plain of Eastern China Influenced by Climate.” *J. Chem.* 2015, 8.

- Yang, Z.P., Lu, W.X., Lonf, Y.Q., Li, P., (2009). “Application and comparison of two prediction models for groundwater levels: a case study in Western Jilin Province. China.” *J. Arid Environ.* 73, 487–492.
- Yoon, H., Jun, S.C., Hyun, Y., Bae, G.O., Lee, K.K., (2011). A comparative study of artificial neural networks and support vector machines for predicting groundwater levels in a coastal aquifer. *J. Hydrol.* 396, 128-138.
- Yue, S., P. Pilon and G. Cavadias. (2002). “Power of Mann-Kendall and Spearman’s rho tests for detecting monotonic trends in hydrological series.” *J. Hydrol.*, 259, 254-271.
- Zhang, Q., Xu, Y., Zhang, Z., Chen, Y. D., ling Liu, C., and Lin, H. (2008). “Spatial and temporal variability of precipitation maxima during 1960-2005 in the Yangtze River basin and possible association with large-scale circulation.” *J. Hydrol.*, 353 (3–4): 215–227.
- Zhang, Q., Xu, C. Y., M. Gemmer, M., Chen, D. and Liu, C. (2009). “Changing properties of precipitation concentration in the Pearl River basin, China.” *Stoch. Environ. Res. Risk Assess.*, 23 (3): 377–385.
- Zhang, K., Yao, Y., Qian, X. and Wang, J. (2019). “Various characteristics of precipitation concentration index and its cause analysis in China between 1960 and 2016.” *Int. J. Climatol.* 39 (12): 4648–4658.



## PUBLICATIONS

1. Chythanya Krishnan and Amai Mahesha. (2022). “Regional Trends and Spatiotemporal Analysis of Rainfall and Groundwater in the West Coast Basins of India”. *J Hydrol Engg.*, ASCE, 27(8), 05022008-1-20. [https://doi.org/10.1061/\(ASCE\)HE.1943-5584.0002177](https://doi.org/10.1061/(ASCE)HE.1943-5584.0002177)
2. Chythanya Krishnan and Amai Mahesha. (2023). “Assessment of Bi-Decadal Groundwater Fluctuations in a Coastal Region Using Innovative Trends and Singular Spectrum Analysis.” *J. of Geol. Soc. of India.*, 1–119. <https://doi.org/10.1007/s12594-023-2273-5>
3. Chythanya Krishnan and Amai Mahesha. (2019). “Impact of Rainfall Trend on Groundwater in Humid, Tropical Coastal Region of India.” *American Geophysical Union Fall Meeting*, Moscone Centre, San Francisco, California, USA, 9 - 13 December 2019.
4. Chythanya Krishnan and Amai Mahesha. (2019). “Trend Analysis of Rainfall and Groundwater in the Netravati Basin of Karnataka. *24th HYDRO-International Conference*, Osmania University, Hyderabad, India. December 18-20, 2019.



## BIODATA

Name Chythanya Krishnan  
Date of Birth 27<sup>th</sup> May 1988  
Father's name Kunhikrishnan K  
Mother's name Usha K K  
Permanent Address Krishna, Koroth house, Near Avyam Kottam,  
P.O. Chirakkal, Kannur -670011, Kerala, India.  
Mail id chythanyakrishnan@gmail.com  
Phone +91-6361607378



### Educational details

2015 - present PhD at Department of Water Resources and Ocean Engineering,  
NITK Surathkal

2011 - 2013 M.Tech in Water Resources Engineering and Management, NITK  
Surathkal.  
CGPA : 9.69 with Gold Medal

2006 – 2010 B.Tech in Civil Engineering, Govt. College of Engineering Kannur  
75% aggregate – Frist Class with Honours

### Research interests

Groundwater hydrology, Rainfall and climate change studies,  
Machine learning in hydrology, Hydrogeology and groundwater  
modelling

### Soft computing skills

ArcGIS, R-statistical software, MODFLOW, MS-Office, SWAT,  
Python